TURKISH SOCIETY OF CARDIOLOGY

October 2025
Volume 53, Number 7

ARCHIVES OF THE TURKISH SOCIETY OF CARDIOLOGY

ORIGINAL ARTICLES

AF in AMI: Comparing GRACE, SYNTAX II, and More
Bilgin Doğan et al.

Lp(a), Coronary Calcification, Bone Density
Yurtseven et al.

HALP Score in Diabetic NSTEMI
Erbay and Aladağ

Erectile Dysfunction and Biventricular Diastolic Dysfunction
Çiçek et al.

Prognostic Value of Inflammatory Indices in Patients with IE
İnan et al.

Frontal QRS-T Angle and Hemodialysis
Kaya et al.

Concomitant CEA and off-pump CAB
Ateş et al.

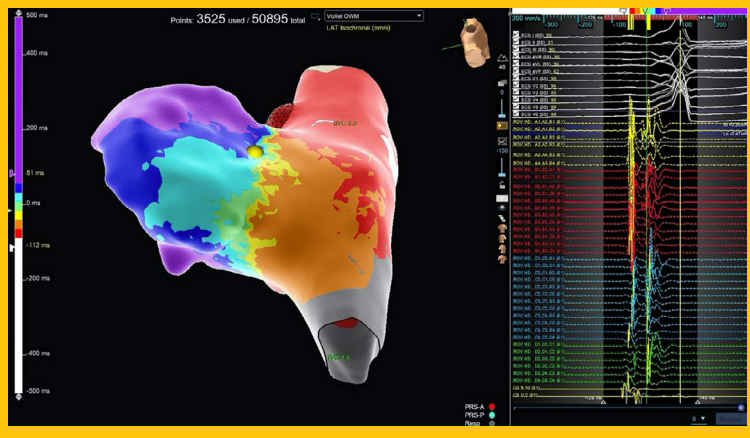

KARE MEDYA

ISSN - 1016 - 5169 eISSN 1308 - 4488
www.archivestsc.com

ARCHIVES OF THE TURKISH SOCIETY OF CARDIOLOGY

Editör / Editor

Dr. Dilek Ural

Önceki Editörler / Former Editors

Dr. Vedat Sansoy
Dr. Altan Onat

Editör Yardımcıları / Associate Editors

Dr. Halil Ataş
Dr. Gamze Babur Güler
Dr. Özcan Başaran
Dr. Serdar Bozyel
Dr. Uğur Canpolat
Dr. Barış Güngör
Dr. Mustafa Ozan Gürsoy
Dr. Meral Kayıkçıoğlu
Dr. Barış Kılıçarslan
Dr. Sanem Nalbantgil
Dr. Kaan Okyay
Dr. Elif Hande Özcan Çetin
Dr. Bahar Pirat
Dr. Taner Şen
Dr. Hakan Taşolar
Dr. Selim Topçu
Dr. Cansın Tulunay Kaya

İstatistik Danışmanı / Statistical Consultant

Aysen Kandemir

Karikatür ve Çizimler / Cartoon and Illustrations

Dr. Levent Pay

Ulusal Bilimsel Danışma Kurulu / National Editorial Board

Nihal Akar Bayram, Ankara
Hakkı Tankut Akay, Ankara
Mehmet Akbulut, Elazığ
Bahri Akdeniz, İzmir
Taylan Akgün, İstanbul
Hakan Altay, İstanbul
Dursun Aras, İstanbul
Alev Arat Özkan, İstanbul
Şakir Arslan, Antalya
Özgür Aslan, İzmir
Enver Atalar, Ankara
Vedat Aytekin, İstanbul
Engin Bozkurt, Ankara
Ceyhun Ceyhan, Aydın
Yüksel Çavuşoğlu, Eskişehir
Ahmet Çelik, Mersin
Muzaffer Değertekin, İstanbul
İrem Dinçer, Ankara
Mustafa Kemal Erol, İstanbul
Mehmet Ertürk, İstanbul
Bülent Görenek, Eskişehir
İbrahim Hakan Güllü, Ankara
Yılmaz Güneş, Bolu
İbrahim Akın İzgi, İstanbul
Can Yücel Karabay, İstanbul
Ergün Barış Kaya, Ankara
Teoman Kılıç, Kocaeli
Mustafa Kılıçkap, Ankara
Serdar Kula, Ankara
Bülent Mutlu, İstanbul
Haldun Müderrisoğlu, Ankara
Ertuğrul Okuyan, İstanbul
Öner Özdoğan, İzmir
Mehmet Özkan, Ardahan
Ebru Özpelit, İzmir
Mahmut Şahin, Samsun
Asife Şahinarslan, Ankara
İbrahim Halil Tanboğa, İstanbul
Ahmet Temizhan, Ankara
Lale Tokgözoğlu, Ankara
Serkan Topaloğlu, Ankara
Eralp Tutar, Ankara
Ercan Tutar, Ankara
Omaç Tüfekçioğlu, Ankara
Ertan Ural, Kocaeli
Mehmet Uzun, İstanbul
Ertan Vuruşkan, Gaziantep
Oğuz Yavuzgil, İzmir
Dilek Yeşilbursa, Bursa
Ertan Yetkin, Mersin
Aylin Yıldırır, Ankara
Ahmet Yıldız, İstanbul
Mustafa Yıldız, İstanbul
Mehmet Birhan Yılmaz, İzmir
Hikmet Yorgun, Ankara
Uygar Çağdaş Yüksel, Ankara

Uluslararası Bilimsel Danışma Kurulu / International Editorial Board

Adrian Baranchuk, Canada
Talantbek Batyraliyev, Kyrgyzstan
Gani Bajraktari, Kosovo
Antonio Bayéde Luna, Spain
Salim Berkinbayev, Kazakhstan
Matteo Cameli, Italy
Alain Cohen-Solal, France
Mirza Dilic, Bosnia and Herzegovina
David Duncker, Germany
Samad Ghaffari, Iran
Hüseyin İnce, Germany
Cemil İzgi, United Kingdom
Sasko Kedev, Macedonia
Erkin Mirrakhimov, Kyrgyzstan
Ulvi Mirzoyev, Azerbaijan
Agnès Pasquet, Belgium
Fausto J. Pinto, Portugal
Belma Pojskić, Bosnia and Herzegovina
Zeljko Reiner, Croatia
Leyla Elif Sade, United States of America
Petar M. Seferovic, Serbia
Patrick W.J. Serruys, Netherlands
Stephen W. Smith, United States of America
Zeynep Özlem Soran, United States of America
Evgeny Shlyakhto, Russia
Dragan Simic, Serbia
Gary Tse, United Kingdom
Murat Tuzcu, United Arab Emirates

Sahibi/Owner

Türk Kardiyoloji Derneği adına
On behalf of the Turkish Society of Cardiology
Muzaffer M. Değertekin

Yazı İşleri Müdürü / Publishing Manager

Dr. Dilek Ural

Yayın Sekreteri / Publication Secretary

Ebru Boz Sandıkçı

Yayın Koordinatörü / Publication Coordinator

Zeynep Sena Pekşen

Yönetim Yeri Adresi / Corresponding Address

Turkish Society of Cardiology
Nish İstanbul A Blok Kat: 8
No: 47-48, Çobançeşme
Sanayi Cad. 11, Yenibosna,
Bahçelievler, İstanbul
Phone: +90 212 221 17 30 - 221 17 38
Fax: +90 212 221 17 54
E-Mail: tkd@tkd.org.tr
URL: http://www.tkd.org.tr

Yayıncı / Publisher

Kare Yayıncılık
www.karepb.com
Circulation : 12

Indexed in PubMed, Europe PMC, Index Medicus, Web of Science, Emerging Sources Citation Index (ESCI), SCOPUS, EMBASE (the Excerpta Medica database), EBSCO, DOAJ, CNKI (China National Knowledge Infrastructure), GENAMICS, Research4Life, Hinari, SCILIT, OUCI, Turkish Medical Index and Turkiye Citation Index./PubMed, Europe PMC, Index Medicus, Web of Science, Emerging Sources Citation Index (ESCI), SCOPUS, EMBASE (Excerpta Medica), EBSCO, DOAJ, CNKI (China National Knowledge Infrastructure), GENAMICS, Research4Life, Hinari, SCILIT, OUCI, TÜBİTAK ULAKBİM Türk Tıp Dizini ve Türkiye Atıf Dizini'nde yer almaktadır.

Issued by the Turkish Society of Cardiology. / Türk Kardiyoloji Derneği'nin yayın organıdır.

Commercial activites are carried out by Turkish Society of Cardiology Economic Enterprise. / Ticari faaliyeti TKD İktisadi İşletmesi'nce yürütülmektedir.

Published eight issues a year. / Yılda sekiz sayı yayınlanır.

Publication Type: Periodical Publication / Yayın Türü: Yaygın Süreli.

KARE MEDYA

Contact
Address: Göztepe Mah., Fahrettin Kerim Gökay Cad., No: 200 Da: 2, Göztepe, Kadıköy, İstanbul, Türkiye
Phone: +90 216 550 61 11 Web: www.karepb.com E-mail: kare@karepb.com

Kare Publishing is a subsidiary of Kare Media.

ARCHIVES OF THE TURKISH SOCIETY OF CARDIOLOGY

CONTENTS/İÇİNDEKİLER

Volume: 53 / Issue: 7 / Year: 2025

ORIGINAL ARTICLES/KLİNİK ÇALIŞMALAR

▶465 **Comparison of CHA_2DS_2-VASc, C_2HEST, HAT_2CH_2, SYNTAX, GRACE, and SYNTAX II Scores for Predicting New-Onset Atrial Fibrillation Complicating Acute Myocardial Infarction**

Akut Miyokard Enfarktüsü Seyrinde Yeni Gelişen Atriyal Fibrilasyonu Öngörmede CHA_2DS_2-VASc, C_2HEST, HAT_2CH_2, SYNTAX, GRACE VE SYNTAX 2 Skorlarının Karşılaştırılması

Nazile Bilgin Doğan, Abdullah Kadir Dolu, Selim Ekinci, Ersin Çağrı Şimşek

▶477 **Association of Lipoprotein(a) with Coronary Artery Calcification and Bone Mineral Density in Elderly Individuals**

İleri Yaştaki Bireylerde Lipoprotein(a)'nın Koroner Arter Kalsifikasyonu ve Kemik Mineral Yoğunluğu ile İlişkisi

Ece Yurtseven, Gizem Timoçin Yığman, Gizem Yaşa, Nigar Bakhshaliyeva, Kayhan Çetin Atasoy, Erol Gürsoy, Kemal Baysal, Saide Aytekin, Vedat Aytekin

▶483 **The Hemoglobin, Albumin, Lymphocyte, and Platelet Score as a Simple Blood-Based Predictor of Residual Coronary Disease Burden in Diabetic Patients with Non-ST-Elevation Myocardial Infarction**

Diyabetik Non-ST Elevasyonlu Miyokard Enfarktüsü Hastalarında Rezidüel Koroner Hastalık Yükünü Öngörmede Hemoglobin, Albümin, Lenfosit ve Trombosit Skorunun Basit Bir Kan Testi Belirteci Olarak Değeri

İlke Erbay, Pelin Aladağ

▶492 **Erectile Dysfunction as a Marker of Subclinical Biventricular Diastolic Dysfunction: A Prospective Echocardiographic Study**

Subklinik Biventriküler Diyastolik Disfonksiyonun Bir Belirteci Olarak Erektil Disfonksiyon: Prospektif Ekokardiyografik Çalışma

Vedat Çiçek, Serkan Akan, Samet Yavuz, Şahhan Kılıç, Almina Erdem, Mert Babaoğlu, Caner Ediz, Ahmet Öz, Tufan Çınar, Ulaş Bağcı

▶501 **Prognostic Value of Inflammatory Indices in Patients with Infective Endocarditis: Peak C-Reactive Protein/Albumin Ratio as a Better Biomarker**

İnfektif Endokarditli Hastalarda İnflamatuar İndekslerin Prognostik Değeri: Pik C-Reaktif Protein/Albümin Oranı Daha İyi Bir Biyobelirteç

Duygu İnan, Alev Kılıçgedik, Ayşe İrem Demirtola Mammadli, Arslan Erdoğan, Duygu Genç Albayrak, Funda Özlem Pamuk, Sevil Tuğrul Yavuz, Fatmatuz Zehra Eroğlu, Cemal Ozanalp, Ahmet İlker Tekkeşin, Ömer Genç

▶510 **Frontal QRS-T Angle as a Prognostic Marker of Long-Term Mortality in Hemodialysis Patients**

Frontal QRS-T Açısının Hemodiyaliz Hastalarında Uzun Dönem Mortaliteyi Öngörmedeki Prognostik Değeri

Çağlar Kaya, Mustafa Ebik, Cihan Öztürk, Merve Akbulut Çakır, Emirhan Çakır, İlhan Kılıç

▶518 **The Outcomes of Concomitant Carotid Endarterectomy and Off-Pump Coronary Artery Bypass Grafting**

Eş Zamanlı Karotis Endarterektomi ve Pompasız Koroner Arter Bypass Greftlemesinin Sonuçları

Mehmet Şanser Ateş, Eray Aksoy, Zümrüt Tuba Demirözü, Sami Gürkahraman

HOW TO?/NASIL YAPALIM?

▶524 **How to Perform Open Window Mapping and Ablation in Patients with Wolff-Parkinson-White Syndrome: A Comprehensive Technical Guide Using CARTO™ and EnSite Electroanatomic Mapping Systems**

Wolff-Parkinson-White Sendromlu Hastalarda Open Window Haritalama ve Ablasyon Nasıl Yapılır: CARTO™ ve EnSite Elektroanatomik Haritalama Sistemleri Kullanılarak Kapsamlı Teknik Kılavuz

Serkan Çay, Meryem Kara, Serhat Koca, Özcan Özeke, Elif Hande Özcan Çetin, Ahmet Korkmaz, Fırat Özcan, Serkan Topaloğlu

CASE REPORTS/OLGU SUNUMLARI

▶536 **Left Anterior Descending Artery to Right Coronary Artery Bifurcation Stenting with Culotte Technique in Acute Inferior Myocardial Infarction**

Akut Alt Duvar Miyokard Enfarktüsünde Sol Ön İnen Koroner Arterden Sağ Koroner Artere Culotte Tekniği ile Bifurkasyon Stentleme İşlemi

Murat Akçay, Ahmet Çınar, Aydın Can Ulusoy, Fatma Rümeysa Karaçeşme, Metin Çoksevim

▶541 **Paradoxical Cerebral and Coronary Embolism in a Young Patient Due to Right Atrial Appendage Aneurysm: A Case Report**

Sağ Atriyal Apendiks Anevrizmasına Bağlı Genç Bir Hastada Paradoksal Serebral ve Koroner Emboli: Bir Olgu Sunumu

Songül Usalp, Safiye Sanem Dereli Bulut, Filiz Çelebi, Emine Altuntaş

CASE IMAGE/OLGU GÖRÜNTÜSÜ

▶545 **Optical Coherence Tomography-Guided Nano-Culotte Stenting for Woven Coronary Artery Bifurcation Lesion**

Woven Koroner Bifürkasyon Lezyonuna Optik Koherens Tomografi Kılavuzlu Nano-Culotte Stentleme

Serkan Kahraman, Ahmet Yaşar Çizgici, Kadir Sadıkoğlu, Ali Kemal Kalkan, Mehmet Ertürk

LETTERS TO THE EDITOR/EDİTÖRE MEKTUPLAR

▶547 **Can Artificial Intelligence Replace Human Peer Review in Cardiovascular Journals?**

Kardiyovasküler Bilimsel Yayınlarda Hakemlik Sürecini Yapay Zeka Üstlenebilir mi?

Sefa Tatar

▶549 **Would the Hemoglobin, Albumin, Lymphocyte, and Platelet Score Help Predict Atrial Fibrillation Recurrence After Cryoballoon Ablation?**

Hemoglobin, Albümin, Lenfosit ve Trombosit Skoru Kriyoballon Ablasyon Sonrası Atriyal Fibrilasyon Tekrarını Tahmin Etmeye Yardımcı Olur mu?

Uğur Canpolat

Authors' Reply/Yazarın Cevabı

▶551 **Reply to the Letter to the Editor: ''Would the Hemoglobin, Albumin, Lymphocyte, and Platelet Score Help Predict Atrial Fibrillation Recurrence After Cryoballoon Ablation?''**

Editöre Mektup Yanıtı: ''Hemoglobin, Albümin, Lenfosit ve Trombosit Skoru Kriyoballon Ablasyon Sonrası Atriyal Fibrilasyon Tekrarını Tahmin Etmeye Yardımcı Olur mu?''

Koray Kalenderoğlu, Mert İlker Hayıroğlu, Tufan Çınar

▶552 **Factors Affecting QT Interval in Patients with Type 2 Diabetes Mellitus and the Effect of Sodium-Glucose Cotransporter 2 Inhibitors**

Tip 2 Diabetes Mellituslu Hastalarda QT Aralığını Etkileyen Faktörler ve Sodyum-Glukoz Kotransporter 2 İnhibitörlerinin Etkisi

Ali Çoner, Can Ramazan Önce, Cemal Köseoğlu

ARCHIVES OF THE TURKISH SOCIETY OF CARDIOLOGY

Official journal of the TURKISH SOCIETY OF CARDIOLOGY

Comparison of CHA_2DS_2-VASc, C_2HEST, HAT_2CH_2, SYNTAX, GRACE, and SYNTAX II Scores for Predicting New-Onset Atrial Fibrillation Complicating Acute Myocardial Infarction

Akut Miyokard Enfarktüsü Seyrinde Yeni Gelişen Atriyal Fibrilasyonu Öngörmede CHA_2DS_2-VASc, C_2HEST, HAT_2CH_2, SYNTAX, GRACE VE SYNTAX 2 Skorlarının Karşılaştırılması

ABSTRACT

Objective: This study evaluated the most effective scoring system for predicting new-onset atrial fibrillation (NOAF) during acute myocardial infarction (AMI). Identifying the best predictive tool may help clinicians select the most appropriate personalized treatment based on individual risk scores to prevent NOAF complicating AMI.

Method: A total of 2,206 patients diagnosed with AMI between June 2021 and January 2023 were included in this study. After excluding cases with missing data, univariable and multivariable analyses were conducted on 1,672 patients to assess the association between baseline characteristics and the development of atrial fibrillation. The CHA_2DS_2-VASC (Congestive heart failure, Hypertension, Age ≥ 75 years, Diabetes mellitus, Stroke/TIA/thromboembolism, Vascular disease, Age 65-74 years, Sex category), C_2HEST (Coronary artery disease, Chronic obstructive pulmonary disease, Hypertension, Elderly [age ≥ 75], Systolic heart failure, Thyroid disease), HAT_2CH_2 (Hypertension, Age > 75, Stroke/TIA, Chronic obstructive pulmonary disease, Heart failure), SYNTAX (Synergy Between PCI with Taxus and Cardiac Surgery), GRACE 2.0 (Global Registry of Acute Coronary Events), and SYNTAX II scores were calculated for each patient.

Results: Receiver operating characteristic (ROC) analysis showed that the SYNTAX score (SxS) had the highest predictive value for NOAF during AMI, with an area under the curve (AUC) of 0.785 (95% confidence interval [CI]: 0.767-0.802, P < 0.001), followed by the SYNTAX II score (SxSII) with an AUC of 0.747 (95% CI: 0.728-0.765, P < 0.001), and the GRACE 2.0 risk score (RS) with an AUC of 0.740 (95% CI: 0.721-0.758, P < 0.001). It was shown that the modified scores (created by incorporating hemoglobin A1c [HbA1c] levels), the primary independent predictive parameter in this study, into the existing risk models demonstrated higher predictive value for NOAF (C-statistic: 0.784-0.794).

Conclusion: Combining HbA1c levels with SxS yielded the highest diagnostic performance for predicting NOAF during AMI. In this study, while SxS outperformed other risk models, the GRACE 2.0 and SxSII scores also demonstrated relatively strong predictive value and were superior to the CHA_2DS_2-VASC, C_2HEST, and HAT_2CH_2 scores for predicting NOAF in the setting of AMI.

Keywords: Acute myocardial infarction, atrial fibrillation, hemoglobin A1c, SYNTAX score

ÖZET

Amaç: Bu çalışma, akut miyokard enfarktüsü (AMI) sırasında ortaya çıkan yeni başlangıçlı atriyal fibrilasyonu (NOAF) öngörmede en etkili skorlama yöntemini belirlemeyi amaçlamıştır. Bu sayede, AMI'ye eşlik eden NOAF'nin önlenmesi için, öngörülen risk skorlarına göre hekimlerin en uygun kişiselleştirilmiş tedaviyi seçmesine rehberlik edilebilir.

Yöntem: Haziran 2021 ile Ocak 2023 arasında toplam 2206 AMI hastası bu çalışmaya dâhil edilmiştir. Eksik veri nedeniyle, 1672 hasta için başlangıç faktörleri ile atriyal fibrilasyon gelişimi arasındaki ilişkileri değerlendirmek üzere tek değişkenli ve çok değişkenli analizler kullanılmıştır. Her bir hasta için CHA_2D_2-VASC, C_2HEST, HAT_2CH_2, SYNTAX, GRACE 2.0 ve SYNTAX II skorları hesaplanmıştır.

Bulgular: AMI sürecinde NOAF'ı öngörmek amacıyla yapılan ROC analizinde, SYNTAX skoru (SxS) için eğri altında kalan alan 0.785 (GA %95 0.767–0.802, P < 0.001) olarak bulunmuş;

ORIGINAL ARTICLE
KLİNİK ÇALIŞMA

Nazile Bilgin Doğan[1]
Abdullah Kadir Dolu[2]
Selim Ekinci[1]
Ersin Çağrı Şimşek[1]

[1]Department of Cardiology, University of Health Sciences Tepecik Training and Research Hospital, İzmir, Türkiye
[2]Department of Cardiology, İzmir Katip Çelebi University Atatürk Training and Research Hospital, İzmir, Türkiye

Corresponding author:
Nazile Bilgin Doğan
✉ dr_nbilgin@yahoo.com

Received: February 19, 2025
Accepted: July 09, 2025

Cite this article as: Bilgin Doğan N, Dolu AK, Ekinci S, Şimşek EÇ. Comparison of CHA_2DS_2-VASc, C_2HEST, HAT_2CH_2, SYNTAX, GRACE, and SYNTAX II Scores for Predicting New-Onset Atrial Fibrillation Complicating Acute Myocardial Infarction. *Turk Kardiyol Dern Ars.* 2025;53(7):465-476.

DOI: 10.5543/tkda.2025.38852

Copyright@Author(s)
Available online at archivestsc.com.
Content of this journal is licensed under a Creative Commons Attribution – NonCommercial-NoDerivatives 4.0 International License.

bunu sırasıyla SYNTAX II skoru (SxSII) 0.747 (GA %95 0.728–0.765, P < 0.001) ve GRACE 2.0 risk skoru (RS) 0.740 (GA %95 0.721–0.758, P < 0.001) izlemiştir. Çalışmanın bağımsız en güçlü öngörücü parametresi olan HbA1c düzeyinin, bu risk skorlarına bir puanlama parametresi olarak eklenmesiyle oluşturulan "modifiye" skorların NOAF'ı öngörmedeki değerinin daha yüksek olduğu gösterilmiştir (C istatistiği, 0.784–0.794).

Sonuç: HbA1c düzeyinin SxS ile birleştirilmesi, AMI sırasında NOAF tahmini açısından en iyi tanısal performansı sağlamıştır. Bu çalışmada, SxS diğer risk skorlarından daha iyi performans gösterirken, GRACE 2.0 risk skoru ile SxSII skorunun da görece yüksek bir öngörü değeri olduğu ve NOAF tahmini açısından CHA_2D_2-VASC, C_2HEST ve HAT_2CH_2 skorlarından daha başarılı olduğu saptanmıştır.

Anahtar Kelimeler: Akut miyokard enfarktüsü, atriyal fibrilasyon, hemoglobin A1c, SYNTAX skoru

Patients with myocardial infarction (MI)[1] frequently develop new-onset atrial fibrillation (NOAF), a condition strongly associated with increased mortality and adverse in-hospital outcomes, including prolonged length of stay, higher complication rates, and an increased need for intensive care or readmission.[2,3] Several clinical risk scores have been developed to assess atrial fibrillation (AF) risk in the general population, such as the Framingham Heart Study (FHS) score, the Atherosclerosis Risk in Communities (ARIC) score, and the Cohorts for Heart and Aging Research in Genomic Epidemiology Atrial Fibrillation (CHARGE-AF) score. Although advanced age, pre-existing heart failure, and extensive myocardial infarction have long been recognized as risk factors for atrial fibrillation during acute myocardial infarction (AMI), particularly in studies from the fibrinolytic therapy era,[4] there is a paucity of research on risk assessment modeling for NOAF in patients undergoing invasive revascularization. Identifying the most effective risk stratification model for NOAF is clinically important, particularly given the wide range of clinical, laboratory, and electrocardiographic parameters available at admission, and the fact that NOAF management in AMI patients remains both controversial and not well understood. Despite the availability of several general AF risk scores, there remains a significant gap in tools specifically designed or validated to predict NOAF in the setting of AMI. Most existing models lack integration of angiographic complexity and contemporary biomarker data, which may limit their clinical applicability in this high-risk population. This study aimed to conduct a comparative validation of the GRACE 2.0 Global Registry of Acute Coronary Events), CHA_2DS_2-VASc (Congestive heart failure, Hypertension, Age ≥75 years, Diabetes mellitus, Stroke/TIA/thromboembolism, Vascular disease, Age 65–74 years, Sex category), C_2HEST (Coronary artery disease, Chronic obstructive pulmonary disease, Hypertension, Elderly \[age ≥75], Systolic heart failure, Thyroid disease), HAT_2CH_2 (Hypertension, Age >75, Stroke/TIA, Chronic obstructive pulmonary disease, Heart failure), SYNTAX (Synergy Between PCI with Taxus and Cardiac Surgery), and SYNTAX II risk scores in predicting the likelihood of NOAF during AMI in patients undergoing invasive treatment.

ABBREVIATIONS

ACC/AHA	American College of Cardiology/ American Heart Association
ACS	Acute coronary syndrome
AMI	Acute myocardial infarction
ARIC	Atherosclerosis Risk in Communities
ASA	Acetylsalicylic acid
AUC	Area under the curve
CABG	Coronary artery bypass grafting
CHARGE-AF	Cohorts for Heart and Aging Research in Genomic Epidemiology Atrial Fibrillation
COPD	Chronic obstructive pulmonary disease
COVID-19	Coronavirus Disease 2019
CULPRIT-SHOCK trial	Culprit Lesion Only PCI versus Multivessel PCI in Cardiogenic Shock
DAPA-HF	Dapagliflozin and Prevention of Adverse Outcomes in Heart Failure
DECLARE-TIMI 58	Dapagliflozin Effect on Cardiovascular Events -Thrombolysis in Myocardial Infarction 58
ECG	Electrocardiogram
ESC	European Society of Cardiology
FHS	Framingham Heart Study
ICCU	Intensive cardiac care unit
LASSO	Least Absolute Shrinkage and Selection Operator
LVEF	Left ventricular ejection fraction
MI	Myocardial infarction
MR	Mitral regurgitation
NOAF	New-onset atrial fibrillation
OAD	Oral antidiabetic drugs
PCI	Percutaneous coronary intervention
ROC	Receiver operating characteristic
SPAP	Systolic pulmonary artery pressure
SYNTAX	Synergy Between PCI with Taxus and Cardiac Surgery
TIA	Transient ischemic attack

Materials and Methods

This retrospective observational cohort study was conducted at two high-volume tertiary invasive cardiology centers in İzmir, Türkiye. All patients diagnosed with AMI and admitted between June 2021 (coinciding with the Turkish Ministry of Health's announcement to normalize lifestyle habits due to low Coronavirus Disease 2019 (COVID-19) case numbers) and January 2023 were included. The diagnosis of AMI was based on clinical evidence of myocardial injury, including necrosis and elevated cardiac troponin levels exceeding the 99th percentile reference limit. Atrial fibrillation was diagnosed by a physician based on electrocardiographic (ECG) findings, in accordance with

established guidelines.[5] All patients were either continuously monitored for at least 24 hours during their stay in the intensive cardiac care unit (ICCU), or received daily 12-lead ECGs (or ECGs in response to new symptoms) throughout their hospitalization in the cardiac ward. Patients were excluded if they met any of the following criteria:

- History of known AF;
- Diagnosis other than acute coronary syndrome (ACS);
- Development of atrial fibrillation while being followed-up in the ICCU for a non-ACS condition;
- Known congenital heart disease;
- Organic mitral regurgitation (MR) (defined as MR due to structural deformities or injury to the leaflets, chordae, and/or papillary muscles leading to incomplete leaflet closure during systole);
- Stenosis (e.g., rheumatic mitral valve disease);
- History of mitral valve endocarditis;
- History of cardiac surgery other than coronary artery bypass grafting (CABG);
- Active infection such as pneumonia;
- Death during catheterization or within 24 hours of ICCU admission;
- Requirement for inotropic support during catheterization or ICCU stay (Figure 1).

New-onset atrial fibrillation was defined as atrial fibrillation detected for the first time during the index hospitalization in patients without a previously documented history of AF, in accordance with the 2020 European Society of Cardiology (ESC) Guidelines for the management of atrial fibrillation.[5] Among the 64 patients diagnosed with NOAF during hospitalization, 18 had atrial fibrillation recorded at the time of admission. In these cases, NOAF was considered to be associated with the acute myocardial infarction, based on the absence of prior AF documentation in national electronic health records and patient charts. Additionally, outpatient ECGs and hospital discharge reports from the preceding 12 months were reviewed to confirm the absence of pre-existing atrial fibrillation. Only patients with clear documentation of sinus rhythm prior to admission—or without any prior AF-related findings—were classified as true new-onset cases. The diagnosis of NOAF was based on 12-lead electrocardiograms recorded at admission, during catheterization, or in the intensive cardiac care unit, provided the episode was long enough to be documented and confirmed by a cardiologist. Patients were continuously monitored for arrhythmias in the ICCU or underwent daily ECGs or symptom-triggered ECGs in the general ward. ST-segment deviation was defined as the presence of ≥ 1 mm (0.1 mV) of ST-segment elevation or depression, measured 60 ms after the J point, observed in at least two contiguous leads on the 12-lead ECG recorded at admission. This assessment was performed manually by two independent cardiologists who were blinded to clinical outcomes. This definition aligns with standard criteria recommended by the American College of Cardiology/American Heart Association

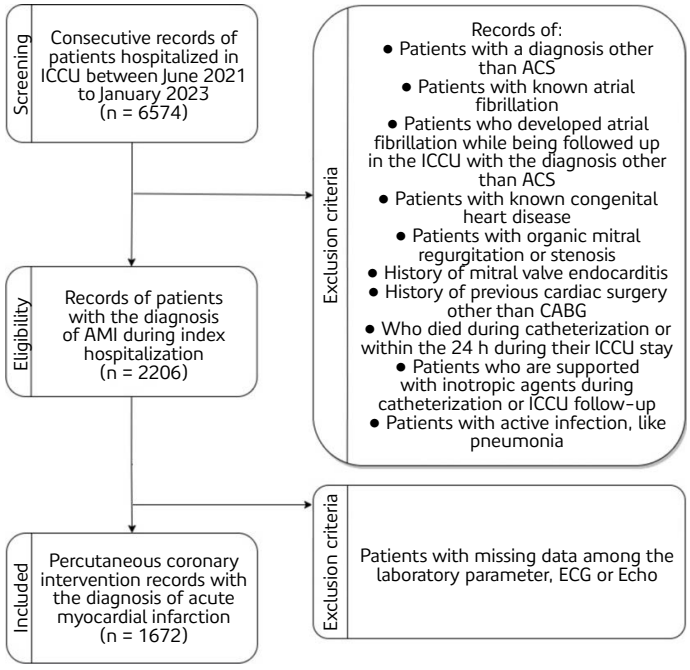

Figure 1. Patient identification flowchart.

(ACC/AHA) guidelines and is consistent with large-scale studies such as GUSTO-I (the Global Utilization of Streptokinase and Tissue Plasminogen Activator for Occluded Coronary Arteries I) and FAST-MI (the French Registry of Acute ST-Elevation or Non-ST-Elevation Myocardial Infarction) studies.[4-6] Baseline demographic, clinical, echocardiographic (performed during the index hospitalization), and angiographic data were collected and analyzed from medical records, procedural reports, and angiographic studies. Patients with ACS were categorized into two groups based on the presence of AF: the NOAF group and the non-NOAF group. Risk scores used in daily clinical practice for assessing in-hospital and long-term morbidity (CHA_2DS_2-VASC, C_2HEST, HAT_2CH_2, SYNTAX, SYNTAX II, and GRACE 2.0) were calculated using available data. The study was conducted in accordance with the principles of the Declaration of Helsinki. Informed consent was obtained from all patients. No artificial intelligence (AI)-assisted technologies, including large language models (LLMs), chatbots, or image generators, were used in the production of this manuscript.

The GRACE 2.0 ACS Risk Calculator (available via the MDCalc Medical Calculator app) was used to compute the GRACE risk score (GRACE RS). This score incorporates eight prognostic variables: ST-segment deviation, age, heart rate, systolic blood pressure, creatinine level, Killip classification, cardiac arrest at presentation, and elevated necrosis biomarkers.[6] Notably, in accordance with our inclusion criteria, ST-segment deviation and elevated troponin levels were considered present ("true") for all patients.

The SYNTAX score (SxS) and SYNTAX score II (SxSII) were calculated using the SYNTAX 2020 application. SxS is a widely recognized scoring algorithm used to assess the degree of complexity of coronary artery disease (CAD). It serves as a comprehensive angiographic grading tool that assists in objective

decision-making between CABG and percutaneous coronary intervention (PCI). The SxSII expands upon the original score by incorporating seven additional clinical variables to guide individualized treatment decisions based on mortality risk: age, creatinine clearance, left ventricular ejection fraction (LVEF), presence of unprotected left main coronary artery disease, peripheral vascular disease, female sex, and chronic obstructive pulmonary disease (COPD).[7]

The CHA_2DS_2-VASC score (which assigns 1 point for congestive heart failure, hypertension, age 65–74 years, diabetes mellitus, vascular disease, and female sex, and 2 points for age 75 and prior stroke or transient ischemic attack [TIA]) has a maximum total of 9 points. It is an effective tool for assessing ischemic stroke risk in patients with AF.[8] Moreover, several previous studies[9,10] have investigated its clinical utility in predicting the development of AF specifically.

For the purpose of predicting atrial fibrillation in the general population, the C_2HEST score, a composite of six parameters, was utilized in a large-scale study conducted in Asia. These parameters include: CAD or chronic obstructive pulmonary disease [1 point each], hypertension [1 point], elderly (age ≥ 75 years) [2 points], systolic heart failure [2 points], and thyroid disease (hyperthyroidism) [1 point].[11]

The HAT_2CH_2 score, developed in 2010, is based on patient age (≥ 75 years) [1 point], hypertension [1 point], stroke or transient ischemic attack [2 points], chronic obstructive pulmonary disease [1 point], and heart failure [2 points]. It was designed to help identify patients at risk of developing persistent AF.[12] In this study, we evaluated all of these risk scores, which are simple tools that can be calculated at the bedside using smartphones or paper charts, for their ability to predict NOAF in patients with AMI. The study was approved by Ethics Committee of Health Sciences University Tepecik Training and Research Hospital Non-Interventional Research Ethics Committee (Approval Number: 2022/04-41, Date: 15.04.2022).

Statistical Analysis

Continuous variables are presented as medians (25^{th}–75^{th} percentiles), while categorical variables are expressed as numbers (n) and percentages (%). Non-parametric tests were chosen for statistical analysis, as the Shapiro-Wilk test indicated that most parameters were not normally distributed, even after logarithmic transformation. The Mann-Whitney U test was used to compare continuous variables between groups. For categorical variables, comparisons were made using Pearson's chi-square test, Yates's chi-square test, or Fisher's exact test. To assess the direction and strength of correlations between non-normally variables, Spearman's correlation coefficients were calculated. The area under the receiver operating characteristic (ROC) curve (AUC) was used to evaluate the predictive performance of the established variables for identifying NOAF. Optimal cut-off values were selected based on the best combination of sensitivity and specificity. To identify variables most strongly associated with NOAF, univariate logistic regression analyses were performed using pre-specified cut-off values. Continuous variables were categorized according to ROC-derived thresholds, while categorical variables significantly associated with NOAF (p-value of 0.05 or less) univariate analysis were included in the multivariate analysis. Variables included in the final model were determined using a backward elimination approach, starting with all statistically significant predictors. Given the heterogeneity in group sizes between NOAF and non-NOAF patients, variable selection was also performed using the Least Absolute Shrinkage and Selection Operator (LASSO) regression to mitigate potential bias and prevent model due to class imbalance. Since the dependent variable in the study is binary, variable selection was based on logistic regression using the LASSO method. Analyses were conducted in R (version 4.4.2) using the "glmnet" package. The LASSO model was optimized for the penalty parameter (lambda) through 5-fold cross-validation, and model fit was evaluated based on the deviance criterion. The optimal model was selected using the "lambda.min" parameter, which corresponds to the lambda value yielding the minimum cross-validated deviance. The regression coefficients from this model were then examined, and variables with non-zero coefficients were considered statistically relevant. All analyses were conducted using IBM SPSS Statistics version 21.0 (IBM Corp., 2012, Armonk, NY, USA), with $P < 0.05$ set as the threshold for statistical significance. A post hoc power analysis was performed based on the difference in hemoglobin A1c (HbA1c) levels between the NOAF (+) and NOAF (–) groups. Assuming a medium effect size (Cohen's d = 0.5), with group sizes of 1,608 and 64, and an alpha level of 0.05, the calculated statistical power was 0.975. This indicates that the sample size was sufficient to detect clinically meaningful differences in HbA1c between the groups.

Results

A total of 2,206 AMI patients were enrolled in the study. Of these, 64 (2.9%) were diagnosed with NOAF during hospitalization. Among the 64 NOAF patients, 18 (28.1%) had arrhythmia at the time of admission, 20 (31.3%) during catheterization in the lab, and 26 (40.6%) during their stay in the ICCU. Due to missing data, variables from 1,672 patents were evaluated in the study.

Regarding patient demographics and comorbidities, those who developed NOAF were significantly older, with a mean age of 63.64 ± 12.93 years, compared to 52.94 ± 10.15 years in the non-NOAF group ($P < 0.001$). The NOAF group also had a higher prevalence of hypertension (53.13% vs. 27.80%, $P < 0.001$), prior coronary artery disease (37.5% vs. 21.95%, $P = 0.013$), and heart failure (23.4% vs. 13.06%, $P = 0.025$), as detailed in Table 1.

The risk of NOAF was significantly higher in patients who were taking acetylsalicylic acid prior to admission, with 33.33% of NOAF patients using aspirin compared to 16.67% in the non-NOAF group (odds ratio [OR]: 2.50, $P = 0.001$). Similarly, statin use before admission was more frequent among NOAF patients (18.8% vs. 5.53%, OR: 4.34, $P < 0.001$). Additionally, the absence of a smoking history was more common in the NOAF group, with 33.33% being non-smokers and 14.04% ex-smokers, compared to 11.73% and 5.86%, respectively, in the non-NOAF group ($P < 0.001$), as shown in Table 1.

The presence of diabetes mellitus did not significantly affect the development of NOAF during AMI (40.6% vs. 33.0%, $P = 0.258$). However, patients who developed NOAF had significantly higher blood glucose levels at admission (181.83 ± 85.23 mg/

Table 1. Baseline clinical characteristics

	Non-NOAF (-) (n = 1608)	NOAF (+) (n = 64)	P
BMI (kg/m²)	26.74 ± 3.74 27.12 (23.74–28.41)	27.43 ± 3.98 27.04 (24.29–29.41)	0.212‖
Age (years)	52.94 ± 10.15 51.00 (47.00–59.00)	63.64 ± 12.93 64.50 (56.00–73.00)	< 0.001‖
Gender			0.351‡
Male, n (%)	1295 (80.53%)	48 (75.00%)	
Female, n (%)	313 (19.47%)	16 (25.00%)	
Previous stroke/TIA, n (%)	90 (5.60%)	5 (7.81%)	0.634§
Hypertension, n (%)	447 (27.80%)	34 (53.13%)	<0.001‡
Prior coronary artery disease (CABG/PCI), n (%)	353 (21.95%)	24 (37.5%)	0.013*
Peripheral artery disease (carotid/peripheral arteries), n (%)	90 (5.60%)	1 (1.56%)	0.265§
Heart failure, n (%)	210 (13.06%)	15 (23.4%)	0.025‡
Chronic renal disease, n (%)	122 (7.59%)	9 (14.06%)	0.098‡
Smoking status			< 0.001†
Current smoker, n (%)	1251 (82.41%)	30 (52.63%)	
Ex-smoker, n (%)	89 (5.86%)	8 (14.04%)	
Non-smoker, n (%)	178 (11.73%)	19 (33.33%)	
Thyroid disease			0.543†
Hypothyroidism	85 (5.3%)	2 (3.1%)	
Hyperthyroidism	21 (1.3%)	0 (0.0%)	
None	1502 (93.4%)	62 (96.9%)	
Chronic obstructive pulmonary disease, n (%)	123 (7.65%)	8 (12.90%)	0.204§
On-admission treatment			
Acetylsalicylic acid, n (%)	268 (16.67%)	21 (33.33%)	0.001§
B-blocker, n (%)	179 (11.13%)	12 (18.75%)	0.056§
ACE-I/ARB, n (%)	536 (33.33%)	24 (37.5%)	0.302‡
Statin, n (%)	89 (5.53%)	12 (18.8%)	< 0.001§

*, Pearson Chi-Square; †, Pearson Exact Chi-Square; ‡, Yates's Chi-Square; §, Fisher's Exact Test; ||, Mann-Whitney U Test. ACE-I, Angiotensin-converting enzyme inhibitor; ARB, Angiotensin receptor blocker; BMI, Body max index; CABG, Coronary artery bypass grafting; PCI, Percutaneous coronary intervention; TIA, Transient ischemic attack.

dL vs. 131.89 ± 52.53 mg/dL, P < 0.001) and higher HbA1c levels (6.98 ± 1.81% vs. 6.16 ± 1.19%, P = 0.007), indicating poorer glycemic control. In terms of lipid and renal parameters, NOAF patients had lower high-density lipoprotein (HDL) levels (39.4 ± 7.34 mg/dL vs. 44.6 ± 7.36 mg/dL, P < 0.001), lower creatinine clearance (75.1 ± 30.6 mL/min vs. 99.7 ± 32.84 mL/min, P < 0.001), and lower total cholesterol levels (186.0 ± 43.38 mg/dL vs. 223.4 ± 49.76 mg/dL, P < 0.001), as summarized in Table 2. Detailed clinical data at admission are presented in Table 2. Patients who developed NOAF had a significantly higher heart rate on admission (93.2 ± 28.8 bpm vs. 82.44 ± 11.34 bpm, P = 0.007) and lower systolic blood pressure (122.6 ± 21.4 mmHg vs. 131.41 ± 21.88 mmHg, P = 0.016) compared to those without NOAF. However, the presence of cardiac arrest on admission was not significantly different between the groups (6.3% in NOAF vs. 14.7% in non-NOAF, P = 0.088). Similarly, Killip class distribution showed no significant difference (Killip class I: 81.3% vs. 83.5%; class II: 17.2% vs. 15.0%; class III: 1.6% in both groups; P = 0.890).

Electrocardiographic, echocardiographic, and angiographic findings are summarized in Table 3. Among the echocardiographic parameters, patients who developed NOAF had a significantly larger left atrial diameter (38.7 ± 4.84 mm vs. 36.32 ± 2.39 mm, P < 0.001), increased left ventricular end-systolic diameter (LVESD) (35.18 ± 7.96 mm vs. 30.51 ± 3.79 mm, P < 0.001), and increased left ventricular end-diastolic diameter (LVEDD) (49.33 ± 6.03 mm vs. 45.39 ± 2.87 mm, P < 0.001). Systolic pulmonary artery pressure (SPAP) was also significantly higher in the NOAF group (37.9 ± 10.2 mmHg vs. 30.0 ± 2.12 mmHg, P < 0.001). Mitral regurgitation, even when mild, was more common among NOAF patients, with 53.1% having any degree of MR compared to 14.8% in the non-NOAF group (P < 0.001). Additionally, patients with NOAF had lower left ventricular ejection fraction (43.11 ± 10.2% vs. 48.43 ± 6.55%, P < 0.001).

The effects of the variables included in the study on NOAF development were assessed using univariate and multivariate analyses. Stepwise logistic regression was performed with variables found to be significant in univariate logistic regression.

Table 2. Laboratory parameters and clinical data at admission

	Non-NOAF (-) (n = 1608)	NOAF (+) (n = 64)	P
Diagnosis			0.206†
NSTEMI	537 (33.40%)	16 (25.0%)	
STEMI	1071 (66.60%)	48 (75.0%)	
Laboratory parameters at admission			
Blood glucose (mg/dL)	131.89 ± 52.53 120.50 (106.00-136.00)	181.83 ± 85.23 154.00 (127.00-226.00)	< 0.001‡
CrC (mL/min)	99.69 ± 32.84 102.50 (65.38-118.94)	75.1 ± 30.6 74.0 (50.0-92.0)	< 0.001‡
TSH (mIU/L)	1.30 ± 0.44 1.19 (0.91-1.50)	1.64 ± 1.35 1.10 (0.71-2.26)	0.922‡
HB (g/dL)	13.98 ± 1.18 14.00 (13.00-14.70)	15.75 ± 1.79 13.60 (11.73-15.35)	0.173‡
HDL (mg/dL)	44.60 ± 7.36 43.00 (40.00-51.00)	39.4 ± 7.34 39.50 (34.30-43.00)	< 0.001‡
Total cholesterol (mg/dL)	223.44 ± 49.76 212.00 (187.00-243.00)	186.00 ± 43.38 183.50 (162.50-217.25)	< 0.001‡
HbA1c (%)	6.16 ± 1.19 6.00 (5.40-6.60)	6.98 ± 1.81 6.20 (5.70-8.10)	0.007‡
Clinical status at admission			
Heart rate (bpm)	82.44 ± 11.34 80.0 (77.0-90.0)	93.2 ± 28.8 85.0 (78.0-120)	0.007‡
Systolic blood pressure (mmHg)	131.41 ± 21.88 130.00 (115.00-150.00)	122.6 ± 21.4 120.00 (107.00-135.00)	0.016‡
Modified killip class			0.890*
Class I	1342 (83.5%)	52 (81.3%)	
Class II	241 (15%)	11 (17.2%)	
Class III	25 (1.6%)	1 (1.6%)	
Cardiac arrest			0.088†
Yes	236 (14.68%)	4 (6.3%)	
No	1372 (85.32%)	60 (93.8%)	

*, Pearson Exact Chi-Square; †, Yates's Chi-Square; ‡, Mann-Whitney U Test. CrC, Creatinine clearance; bpm, Beats per minute; HB, Hemoglobin; HDL, High-density lipoprotein; NSTEMI, Non-ST-elevation myocardial infarction; STEMI, ST-elevation myocardial infarction; TSH, Thyroid-stimulating hormone.

Additionally, to address the class imbalance between NOAF and non-NOAF groups and to prevent model overfitting, LASSO regression was used for variable selection. After including all candidate variables in the model, a LASSO regression analysis was performed. Variables with coefficients shrunk to zero by the penalty parameter (lambda) were excluded from the final model, and only those with non-zero coefficients were retained. The variables that remained in the model following LASSO penalization, indicating their relative contribution to the model, are listed below: Age (coefficient: 0.27005); time from symptom onset to reperfusion (4–12 hours) (0.19003); > 12 hours (0.27992); blood glucose level (0.1800); HbA1C (0.349906); systolic blood pressure (-0.220029); number of ischemic ST-segment elevation leads (0.3099); left ventricular end-diastolic diameter (0.21009); and presence of mitral regurgitation (reference: none) (0.28997). These variables, identified by having non-zero coefficients, were considered the most informative predictors retained in the final LASSO-selected model. The major predictors of NOAF were determined accordingly, as shown in Table 4. In the final multivariate logistic regression analysis, several variables were identified as independent predictors of NOAF during acute myocardial infarction: Age ≥ 60 years was associated with a significantly increased risk (OR: 2.103; 95% confidence interval [CI]: 1.378–3.134; P < 0.001). Compared to patients who received reperfusion within 4 hours, those treated between 4–12 hours had a moderately increased risk (OR: 1.912; 95% CI: 1.134–3.221; P = 0.015), while those treated after 12 hours had a substantially higher risk (OR: 2.708; 95% CI: 1.619–4.382; P < 0.001). Elevated blood glucose levels (≥ 127 mg/dL; OR: 1.593; 95% CI: 1.087–2.408; P = 0.015) and high HbA1c levels (≥5.6%; OR: 2.841; 95% CI: 1.923–4.195; P < 0.001) were also significant predictors of NOAF. Low systolic blood pressure (≤125 mmHg) was found to be a predictive factor (OR: 0.693; 95% CI: 0.509–0.944; P = 0.028). Additional independent risk factors included a higher number of ischemic ST-segment derivations (≥ 5 leads) (OR: 2.482; 95% CI: 1.517–4.062; P < 0.001), increased left ventricular end-diastolic diameter (≥ 48 mm) (OR: 2.011; 95% CI: 1.211–3.197; P = 0.006), and the presence of any grade of mitral regurgitation (OR: 1.864; 95% CI: 1.090–3.126; P = 0.012).

Table 3. Electrocardiographic, echocardiographic, and coronary angiographic findings during hospitalization

	Non-NOAF (-) (n = 1608)	NOAF (+) (n = 64)	P
Electrocardiographic parameters at admission			
Ischemic ST derivation lead number	4.17 ± 2.36 4.00 (2.00-6.00)	4.91 ± 2.25 6.00 (3.00-6.00)	0.012‡
Echocardiographic parameters			
Left atrial size (mm)	36.32 ± 2.39 36.0 (35.0-37.0)	38.7 ± 4.84 38.0 (36.0-42.0)	< 0.001‡
LVEF (%)	48.43 ± 6.55 50.0 (41.25-50.0)	43.11 ± 10.2 45.0 (39.0-50.0)	< 0.001‡
LVESD (mm)	30.51 ± 3.79 31.0 (28.0-33.0)	35.18 ± 7.96 35.0 (30.0-40.0)	< 0.001‡
LVEDD (mm)	45.39 ± 2.87 45.0 (44.0-47.0)	49.33 ± 6.03 48.0 (46.0-53.0)	< 0.001‡
Mitral regurgitation			< 0.001*
None	1332 (82.8%)	26 (40.6%)	
Mild	238 (14.8%)	34 (53.1%)	
Moderate	38 (2.4%)	4 (6.3%)	
SPAP (mmHg)	30.00 ± 2.12 30.0 (29.0-32.50)	37.9 ± 10.2 36.0 (35.0-42.3)	< 0.001‡
Coronary angiographic parameters			
SYNTAX score	11.47 ± 6.53 8.00 (8.00-14.5)	21.25 ± 10.1 22.0 (14.0-26.0)	< 0.001‡
No-reflow phenomenon	43 (3.0%)	3 (4.7%)	0.692†
Time from symptom onset to reperfusion			< 0.001†
<4 hours	1430 (88.93%)	31 (48.4%)	
4–12 hours	178 (11.07%)	14 (21.9%)	
>12 hours	0 (0.0%)	19 (29.7%)	

*, Pearson Chi-Square; †, Fisher's Exact Chi-Square; ‡, Mann-Whitney U Test. LVEDD, Left ventricular end-diastolic diameter; LVEF, Left ventricular ejection fraction; LVESD, Left ventricular end-systolic diameter; SPAP, Systolic pulmonary arterial pressure.

In this study, we found that each risk score can be used to predict NOAF complicating AMI (Table 5). Patients with the following values had an increased risk of developing NOAF during AMI: SxS RS ≥ 16.1, SxSII RS ≥ 26.2, GRACE 2.0 ≥ 122, CHA_2DS_2-VASC RS ≥ 3, C_2HEST RS ≥ 3, or HAT_2CH_2 RS ≥ 1. ROC analysis showed that the AUC of the SxS for predicting NOAF in the setting of AMI was 0.785 (95% CI: 0.767–0.802, P < 0.001), followed by SxSII (AUC: 0.747; 95% CI: 0.728–0.765, P < 0.001), and the GRACE 2.0 risk score (AUC: 0.740; 95% CI: 0.721–0.758, P < 0.001) (Table 6). Based on these results, SxS was identified as the most predictive RS for NOAF complicating AMI (Figure 2).

A new scoring model was developed by combining HbA1c level, identified as the most predictive risk factor for NOAF, with each of the risk scores included in the study. This combined approach was found to be superior in predicting NOAF in the context of AMI. ROC analysis demonstrated the following AUC values for the new scoring models in predicting NOAF in the context of AMI: 0.794 (95% CI: 0.764–0.808, P < 0.001) for SxS, 0.790 (95% CI: 0.734–0.812, P < 0.001) for SxSII, 0.784 (95% CI: 0.750–0.795, P < 0.001) for the GRACE 2.0 risk score, 0.705 (95% CI: 0.657–0.707, P < 0.001) for the CHA_2DS_2-VASc score, 0.673 (95% CI: 0.674–0.723, P < 0.001) for the C_2HEST score, and 0.650 (95% CI: 0.627–0.678, P < 0.001) for the HAT_2CH_2 score.

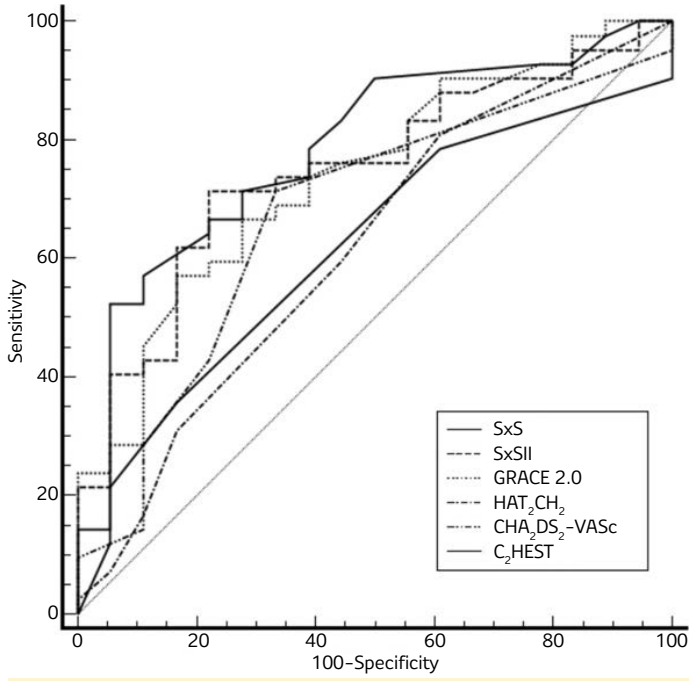

Figure 2. Receiver operating characteristic (ROC) curve analysis of risk scores for predicting new-onset atrial fibrillation (NOAF) during acute myocardial infarction (AMI).

Table 4. Univariate and multivariable logistic regression analyses of independent predictors of new-onset atrial fibrillation (NOAF)

Variables	Univariate analysis		Multivariable analysis	
	OR (95% CI)	P	OR (95% CI)	P
Age	1.09 (1.06–1.11)	< 0.001	**2.103 (1.378–3.134)**	**< 0.001**
HT (Ref: None)	2.946 (1.787–4.858)	< 0.001		
CAD (Ref: None)	3.000 (1.786–5.039)	< 0.001		
HF (Ref: None)	5.204 (2.835–9.550)	< 0.001		
Time from symptom onset to reperfusion (Ref: <4 hours)	4–12 hours: > 3.310 (1.666–6.5742) >12 hours: > Inf.	< 0.001 0.972	**4–12 hours: >1.912 (1.134–3.221)** **>12 hours: >2.708 (1.619–4.382)**	**0.015** **< 0.001**
Blood glucose level	1.009 (1.006–1.012)	< 0.001	**1.593 (1.087–2.408)**	**0.015**
Creatinine clearance	0.979 (0.971–0.986)	< 0.001		
HDL	0.892 (0.848–0.937)	< 0.001		
Total cholesterol	0.976 (0.966–0.986)	< 0.001		
HbA1c	1.484 (1.220–1.807)	< 0.001	**2.841 (1.923–4.195)**	**< 0.001**
Heart rate	1.050 (1.040–1.071)	< 0.001		
Systolic blood pressure	0.980 (0.965–0.994)	0.005	**0.693 (0.509–0.944)**	**0.028**
Ischemic ST derivation lead count	1.140 (1.026–1.267)	0.015	**2.482 (1.517–4.062)**	**< 0.001**
Left atrial size	1.360 (1.240–1.480)	< 0.001		
LVEF	0.885 (0.850–0.921)	< 0.001		
LVESD	1.300 (1.210–1.390)	< 0.001		
LVEDD	1.440 (1.320–1.580)	< 0.001	**2.011 (1.211–3.197)**	**0.006**
Mitral regurgitation (Ref: None)	9.692 (5.748–16.341)	< 0.001	**1.864 (1.091–3.126)**	**0.012**
SPAP	1.580 (1.250–2.00)	< 0.001		
Acetylsalicylic acid use	2.500 (1.462–4.272)	< 0.001		
Statin use (Ref: None)	4.340 (2.242–8.400)	< 0.001		

CAD, Coronary artery disease; HDL, High-density lipoprotein; HF, Heart failure; HT, Hypertension; LVEDD, Left ventricular end-diastolic diameter; LVEF, Left ventricular ejection fraction; LVESD, Left ventricular end-systolic diameter; SPAP, Systolic pulmonary artery pressure.

Table 5. Risk scores

	Non-NOAF (-) (n = 1608)	NOAF (+) (n = 64)	P
SYNTAX score	11.48 ± 6.53 8.00 (8.00-14.50)	21.25 ± 10.1 22.0 (14.0-26.0)	< 0.001*
CHA_2DS_2-VASc	2.44 ± 1.57 2.00 (1.00-3.00)	3.41 ± 1.76 3.00 (2.00-4.25)	< 0.001*
C_2HEST	1.89 ± 0.99 2.00 (1.00-2.00)	2.38 ± 1.36 2.00 (2.00-3.00)	0.002*
HAT_2CH_2	1.39 ± 1.46 1.00 (0.00-2.00)	2.02 ± 1.49 2.00 (1.00-3.00)	< 0.001*
SYNTAX II score	22.59 ± 9.36 22.80 (14.20-26.10)	35.42 ± 13.27 34.0 (26.2-46.0)	< 0.001*
GRACE 2.0	102.44 ± 23.54 102.00 (85.00-120.00)	129.78 ± 26.01 134 (110-146)	< 0.001*

*, Mann-Whitney U Test.

Discussion

Atrial fibrillation, the most common clinical arrhythmia, frequently occurs as a complication of AMI and serves as an independent predictor of adverse outcomes.[3,13,14] In this study, the SYNTAX score demonstrated the best diagnostic performance for predicting NOAF in the context of AMI, followed by the GRACE 2.0 RS and SYNTAX II scores. These three scores outperformed CHA_2D_2-VASc, C_2HEST, and HAT_2CH_2 scores. Notably, the predictive performance of the SYNTAX score was further enhanced by incorporating HbA1c levels, resulting in a modified model that combines both anatomical and metabolic risk factors. This combined SYNTAX

Table 6. Pairwise comparison of receiver operating characteristic (ROC) curves

	SYNTAX	C_2HEST	CHA_2DS_2-VASc	HAT_2CH_2	GRACE 2.0	SYNTAX II
SYNTAX score	AUC: 0.785	–	–	–	–	–
C_2HEST	P < 0.001	AUC: 0.618	–	–	–	–
CHA_2DS_2-VASc	P = 0.018	P = 0.021	AUC: 0.672	–	–	–
HAT_2CH_2	P < 0.001	P = 0.976	P = 0.016	AUC: 0.617	–	–
GRACE 2.0	P = 0.262	P = 0.001	P = 0.045	P < 0.001	AUC: 0.740	–
SYNTAX II score	P = 0.317	P < 0.001	P = 0.018	P < 0.001	P = 0.810	AUC: 0.747

+ HbA1c model achieved a higher AUC (0.794) compared to the SYNTAX score alone (0.785), suggesting improved discrimination for NOAF prediction. This improvement can be attributed to the complementary nature of the included parameters: while the SYNTAX score reflects the complexity of coronary artery disease, HbA1c represents chronic metabolic stress, which contributes to atrial structural remodeling and arrhythmogenesis. Therefore, integrating these parameters may offer a more holistic risk stratification tool in the setting of acute MI. Additionally, several clinical and echocardiographic parameters identified in our study as significant predictors of NOAF during AMI have also been reported in previous research. For instance, left atrial enlargement and increased left ventricular end-diastolic diameter have consistently been associated with a higher risk of NOAF, likely due to elevated atrial pressure and stretch.[15] Similarly, mitral regurgitation, even when mild, has been found to contribute to NOAF development by increasing left atrial volume and promoting electrical remodeling.[16] In addition, prolonged time from symptom onset to reperfusion (> 4 hours), which was significant in our analysis, has been shown in earlier reports to increase ischemic burden and sympathetic activation, both of which predispose patients to atrial fibrillation.[17] ST-segment deviation on admission electrocardiogram (ECG), another predictor in our model, is also supported by prior research as a marker of widespread ischemia and atrial irritability.[18] These consistent findings across studies support the robustness of our model and highlight the multifactorial nature of NOAF during AMI. In our study, the CHA_2DS_2-VASc, C_2HEST, and HAT_2CH_2 scores demonstrated relatively poor predictive performance for NOAF in the setting of AMI. These scores were originally developed for general AF risk assessment in broader outpatient or community-based populations, not for acute ischemic settings. One possible reason for their limited utility is that they do not incorporate acute-phase variables such as infarct size, ischemic burden, or angiographic complexity, all of which may play a significant role in NOAF development during AMI. Additionally, these scores lack integration of acute metabolic and hemodynamic parameters (e.g., blood glucose, HbA1c, troponin, or ST-segment changes), which have been shown to influence arrhythmogenesis in acute coronary syndromes. Therefore, the application of these scores in this high-risk inpatient population may not reflect the true burden of NOAF risk.

In our study, the use of acetylsalicylic acid (ASA) and statins was more common among patients who developed NOAF. Interestingly, regression analysis revealed that ASA and statin users had a 2.5-fold (P = 0.001) and 4.34-fold (P < 0.001) increased risk of NOAF, respectively (Table 1). However, this finding is likely influenced by confounding factors, as these medications are more frequently prescribed to patients with a higher burden of coronary artery disease and comorbidities. Therefore, this observed association should be interpreted with caution and not assumed to be causal.

When HbA1c, the main independent predictor identified in our cohort, was added to the risk scores as an additional parameter, the predictive accuracy for NOAF during AMI improved noticeably. Atrial fibrillation complicating AMI has been reported to have a wide incidence range, from 2.3% and 21%.[1,19,20] In our study, the incidence of NOAF was 2.92%, which is consistent with previous reports, particularly those focusing on NOAF occurring during hospitalization in the modern revascularization era.[1,21,22]

Various studies have explored the predictors of NOAF in the context of AMI, identifying numerous significant and independent factors.[4,23] Various studies have demonstrated that the onset of NOAF during ACS involves multiple mechanisms. Although the precise cause remains uncertain, one potential mechanism is inflammation, a shared feature in both NOAF and CAD. The effects of inflammation on coronary arteries depends on multiple factors, one of which is elevated blood glucose levels due to uncontrolled or undiagnosed diabetes. Interestingly, a history of diabetes was not a predictor of clinical outcomes in the current study. Regardless of diabetes status, a high blood glucose level or elevated HbA1c on admission was associated with an increased risk of NOAF complicating AMI in our cohort. The literature reports varying HbA1c cut-off values associated with atherosclerosis, demonstrating increased CAD risk even among non-diabetic individuals.[24] According to the American Diabetes Association, the prediabetic range is defined as an HbA1c of 5.7–6.4.[25] In our study, an HbA1c threshold of ≥ 5.6 emerged as the most influential independent predictor of NOAF among AMI patients. This finding may be explained by the hypothesis that diabetes-related end-organ damage—reflected by elevated HbA1c levels in patients who developed NOAF and detected via coronary anatomy and calcification scores—provides a more accurate measure of risk in this population than metabolic markers alone. Several mechanisms may underlie the relationship between elevated HbA1c and NOAF development in the setting of AMI. Chronic hyperglycemia contributes to left atrial structural remodeling through increased oxidative stress, inflammation, and interstitial fibrosis, all of which can alter atrial electrophysiology and promote arrhythmogenesis. Moreover, elevated HbA1c levels are indicative of poor glycemic control, insulin resistance,

and metabolic dysregulation, all of which are independently associated with atrial fibrillation in both diabetic and non-diabetic populations. These pathophysiological changes may explain why HbA1c emerged as the strongest independent predictor of NOAF in our study. Although the exact number of patients receiving sodium-glucose cotransporter 2 (SGLT2) inhibitor therapy in our cohort is unknown—due to the classification of antidiabetic treatment into broader categories (i.e., oral antidiabetic drugs [OAD], insulin, or a combination of both)—emerging evidence suggests that these agents may reduce the incidence of atrial fibrillation. This benefit is believed to occur through mechanisms such as favorable cardiac remodeling, reduction of oxidative stress, and improvement in metabolic profiles. Several large trials and meta-analyses (e.g., DECLARE-TIMI 58 [Dapagliflozin Effect on Cardiovascular Events-Thrombolysis in Myocardial Infarction 58], DAPA-HF [Dapagliflozin and Prevention of Adverse Outcomes in Heart Failure]) have reported a reduced risk of AF in patients treated with SGLT2 inhibitors. While our dataset does not allow for a direct evaluation of this association, the strong link between elevated HbA1c and NOAF supports the hypothesis that targeting glycemic control—potentially through SGLT2 inhibitors—could serve as a preventive strategy against NOAF in the post-MI setting. Future studies are warranted to explore this potential therapeutic benefit. An angiographic tool for assessing CAD complexity, the SYNTAX score is commonly used in clinical practice.[26] Drawing on data from the SYNTAX trial, SxS was originally developed to predict clinical outcomes in stable patients presenting with three-vessel and/or left main disease who underwent PCI or CABG.[27,28] Subsequently, the SxS was applied across a broader range of patient populations with various clinical scenarios, including those presenting with ACS and undergoing primary PCI.[29,30] Patients with a higher SYNTAX score are known to have more jeopardized myocardium under ischemia, and this was reflected in our study, where widespread ST-segment deviation on admission ECG emerged as an independent predictor of NOAF. To complement angiographic data with clinical variables, the SYNTAX score II was developed. In our study, SxSII was found to be as helpful as the SxS in predicting NOAF complicating AMI, but not superior.

Although low HDL-cholesterol and statin use have been previously associated with atrial fibrillation in various studies, these variables did not remain independent predictors of NOAF in our multivariate model.[31] Nevertheless, their established roles in modulating systemic inflammation and atherosclerotic burden may still contribute indirectly to arrhythmic risk, particularly in patients with chronic dyslipidemia.[32]

Among the echocardiographic parameters evaluated, only mitral regurgitation was identified as an independent predictor of NOAF in our model (OR: 1.864; 95% CI: 1.090–3.126; P = 0.012). While variables such as left ventricular end-systolic diameter, left atrial diameter, and systolic pulmonary artery pressure (SPAP) have been associated with atrial pressure and structural remodeling in previous studies, they did not retain statistical significance in our multivariate analysis.[33,34] This suggests that volume overload, as reflected by MR, may play a more dominant role in the development of atrial fibrillation during AMI in this patient cohort.

Other independent predictors of NOAF in the setting of AMI included age, heart rate, systolic blood pressure, and creatinine level, all of which are among the eight prognostic variables included in the GRACE 2.0 RS. Initially developed from the GRACE registry, the GRACE risk score (2.0) was later validated in the French FAST-MI 2005 registry for both acute ST-elevation and non-ST-elevation MI.[6] This updated risk assessment model is important for its simplicity and compatibility with handheld electronic devices and smartphones. It predicts mortality at 6 months, 1 year, and 3 years in patients with ACS. Notably, the occurrence of NOAF during AMI has consistently been associated with worse clinical outcomes, including higher rates of in-hospital mortality, ischemic stroke, and long-term mortality.[4,35,36] Therefore, it is not surprising that the GRACE 2.0 RS proved valuable in predicting NOAF in patients with AMI. In our multivariate model, two key components of the GRACE score—age and systolic blood pressure—were independently associated with the development of NOAF, further supporting the relevance of this risk score in this clinical context. According to current guidelines, moderate- or high-risk GRACE scores in ACS patients are associated with worse clinical outcomes,[6] which may also reflect a higher risk for NOAF during AMI. In our study, a GRACE (2.0) risk score above 122 defined this high-risk subgroup. The GRACE 2.0 score, which is calculated using clinical data independent of coronary angiographic findings, was shown to be nearly as effective as the SxSII score in predicting NOAF complicating AMI, supporting its practical utility.

Etiologies of AF during AMI, aside from inflammation, include excessive sympathetic stimulation, pressure overload of the left or right ventricle, and hypoxia.[1,2,37] All of these factors are commonly seen in patients with heart failure. Elevated heart rates and reduced systolic blood pressure likely indicate hemodynamic compromise, a relationship further supported by their association with heart failure and markers of more extensive MI, such as a lower ejection fraction.[38,39] A sub-analysis of the CULPRIT-SHOCK trial (Culprit Lesion Only PCI versus Multivessel PCI in Cardiogenic Shock) found that 52 of 142 patients (37%) with cardiogenic shock complicating AMI developed new-onset AF during their initial hospital stay.[40] However, in our study, the two GRACE RS components (cardiac arrest at admission and Killip class (signs/symptoms)) did not affect the occurrence of NOAF during AMI, likely due to non-homogeneous sample sizes in these subgroups. However, this finding is not clinically significant and represents one of the limitations of the study.

Although the CHA_2DS_2-VASc score is widely used to assess ischemic stroke risk in patients with AF,[41] its role in predicting the onset of AF has been evaluated in several studies.[9,42] In an ACS cohort, Mitchell et al.[43] demonstrated that neither the $CHADS_2$ nor CHA_2DS_2-VASc scores were effective in predicting incident AF. Similarly, in our study, even after modifying the CHA_2DS_2-VASc score by incorporating HbA1c levels, its diagnostic performance remained relatively poor, with C-statistics of 0.705 and 0.672, respectively. The C_2HEST score, which has been widely studied in Asian populations, has shown superior predictive performance for incident AF compared to the $CHADS_2$, CHA_2DS_2-VASc, and HATCH scores in the general population.[11]

Additionally, studies have explored the use of the HAT_2CH_2 score to predict AF in various patient populations, such as those with cancer[44] or patients presenting to the emergency department.[45] Despite the poor predictive performance of the CHA_2DS_2-VASc score, both the HAT_2CH_2 and C_2HEST scores performed even worse in our study. This discrepancy may be explained by the low prevalence of COPD—a key component of both the HAT_2CH_2 and C_2HEST scores—within our study population. Furthermore, the study's primary outcome may be influenced by the fact that the research sample consisted exclusively of AMI patients, a clinical setting in which risk scores such as SYNTAX, GRACE 2.0, and SYNTAX II are more likely to provide predictive value in assessing disease severity.

Limitations

The relatively small sample size of patients with NOAF may limit the strength of independent predictors identified through multivariate analysis, potentially affecting the comprehensiveness of our conclusions. It is also possible that some asymptomatic paroxysmal AF cases in the non-NOAF group went undetected due to minimal diagnostic monitoring in the cardiology department—where only one daily 12-lead ECG was performed. Additionally, individuals with asymptomatic AF prior to the index AMI may have been misclassified as NOAF, despite our exclusion of patients with documented AF. Although the study included patients with AMI, the majority were ST-elevation myocardial infarction (STEMI) cases, as both participating centers functioned as primary PCI hubs for İzmir Province.

Conclusion

In this study, we demonstrated that the SYNTAX RS has clinically relevant superiority over other risk scores in predicting NOAF among patients with AMI. Additionally, HbA1c emerged as an important biomarker for NOAF, independent of the patient's diabetes status. A modified SxS created by adding HbA1C to the original SxS, was shown to have better predictive value for NOAF in the setting of AMI.

Ethics Committee Approval: Ethics committee approval was obtained from Ethics Committee of Health Sciences University Tepecik Training and Research Hospital Non-Interventional Research Ethics Committee (Approval Number: 2022/04-41, Date: 15.04.2022).

Informed Consent: Informed consent was obtained from all patients.

Conflict of Interest: The authors have no conflicts of interest to declare.

Funding: The authors declared that this study received no financial support.

Use of AI for Writing Assistance: No artificial intelligence (AI)-assisted technologies, including large language models (LLMs), chatbots, or image generators, were used in the production of this manuscript.

Author Contributions: Concept – N.B.D., A.K.D., S.E., E.Ç.Ş.; Design – N.B.D., E.Ç.Ş.; Supervision – N.B.D., E.Ç.Ş.; Resource – N.B.D., A.K.D., S.E.; Materials – N.B.D., A.K.D., S.E.; Data Collection and/or Processing – N.B.D., A.K.D.; Analysis and/or Interpretation – N.B.D.; Literature Review – N.B.D., E.Ç.Ş.; Writing – N.B.D.; Critical Review – E.Ç.Ş.

Acknowledgments: Assistant Professor Dr. Muzaffer Bilgin is kindly acknowledged for contributing to the statistical analysis.

Peer-review: Externally peer-reviewed.

References

1. Schmitt J, Duray G, Gersh BJ, Hohnloser SH. Atrial fibrillation in acute myocardial infarction: A systematic review of the incidence, clinical features and prognostic implications. *Eur Heart J*. 2009;30(9):1038-1045. [CrossRef]
2. Pay L, Kolak Z, Çakır B, Kamber T, Yazıcı S. Atrial fibrillation-related acute myocardial infarction and acute mesenteric ischemia. *Turk Kardiyol Dern Ars*. 2021;49(5):410-413. [CrossRef]
3. Angeli F, Reboldi G, Garofoli M, et al. Atrial fibrillation and mortality in patients with acute myocardial infarction: A systematic overview and meta-analysis. *Curr Cardiol Rep*. 2012;14(5):601-610. [CrossRef]
4. Crenshaw BS, Ward SR, Granger CB, Stebbins AL, Topol EJ, Califf RM. Atrial fibrillation in the setting of acute myocardial infarction: The GUSTO-I experience. Global Utilization of Streptokinase and TPA for Occluded Coronary Arteries. *J Am Coll Cardiol*. 1997;30(2):406-413. [CrossRef]
5. Hindricks G, Potpara T, Dagres N, et al. 2020 ESC Guidelines for the diagnosis and management of atrial fibrillation developed in collaboration with the European Association for Cardio-Thoracic Surgery (EACTS): The Task Force for the diagnosis and management of atrial fibrillation of the European Society of Cardiology (ESC) Developed with the special contribution of the European Heart Rhythm Association (EHRA) of the ESC. *Eur Heart J*. 2021;42(5):373-498. Erratum in: *Eur Heart J*. 2021;42(5):507. Erratum in: *Eur Heart J*. 2021;42(5):546-547. Erratum in: *Eur Heart J*. 2021;42(40):4194.
6. Fox KA, FitzGerald G, Puymirat E, et al. Should patients with acute coronary disease be stratified for management according to their risk? Derivation, external validation and outcomes using the updated GRACE risk score. *BMJ Open*. 2014;4(2):e004425. [CrossRef]
7. Farooq V, van Klaveren D, Steyerberg EW, et al. Anatomical and clinical characteristics to guide decision making between coronary artery bypass surgery and percutaneous coronary intervention for individual patients: Development and validation of SYNTAX score II. *Lancet*. 2013;381(9867):639-650. [CrossRef]
8. European Heart Rhythm Association; European Association for Cardio-Thoracic Surgery; Camm AJ, et al. Guidelines for the management of atrial fibrillation: The Task Force for the Management of Atrial Fibrillation of the European Society of Cardiology (ESC). *Eur Heart J*. 2010;31(19):2369-429. Erratum in: *Eur Heart J*. 2011;32(9):1172.
9. Saliba W, Gronich N, Barnett-Griness O, Rennert G. Usefulness of CHADS2 and CHA2DS2-VASc scores in the prediction of new-onset atrial fibrillation: A population-based study. *Am J Med*. 2016;129(8):843-849. [CrossRef]
10. Lau KK, Chan PH, Yiu KH, et al. Roles of the CHADS2 and CHA2DS2-VASc scores in post-myocardial infarction patients: Risk of new occurrence of atrial fibrillation and ischemic stroke. *Cardiol J*. 2014;21(5):474-483. [CrossRef]
11. Li YG, Pastori D, Farcomeni A, et al. A Simple Clinical Risk Score (C2HEST) for predicting incident atrial fibrillation in Asian subjects: Derivation in 471,446 Chinese subjects, with internal validation and external application in 451,199 korean subjects. *Chest*. 2019;155(3):510-518. [CrossRef]
12. de Vos CB, Pisters R, Nieuwlaat R, et al. Progression from paroxysmal to persistent atrial fibrillation clinical correlates and prognosis. *J Am Coll Cardiol*. 2010;55(8):725-731. [CrossRef]
13. Bishara R, Telman G, Bahouth F, Lessick J, Aronson D. Transient atrial fibrillation and risk of stroke after acute myocardial infarction. *Thromb Haemost*. 2011;106(5):877-884. [CrossRef]
14. Jabre P, Roger VL, Murad MH, et al. Mortality associated with atrial fibrillation in patients with myocardial infarction: A systematic review and meta-analysis. *Circulation*. 2011;123(15):1587-1593. [CrossRef]

15. Essayagh B, Antoine C, Benfari G, et al. Prognostic implications of left atrial enlargement in degenerative mitral regurgitation. *J Am Coll Cardiol*. 2019;74(7):858-870. [CrossRef]
16. Van Laer SL, Verreyen S, Winkler KM, et al. Effect of mitral regurgitation on thrombotic risk in patients with nonrheumatic atrial fibrillation: A new CHA2DS2-VASc score risk modifier? *Am J Cardiol*. 2021;145:69-76. [CrossRef]
17. Calé R, Pereira H, Pereira E, et al. Time to reperfusion in high-risk patients with myocardial infarction undergoing primary percutaneous coronary intervention. *Rev Port Cardiol (Engl Ed)*. 2019;38(9):637-646. [CrossRef]
18. Yamashita T, Murakawa Y, Ajiki K, Omata M. Incidence of induced atrial fibrillation/flutter in complete atrioventricular block. A concept of 'atrial-malfunctioning' atrio-hisian block. *Circulation*. 1997;95(3):650-654. [CrossRef]
19. Kalarus Z, Svendsen JH, Capodanno D, et al. Cardiac arrhythmias in the emergency settings of acute coronary syndrome and revascularization: An European Heart Rhythm Association (EHRA) consensus document, endorsed by the European Association of Percutaneous Cardiovascular Interventions (EAPCI), and European Acute Cardiovascular Care Association (ACCA). *Europace*. 2019;21(10):1603-1604. Erratum in: *Europace*. 2019 Oct 1;21(10):1604. [CrossRef]
20. Dai Y, Yang J, Gao Z, et al. Atrial fibrillation in patients hospitalized with acute myocardial infarction: Analysis of the china acute myocardial infarction (CAMI) registry. *BMC Cardiovasc Disord*. 2017;17(1):2. [CrossRef]
21. McManus DD, Huang W, Domakonda KV, et al. Trends in atrial fibrillation in patients hospitalized with an acute coronary syndrome. *Am J Med*. 2012;125(11):1076-1084. [CrossRef]
22. Rene AG, Généreux P, Ezekowitz M, et al. Impact of atrial fibrillation in patients with ST-elevation myocardial infarction treated with percutaneous coronary intervention (from the HORIZONS-AMI [Harmonizing Outcomes With Revascularization and Stents in Acute Myocardial Infarction] trial). *Am J Cardiol*. 2014;113(2):236-242. [CrossRef]
23. Wong CK, White HD, Wilcox RG, et al. Significance of atrial fibrillation during acute myocardial infarction, and its current management: Insights from the GUSTO-3 trial. *Card Electrophysiol Rev*. 2003;7(3):201-207. [CrossRef]
24. Sarwar N, Aspelund T, Eiriksdottir G, et al. Markers of dysglycaemia and risk of coronary heart disease in people without diabetes: Reykjavik prospective study and systematic review. *PLoS Med*. 2010;7(5):e1000278. [CrossRef]
25. American Diabetes Association. 2. Classification and diagnosis of diabetes: Standards of Medical Care in Diabetes-2018. *Diabetes Care*. 2018;41(Suppl 1):S13-S27. [CrossRef]
26. Sianos G, Morel MA, Kappetein AP, et al. The SYNTAX Score: An angiographic tool grading the complexity of coronary artery disease. *EuroIntervention*. 2005;1(2):219-227.
27. Serruys PW, Onuma Y, Garg S, et al. Assessment of the SYNTAX score in the Syntax study. *EuroIntervention*. 2009;5(1):50-56. [CrossRef]
28. Serruys PW, Morice MC, Kappetein AP, et al. Percutaneous coronary intervention versus coronary-artery bypass grafting for severe coronary artery disease. *N Engl J Med*. 2009;360(10):961-72. Erratum in: *N Engl J Med*. 2013;368(6):584. [CrossRef]
29. Capodanno D, Di Salvo ME, Cincotta G, Miano M, Tamburino C, Tamburino C. Usefulness of the SYNTAX score for predicting clinical outcome after percutaneous coronary intervention of unprotected left main coronary artery disease. *Circ Cardiovasc Interv*. 2009;2(4):302-308. [CrossRef]
30. Caixeta A, Généreux P, Palmerini T, et al. Prognostic utility of the SYNTAX score in patients with single versus multivessel disease undergoing percutaneous coronary intervention (from the Acute Catheterization and Urgent Intervention Triage StrategY [ACUITY] trial). *Am J Cardiol*. 2014;113(2):203-210. [CrossRef]
31. Reiner Ž, Muačević-Katanec D, Katanec D, Tedeschi-Reiner E. Low HDL-cholesterol - An important risk factor for cardiovascular diseases. *Lijec Vjesn*. 2011;133:111-116. [Article in Bosnian]
32. Almeida SO, Budoff M. Effect of statins on atherosclerotic plaque. *Trends Cardiovasc Med*. 2019;29(8):451-455. [CrossRef]
33. Wang W, Buehler D, Martland AM, Feng XD, Wang YJ. Left atrial wall tension directly affects the restoration of sinus rhythm after Maze procedure. *Eur J Cardiothorac Surg*. 2011;40(1):77-82. [CrossRef]
34. Kettlewell S, Burton FL, Smith GL, Workman AJ. Chronic myocardial infarction promotes atrial action potential alternans, afterdepolarizations, and fibrillation. *Cardiovasc Res*. 2013;99(1):215-224. [CrossRef]
35. Wong CK, White HD, Wilcox RG, et al. New atrial fibrillation after acute myocardial infarction independently predicts death: The GUSTO-III experience. *Am Heart J*. 2000;140(6):878-885. [CrossRef]
36. Lehto M, Snapinn S, Dickstein K, Swedberg K, Nieminen MS; OPTIMAAL investigators. Prognostic risk of atrial fibrillation in acute myocardial infarction complicated by left ventricular dysfunction: The OPTIMAAL experience. *Eur Heart J*. 2005;26(4):350-356. [CrossRef]
37. Lopes RD, Pieper KS, Horton JR, et al. Short- and long-term outcomes following atrial fibrillation in patients with acute coronary syndromes with or without ST-segment elevation. *Heart*. 2008;94(7):867-873. [CrossRef]
38. Eldar M, Canetti M, Rotstein Z, et al. Significance of paroxysmal atrial fibrillation complicating acute myocardial infarction in the thrombolytic era. SPRINT and Thrombolytic Survey Groups. *Circulation*. 1998;97(10):965-970. [CrossRef]
39. Pedersen OD, Bagger H, Køber L, Torp-Pedersen C. The occurrence and prognostic significance of atrial fibrillation/-flutter following acute myocardial infarction. TRACE Study group. TRAndolapril Cardiac Evalution. *Eur Heart J*. 1999;20(10):748-754. [CrossRef]
40. Feistritzer HJ, Desch S, Zeymer U, et al. Prognostic impact of atrial fibrillation in acute myocardial infarction and cardiogenic shock. *Circ Cardiovasc Interv*. 2019;12(6):e007661. [CrossRef]
41. European Heart Rhythm Association; European Association for Cardio-Thoracic Surgery; Camm AJ, et al. Guidelines for the management of atrial fibrillation: The Task Force for the Management of Atrial Fibrillation of the European Society of Cardiology (ESC). *Eur Heart J*. 2010;31(19):2369-2429. Erratum in: *Eur Heart J*. 2011;32(9):1172.
42. Lau KK, Chan PH, Yiu KH, et al. Roles of the CHADS2 and CHA2DS2-VASc scores in post-myocardial infarction patients: Risk of new occurrence of atrial fibrillation and ischemic stroke. *Cardiol J*. 2014;21(5):474-483. [CrossRef]
43. Mitchell LB, Southern DA, Galbraith D, et al. Prediction of stroke or TIA in patients without atrial fibrillation using CHADS2 and CHA2DS2-VASc scores. *Heart*. 2014;100(19):1524-1530. [CrossRef]
44. Hu WS, Lin CL. Comparison of CHA2DS2-VASc, CHADS2 and HATCH scores for the prediction of new-onset atrial fibrillation in cancer patients: A nationwide cohort study of 760,339 study participants with competing risk analysis. *Atherosclerosis*. 2017;266:205-211. [CrossRef]
45. Barrett TW, Self WH, Wasserman BS, McNaughton CD, Darbar D. Evaluating the HATCH score for predicting progression to sustained atrial fibrillation in ED patients with new atrial fibrillation. *Am J Emerg Med*. 2013;31(5):792-797. [CrossRef]

ARCHIVES OF THE TURKISH SOCIETY OF CARDIOLOGY

Official journal of the TURKISH SOCIETY OF CARDIOLOGY

Association of Lipoprotein(a) with Coronary Artery Calcification and Bone Mineral Density in Elderly Individuals

İleri Yaştaki Bireylerde Lipoprotein(a)'nın Koroner Arter Kalsifikasyonu ve Kemik Mineral Yoğunluğu ile İlişkisi

ABSTRACT

Objective: Coronary artery calcification (CAC) and osteoporosis are common age-related conditions that may share underlying mechanisms such as inflammation and lipid dysregulation. Lipoprotein(a) [Lp(a)] has been suggested as a potential contributor to both processes. This study aims to investigate the relationship between CAC, bone mineral density (BMD), and Lp(a) levels in a statin-naive elderly population.

Method: This retrospective study included 310 patients aged ≥ 55 years who underwent coronary computed tomography angiography and Lp(a) measurement. CAC was assessed visually, and BMD was measured using vertebral Hounsfield units. Patients were stratified into three groups according to Lp(a) levels: ≤ 30, 30–49, and ≥ 50 mg/dL. Propensity score matching was performed for age and sex.

Results: Patients with CAC had higher Lp(a) levels [36.4 ± 33.2 vs. 21.7 ± 27.8 mg/dL, P < 0.001], lower high-density lipoprotein cholesterol (HDL-C) [52.6 ± 14.6 vs. 57.5 ± 17.9 mg/dL, P = 0.010], and lower BMD [152.9 ± 50.2 vs. 169.1 ± 51.0 HU, P = 0.009]. In multivariate analysis, both Lp(a) and HDL-C were independent predictors of CAC. Low BMD and CAC prevalence increased stepwise across Lp(a) strata: in patients with Lp(a) ≤ 30 mg/dL, low BMD was present in 28.9% and CAC in 52.6%; in those with Lp(a) 30–49 mg/dL, 37.2% and 66.7%; and in those with Lp(a) ≥ 50 mg/dL, 58.6% and 80.3%, respectively (P = 0.002 and P = 0.001).

Conclusion: Elevated Lp(a) is associated with both CAC and low BMD. Lp(a) ≥ 50 mg/dL may serve as a shared biomarker to identify individuals at risk for concurrent vascular and skeletal deterioration.

Keywords: Atherosclerosis, bone mineral density, coronary artery calcification, lipoprotein(a), osteoporosis

ÖZET

Amaç: Koroner arter kalsifikasyonu (KAK) ve osteoporoz, yaşa bağlı gelişen, inflamasyon ve lipid düzensizliği gibi ortak mekanizmalara sahip, birbiriyle ilişkili patolojilerdir. Lipoprotein(a) [Lp(a)], her iki sürece de katkıda bulunabilecek potansiyel bir faktör olarak önerilmiştir. Bu çalışmanın amacı, statin kullanmamış ileri yaştaki bireylerde KAK, kemik mineral yoğunluğu (KMY) ve Lp(a) düzeyleri arasındaki ilişkiyi araştırmaktır.

Yöntem: Bu retrospektif çalışmaya, bilgisayarlı tomografik koroner anjiyografisi ve Lp(a) ölçümü yapılmış, ≥ 55 yaş olan 310 hasta dahil edildi. KAK görsel olarak değerlendirildi, KMY ise vertebral Hounsfield birimleri kullanılarak ölçüldü. Hastalar Lp(a) düzeylerine göre, ≤ 30, 30–49 ve ≥ 50 mg/dL olarak üç gruba ayrıldı. Yaş ve cinsiyet için eğilim skoru eşleştirmesi yapıldı.

Bulgular: KAK bulunan hastalarda Lp(a) düzeyleri daha yüksek [36,4 ± 33,2 vs. 21,7 ± 27,8 mg/dL, P < 0,001], HDL-K düzeyleri daha düşük [52,6 ± 14,6 vs. 57,5 ± 17,9 mg/dL, P = 0,010] ve KMY daha düşük [152,9 ± 50,2 vs. 169,1 ± 51,0 HU, P = 0,009] idi. Çok değişkenli analizde hem Lp(a) hem de HDL-K, KAK'ın bağımsız belirleyicileri olarak bulundu. Düşük KMY ve KAK prevalansının, Lp(a) gruplarına göre kademeli olarak arttığı izlendi; Lp(a) ≤ 30 mg/dL olanlarda düşük KMY %28,9 ve KAK %52,6; Lp(a) 30–49 mg/dL olanlarda %37,2 ve %66,7; Lp(a) ≥ 50 mg/dL olanlarda %58,6 ve %80,3 (P = 0,002 ve P = 0,001) olarak saptandı.

Sonuç: Yüksek Lp(a) düzeyleri hem KAK hem de düşük KMY ile ilişkilidir. Lp(a) ≥ 50 mg/dL, hem damar hem kemik yapısında eş zamanlı bozulma riski taşıyan bireyleri belirlemede ortak bir biyobelirteç olarak kullanılabilir.

Anahtar Kelimeler: Ateroskleroz, kemik mineral yoğunluğu, koroner arter kalsifikasyonu, lipoprotein a, osteoporoz

ORIGINAL ARTICLE
KLİNİK ÇALIŞMA

Ece Yurtseven[1]
Gizem Timoçin Yığman[2]
Gizem Yaşa[3]
Nigar Bakhshaliyeva[3]
Kayhan Çetin Atasoy[2]
Erol Gürsoy[1]
Kemal Baysal[1]
Saide Aytekin[1]
Vedat Aytekin[1]

[1]*Department of Cardiology, Koç University Faculty of Medicine, İstanbul, Türkiye*
[2]*Department of Radiology, Koç University Faculty of Medicine, İstanbul, Türkiye*
[3]*Koç University Faculty of Medicine, İstanbul, Türkiye*

Corresponding author:
Ece Yurtseven
✉ eyurtseven@kuh.ku.edu.tr

Received: August 12, 2025
Accepted: August 26, 2025

Cite this article as: Yurtseven E, Yığman GT, Yaşa G, et al. Association of Lipoprotein(a) with Coronary Artery Calcification and Bone Mineral Density in Elderly Individuals. *Turk Kardiyol Dern Ars.* 2025;53(7):477–482.

DOI: 10.5543/tkda.2025.87282

Copyright@Author(s)
Available online at archivestsc.com. Content of this journal is licensed under a Creative Commons Attribution – NonCommercial-NoDerivatives 4.0 International License.

Arterial calcification, a process closely associated with atherosclerosis, results from the accumulation of hydroxyapatite crystals within the arterial extracellular matrix.[1] It represents an active, cell-controlled process resembling bone formation, involving vascular smooth muscle cell transdifferentiation and extracellular matrix remodeling.[2] While medial calcification predominantly affects peripheral arteries and is commonly related to diabetes and chronic kidney disease, intimal calcification in coronary arteries is primarily related to atherosclerosis and reflects an inflammatory process.[3] Advancement of coronary artery calcification (CAC) is closely related to an increased risk of cardiovascular events and is therefore considered a clinically relevant marker for risk stratification in asymptomatic individuals.[3] Recent guidelines recommend incorporating coronary calcium scoring alongside traditional cardiovascular risk factors to improve risk prediction accuracy.[3] Arterial calcification advances with aging, and osteoporosis frequently coexists as a common age-related comorbidity.

Osteoporosis, caused by low bone mineral density (BMD) leading to an increased risk of fractures, shares multiple pathophysiological mechanisms with vascular calcification, including chronic inflammation, oxidative stress, and dysregulated mineral metabolism.[4,5] This interaction is often referred to as the "bone–vascular axis."[4] Given this overlap, recent studies have emphasized the value of opportunistic screening for osteoporosis using coronary computed tomography (CT) scans. In patients undergoing CT for CAC scoring, vertebral bone attenuation can be simultaneously assessed, providing a cost-effective strategy to identify those at risk for low BMD.[6] The shared mechanisms between osteoporosis and arterial calcification have raised the possibility of common biomarkers related to the presence of both conditions.

Increased Lp(a) concentration has been consistently linked to a higher cardiovascular risk, and its clinical significance has become more widely recognized in recent years.[7] Lp(a) also promotes vascular calcification by enhancing inflammation, increasing the burden of oxidized phospholipids, and stimulating osteogenic differentiation of vascular smooth muscle cells.[8] While several studies have demonstrated an association between Lp(a) and the presence or progression of coronary artery calcification, some studies have failed to replicate this relationship, highlighting the need for further investigation.[9,10] Due to its possible interaction with bone metabolism, Lp(a) has also been investigated as a potential link between atherosclerosis and osteoporosis.[11] Although some studies have reported a negative correlation between Lp(a) levels and BMD or fracture risk, some large prospective cohort studies have not confirmed this association.[12,13] Despite these inconsistent findings, the possible role of Lp(a) in both vascular calcification and bone loss remains a subject of scientific interest due to shared underlying mechanisms.

In light of these conflicting findings, we aimed to investigate the relationships between coronary artery calcification, Lp(a) levels, and bone mineral density in a single cohort of patients who had coronary computed tomography angiography (CCTA). Understanding these associations may help raise awareness for considering screening for osteoporosis or coronary calcification in the presence of high Lp(a) levels and may enable earlier risk identification and clinical intervention.

ABBREVIATIONS

AHA	the American Heart Association
BMD	Bone mineral density
BMI	Body mass index
CAC	Coronary artery calcification
CCTA	Coronary computed tomography angiography
CT	Computed tomography
CVD	Cardiovascular disease
ECG	Electrocardiogram
eGFR	Estimated glomerular filtration rate
HDL-C	High-density lipoprotein cholesterol
hs-CRP	High-sensitivity C-reactive protein
LDL-C	Low-density lipoprotein cholesterol
Lp(a)	Lipoprotein(a)
MDRD	The Modification of Diet in Renal Disease
ROI	Region of interest

Materials and Methods

This retrospective study, which received approval from the Ethics Committee of Koç University School of Medicine (Approval Number: 2025.222.IRB2.102, Date: 15.05.2025), was undertaken in compliance with the Declaration of Helsinki. The study included patients aged 55 years or older who underwent Lp(a) measurement and CCTA at our university hospital between January 2018 and January 2023. Participants signed written informed consent.

Patients with a history of cardiovascular disease (CVD) were excluded from the study. CVD was defined as a history of myocardial infarction, unstable angina, ≥ 50% stenosis in the epicardial coronary arteries confirmed by prior computed tomography or conventional invasive angiography, ischemia detected on stress imaging, or previous coronary revascularization. Patients receiving statin therapy were also excluded. In addition, individuals with significant arrhythmias, valvular heart disease, cardiomyopathy, or pulmonary heart disease were not included.

In addition, individuals with chronic liver disease, chronic kidney disease with estimated glomerular filtration rate (eGFR) < 45 mL/min/1.73m^2, active cancer or a history of cancer, and women on hormone replacement therapy were not eligible. Considering the effect of Lp(a) on inflammation, patients with signs of acute infection or inflammation [high-sensitivity C-reactive protein (hs-CRP) > 10 mg/L, leukocytosis (white blood cell count > 11 × 10^9 cells/L), fever > 38°C, or antibiotic use] were also excluded.

Data on age, sex, smoking status, the presence of hypertension and diabetes, body mass index (BMI), and laboratory findings including fasting glucose, HbA1c, creatinine, estimated glomerular filtration rate, total cholesterol, low-density lipoprotein cholesterol (LDL-C), triglycerides, high-density lipoprotein cholesterol (HDL-C), and Lp(a) levels were collected. The Modification of Diet in Renal Disease (MDRD) formula was used to calculate eGFR.[5] Hypertension was considered present if

Table 1. Baseline characteristics of study population

Variables	CAC (-) (n = 124)	CAC (+) (n = 186)	P
Age (mean ± SD)	66.96 ± 7.09	68.26 ± 6.78	0.106
Sex (female), n (%)	75 (60.5)	96 (51.6)	0.131
BMI, kg/m^2 (mean ± SD)	28.29 ± 5.54	29.55 ± 5.35	0.068
Smokers, n (%)	40 (32.2)	65 (34.9)	0.627
Hypertension, n (%)	63 (50.8)	121 (65.05)	**0.012**
Diabetes, n (%)	33 (26.6)	66 (35.5)	0.101
eGFR, mL/min/1.73 m^2 (mean ± SD)	83.67 ± 19.95	80.83 ± 20.23	0.232
Glucose, mg/dL (mean ± SD)	112.97 ± 30.95	119.05 ± 40.06	0.165
HbA1C, % (mean ± SD)	6.08 ± 0.81	6.86 ± 5.01	0.211
Total cholesterol, mg/dL (mean ± SD)	201.06 ± 52.78	201.95 ± 55.02	0.887
HDL-C, mg/dL (median, Q1-Q3)*	58 (45-66.5)	51 (42.75-60.25)	**0.041**
LDL-C, mg/dL, mean ± SD	128.88 ± 48.73	130.81 ± 50.43	0.738
Triglycerides, mg/dL (median, Q1-Q3)*	121 (84-175.5)	140 (106-184)	0.118
hsCRP, mg/L (median, Q1-Q3)*	1.9 (1-3.7)	2.1 (1.15-4.8)	0.916
Lp(a), mg/dL (median, Q1-Q3)*	14 (5.25-25.75)	27 (10-52)	**<0.001**
Bone mineral density (mean ± SD)	169.12 ± 51.03	152.86 ± 50.20	**0.009**
Coronary stenosis > 50%	31 (25.00)	77 (41.39)	**0.004**

BMI, Body mass index; CAC, Coronary artery calcification; eGFR, Estimated glomerular filtration rate; HDL-C, High-density lipoprotein cholesterol; hsCRP, High-sensitivity c-reactive protein; LDL-C, Low-density lipoprotein cholesterol; Lp(a), Lipoprotein (a). *Nonparametric analyses were performed due to the absence of a normal distribution.

previously diagnosed or if repeated office blood pressure readings were consistently over 140/90 mmHg. Diabetes was identified based on a prior diagnosis or laboratory findings of fasting glucose ≥ 126 mg/dL or HbA1c ≥ 6.5%. Lp(a) levels were determined by an immunoturbidimetric method using the Roche Cobas Tina-quant Lipoprotein(a) Gen 2 kit in the institution's laboratory.

CCTA images of eligible patients were retrospectively analyzed. Scans were acquired using 64-slice and 128-slice scanners (Somatom Definition AS, Siemens Healthineers) with retrospective electrocardiogram (ECG) gating to synchronize image acquisition with the cardiac cycle. A 70–90 mL dose of intravenous contrast (iopromide) was injected at 4–5 mL/s, then flushed with 40 mL of saline. Bolus tracking was used with a threshold of 100 HU in the ascending aorta. Image reconstruction was performed with a medium-soft tissue kernel, an interval of 0.5 mm, and a slice thickness of 0.75 mm.

CAC was visually assessed based on 18 coronary artery segments, following the American Heart Association (AHA) classification. All scans were independently reviewed by an experienced cardiologist and an experienced radiologist, both blinded to clinical data. Any discrepancies between the readers were resolved by consensus.

Thoracic vertebral bone density was measured on axial bone window images with a slice thickness of 1.5 mm, along with sagittal reformatted images. The seventh thoracic vertebra (T7) was used for the assessment due to its consistent visualization across scans and acceptable distance from the aortic calcification zone. A circular region of interest (ROI) was manually placed in the anterior trabecular part of the vertebral body, avoiding cortical bone and vascular structures.

Statistical analyses were carried out using SPSS version 28.0 (SPSS Inc., Chicago, IL, USA) and GraphPad Prism 10.5.0 (GraphPad Software, San Diego, USA). Propensity score matching was performed to eliminate age and sex differences between the CAC groups. After excluding 56 cases, the analysis continued with a total of 310 age- and sex-matched patients, of whom 124 did not have CAC and 186 had CAC.

The Kolmogorov-Smirnov test was used to evaluate the distribution of continuous variables. If the continuous data were normally distributed, they were presented as mean ± standard deviation (SD); if the distribution was not normal, continuous data were presented as median with interquartile range (IQR). Categorical variables were reported as counts and percentages. Categorical data were compared using the Chi-square test, continuous data with a normal distribution were compared using the Student's t-test, and data without a normal distribution were compared using the Mann–Whitney U test. To identify independent predictors, logistic regression analyses, including both univariate and multivariate, were conducted. Statistical significance was defined as a two-tailed p-value of less than 0.05.

Although bone mineral density was primarily analyzed as a continuous variable, it was also categorized into two groups, low and high BMD, using the cohort mean value of 173 as the cutoff, to allow for analyses requiring categorical variables. Similarly, although Lp(a) was mainly treated as a continuous variable, to evaluate the potential effects of commonly used Lp(a) thresholds recommended by the European Atherosclerosis Society on BMD and arterial calcification, the cohort was further classified into three groups according to Lp(a) levels: ≤ 30 mg/dL, > 30 and < 50 mg/dL, and ≥ 50 mg/dL.[14]

Table 2. Independent predictors of coronary artery calcification (CAC)

Variables	OR	95% CI	P
Model 1			
Hypertension	1.461	0.858–2.489	0.163
HDL-C	0.976	0.960–0.993	0.004
Lp(a)	1.017	1.007–1.028	<0.001
Bone mineral density	0.996	0.991–1.001	0.149
Model 2			
Hypertension	1.49	0.863–2.574	0.152
HDL-C	0.983	0.966–0.999	0.043
Lp(a)	1.013	1.003–1.024	0.012
Bone mineral density	0.996	0.991–1.001	0.141
Coronary stenosis > 50%	3.537	1.765–7.088	<0.001

OR, Odd ratios; CI, Confidence interval; HDL-C, High-density lipoprotein cholesterol; Lp(a), Lipoprotein (a).

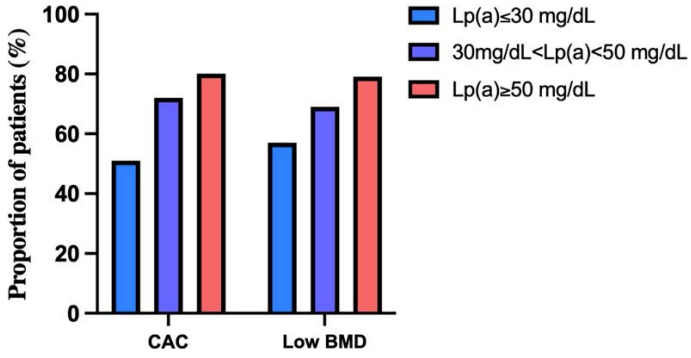

Figure 1. Proportions of patients with coronary artery calcification (CAC) and low bone mineral density (BMD) across Lp(a) categories. Patients were stratified into three groups based on guideline-recommended Lp(a) thresholds: ≤ 30 mg/dL, 30–49 mg/dL, and ≥ 50 mg/dL. The prevalence of CAC and low BMD increased with higher Lp(a) levels.

Results

Following propensity score matching, the baseline characteristics of patients with and without CAC were compared (Table 1). Among the age- and sex-matched cohort, patients with CAC had a higher prevalence of hypertension (65.1% vs. 50.8%, P = 0.012), coronary stenosis > 50% (41.4% vs. 25.0%, P = 0.004) compared to those without CAC. Additionally, HDL-C levels were significantly lower [51 mg/dL (Q1-Q3: 42.75–60.25) vs. 58 mg/dL (Q1-Q3: 41–64), P = 0.041], and median Lp(a) levels were significantly elevated in patients with CAC [27 mg/dL (Q1-Q3: 10–52) vs. 14 mg/dL (Q1-Q3: 5.25–25.75) P < 0.001]. Furthermore, BMD was significantly lower in the CAC group compared to the non-CAC group (152.86 ± 50.20 vs. 169.12 ± 51.03, P = 0.009).

Independent predictors of CAC were identified using multivariate logistic regression analysis across two models (Table 2). In the first model, variables that were statistically significant in the univariate analysis, excluding coronary stenosis > 50%, were included. Higher Lp(a) levels (odds ratio [OR]: 1.017; 95% confidence interval [CI]: 1.007–1.028; P < 0.001) and lower HDL-C levels (OR: 0.976; 95% CI: 0.960–0.993; P = 0.004) were independently associated with CAC. In contrast, hypertension and BMD were not independently associated with CAC in this model. In the second model, coronary stenosis > 50% was added to the regression analysis. Lp(a) levels (OR: 1.013; 95% CI: 1.003–1.024; P = 0.012), lower HDL-C levels (OR: 0.983; 95% CI: 0.966–0.999; P = 0.043), and the presence of significant coronary stenosis (OR: 3.537; 95% CI: 1.765–7.088; P < 0.001) continued to show an independent association with CAC. Similar to the first model, hypertension and BMD did not show significant associations. Correlation analysis was performed between BMD and lipoprotein levels. BMD was not significantly correlated with LDL-C, HDL-C, triglycerides, or total cholesterol. However, a weak but statistically significant negative correlation was observed between BMD and Lp(a) levels (r = -0.136, P = 0.020). Patients were stratified into two groups based on the mean BMD of the cohort (173 HFU). While total cholesterol, HDL-C, LDL-C, and triglyceride levels did not differ significantly between the groups, Lp(a) levels were significantly higher in the low BMD group [24.00 (8.00–48.00) vs. 14.00 (6.00–34.50) mg/dL, p = 0.006]. A comparison of other characteristics is presented in Appendix 1. In addition, Lp(a) level was identified as an independent predictor of low BMD after adjustment for age and sex (OR: 1.010; 95% CI: 1.001–1.019).

When patients were classified based on guideline-recommended Lp(a) cut-off levels, the highest proportions of CAC (80.3%) and low BMD (79.3%) were in the group with Lp(a) ≥ 50 mg/dL. This was followed by the group with Lp(a) between 30 and 50 mg/dL, in which 72% had CAC and 69% had low BMD. The lowest proportions were seen in patients with Lp(a) ≤ 30 mg/dL, where 51% had CAC and 57.8% had low BMD (Figure 1). Mean BMD was highest in patients with Lp(a) ≤ 30 mg/dL (167.0 HFU), and significantly lower in those with Lp(a) between 30–49 mg/dL (144.5 HFU, P = 0.015) and Lp(a) ≥ 50 mg/dL (140.3 HFU, P = 0.001) (Figure 2). BMD was not significantly different between the 30–49 mg/dL and ≥ 50 mg/dL groups (P = 0.902).

Discussion

In this study of statin-naive individuals aged 55 years and older, patients with CAC were found to have lower HDL-C levels and higher Lp(a) levels. Both low HDL-C and elevated Lp(a) remained independent predictors of CAC, even after adjusting for coronary stenosis > 50%. We also demonstrated that low BMD was associated with elevated Lp(a) in our cohort. Furthermore, patients with Lp(a) ≥ 50 mg/dL had the highest prevalence of CAC and the lowest mean BMD, suggesting a potential shared mechanism linking Lp(a) with both vascular and skeletal pathology.

To minimize the influence of potential confounders, we restricted our analysis to individuals aged ≥ 55 years, an age group in which both osteoporosis and vascular calcification become more common. Furthermore, Lp(a) levels are known to rise following menopause in women, which may have contributed to the associations observed.[15] Statin users were excluded from the study, as statins may accelerate CAC independent of their lipid-lowering effect, potentially biasing the assessment of calcification severity.[16]

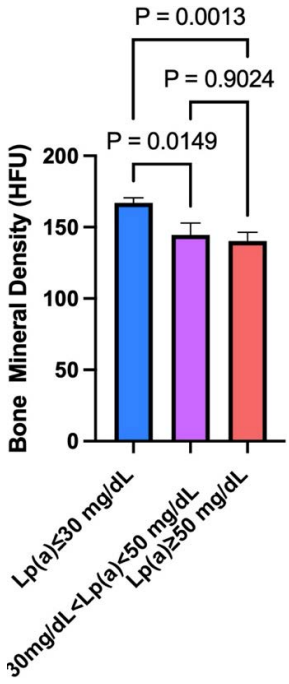

Figure 2. Mean bone mineral density (BMD) across Lp(a) categories. Patients were stratified into three groups based on Lp(a) levels: ≤ 30 mg/dL, 30–49 mg/dL, and ≥ 50 mg/dL. A trend toward lower BMD was observed with increasing Lp(a) levels.

CAC is associated with advanced atherosclerosis and increased cardiovascular risk; therefore, identifying factors related to CAC is crucial for developing effective prevention strategies. The role of Lp(a) in atherosclerosis and degenerative aortic stenosis is well established, and numerous observational studies and meta-analyses support the contribution of Lp(a) to the progression of CAC.[9,14,17] Consistent with these findings, our study demonstrated that Lp(a) levels were significantly higher in patients with CAC, and Lp(a) was found to be independently associated with CAC. In contrast, a recent prospective study did not find a significant relationship between Lp(a) and CAC.[10] While the prospective design is valuable for exploring causal relationships, certain limitations, particularly the relatively young mean age of participants (around 40 years) and the short follow-up period (3–5 years), may have hindered the ability to capture the long-term effects of Lp(a) on vascular calcification. Further longitudinal studies involving older populations and longer follow-up durations are needed to definitively assess the contribution of Lp(a) to CAC. We also demonstrated that HDL-C levels were lower in the CAC group and that low HDL-C was an independent predictor of CAC. This finding aligns with the well-established role of low HDL-C as a cardiovascular risk enhancer. Numerous studies have investigated the relationship between lipid parameters and CAC. While some have reported an association between low HDL-C levels and increased CAC, others have failed to confirm this relationship or have suggested a U-shaped association instead.[18–20] These discrepancies may be attributed to differences in HDL-C subfractions and the functional properties of HDL particles.[21]

Osteoporosis and vascular calcification are increasingly recognized as interrelated conditions that share common pathophysiological mechanisms. These mechanisms may promote both osteoclast-mediated bone resorption and vascular smooth muscle cells' osteogenic differentiation, thereby contributing to bone loss and vascular calcification.[4] In line with this concept, the impact of atherogenic risk factors associated with vascular calcification on bone density and osteoporosis, particularly the influence of lipid parameters, has been investigated in numerous studies. In agreement with our findings, Pliatsika et al.[12] reported a relationship between high Lp(a) levels and low BMD. However, a UK Biobank study did not demonstrate a consistent association between Lp(a) levels and osteoporotic fractures; instead, it identified Lp(a) as a potential risk enhancer for osteoporosis only during the one-year follow-up period.[22] Similarly, Haring et al.[13] reported no significant difference in BMD prevalence across Lp(a) quintiles in postmenopausal women. In contrast, our study demonstrated that in women aged ≥ 55 years, the prevalence of low BMD increased progressively across Lp(a) strata (26.7%, 30.3%, and 52.3%, respectively; P = 0.010). The discrepancies among these studies may be attributed to differences in cohort characteristics, genetic backgrounds, and the Lp(a) cut-off values used for classification. Nevertheless, the stepwise increase in both CAC and low BMD prevalence across ascending Lp(a) strata in our cohort further supports the potential value of Lp(a) as a shared biomarker. Notably, patients with Lp(a) ≥ 50 mg/dL, a threshold recommended by the European Atherosclerosis Society for enhanced cardiovascular risk, had both the highest CAC prevalence and the lowest BMD, suggesting that Lp(a) elevation may serve as a useful marker to prompt further cardiovascular and osteoporosis screening. Furthermore, despite the clear association between CAC and lower BMD in univariate analysis, BMD was not identified as an independent predictor of CAC in multivariate models. This may be due to the confounding influence of Lp(a), a shared risk factor included in the model.

Our study has several strengths, including the use of a well-defined cohort with comprehensive imaging and laboratory assessments, and adjustment for potential confounders through propensity score matching. However, it also has limitations. A cross-sectional design prevents establishing causality and the use of a single Lp(a) measurement does not reflect long-term exposure or variability. Additionally, BMD assessment was performed opportunistically from non-dedicated CT scans, which, although practical, may not accurately capture fracture risk.

Conclusion

In conclusion, our study demonstrates that elevated Lp(a) levels are associated with both coronary artery calcification and lower bone mineral density in a Turkish cohort aged ≥ 55 years, suggesting that Lp(a) may play a dual role in promoting both vascular and skeletal deterioration. Further prospective, longitudinal studies will clarify causality and explore whether Lp(a)-lowering interventions may simultaneously reduce cardiovascular and osteoporotic risk.

Ethics Committee Approval: Ethics committee approval was obtained from Ethics Committee of Koç University School of Medicine (Approval Number: 2025.222.IRB2.102, Date: 15.05.2025).

Informed Consent: Participants signed written informed consent.

Conflict of Interest: The authors have no conflicts of interest to declare.

Funding: The authors declared that this study received no financial support.

Use of AI for Writing Assistance: Artificial intelligence tools were not used in the study or in the preparation of the article.

Author Contributions: Concept – E.Y.; Design – E.Y., K.Ç.A.; Supervision – K.B., S.A., V.A.; Resource – E.G., K.B.; Materials – E.G., K.B., V.A.; Data Collection and/or Processing – G.T.Y., G.Y., N.B.; Analysis and/or Interpretation – E.Y., G.T.Y.; Literature Review – E.Y., G.Y., N.B.; Writing – E.Y.; Critical Review – S.A., V.A.

Peer-review: Externally peer-reviewed.

References

1. Chen NX, Moe SM. Vascular calcification: pathophysiology and risk factors. *Curr Hypertens Rep*. 2012;14(3):228–237. [CrossRef]
2. Lee SJ, Lee IK, Jeon JH. Vascular Calcification-New Insights Into Its Mechanism. *Int J Mol Sci*. 2020 Apr 13;21(8):2685. [CrossRef]
3. Onnis C, Virmani R, Kawai K, et al. Coronary Artery Calcification: Current Concepts and Clinical Implications. *Circulation*. 2024;149(3):251–266. [CrossRef]
4. Sun Y, Huang D, Zhang Y. The bone-vascular axis: the link between osteoporosis and vascular calcification. *Mol Cell Biochem*. 2025;480(6):3413–3427. [CrossRef]
5. Manubolu VS, Mao S, Kinninger A, et al. Association between coronary artery calcium and thoracic spine bone mineral density: Multiethnic Study of Atherosclerosis (MESA). *Nutr Metab Cardiovasc Dis*. 2023;33(3):532–540. [CrossRef]
6. Luo J, Wang Q, Liu W, et al. Computed tomography provides a "one-stop-shop" targeted analysis for coronary artery calcification and osteoporosis: a review. *Front Endocrinol (Lausanne)*. 2025;16:1356831. [CrossRef]
7. Patel AP, Wang M, Pirruccello JP, et al. Lp(a) (Lipoprotein[a]) Concentrations and Incident Atherosclerotic Cardiovascular Disease: New Insights From a Large National Biobank. *Arterioscler Thromb Vasc Biol*. 2021;41(1):465–474. [CrossRef]
8. Rogers MA, Atkins SK, Zheng KH, et al. Lipoprotein(a) Induces Vesicular Cardiovascular Calcification Revealed With Single-Extracellular Vesicle Analysis. *Front Cardiovasc Med*. 2022;9:778919. [CrossRef]
9. Martignoni FV, Rl Júnior JE, Marques IR, et al. The association of lipoprotein(a) and coronary artery calcium in asymptomatic patients: a systematic review and meta-analysis. *Eur J Prev Cardiol*. 2024;31(6):732–741. [CrossRef]
10. Sung DE, Rhee EJ, Lee JY, Lee MY, Sung KC. Elevated lipoprotein(a) is not linked to coronary artery calcification incidence or progression. *Eur J Prev Cardiol*. 2025;32(9):746–755. [CrossRef]
11. Kanno Y, Ishisaki A, Kawashita E, et al. Plasminogen/plasmin modulates bone metabolism by regulating the osteoblast and osteoclast function. *J Biol Chem*. 2011;286(11):8952–8960. Erratum in: *J Biol Chem*. 2014;289(22):15154. [CrossRef]
12. Pliatsika P, Antoniou A, Alexandrou A, et al. Serum lipid levels and bone mineral density in Greek postmenopausal women. *Gynecol Endocrinol*. 2012;28(8):655–660. [CrossRef]
13. Haring B, Crandall CJ, Carbone L, et al. Lipoprotein(a) plasma levels, bone mineral density and risk of hip fracture: a post hoc analysis of the Women's Health Initiative, USA. *BMJ Open*. 2019;9(4):e027257. [CrossRef]
14. Kronenberg F, Mora S, Stroes ESG, et al. Lipoprotein(a) in atherosclerotic cardiovascular disease and aortic stenosis: a European Atherosclerosis Society consensus statement. *Eur Heart J*. 2022;43(39):3925–3946. [CrossRef]
15. Derby CA, Crawford SL, Pasternak RC, Sowers M, Sternfeld B, Matthews KA. Lipid changes during the menopause transition in relation to age and weight: the Study of Women's Health Across the Nation. *Am J Epidemiol*. 2009;169(11):1352–1361. [CrossRef]
16. Ngamdu KS, Ghosalkar DS, Chung HE, et al. Long-term statin therapy is associated with severe coronary artery calcification. *PLoS One*. 2023;18(7):e0289111. [CrossRef]
17. Singh SS, van der Toorn JE, Sijbrands EJG, de Rijke YB, Kavousi M, Bos D. Lipoprotein(a) is associated with a larger systemic burden of arterial calcification. *Eur Heart J Cardiovasc Imaging*. 2023;24(8):1102–1109. [CrossRef]
18. Pedrosa JF, Ribeiro ALP, Santana PC, Araújo LF, Barreto SM. Relation of Thoracic Aortic and Coronary Artery Calcium to Cardiovascular Risk Factors (from The Brazilian Longitudinal Study of Adult Health [ELSA-Brazil]). *Am J Cardiol*. 2019;124(11):1655–1661. [CrossRef]
19. Generoso G, Bensenor IM, Santos RD, et al. High-density Lipoprotein-cholesterol Subfractions and Coronary Artery Calcium: The ELSA-Brasil Study. *Arch Med Res*. 2019;50(6):362–367. [CrossRef]
20. Sandesara PB, Mehta A, O'Neal WT, et al. Association of Elevated High-Density Lipoprotein Cholesterol and Particle Concentration With Coronary Artery Calcium: The Multi-Ethnic Study of Atherosclerosis. *Circ Cardiovasc Imaging*. 2020;13(7):e010473. [CrossRef]
21. Rizzo M, Otvos J, Nikolic D, Montalto G, Toth PP, Banach M. Subfractions and subpopulations of HDL: an update. *Curr Med Chem*. 2014;21(25):2881–2891. [CrossRef]
22. Xiong X, Lui DTW, Ju C, et al. Associations of Serum Lipid Traits With Fracture and Osteoporosis: A Prospective Cohort Study From the UK Biobank. *J Cachexia Sarcopenia Muscle*. 2024;15(6):2669–2683. [CrossRef]

Appendix 1. Baseline characteristics stratified by bone mineral density groups

Variables	Lower BMD (≤ 173 HFU) (n = 187)	Higher BMD (≤ 173 HFU) (n = 105)	P
Age (mean± SD)	69.34 ± 6.50	65.25 ± 6.82	**<0.001**
Sex (female) n (%)	123 (65.8%)	41 (39.0%)	**<0.001**
BMI,m^2/ kg (mean± SD)	29.33 ± 5.18	28.56 ± 5.46	0.268
Smokers, n (%)	59 (33.1%)	37 (36.6%)	0.556
Hypertension, n (%)	121 (64.7%)	54 (51.4%)	0.026
Diabetes, n (%)	64 (34.2%)	32 (30.5%)	0.513
eGFR ml/min/1.73 m^2 (mean± SD)	80.86 ± 19.10	85.38 ± 20.85	0.066
Glucose mg/dL (mean± SD)	115.44 ± 36.23	119.10 ± 34.79	0.411
HbA1C, % (mean± SD)	6.78 ± 4.97	6.23 ± 0.98	0.417
Total cholesterol, mg/dL(mean± SD)	203.35 ± 56.61	200.29 ± 49.48	0.646
HDL-C mg/dL (median, Q1-Q3)*	52 (43.75-64)	51.00 (43.00-60.50)	0.402
LDL-C, mg/dL (mean± SD)	131.11 ± 45.24	130.04 ± 51.65	0.859
Triglycerides, mg/dL (median, Q1-Q3)*	137.00 (105.00-184.00)	132.00 (92.50-174.50)	0.266
hsCRP mg/L (median, Q1-Q3)*	2.00 (1.00-4.05)	2.1 (1.10-5.00)	0.565
Lp(a), mg/dL (median, Q1-Q3)*	24.00 (8.00-48.00)	14 (6.00-34.50)	**0.006**
Bone mineral density (mean± SD)	127.21 ± 28.02	212.64 ± 34.75	**<0.001**
CAC (%)	127 (70.2%)	54 (51.9%)	**0.002**

BMD, Bone mineral density; BMI, body mass index; CAC, Coronary artery calcification; eGFR, estimated glomerular filtration rate; HDL-C, high density lipoprotein cholesterol; hsCRP, high sensitive C reactive protein; LDL-C,low density lipoprotein cholesterol; Lp(a), lipoprotein (a). * Nonparametric analyses were performed due to the absence of a normal distribution.

ARCHIVES OF THE TURKISH SOCIETY OF CARDIOLOGY

Official journal of the TURKISH SOCIETY OF CARDIOLOGY

The Hemoglobin, Albumin, Lymphocyte, and Platelet Score as a Simple Blood-Based Predictor of Residual Coronary Disease Burden in Diabetic Patients with Non-ST-Elevation Myocardial Infarction

Diyabetik Non-ST Elevasyonlu Miyokard Enfarktüsü Hastalarında Rezidüel Koroner Hastalık Yükünü Öngörmede Hemoglobin, Albümin, Lenfosit ve Trombosit Skorunun Basit Bir Kan Testi Belirteci Olarak Değeri

ABSTRACT

Objective: Patients with type 2 diabetes mellitus (T2DM) and non-ST-elevation myocardial infarction (NSTEMI) are at increased risk of incomplete revascularization and adverse outcomes. Simple biomarkers to predict residual disease burden and prognosis are clinically valuable. The hemoglobin, albumin, lymphocyte, and platelet (HALP) score reflects inflammation and nutritional status. This study evaluated the association of the HALP score with the residual Synergy Between Percutaneous Coronary Intervention with Taxus and Cardiac Surgery (SYNTAX) score (rSS) and 12-month major adverse cardiovascular events (MACE) in T2DM patients with NSTEMI.

Method: This retrospective study included 210 diabetic patients. Participants were stratified into three groups based on rSS (0, 1–8, > 8). HALP scores were calculated from admission laboratory values, and outcomes were followed for 12 months. Associations between HALP and rSS were assessed using Spearman correlation and multivariable regression. Receiver operating characteristic (ROC) analysis identified a HALP cut-off value for predicting high rSS. The prognostic value for MACE was evaluated using Cox regression and Kaplan-Meier analysis.

Results: HALP scores were significantly lower in patients with rSS > 8 ($P < 0.001$) and were negatively associated with rSS ($\beta = -0.344$, $P < 0.001$). The optimal HALP score cut-off for predicting rSS > 8 was 2.96, with 78% sensitivity and 77% specificity. Patients with HALP ≤ 2.96 had a higher prevalence of rSS > 8 (43.7% vs. 6.5%) and experienced more MACE over 12 months (29.6% vs. 13.7%, $P = 0.005$). In Cox analysis, a low HALP score (≤ 2.96) was an independent predictor of MACE, along with age and C-reactive protein (CRP) levels (hazard ratio = 1.916, $P = 0.045$).

Conclusion: Lower HALP scores are associated with higher residual disease burden and worse outcomes. The HALP score may serve as a practical tool for risk stratification in patients with diabetic NSTEMI.

Keywords: Hemoglobin, albumin, lymphocyte, and platelet score, major adverse cardiovascular events, non-ST-elevation myocardial infarction, residual SYNTAX score, type 2 diabetes mellitus

ÖZET

Amaç: Tip 2 diabetes mellitus (T2DM) ve non-ST elevasyonlu miyokard enfarktüsü (NSTEMI) olan hastalar, yetersiz koroner revaskülarizasyon ve olumsuz klinik sonuçlar açısından artmış risk taşır. Rezidüel hastalık yükünü ve prognozu öngörebilecek basit biyobelirteçlerin belirlenmesi klinik açıdan önemlidir. Hemoglobin, albümin, lenfosit ve trombosit düzeylerine dayanan HALP skoru, inflamasyon ve beslenme durumunu yansıtan yeni bir göstergedir. Bu çalışma, HALP skorunun rezidüel SYNTAX skoru (rSS) ile ilişkisini ve T2DM'li NSTEMI hastalarında 12 aylık majör advers kardiyovasküler olaylar (MACE) üzerindeki prognostik değerini değerlendirmeyi amaçladı.

Yöntem: Bu retrospektif çalışmaya, NSTEMI tanısıyla perkütan koroner girişim (PCI) uygulanan 210 T2DM hastası dahil edildi. Hastalar, rSS değerlerine göre üç gruba ayrıldı (0, 1–8, >8). HALP skorları yatış laboratuvar verilerinden hesaplandı ve hastalar 12 ay boyunca takip edildi. HALP ile rSS arasındaki ilişkiler Spearman korelasyonu ve çok değişkenli regresyon analizi ile

ORIGINAL ARTICLE
KLİNİK ÇALIŞMA

İlke Erbay

Pelin Aladağ

Department of Cardiology, Bülent Ecevit University Faculty of Medicine, Zonguldak

Corresponding author:
İlke Erbay
✉ ilkeerbay@gmail.com

Received: June 24, 2025
Accepted: August 03, 2025

Cite this article as: Erbay İ, Aladağ P. The Hemoglobin, Albumin, Lymphocyte, and Platelet Score as a Simple Blood-Based Predictor of Residual Coronary Disease Burden in Diabetic Patients with Non-ST-Elevation Myocardial Infarction. *Turk Kardiyol Dern Ars.* 2025;53(7):483–491.

DOI: 10.5543/tkda.2025.71080

Copyright@Author(s)
Available online at archivestsc.com.
Content of this journal is licensed under a Creative Commons Attribution – NonCommercial-NoDerivatives 4.0 International License.

değerlendirildi. ROC analizi, yüksek rSS öngörüsü için optimal HALP eşik değerini belirledi. MACE öngörüsüne yönelik analizlerde Cox regresyonu ve Kaplan–Meier yöntemleri kullanıldı.

Bulgular: HALP skoru, rSS > 8 olan hastalarda anlamlı olarak daha düşüktü (P < 0,001). Çok değişkenli doğrusal regresyon analizinde HALP, rSS ile negatif yönde bir ilişki gösterdi (β = –0,344, p<0,001). HALP skoru için 2,96'lık eşik değeri, rSS > 8'i %78 duyarlılık ve %77 özgüllükle öngördü. HALP ≤ 2,96 olan hastalarda, HALP > 2,96 olanlara göre rSS > 8 prevalansı (%43,7 vs. %6,5) ve 12 ay içinde MACE sıklığı (%29,6 vs. %13,7, P = 0,005) daha yüksekti. Cox analizinde düşük HALP skoru (HALP ≤2,96), yaş ve CRP düzeyleriyle birlikte 12 aylık MACE için bağımsız bir öngörücü olarak bulundu (HR=1,916, P = 0,045).

Sonuç: Düşük HALP skorları, daha fazla rezidüel koroner hastalık yükü ve kötü klinik sonuçlarla ilişkili bulunmuştur. HALP skoru, T2DM'li NSTEMI hastalarında risk sınıflandırması için pratik ve erişilebilir bir araç olabilir.

Anahtar Kelimeler: Hemoglobin, albümin, lenfosit ve trombosit skoru, majör kardiyovasküler olaylar, tip 2 diabetes mellitus; non-ST elevasyonlu miyokard enfarktüsü, rezidüel SYNTAX skoru

Cardiovascular diseases (CVDs) remain the leading cause of morbidity and mortality worldwide, despite considerable advances in diagnosis and therapeutic strategies.[1] Among CVDs, coronary artery disease (CAD) is the most common and is often complicated by comorbid conditions such as type 2 diabetes mellitus (T2DM), which significantly worsens clinical outcomes.[2] Non-ST-elevation myocardial infarction (NSTEMI), a common manifestation of acute coronary syndromes, is frequently observed in diabetic patients and is associated with a higher risk of adverse cardiovascular events and poorer long-term prognosis compared to non-diabetic individuals.[3] However, there remains a clinical need for a simple, accessible, and reliable prognostic marker to help predict adverse outcomes in this high-risk population.

In recent years, inflammation- and nutrition-based indices, such as the systemic immune-inflammation index, the prognostic nutrition index, and the C-reactive protein (CRP) to albumin ratio, have been increasingly used to predict clinical outcomes in patients with acute coronary syndromes. These markers reflect the complex interplay between systemic inflammation, immune dysregulation, and nutritional status, which is particularly relevant in patients with diabetes and CAD.[4-7] Among these indices, the hemoglobin, albumin, lymphocyte, and platelet (HALP) score has garnered interest due to its prognostic relevance in systemic diseases.

The HALP score is a novel composite biomarker that reflects both systemic inflammation and nutritional status. Originally investigated in oncology, it has recently been shown to predict adverse outcomes in CVDs.[8] Each of its components has been individually associated with cardiovascular risk. Anemia and hypoalbuminemia, commonly observed in T2DM patients, reflect malnutrition and chronic inflammation and have been independently linked to poor outcomes after myocardial infarction (MI).[9,10] Low lymphocyte counts have been reported to be associated with increased mortality in patients with CAD.[11] In addition, platelet hyperactivity, which is common in diabetic patients, contributes to atherothrombosis and increases vascular inflammation, potentially worsening clinical outcomes in acute coronary syndrome.[12]

While the HALP score reflects systemic inflammation and nutritional status, the anatomical extent of CAD is better assessed using angiographic tools such as the residual Synergy Between Percutaneous Coronary Intervention with Taxus and Cardiac Surgery (SYNTAX) score (rSS). Residual CAD after the index event is a known predictor of poor outcomes, and the rSS is a validated tool used to quantify this burden.[13,14] In addition to anatomical complexity, residual coronary disease may also be influenced by systemic factors such as inflammation and nutritional status.[15] Despite growing recognition of the role of systemic factors in post-MI outcomes, their relationship with residual CAD burden remains unclear in diabetic patients.

The aim of this study was to evaluate the association between the HALP score and the rSS after primary percutaneous coronary intervention (pPCI), as well as to assess its prognostic value in predicting major adverse cardiovascular events (MACE) in patients with T2DM and NSTEMI.

ABBREVIATIONS

AUC	Area under the curve
bSS	Baseline SYNTAX score
CABG	Coronary artery bypass grafting
CAD	Coronary artery disease
CI	Confidence interval
CRP	C-reactive protein
CVD	Cardiovascular disease
DAPT	Dual antiplatelet therapy
GRACE	Global Registry of Acute Coronary Events
HALP	Hemoglobin, albumin, lymphocyte, and platelet score
HbA1c	Glycated hemoglobin
HR	Hazard ratio
IRA	Infarct-related artery
IQR	Interquartile range
LAD	Left anterior descending
LDL-C	Low-density lipoprotein cholesterol
LMCA	Left main coronary artery
MACE	Major adverse cardiovascular events
MI	Myocardial infarction
NSTEMI	Non-ST-elevation myocardial infarction
PCI	Percutaneous coronary intervention
ROC	Receiver operating characteristic
rSS	Residual SYNTAX score
SD	Standard deviation
STEMI	ST-elevation myocardial infarction
T2DM	Type 2 diabetes mellitus

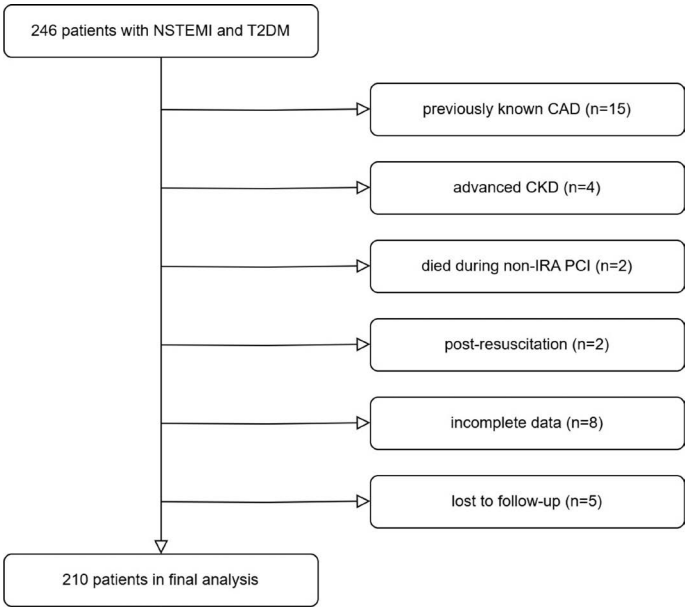

Figure 1. Study flow chart.

CAD, Coronary artery disease; CKD, Chronic kidney disease; IRA, Infarct-related artery; NSTEMI, Non–ST-segment elevation myocardial infarction; PCI, Percutaneous coronary intervention; T2DM, Type 2 diabetes mellitus.

Materials and Methods

Study Design and Population

This retrospective observational study included 246 consecutive patients with a diagnosis of NSTEMI and a known history of T2DM who were admitted to the emergency department of Bülent Ecevit University Hospital and underwent pPCI between January 2022 and January 2024.

Patients were excluded if they had a known history of CAD, active or chronic inflammatory disorders, hematologic malignancies, severe hepatic or renal dysfunction, ongoing chemotherapy or immunosuppressive therapy, chronic glucocorticoid use, cardiogenic shock, cardiopulmonary arrest requiring resuscitation, pregnancy, use of thrombolytic agents, referral for emergency coronary artery bypass grafting (CABG) surgery, underwent surgical revascularization during follow-up, or had missing data, including blood count parameters. After applying these exclusion criteria, 210 patients were included in the final analysis (Figure 1).

Baseline demographic, clinical, and laboratory data were retrospectively collected from the hospital's electronic medical records. The HALP score was calculated using complete blood count and biochemical parameters. All patients were followed for 12 months after discharge for the occurrence of clinical outcomes.

Laboratory Measurements and HALP Score Calculation

Hemoglobin, lymphocyte, and platelet counts were measured using an automated hematology analyzer (UniCel DxH 800, Beckman Coulter, USA), and serum albumin levels were measured using standard automated biochemistry analyzers available in the hospital laboratory. Blood samples for these measurements were obtained on the day of admission, prior to coronary angiography. The HALP score was calculated using the following formula:

HALP = hemoglobin (g/L) × albumin (g/L) × lymphocyte count (10^3/μL) / platelet count (10^3/μL).

Angiographic Evaluation and Percutaneous Coronary Intervention

All patients underwent coronary angiography via the femoral or radial artery upon admission. In accordance with current guidelines for NSTEMI, routine pre-angiography loading with dual antiplatelet therapy (DAPT) was not performed. Instead, 300 mg of acetylsalicylic acid and a loading dose of either 600 mg clopidogrel or 180 mg ticagrelor were administered during or immediately after the procedure, based on the revascularization strategy and clinical judgment.[16] Unfractionated heparin was administered intravenously during the procedure at a dose of 70–100 U/kg, with additional doses given as needed to maintain adequate anticoagulation. Primary percutaneous coronary intervention was performed based on angiographic findings, targeting only the culprit lesion or lesions deemed responsible for the acute presentation. Treatment involved either balloon angioplasty alone or drug-eluting stent implantation, according to the operator's discretion and lesion characteristics.

Definitions

Non-ST-elevation myocardial infarction was defined as chest pain or angina-equivalent symptoms without persistent ST-segment elevation on electrocardiography, accompanied by elevated cardiac troponin levels above the 99th percentile upper reference limit, with a dynamic change indicative of acute myocardial injury.[16]

The baseline SYNTAX score (bSS) and rSS were calculated by summing the individual scores of all coronary lesions with ≥ 50% diameter stenosis in vessels measuring at least 1.5 mm. Residual SYNTAX scores were classified as follows: a score of 0 indicated complete revascularization; scores of 1–8 were defined as low-to-moderate residual disease burden; and scores greater than 8 were considered high residual disease burden, as previously described.[17] All angiographic variables relevant to the bSS and rSS were assessed by two experienced cardiologists trained in SYNTAX scoring, who were blinded to procedural data and clinical outcomes. In case of disagreement, the final score was determined by consensus.

In our study, rSS was calculated after infarct-related artery (IRA) revascularization and, when applicable, following any additional non-IRA PCI procedures performed prior to discharge. If no further revascularization was planned after discharge, the same rSS value was used for follow-up analysis. In patients who underwent staged PCI on non-IRA vessels after discharge, the final rSS was recalculated based on the most recent angiographic procedure and used to assess follow-up outcomes. These elective interventions were typically performed within 10 to 30 days after the index procedure. In total, 35.2% (n = 74) of patients underwent staged PCI either during hospitalization or within the early post-discharge period.

Type 2 diabetes mellitus was defined as a prior diagnosis of diabetes treated with oral hypoglycemic agents and/or insulin, or based on laboratory criteria at admission: random plasma glucose ≥ 200 mg/dL or glycated hemoglobin (HbA1c) ≥ 6.5%.[18] Hypertension was defined as a prior diagnosis of hypertension,

use of antihypertensive medications, or a systolic blood pressure ≥ 140 mmHg and/or diastolic blood pressure ≥ 90 mmHg. Hyperlipidemia was defined as a known diagnosis of dyslipidemia, use of lipid-lowering therapy, or total cholesterol ≥ 200 mg/dL, low-density lipoprotein cholesterol (LDL-C) ≥ 130 mg/dL, or triglycerides ≥ 150 mg/dL. Smoking was defined as current smoking or a history of smoking with a cumulative exposure of at least 10 pack-years, regardless of current status.

Follow-up and Outcomes

Follow-up began after completion of the full revascularization strategy, including staged PCI procedures when applicable. For patients who did not undergo further intervention after discharge, follow-up was initiated at the time of hospital discharge. All patients were followed for 12 months to assess the occurrence of MACE.

The primary outcome was the occurrence of MACE, defined as a composite of all-cause mortality and non-fatal myocardial infarction during the follow-up period. Outcome data were obtained retrospectively through review of hospital records, outpatient follow-up notes, and the national electronic health record system when available.

The study protocol was approved by the Ethics Committee of Zonguldak Bülent Ecevit University Non-Interventional Clinical Research Ethics Committee (Approval Number: 2025/10, Date: 21.05.2025), and all procedures were conducted in accordance with the ethical standards of the Declaration of Helsinki. Informed consent was waived due to the retrospective design of the study. The authors confirm that no artificial intelligence (AI)-assisted technologies (such as large language models [LLMs], chatbots, or image generators) were used in the production of this manuscript.

Statistical Analysis

All statistical analyses were performed using IBM SPSS Statistics version 26.0 (IBM Corp., Armonk, NY, USA). The distribution of continuous variables was assessed using the Kolmogorov-Smirnov test. Variables with a normal distribution were expressed as mean ± standard deviation (SD), while those with a non-normal distribution were presented as median with interquartile range (IQR). Categorical variables were reported as frequencies and percentages. Patients were categorized into three groups based on their rSS (rSS = 0, rSS = 1-8, and rSS > 8), and baseline clinical, laboratory, and angiographic characteristics were compared across groups using one-way analysis of variance (ANOVA) or the Kruskal-Wallis test for continuous variables, and the chi-square or Fisher's exact test for categorical variables. To assess the relationship between HALP score and rSS, Spearman correlation analysis was performed. Additionally, multivariable linear regression analysis was conducted to identify independent predictors of rSS, including variables with a p-value < 0.10 in univariable analysis. Receiver operating characteristic (ROC) curve analysis was used to evaluate the performance of the HALP score in predicting high residual coronary disease burden (rSS > 8). The optimal HALP cut-off value of 2.96, determined using the Youden index, was used to stratify patients into two groups (HALP ≤ 2.96 and HALP > 2.96) for further analyses. The prognostic value of the HALP score for predicting 12-month MACE was assessed using Cox proportional hazards regression analysis. Variables with a p-value < 0.10 in univariable analysis were entered into the multivariable model. Kaplan-Meier survival curves were generated according to HALP categories, and survival differences were evaluated using the log-rank test. A two-tailed p-value < 0.05 was considered statistically significant.

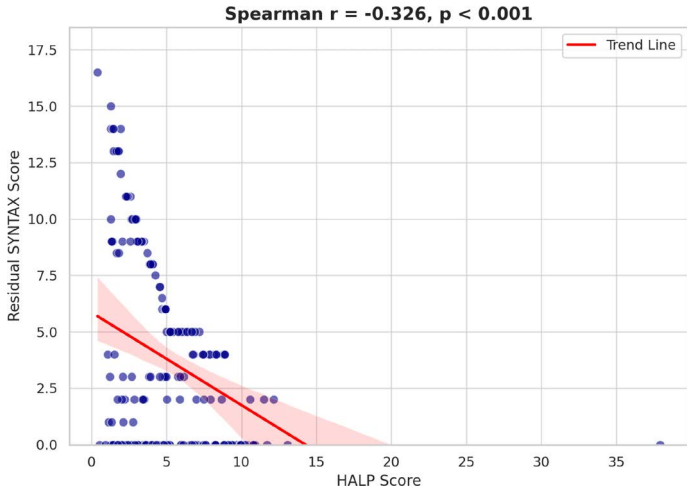

Figure 2. Association between HALP score and residual SYNTAX score.

HALP, Hemoglobin, albumin, lymphocyte, and platelet.

Results

A total of 210 patients with T2DM and NSTEMI were divided into three groups based on rSS: rSS = 0 (n = 86), rSS = 1-8 (n = 84), and rSS > 8 (n = 40). Baseline demographic, clinical, angiographic, and laboratory characteristics according to rSS groups are summarized in Table 1. Patients with rSS > 8 were significantly older and had higher Global Registry of Acute Coronary Events (GRACE) scores (P < 0.001). Angiographically, these patients had higher bSS, more frequent involvement of the left main coronary artery (LMCA) and left anterior descending artery (LAD), and a higher rate of staged PCI (all P < 0.001). Laboratory analyses showed that patients in the rSS > 8 group had significantly lower lymphocyte counts and HALP scores (P = 0.013 and P < 0.001, respectively), as well as higher levels of HbA1c, CRP, and LDL-C (P < 0.001, P = 0.001, and P = 0.006, respectively).

Association Between HALP Score and rSS

Spearman correlation analysis revealed a significant inverse relationship between HALP score and rSS (r = -0.326, P < 0.001) (Figure 2). In the multivariable linear regression analysis, the HALP score was independently associated with rSS (β = -0.344, P < 0.001) (Table 2).

Predictive Performance of the HALP Score for High rSS

ROC curve analysis was performed to evaluate the ability of the HALP score to predict high residual coronary disease burden, defined as rSS > 8. The analysis showed that the HALP score had an area under the curve (AUC) of 0.848 (P < 0.001) for predicting rSS > 8. The optimal cut-off value of HALP 2.96 provided a sensitivity of 78% and a specificity of 77% (Figure 3).

Table 1. Baseline characteristics according to residual synergy between percutaneous coronary intervention with taxus and cardiac surgery (SYNTAX) score groups

	rSS = 0 (n = 86)	rSS = 1–8 (n = 84)	rSS > 8 (n = 40)	P
Age, years	66.0 (59.0–69.3)	62.5 (53.0–69.0)	75.0 (68.0–77.7)	< 0.001
Male sex, n (%)	64 (74.4)	59 (70.2)	23 (57.5)	0.156
BMI, kg/m²	28.1 (26.3–31.9)	28.2 (25.9–30.9)	27.1 (25.0–30.3)	0.249
Smoking status, n (%)	52 (60.5)	42 (50.0)	30 (75.0)	0.028
HT, n (%)	64 (74.4)	55 (65.5)	34 (85.0)	0.067
HL, n (%)	50 (58.1)	53 (63.1)	30 (75.0)	0.188
COPD, n (%)	5 (5.8)	9 (10.7)	7 (17.5)	0.121
History of stroke, n (%)	7 (8.1)	7 (8.3)	1 (2.5)	0.447
CKD, n (%)	20 (23.3)	24 (28.6)	21 (52.5)	0.004
AF, n (%)	8 (9.3)	6 (7.1)	2 (5.0)	0.683
GRACE score	120.8 ± 16.1	124.3 ± 20.4	137.3 ± 23.5	< 0.001
bSS	7.0 (4.7–9.0)	9.5 (7.0–13.0)	18.5 (16.6–20.0)	< 0.001
rSS	0.0 (0.0–0.0)	4.0 (3.0–5.0)	10.0 (9.0–13.0)	< 0.001
HR, beats/min	82.5 ± 11.2	81.8 ± 15.1	78.9 ± 14.9	0.375
Diastolic BP, mmHg	80.6 ± 10.0	77.6 ± 15.6	78.8 ± 10.7	0.306
Systolic BP, mmHg	137.2 ± 19.2	136.2 ± 22.0	139.8 ± 21.2	0.668
Killip class				0.017
Class I, n (%)	80 (93.0)	74 (88.1)	29 (72.5)	
Class II, n (%)	6 (7.0)	9 (10.7)	8 (20.0)	
Class III, n (%)	0 (0.0)	1 (1.2)	3 (7.5)	
Infarct-related artery involvement				
LMCA, n (%)	0 (0.0)	0 (0.0)	2 (5.0)	0.014
LAD and/or its branches, n (%)	40 (46.5)	26 (31.0)	23 (57.5)	0.007
Cx and/or its branches, n (%)	27 (31.4)	20 (23.8)	5 (12.5)	0.071
RCA and/or its branches, n (%)	19 (22.1)	38 (45.2)	12 (30.0)	0.108
Other affected vessels				
LMCA, n (%)	0 (0.0)	1 (1.2)	4 (10.0)	< 0.001
LAD and/or its branches, n (%)	0 (0.0)	25 (29.8)	7 (17.5)	0.008
Cx and/or its branches, n (%)	0 (0.0)	33 (39.3)	17 (42.5)	< 0.001
RCA and/or its branches, n (%)	0 (0.0)	18 (21.4)	12 (30.0)	< 0.001
PCI performed at different time, n (%)	0 (0.0)	46 (54.8)	28 (70.0)	< 0.001
LVEF, %	50.0 (45.7–55.0)	50.0 (45.0–55.0)	48.0 (42.0–50.0)	0.006
LV-EDD, mm	50.0 (47.0–53.0)	50.5 (48.0–55.0)	50.0 (45.0–52.7)	0.157
LA, mm	39.0 (36.0–41.0)	39.0 (36.2–41.0)	38.5 (37.0–41.0)	0.630
Hemoglobin, g/dL	13.3 ± 2.0	13.4 ± 1.6	12.9 ± 1.8	0.304
RBC, $\times 10^6$/μL	4.6 ± 0.5	4.5 ± 0.6	4.6 ± 0.6	0.517
WBC, $\times 10^3$/μL	8.6 (7.1–11.4)	8.3 (7.0–10.6)	8.8 (7.0–11.1)	0.754
Neutrophil, $\times 10^3$/μL	5.9 (4.6–8.9)	5.7 (4.6–8.9)	5.7 (4.4–7.7)	0.843
Lymphocyte, $\times 10^3$/μL	1.7 (1.2–2.4)	1.7 (1.4–2.3)	1.4 (1.0–1.7)	0.013
Monocyte, $\times 10^3$/μL	0.6 (0.4–0.7)	0.5 (0.4–0.7)	0.6 (0.5–0.8)	0.418
Platelet, $\times 10^3$/μL	228.0 (175.0–278.2)	230.0 (188.2–265.5)	233.5 (192.5–270.7)	0.795
Albumin, g/dL	41.0 (39.0–43.2)	41.0 (39.0–44.0)	41.0 (40.0–43.0)	0.686
HALP score	4.9 (2.4–9.0)	5.0 (3.9–6.8)	2.3 (1.5–2.9)	< 0.001
Creatinine, mg/dL	0.9 (0.8–1.1)	1.0 (0.9–1.2)	1.1 (0.8–1.6)	0.023

Table 1 (cont). Baseline characteristics according to residual synergy between percutaneous coronary intervention with taxus and cardiac surgery (SYNTAX) score groups

	rSS = 0 (n = 86)	rSS = 1–8 (n = 84)	rSS > 8 (n = 40)	P
eGFR, mL/min/1.73 m²	72.3 ± 14.1	68.6 ± 14.6	64.9 ± 17.7	0.033
Glucose, mg/dL	155.5 (118.7–225.7)	167.0 (122.2–240.2)	230.0 (131.2–293.0)	0.043
HbA1c, %	7.6 (6.8–9.1)	8.1 (6.9–9.7)	9.4 (8.4–10.6)	<0.001
CRP, mg/L	4.0 (2.0–7.0)	4.8 (2.3–10.5)	9.3 (4.2–16.5)	0.001
ALT, U/L	21.5 (15.0–31.2)	19.5 (14.0–29.0)	18.0 (12.0–26.7)	0.158
Total cholesterol, mg/dL	202.5 ± 39.4	202.1 ± 42.5	221.9 ± 45.8	0.030
Non-HDL cholesterol, mg/dL	143.4 ± 43.2	145.8 ± 44.1	172.7 ± 48.7	0.002
LDL, mg/dL	126.0 ± 31.3	132.7 ± 36.8	147.8 ± 39.8	0.006
HDL, mg/dL	40.0 (35.0–46.0)	38.5 (34.0–45.7)	39.5 (34.2–44.7)	0.894
TG, mg/dL	157.0 (107.7–213.5)	135.5 (92.5–233.0)	187.0 (155.5–287.7)	0.003

AF, Atrial fibrillation; ALT, Alanine aminotransferase; BMI, Body mass index; BP, Blood pressure; bSS, Baseline SYNTAX score; CKD, Chronic kidney disease; COPD, Chronic obstructive pulmonary disease; CRP, C-Reactive protein; Cx, Circumflex artery; eGFR, Estimated glomerular filtration rate; GRACE, Global registry of acute coronary events; HbA1c, Hemoglobin A1c; HDL, High-density lipoprotein; HL, Hyperlipidemia; HR, Heart rate; HT, Hypertension; LA, Left atrial diameter; LAD, Left anterior descending artery; LDL, Low-density lipoprotein; LV-EDD, Left ventricular end-diastolic diameter; LVEF, Left ventricular ejection fraction; Non-HDL, Non-high-density lipoprotein; PCI, Percutaneous coronary intervention; RBC, Red blood cell count; RCA, Right coronary artery; rSS, Residual SYNTAX score; TG, Triglycerides; WBC, White blood cell count.

Table 2. Multivariable linear regression analysis for predictors of residual synergy between percutaneous coronary intervention with taxus and cardiac surgery (SYNTAX) score

	Beta coefficient	95% CI	P
Age, years	0.049	0.003–0.095	0.037
Male sex¶	0.114	-1.068–1.296	0.849
HT¶	0.732	-0.470–1.933	0.231
CRP, mg/L	0.062	0.012–0.112	0.016
LVEF, %	-0.042	-0.122–0.039	0.305
eGFR, mL/min/1.73 m²	-0.020	-0.056–0.016	0.277
HbA1c, %	0.422	0.136–0.708	0.004
HALP score	-0.344	-0.488– -0.201	< 0.001

Model R^2 = 0.249; Adjusted R^2 = 0.219. ¶: Retained in the model due to clinical relevance despite non-significance. Other variables with P < 0.10 in univariate analysis were included in the multivariate model. CI, Confidence interval; CRP, C-Reactive protein; eGFR, Estimated glomerular filtration rate; HALP, Hemoglobin, albumin, lymphocyte, and platelet score; HbA1c, Glycated hemoglobin; HT, Hypertension; LVEF, Left ventricular ejection fraction.

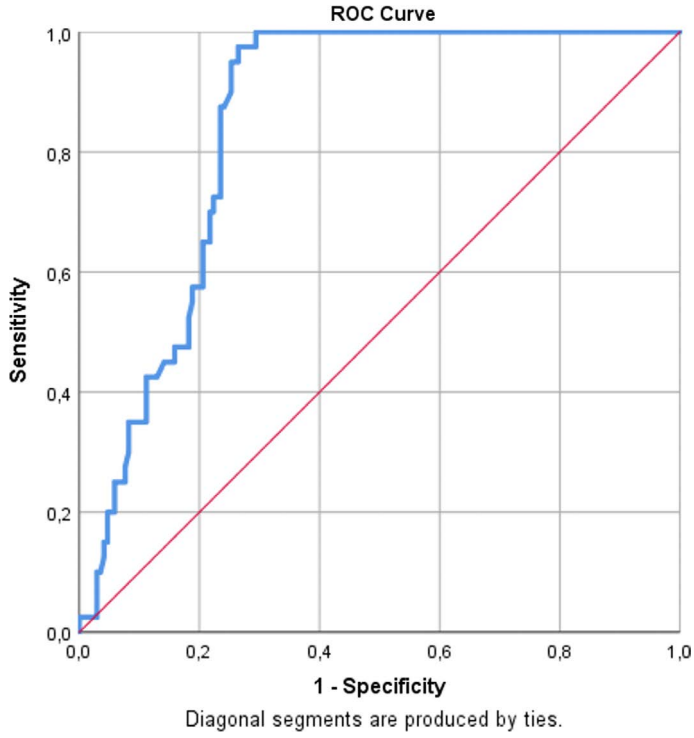

Figure 3. ROC curve analysis of the HALP score for predicting residual SYNTAX score > 8. At the optimal cut-off value of HALP < 2.96, the AUC was 0.848, with a sensitivity of 78%, specificity of 77% (95% CI: 0.802–0.901, P < 0.001).

AUC, Area under the curve; HALP, Hemoglobin, albumin, lymphocyte, and platelet; ROC, Receiver operating characteristic.

Clinical Outcomes According to HALP Score

Based on the ROC-derived cut-off, patients were categorized into two groups: HALP > 2.96 (n = 139) and HALP ≤ 2.96 (n = 71). As shown in Table 3, the proportion of patients with rSS > 8 was significantly higher in the HALP ≤ 2.96 group (43.7% vs. 6.5%, P < 0.001). During the 12-month follow-up, MACE occurred more frequently in the low HALP group (29.6% vs. 13.7%, P = 0.005). Non-fatal MI was also more common (15.5% vs. 6.5%, P = 0.035), while the difference in all-cause mortality was not statistically significant (14.2% vs. 7.1%, P = 0.108).

Prognostic Value of HALP Score for 12-Month Outcome

According to univariate Cox regression analysis, age, CRP level, rSS > 8, HALP ≤ 2.96, and the presence of an LMCA lesion were all significantly associated with MACE. In the multivariable model, HALP ≤ 2.96 remained an independent predictor of MACE (hazard ratio [HR] = 1.916, 95% confidence interval [CI]: 1.013–3.621, P = 0.045), along with age (HR = 1.036, P = 0.026) and CRP (HR = 1.026, P = 0.011) (Table 4).

Table 3. Comparison of residual synergy between percutaneous coronary intervention with taxus and cardiac surgery (SYNTAX) score and clinical outcomes based on receiver operating characteristic (ROC)-derived hemoglobin, albumin, lymphocyte, and platelet (HALP) score cut-off

	HALP score > 2.96 (n = 139)	HALP score ≤ 2.96 (n = 71)	P
rSS group, n (%)			< 0.001
rSS = 0	59 (42.4)	27 (38.0)	
rSS = 1-8	71 (51.1)	13 (18.3)	
rSS > 8	9 (6.5)	31 (43.7)	
Non-fatal MI, n (%)	9 (6.5)	11 (15.5)	0.035
All-cause mortality, n (%)	10 (7.1)	10 (14.2)	0.108
MACE*, n (%)	19 (13.7)	21 (29.6)	0.005

*MACE was defined as a composite of non-fatal myocardial infarction and all-cause mortality. HALP, Hemoglobin, albumin, lymphocyte, and platelet score; MACE, Major adverse cardiovascular events; MI, Myocardial infarction; ROC, Receiver operating characteristic; rSS, Residual SYNTAX score.

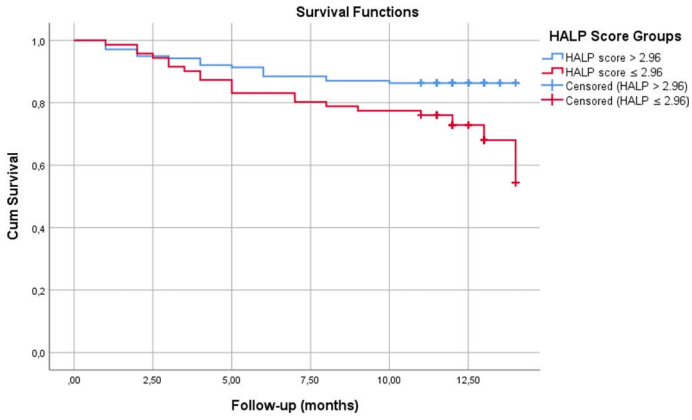

Figure 4. Kaplan-Meier survival curves based on HALP score groups over a 12-month follow-up period. Patients with a HALP score ≤ 2.96 had significantly lower cumulative survival compared to those with a HALP score > 2.96 during the follow-up period (Log-rank test: χ^2=6.951, df=1, P = 0.008).

HALP, Hemoglobin, albumin, lymphocyte, and platelet; Cum Survival, Cumulative survival.

Table 4. Cox regression analysis for determining the risk factors associated with 12-month major adverse cardiovascular events (MACE)

	Univariate analysis		Multivariable analysis	
	HR (95% CI)	P	HR (95% CI)	P
Age, years	1.044 (1.012–1.076)	0.006	1.036 (1.004–1.068)	0.026
Male sex¶	0.823 (0.430–1.577)	0.557		
Smoking	1.878 (0.937–3.762)	0.076		
HT¶	0.949 (0.474–1.901)	0.883		
CRP, mg/L	1.026 (1.007–1.045)	0.006	1.026 (1.006–1.047)	0.011
LVEF, %	0.981 (0.939–1.024)	0.382		
eGFR, mL/min/1.73 m²	0.995 (0.975–1.016)	0.651		
HbA1c, %	1.012 (0.861–1.189)	0.888		
rSS >8	2.844 (1.508–5.363)	0.001		
HALP score ≤ 2.96	2.243 (1.206–4.174)	0.011	1.916 (1.013–3.621)	0.045
LMCA lesion	2.617 (1.094–6.258)	0.031		

The final Cox model had a –2 log likelihood of 411.835. ¶: Included variables had P < 0.10 in univariate analysis or were retained based on clinical relevance. HR, Hazard ratio; CI, Confidence interval; CRP, C-reactive protein; eGFR, Estimated glomerular filtration rate; HALP, Hemoglobin, albumin, lymphocyte, and platelet score; HbA1c, glycated hemoglobin; HT, Hypertension; LMCA, Left main coronary artery; LVEF, Left ventricular ejection fraction; MACE, Major adverse cardiovascular events; rSS, Residual SYNTAX score.

Kaplan-Meier analysis showed a significant difference in cumulative survival between the two HALP groups at 12 months. Patients with HALP ≤ 2.96 had a lower survival rate compared to those with HALP > 2.96 (log-rank test: χ^2 = 6.951, P = 0.008) (Figure 4).

Discussion

This study evaluated the relationship between the HALP score, a composite biomarker reflecting systemic inflammation and nutritional status, and residual coronary disease burden, as measured by the rSS, in patients with T2DM and NSTEMI. Our main findings demonstrated that lower HALP scores were significantly associated with higher rSS values. A HALP score below the ROC-derived threshold of 2.96 independently predicted high residual disease burden (rSS > 8). Furthermore, patients with HALP ≤ 2.96 experienced a significantly higher incidence of MACE over the 12-month follow-up. In multivariable Cox regression analysis, a low HALP score remained an independent predictor of MACE, alongside older age and elevated CRP levels.

The important role of inflammation and nutritional status in the development of diabetes mellitus (DM) and CVD is well established.[19] In patients with T2DM, persistent low-grade inflammation, immune dysregulation, and metabolic disturbances lead to characteristic alterations in hematologic and biochemical parameters.[20-22] Among these, anemia, reflected by low hemoglobin levels, has been associated with increased cardiovascular mortality.[23] Similarly, hypoalbuminemia has been identified as a predictor of adverse cardiovascular outcomes in diabetic patients.[24] Lymphopenia, as also observed in our study

among patients with high rSS (rSS > 8), has been associated with increased cardiovascular risk in individuals with T2DM.[25] Elevated platelet counts, reflecting a prothrombotic and inflammatory state, have also been implicated in the development of atherosclerosis and cardiovascular events in this population.[26]

The HALP score is a novel biomarker that integrates hemoglobin and albumin levels with lymphocyte and platelet counts, reflecting both nutritional and inflammatory status. Although each of these components has been individually associated with cardiovascular outcomes in patients with T2DM, their combined relationship with angiographic disease burden has not previously been investigated in this population.

Recent studies have further highlighted the prognostic value of the HALP score in diabetic populations. Lower HALP scores have been identified as independent risk factors for microvascular complications such as diabetic nephropathy and retinopathy and have shown a negative association with both glomerular filtration rate and retinal vascular damage.[27] More importantly, a large-scale cohort analysis demonstrated that the HALP score was independently and inversely correlated with both all-cause and cardiovascular mortality in individuals with diabetes or prediabetes.[28] In line with these findings, our results showed that patients with higher rSS had significantly lower HALP values, highlighting a possible mechanistic pathway through which systemic metabolic imbalance contributes to incomplete coronary revascularization.

Systemic disturbances in patients with T2DM contribute to vascular dysfunction and progressive atherosclerosis.[29,30] A significant relationship was identified between lower HALP scores and higher rSS, which proved to be robust in multivariable linear regression analysis. Given that the rSS reflects the extent of unrevascularized coronary atherosclerosis, the HALP score may serve as an indirect indicator of diffuse atherosclerotic burden in diabetic patients.

A cut-off value of 2.96 demonstrated the HALP score's ability to distinguish patients with rSS > 8 in our study. A recent study by Ilis et al.[31] also showed that the HALP score had prognostic value in patients with NSTEMI, independent of diabetes status, reporting that a threshold of 2.62 predicted in-hospital mortality. In our study, patients with HALP scores ≤ 2.96 experienced significantly higher rates of non-fatal MI and overall MACE during the 12-month follow-up. Given its previously reported association with in-hospital mortality,[31,32] the HALP score may also be useful in identifying long-term risk in diabetic patients with NSTEMI.

Our multivariable Cox regression analysis showed that the HALP score was an independent predictor of 12-month MACE, while HbA1c was not. This discrepancy may be explained by collinearity, as the HALP score includes hemoglobin and albumin, parameters influenced by both glycemic control and nutritional status. Moreover, markers of inflammation and nutrition may provide prognostic information that extends beyond traditional glycemic metrics in diabetic patients with acute coronary syndromes. A recent meta-analysis by Pan et al.[33] demonstrated that HbA1c was not significantly associated with short-term mortality in diabetic patients with acute coronary syndrome, suggesting that conventional glycemic markers may not fully capture cardiovascular risk in this population.[34] In contrast, composite indices such as the HALP score have been shown to reflect both inflammation and systemic resilience. For example, Liu et al.[35] reported that the HALP score independently predicted no-reflow and long-term MACE in patients with ST-segment elevation myocardial infarction (STEMI), while Zhao et al.[28] found an inverse relationship between HALP and cardiovascular mortality in a large diabetic cohort from the National Health and Nutrition Examination Survey (NHANES) database. These findings support the idea that the HALP score, previously linked to in-hospital mortality in acute coronary syndrome patients, may also help identify diabetic patients with NSTEMI who are at increased risk of long-term adverse cardiovascular outcomes. In our study, this was reflected by a significantly higher incidence of MACE, primarily driven by non-fatal MI.

This study has certain limitations. The data were collected retrospectively, so not all potential confounding factors could be controlled. The results reflect the experience of a single center and may not be generalizable to other clinical settings. The HALP score was calculated only at admission; therefore, we were unable to evaluate changes over time. We included only patients with NSTEMI and T2DM, allowing for a focused analysis but limiting the applicability of the findings to broader populations. Variations in the timing of staged PCI procedures (typically 10 to 30 days post-procedure) may have introduced heterogeneity in rSS calculation. Additionally, follow-up began after PCI procedures for non-IRAs, which may have contributed to variability in follow-up timing. Finally, the strict exclusion criteria, including the absence of previously known CAD, resulted in a more homogeneous but smaller study population.

Conclusion

In patients with NSTEMI and T2DM, lower HALP scores were independently associated with both higher residual coronary disease burden and an increased risk of adverse cardiovascular events. Integrating the HALP score into clinical workflows, alongside tools such as the GRACE score, may offer a practical approach to identifying high-risk diabetic patients with NSTEMI.

Ethics Committee Approval: Ethics committee approval was obtained from Zonguldak Bülent Ecevit University Non-Interventional Clinical Research Ethics Committee (Approval Number: 2025/10, Date: 21.05.2025).

Informed Consent: Informed consent was waived due to the retrospective design of the study.

Conflict of Interest: The authors have no conflicts of interest to declare.

Funding: The authors declared that this study received no financial support.

Use of AI for Writing Assistance: The authors confirm that no artificial intelligence (AI)-assisted technologies (such as large language models [LLMs], chatbots, or image generators) were used in the production of this manuscript.

Author Contributions: Concept – İ.E.; Design – İ.E., P.A.; Supervision – İ.E.; Resource – İ.E., P.A..; Materials – P.A.; Data Collection and/or Processing – İ.E., P.A.; Analysis and/or Interpretation – İ.E.; Literature Review – İ.E., P.A.; Writing – İ.E.; Critical Review – P.A.

Peer-review: Externally peer-reviewed.

References

1. Roth GA, Mensah GA, Johnson CO, et al. Global burden of cardiovascular diseases and risk factors, 1990–2019: Update from the GBD 2019 study. *J Am Coll Cardiol*. 2020;76(25):2982–3021. [CrossRef]
2. Einarson TR, Acs A, Ludwig C, Panton UH. Prevalence of cardiovascular disease in type 2 diabetes: A systematic literature review of scientific evidence from across the world in 2007–2017. *Cardiovasc Diabetol*. 2018;17(1):83. [CrossRef]
3. Skoda R, Nemes A, Bárczi G, et al. Survival of myocardial infarction patients with diabetes mellitus at the invasive era (Results from the városmajor myocardial infarction registry). *J Clin Med*. 2023;12(3):917. [CrossRef]
4. Luo J, Qin X, Zhang X, et al. Prognostic implications of systemic immune-inflammation index in myocardial infarction patients with and without diabetes: Insights from the NOAFCAMI-SH registry. *Cardiovasc Diabetol*. 2024;23(1):41. [CrossRef]
5. Peng Y, Lin A, Luo B, Chen L, Lin Y. The effect of prognostic nutritional index on diabetic patients with myocardial infarction. *Diabetol Metab Syndr*. 2024;16(1):179. [CrossRef]
6. Li T, Yuan D, Wang P, et al. Association of prognostic nutritional index level and diabetes status with the prognosis of coronary artery disease: A cohort study. *Diabetol Metab Syndr*. 2023;15(1):58. [CrossRef]
7. Li J, Zhu P, Li Y, et al. A novel inflammatory biomarker, high-sensitivity C-reactive protein-to-albumin ratio, is associated with 5-year outcomes in patients with type 2 diabetes who undergo percutaneous coronary intervention. *Diabetol Metab Syndr*. 2023;15(1):14. [CrossRef]
8. Pan H, Lin S. Association of hemoglobin, albumin, lymphocyte, and platelet score with risk of cerebrovascular, cardiovascular, and all-cause mortality in the general population: Results from the NHANES 1999–2018. *Front Endocrinol (Lausanne)*. 2023;14:1173399. [CrossRef]
9. Sarnak MJ, Tighiouart H, Manjunath G, et al. Anemia as a risk factor for cardiovascular disease in The Atherosclerosis Risk in Communities (ARIC) study. *J Am Coll Cardiol*. 2002;40(1):27–33. [CrossRef]
10. Oduncu V, Erkol A, Karabay CY, et al. The prognostic value of serum albumin levels on admission in patients with acute ST-segment elevation myocardial infarction undergoing a primary percutaneous coronary intervention. *Coron Artery Dis*. 2013;24(2):88–94. [CrossRef]
11. Ommen SR, Gibbons RJ, Hodge DO, Thomson SP. Usefulness of the lymphocyte concentration as a prognostic marker in coronary artery disease. *Am J Cardiol*. 1997;79(6):812–814. [CrossRef]
12. Angiolillo DJ, Bernardo E, Sabaté M, et al. Impact of platelet reactivity on cardiovascular outcomes in patients with type 2 diabetes mellitus and coronary artery disease. *J Am Coll Cardiol*. 2007;50(16):1541–1547. [CrossRef]
13. Farooq V, Serruys PW, Bourantas CV, et al. Quantification of incomplete revascularization and its association with five-year mortality in the synergy between percutaneous coronary intervention with taxus and cardiac surgery (SYNTAX) trial validation of the residual SYNTAX score. *Circulation*. 2013;128(2):141–151. [CrossRef]
14. Yan L, Li P, Wang Y, et al. Impact of the residual SYNTAX score on clinical outcomes after percutaneous coronary intervention for patients with chronic renal insufficiency. *Catheter Cardiovasc Interv*. 2020;95(Suppl 1):606–615. [CrossRef]
15. Altunova M, Karakayalı M, Kahraman S, et al. Systemic immune-inflammatory index is associated with residual SYNTAX score in patients with ST-segment elevation myocardial infarction. *Anatol J Cardiol*. 2023;27(8):472–478. [CrossRef]
16. Byrne RA, Rossello X, Coughlan JJ, et al. 2023 ESC Guidelines for the management of acute coronary syndromes. *Eur Heart J*. 2023;44(38):3720–3826. [CrossRef]
17. Généreux P, Palmerini T, Caixeta A, et al. Quantification and impact of untreated coronary artery disease after percutaneous coronary intervention: The residual SYNTAX (Synergy Between PCI with Taxus and Cardiac Surgery) score. *J Am Coll Cardiol*. 2012;59(24):2165–2174. [CrossRef]
18. American Diabetes Association Professional Practice Committee. 2. Diagnosis and classification of diabetes: Standards of Care in Diabetes–2024. *Diabetes Care*. 2024;47(Suppl 1):S20–S42. [CrossRef]
19. Zhang J, Fan X, Xu Y, et al. Association between inflammatory biomarkers and mortality in individuals with type 2 diabetes: NHANES 2005–2018. *Diabetes Res Clin Pract*. 2024;209:111575. [CrossRef]
20. Tsalamandris S, Antonopoulos AS, Oikonomou E, et al. The role of inflammation in diabetes: Current concepts and future perspectives. *Eur Cardiol*. 2019;14(1):50–59. [CrossRef]
21. Li H, Zou L, Long Z, Zhan J. Immunometabolic alterations in type 2 diabetes mellitus revealed by single-cell RNA sequencing: Insights into subtypes and therapeutic targets. *Front Immunol*. 2025;15:1537909. [CrossRef]
22. Pellegrini V, La Grotta R, Carreras F, et al. Inflammatory trajectory of type 2 diabetes: Novel opportunities for early and late treatment. *Cells*. 2024;13(19):1662. [CrossRef]
23. Zoppini G, Targher G, Chonchol M, et al. Anaemia, independent of chronic kidney disease, predicts all-cause and cardiovascular mortality in type 2 diabetic patients. *Atherosclerosis*. 2010;210(2):575–580. [CrossRef]
24. Jhund PS, McMurray JJ, Chaturvedi N, et al. Mortality following a cardiovascular or renal event in patients with type 2 diabetes in the ALTITUDE trial. *Eur Heart J*. 2015;36(36):2463–2469. [CrossRef]
25. Zidar DA, Al-Kindi SG, Liu Y, et al. association of lymphopenia with risk of mortality among adults in the US general population. *JAMA Netw Open*. 2019;2(12):e1916526. [CrossRef]
26. Colwell JA, Nesto RW. The platelet in diabetes: Focus on prevention of ischemic events. *Diabetes Care*. 2003;26(7):2181–2188. [CrossRef]
27. Tel BMA, Tel MR, Bilgin S, Duman TT, Aktas G. Diagnostic value of HALP score in detecting diabetic nephropathy in patients with type 2 diabetes mellitus. *Ibnosina J Med Biomed Sci*. 2024;16(3):116–122. [CrossRef]
28. Zhao P, Zhang Z, Li M, Hao J, Wang Y. Association between hemoglobin-albumin-lymphocyte-platelet score and all-cause or cardiovascular mortality in patients with diabetes or prediabetes: Mediated effects of renal function. *BMC Cardiovasc Disord*. 2025;25(1):331. [CrossRef]
29. Wang S, Jia B, Niu S, Chen S. Relationship between the hemoglobin, albumin, lymphocyte count, platelet count (HALP) score and type 2 diabetes retinopathy. *Diabetes Metab Syndr Obes*. 2024;17:2693–2706. [CrossRef]
30. Paneni F, Beckman JA, Creager MA, Cosentino F. Diabetes and vascular disease: Pathophysiology, clinical consequences, and medical therapy: Part I. *Eur Heart J*. 2013;34(31):2436–2443. [CrossRef]
31. Ilis D, Arslan A, Artac I, et al. Prognostic value of HALP score in predicting in-hospital mortality in patients with NSTEMI. *Biomark Med*. 2025;19(5):139–147. [CrossRef]
32. Karakayali M, Omar T, Artac I, et al. The prognostic value of HALP score in predicting in-hospital mortality in patients with ST-elevation myocardial infarction undergoing primary percutaneous coronary intervention. *Coron Artery Dis*. 2023;34(7):483–488. [CrossRef]
33. Pan W, Lu H, Lian B, Liao P, Guo L, Zhang M. Prognostic value of HbA1c for in-hospital and short-term mortality in patients with acute coronary syndrome: A systematic review and meta-analysis. *Cardiovasc Diabetol*. 2019;18(1):169. [CrossRef]
34. Zheng Y, Huang Y, Li H. Hemoglobin albumin lymphocyte and platelet score and all-cause mortality in coronary heart disease: A retrospective cohort study of NHANES database. *Front Cardiovasc Med*. 2023;10:1241217. [CrossRef]
35. Liu H, Zhang F, Li Y, et al. The HALP score predicts no-reflow phenomenon and long-term prognosis in patients with ST-segment elevation myocardial infarction after primary percutaneous coronary intervention. *Coron Artery Dis*. 2025;36(4):273–280. [CrossRef]

ARCHIVES OF THE TURKISH SOCIETY OF CARDIOLOGY

Official journal of the TURKISH SOCIETY OF CARDIOLOGY

Erectile Dysfunction as a Marker of Subclinical Biventricular Diastolic Dysfunction: A Prospective Echocardiographic Study

Subklinik Biventriküler Diyastolik Disfonksiyonun Bir Belirteci Olarak Erektil Disfonksiyon: Prospektif Ekokardiyografik Çalışma

ABSTRACT

Objective: Erectile dysfunction (ED) and cardiovascular disease share common vascular pathologies, particularly endothelial dysfunction and atherosclerosis. Growing evidence indicates that ED may serve as an early indicator of underlying cardiac abnormalities, particularly diastolic dysfunction (DD), even in the absence of clinically apparent cardiovascular disease.

Method: This prospective, single-center study included 87 patients with ED, matched with 53 healthy controls based on age and body mass index. The severity of ED was assessed using the International Index of Erectile Function (IIEF) and categorized as mild, moderate, or severe. Diastolic dysfunction was evaluated according to established guidelines.

Results: Patients with ED exhibited significant impairments in left ventricular diastolic function, including reduced E/A and e′ velocities, prolonged isovolumetric relaxation time (IVRT), and left atrial (LA) enlargement. A correlation was observed between the severity of ED and worsening right ventricular (RV) diastolic indices, specifically reduced RV e′ and elevated RV E/e′ ratios. Notably, LA enlargement and prolonged IVRT emerged as independent predictors of ED.

Conclusion: Erectile dysfunction is independently associated with subclinical biventricular DD, even in the absence of overt cardiovascular disease. Echocardiography may help detect subclinical cardiac dysfunction in men with ED and improve cardiovascular risk assessment.

Keywords: Diastolic dysfunction, erectile dysfunction, transthoracic echocardiography

ÖZET

Amaç: Erektil disfonksiyon (ED) ile kardiyovasküler hastalıklar, özellikle endotel disfonksiyonu ve ateroskleroz gibi benzer vasküler patolojileri paylaşmaktadır. Artan kanıtlar, klinik kardiyovasküler hastalık bulunmasa dahi, ED'nin altta yatan kardiyak anormalliklerin, özellikle diyastolik disfonksiyonun (DD) erken bir belirtisi olabileceğini göstermektedir.

Yöntem: Bu prospektif, tek merkezli çalışmada, yaş ve beden kitle indeksi açısından eşleştirilmiş 87 ED hastası ile 53 sağlıklı birey karşılaştırılmıştır. ED şiddeti, Uluslararası Erektil Fonksiyon İndeksi (IIEF) kullanılarak değerlendirilmiş ve hafif, orta ve ağır ED olarak sınıflandırılmıştır. Diyastolik fonksiyon, kılavuzlara uygun şekilde ekokardiyografi ile değerlendirilmiştir.

Bulgular: ED'li hastalarda sol ventrikül DD'sinde anlamlı bozulmalar gözlenmiştir; bunlar azalmış E/A ve e′ hızları, uzamış interventriküler gevşeme süresi (IVRT) ve sol atriyum (LA) genişlemesi ile karakterizedir. ED şiddetindeki artışla birlikte, sağ ventrikül (RV) diyastolik parametrelerinde bozulmalar (düşük RV e′, artmış RV E/e′ oranı) arasında korelasyon saptanmıştır. Özellikle LA genişlemesi ve IVRT, ED'nin bağımsız belirleyicileri olarak tanımlanmıştır.

Sonuç: ED, belirgin kardiyovasküler hastalık olmasa bile subklinik biventriküler DD ile bağımsız olarak ilişkilidir. ED'li erkeklerde transtorasik ekokardiyografi ile yapılacak değerlendirme, gizli kardiyak disfonksiyonun erken saptanmasına katkı sağlayabilir ve kardiyovasküler risk değerlendirmesini iyileştirebilir.

Anahtar Kelimeler: Diyastolik disfonksiyon, erektil disfonksiyon, transtorasik ekokardiyografi

ORIGINAL ARTICLE
KLİNİK ÇALIŞMA

Vedat Çiçek[1,2]
Serkan Akan[3]
Samet Yavuz[4]
Şahhan Kılıç[5]
Almina Erdem[4]
Mert Babaoğlu[4]
Caner Ediz[6]
Ahmet Öz[7]
Tufan Çınar[8]
Ulaş Bağcı[1]

[1]*Machine and Hybrid Intelligence Laboratory, Department of Radiology, Northwestern University, Chicago, IL, USA*
[2]*Tatvan State Hospital, Bitlis, Türkiye*
[3]*Department of Urology, University of Health Sciences Fatih Sultan Mehmet Training and Research Hospital, Istanbul, Türkiye*
[4]*Department of Cardiology, Sultan II Abdulhamid Han Training and Research Hospital, Health Sciences University, Istanbul, Türkiye*
[5]*Department of Cardiology, Çorlu State Hospital, Tekirdağ, Türkiye*
[6]*Department of Urology, Sultan Abdulhamid Han Training and Research Hospital, Istanbul, Türkiye*
[7]*Department of Cardiology, İstanbul Training and Research Hospital, Istanbul, Türkiye*
[8]*School of Medicine, University of Maryland, Baltimore, USA*

Corresponding author:
Vedat Çiçek
✉ vedatacicek@gmail.com

Received: June 06, 2025
Accepted: July 21, 2025

Cite this article as: Çiçek V, Akan S, Yavuz S, et al. Erectile Dysfunction as a Marker of Subclinical Biventricular Diastolic Dysfunction: A Prospective Echocardiographic Study. *Turk Kardiyol Dern Ars.* 2025;53(7):492–500.

DOI: 10.5543/tkda.2025.95270

Copyright@Author(s)
Available online at archivestsc.com. Content of this journal is licensed under a Creative Commons Attribution – NonCommercial-NoDerivatives 4.0 International License.

Erectile dysfunction (ED) is characterized by the persistent inability to achieve or maintain an erection sufficient for satisfactory sexual activity, affecting nearly one-third of men over the age of 40.[1] There is a notable overlap in the risk factors for

ED and cardiovascular disease (CVD), including advancing age, hypertension, hyperlipidemia, smoking, obesity, and diabetes. These shared risk factors suggest a common underlying vascular pathophysiology, particularly involving endothelial dysfunction and atherosclerosis.[1-3]

While atherosclerosis is a systemic condition, its clinical signs often do not appear simultaneously across different vascular territories, likely due to differences in vessel size.[4] The smaller penile arteries, for instance, which measure 1–2 mm in diameter, may become obstructed earlier and exhibit symptoms sooner than larger arteries, such as the coronary arteries.[5] Additionally, microvascular dysfunction, a hallmark of endothelial impairment, has been strongly associated with left ventricular diastolic dysfunction, an early marker of CVD.[6] However, the specific connection between ED and left ventricular diastolic dysfunction (LV DD) has not been thoroughly investigated.

Accurate evaluation of diastolic function is critical, and echocardiography is the primary non-invasive method for assessing abnormalities in cardiac relaxation.[7] Current guidelines recommend assessing cardiovascular risk in men presenting with ED, even in the absence of overt heart disease. Yet, echocardiographic evaluations are not routinely performed in these patients, despite their potential to reveal subclinical cardiac dysfunction related to endothelial health.[8] Consequently, this study aims to explore the relationship between ED and DD parameters as assessed by echocardiography.

Materials and Methods

Study Design

This was a prospective, single-center study conducted at a regional hospital. All procedures were conducted in accordance with institutional regulations and established clinical guidelines to ensure the integrity of the research. Ethical approval was obtained from University of Health Sciences Istanbul Training and Research Hospital Clinical Research Ethics Committee (Approval Number: 2504, Date: 04.09.2020). Written informed consent was obtained from each participant or their authorized representative prior to enrollment. The research protocol adhered to the ethical principles outlined in the Declaration of Helsinki (1975).

Study Population

Between October 2020 and September 2024, male participants presenting to the urology outpatient clinic with complaints of ED were evaluated for eligibility. Eligible participants were men aged 18 to 65 who reported erectile difficulties in at least 25% of sexual encounters over the previous six months and had maintained a stable sexual partnership for at least one year. Exclusion criteria included a history of significant pelvic surgery, neurological or spinal trauma, poorly controlled diabetes, end-stage renal disease, hormonal disorders such as hypothyroidism or hypogonadism, and a diagnosis of premature ejaculation. Participants with urinary tract stones, infections, malignancies, known cardiac conditions, or cardiac-related symptoms were also excluded. Men using exogenous testosterone or receiving treatment with thiazide diuretics, beta-blockers, or spironolactone were also excluded. While patients with a clinical diagnosis of hypogonadism or other hormonal disorders were excluded, routine measurements of serum total testosterone or gonadal hormones were not performed for all participants. This decision was based on the primary focus of the study being echocardiographic correlates of ED in cardiovascular asymptomatic individuals. A total of 87 eligible participants were assigned to the ED group. The control group consisted of 53 male patients with normal erectile function, presenting with unrelated complaints. Both groups were matched for age and body mass index (BMI). All participants underwent a comprehensive physical examination, including measurements of height, weight, BMI, and blood pressure. To rule out cardiovascular diseases, a standardized cardiovascular assessment was conducted by a cardiologist. This evaluation included a detailed medical history focused on symptoms such as chest pain, dyspnea, palpitations, and syncope; a 12-lead resting electrocardiogram (ECG); and transthoracic echocardiography (TTE) to assess cardiac structure and function, including left ventricular ejection fraction and valvular status. Any participant with abnormal findings suggestive of underlying cardiovascular disease was excluded from the study.

Erectile Dysfunction Evaluation

Erectile function was assessed using the International Index of Erectile Function (IIEF) score, a widely recognized, multidimensional, self-administered questionnaire that thoroughly evaluates male sexual health. The IIEF comprises 15 insightful questions covering five essential domains: erectile function, orgasmic function, sexual desire, intercourse satisfaction, and overall satisfaction. Based on the scores, individuals were categorized into distinct levels of erectile dysfunction: no ED (26–30), mild ED Grade 1 (17–25), moderate ED Grade 2 (11–16), or severe ED Grade 3 (0–10).[9]

Transthoracic Echocardiography

Transthoracic echocardiographic assessments, incorporating advanced two-dimensional and Doppler imaging techniques, were performed by two experienced cardiologists using the Vivid E7 imaging platform (General Electric, USA). Comprehensive evaluations of cardiac chamber dimensions were conducted

ABBREVIATIONS

A	Late diastolic transmitral velocity
BMI	Body mass index
CVD	Cardiovascular disease
DT	Deceleration time
E	Early diastolic transmitral velocity
ECG	Electrocardiogram
ED	Erectile dysfunction
HFpEF	Heart failure with preserved ejection fraction
IIEF	International Index of Erectile Function
IVRT	Isovolumic relaxation time
LA	Left atrial
LAAP	Left atrial anteroposterior diameter
LV DD	Left ventricular diastolic dysfunction
PASP	Pulmonary artery systolic pressure
RA	Right atrial
RV	Right ventricular
TR	Tricuspid regurgitation
TTE	Transthoracic echocardiography

Table 1. Demographic characteristics of the study cohort

	ED (+) (n = 87)	ED (–) (n = 53)	P
ED Grade 1	15 (17.24%)		
ED Grade 2	50 (57.47%)		
ED Grade 3	22 (25.29%)		
Age, years	52 (50.7 ± 10.7)	54 (52.7 ± 10.7)	0.349
Body mass index, kg/m^2	27.1 (28.5 ± 4.8)	26.8 (27.6 ± 4.8)	0.166
Systolic blood pressure, mmHg	130 (129 ± 15.3)	124 (127 ± 15.3)	0.394
Diastolic blood pressure, mmHg	80 (95.1 ± 93.7)	75 (74 ± 93.7)	0.005
Current smokers	56 (64.3%)	1 (2%)	< 0.001
Hypertension	46 (52.8%)	20 (37.7%)	0.082
Diabetes mellitus	29 (33.3%)	6 (11.3%)	1.000
Hyperlipidemia	24 (27.5%)	10 (18.8%)	0.243

ED, Erectile dysfunction.

through standard two-dimensional imaging. Key measurements included left atrial (LA) diameter, area, and volume; right atrial (RA) diameter, area, and volume; and pulmonary artery systolic pressure (PASP). Additionally, Tricuspid Annular Plane Systolic Excursion (TAPSE), as well as left ventricular and right ventricular (RV) diameters, volumes, and global function, along with tricuspid regurgitation (TR) jet velocity, were assessed in strict accordance with the guidelines of the American Society of Echocardiography.[10]

Early (E) and late (A) diastolic mitral inflow velocities were meticulously recorded using pulsed-wave Doppler imaging from the apical four-chamber view. To accurately assess diastolic performance, tissue Doppler imaging was employed to quantify early diastolic (e′) velocities at both the lateral and septal regions of the mitral annulus. The e′ velocity, along with the E/e′ ratio, served as powerful indicators of diastolic function, offering critical insights into left ventricular filling pressures and overall diastolic efficiency.[11]

Statistical Analysis

All statistical analyses were conducted using Jamovi software (version 2.6.22; The Jamovi Project, Sydney, Australia), with a two-tailed significance level set at $P < 0.05$. The Kolmogorov-Smirnov test was used to evaluate the normal distribution of continuous data. As the data were not normally distributed, the Mann-Whitney U test was applied to compare two independent groups. For comparisons involving more than two groups, the Kruskal-Wallis test was used, followed by the Dwass-Steel-Critchlow-Fligner procedure for post hoc analysis. Spearman correlation analysis was performed to examine relationships between continuous variables. Additionally, logistic regression analysis was employed to assess the impact of independent variables on categorical outcomes, ensuring a comprehensive understanding of the underlying dynamics.

Results

The study included a total of 140 participants, divided into a control group with 53 individuals (37.9%) and a patient group with 87 individuals (62.1%) experiencing ED, classified into grades 1, 2, and 3. Specifically, 15 individuals (17.24%) had ED grade 1, 50 individuals (57.47%) had ED grade 2, and 22 individuals (25.29%) had ED grade 3. A summary of the demographic and clinical characteristics of the participants is presented in Table 1. Statistical analysis revealed no significant differences between the ED and control groups regarding age, BMI, or systolic blood pressure ($P > 0.05$). Regarding comorbidities, hypertension was present in 52.8% of patients with ED and 37.7% of controls ($P = 0.082$). Diabetes mellitus was observed in 33.3% of the ED group compared to 11.3% in the control group ($P = 1.000$), and hyperlipidemia in 27.5% versus 18.8%, respectively ($P = 0.243$). Notably, smoking was significantly more common in the ED group (64.3%) than in controls (2%), with a statistically significant difference ($P < 0.001$). While the prevalence of traditional cardiovascular risk factors was numerically higher in the ED group, only smoking reached statistical significance (Table 1).

Patients with ED exhibited significantly increased LA and RA volumes when compared to the control group ($P < 0.05$) (Table 2). Additionally, they showed higher values in LV end-systolic diameter, LA size, deceleration time (DT), and E. Conversely, the patient group demonstrated marked reductions in E/A ratio, e′, RV E, and RV e′, while a′ was significantly elevated compared to controls. Importantly, isovolumic relaxation time (IVRT) was also significantly prolonged in the patient group, suggesting impaired DD ($P < 0.05$) (Table 2). There was no statistically significant difference in PASP between the ED group (29.2 ± 1.6 mmHg) and the control group (28.5 ± 1.4 mmHg; $P = 0.088$). Tricuspid regurgitation jet velocity was evaluated in both groups, with a mean velocity of 2.65 ± 0.35 m/s in the ED group and 2.59 ± 0.31 m/s in the control group ($P = 0.148$). Although the difference was not statistically significant, the trend toward higher TR velocities in the ED group may reflect subtle elevations in right-sided pressures associated with early DD, as shown in Table 2.

Differences between the ED grades (ED1, ED2, and ED3) were analyzed, revealing statistically significant differences in E, E/A ratio, RV E, RV e′, and the RV E/RV e′ ratio ($P < 0.05$) (Table 3). Significant variations in E values were noted between ED1 and ED3; in RV E between the control group and ED1 and ED2; in RV e′ between ED1 and ED2 and ED3; and in the RV E/RV e′ ratio between ED1 and ED2 and ED3 ($P < 0.05$).

Table 2. Comparative analysis of echocardiographic variables between study groups

	ED (+) (n = 87)		ED (-) (n = 53)		P
	Mean ± SD	Median (IQR)	Mean ± SD	Median (IQR)	
LVEF, %	61.13 ± 2.98	60 (3)	60.69 ± 4.48	60 (3)	0.554
LVEDD, mm	47.48 ± 4.33	47 (6.5)	47.81 ± 5.24	47 (8)	0.532
LVESD, mm	35.61 ± 21.39	33 (5)	31.6 ± 5.57	30 (8)	0.023*
IVSD, mm	10.97 ± 1.88	11 (2.5)	10.47 ± 1.64	10 (1)	0.155
LVPWD, mm	10.24 ± 1.27	10 (2)	10 ± 1.48	10 (2)	0.144
LAAP, mm	42.11 ± 6.89	40 (11)	37.99 ± 5.13	38 (5)	0.001*
LAA, cm^2	16.67 ± 3.2	16.6 (3.6)	17.84 ± 3.97	17.2 (3.7)	0.099
LAV, mL	40.68 ± 4.48	40 (5)	37.4 ± 5.34	37 (6.5)	0.0001*
LAVI, mL/m^2	21.99 ± 2.42	21.5 (2.7)	20.22 ± 2.89	20 (3.5)	0.0002*
E, cm/s	60.92 ± 16.27	59 (21.5)	78.53 ± 21.54	78 (24)	0.0001*
A, cm/s	67.61 ± 15.89	66 (22)	66.94 ± 17.24	64 (23)	0.747
RV MID, mm	29.76 ± 4.63	30 (6)	29.79 ± 3.85	31 (5)	0.680
RV annular, cm	35.78 ± 5.04	36 (7)	37.3 ± 3.21	37 (3)	0.063
RAA, cm^2	15.01 ± 3.43	14.7 (4.85)	15.7 ± 3.24	15.2 (4.1)	0.146
RAV, mL	40.06 ± 3.85	39 (6)	35.77 ± 4.79	35 (7)	0.0001*
RA, mm	47.17 ± 5.08	47 (7)	48.62 ± 4.67	49 (7)	0.059
TAPSE, mm	23.46 ± 3.56	23 (5)	24 ± 3.25	24 (4)	0.337
PASB, mmHg	29.2 ± 1.6	29 (3)	28.5 ± 1.4	28 (2.5)	0.088
TR, m/s	2.65 ± 0.35	2.60	2.59 ± 0.31	2.55	0.148
Aortic flow, m/s	1.14 ± 0.24	1.1 (0.32)	1.15 ± 0.21	1.08 (0.26)	0.942
IVRT, ms	110.28 ± 47.83	100 (65.5)	73.49 ± 23.42	69 (33)	0.0001*
DT, ms	125.46 ± 56.36	115 (57)	123.79 ± 42.33	114 (57)	0.737
E/A ratio	0.94 ± 0.31	0.86 (0.49)	1.28 ± 0.54	1.34 (0.91)	0.0001*
e’	13.7 ± 10.5	11 (5.5)	14.11 ± 5.83	14 (8)	0.022*
a'	10.51 ± 3.35	11 (4)	9.19 ± 2.95	9 (5)	0.008*
E/e’ ratio	5.75 ± 3.03	5.2 (1.93)	6.34 ± 3.4	5.33 (1.96)	0.457
RV E	52.29 ± 33.17	50 (15)	60.26 ± 15.68	60 (17)	0.0001*
RV e’	13.49 ± 7.73	12 (5.5)	13.91 ± 3.4	15 (4)	0.003*
RV E/RV e’ ratio	4.81 ± 3.14	4.25 (2.46)	4.53 ± 1.38	4.18 (1.15)	0.997
RV A	50.52 ± 17.18	48 (17)	47.94 ± 15.91	42 (24)	0.343
RV a'	14.31 ± 4.04	14 (4)	14.23 ± 3.95	13 (5)	0.749

*Statistically significant (Mann-Whitney U test). A (cm/s), Late Diastolic Mitral Inflow Velocity; a', Late Diastolic Mitral Annular Velocity (Tissue Doppler); DT, Deceleration Time; E (cm/s), Early Diastolic Mitral Inflow Velocity; é, Early Diastolic Mitral Annular Velocity (Tissue Doppler); EF, Ejection Fraction; IVRT, Isovolumetric Relaxation Time; IVSD, Interventricular Septal Diameter; LAA, Left Atrial Area; LAAP, Left Atrial Anteroposterior Diameter; LAV (mL), Left Atrial Volume; LAVI (mL/m2), Left Atrial Volume Index; LVEDD, Left Ventricular End-Diastolic Diameter; LVESD, Left Ventricular End-Systolic Diameter; LVPWD, Left Ventricular Posterior Wall Diameter; PASB (mmHg), Pulmonary Artery Systolic Pressure; RA, Right Atrial Diameter; RAA, Right Atrial Area; RAV (mL), Right Atrial Volume; RV A, Right Ventricular Late Diastolic Inflow Velocity; RV a', Right Ventricular Late Diastolic Annular Velocity; RV Annular, Right Ventricular Annular Diameter; RV E, Right Ventricular Early Diastolic Inflow Velocity; RV é, Right Ventricular Early Diastolic Annular Velocity; RV E/RV é, Ratio of RV Early Diastolic Inflow to Annular Velocity; RV Mid, Right Ventricular Mid-Cavity Diameter; TAPSE, Tricuspid Annular Plane Systolic Excursion; TR (m/s), Tricuspid Regurgitation Jet Velocity.

To evaluate the impact of variables that showed significant differences between groups, logistic regression analysis was conducted. In the univariate logistic regression, left atrial anteroposterior diameter (LAAP), LA and RA volumes, and IVRT demonstrated a statistically significant positive association with the patient group compared to controls ($P < 0.05$). In the multivariate logistic regression analysis, LAAP and IVRT remained significantly associated with the patient group ($P < 0.05$) (Table 4).

Figure 1 illustrates representative echocardiographic findings from a patient with erectile dysfunction. Panel A, obtained in the parasternal long-axis view, reveals left atrial enlargement. Panel B shows a reduced E/A ratio on mitral inflow Doppler, consistent with impaired diastolic filling. Tissue Doppler imaging of the mitral annulus in Panel C (lateral) and Panel D (septal) demonstrates reduced e’ velocities, further indicating diastolic dysfunction. Panels E and F present left atrial area and volume measurements,

Table 3. Comparative analysis of echocardiographic parameters based on erectile dysfunction severity

	Mild ED (n = 15)		Moderate ED (n = 50)		Severe ED (n = 22)		P*	P**
	Mean ± SD	Median (IQR)	Mean ± SD	Median (IQR)	Mean ± SD	Median (IQR)		
E	55.27 ± 13.2	52 (21)	61.56 ± 18.09	18.09 (25.5)	63.32 ± 13.26	59 (14)	< 0.001*	01; 03
A	64.6 ± 16.15	64 (25)	68.3 ± 16.61	16.61 (19.8)	68.09 ± 14.44	67.5 (19)	0.838	
E/A ratio	0.9 ± 0.31	0.75 (0.26)	0.94 ± 0.33	0.33 (0.52)	0.97 ± 0.26	0.89 (0.48)	0.005*	02
e′	19.4 ± 17.8	11 (6.5)	13.06 ± 9.27	9.27 (6)	11.27 ± 3.06	11 (2.75)	0.099	
a'	10.93 ± 2.31	11 (2.5)	10.18 ± 3.58	3.58 (5)	10.95 ± 3.46	11 (5)	0.055	
E/é ratio	4.44 ± 1.99	5.11 (1.4)	6.01 ± 3.41	3.41 (2.28)	6.05 ± 2.51	5.38 (1.6)	0.384	
RV E	37.87 ± 15.83	39 (16.5)	53.08 ± 31.55	31.55 (16)	60.32 ± 42.4	52 (16.8)	< 0.001*	01; 02; 12; 13
RV e′	18.4 ± 11.41	14 (7.5)	13.12 ± 7.31	7.31 (5.75)	10.97 ± 3.04	10 (4)	0.001*	02; 03
RV E/RV e′ ratio	2.9 ± 1.59	2.79 (1.45)	4.96 ± 3.01	3.01 (2.34)	5.78 ± 3.72	4.42 (3.08)	0.004*	01; 12; 13
RV A	52.6 ± 13.6	48 (16.5)	51.2 ± 20.2	20.2 (18.8)	47.55 ± 10.98	48 (12)	0.644	
RV a'	14.6 ± 2.23	14 (2)	14.28 ± 4.97	4.97 (6)	14.19 ± 2.37	14.5 (2.75)	0.961	

*Kruskal–Wallis Test; **Dwass–Steel–Critchlow–Fligner pairwise comparisons. A, Peak Late Diastolic Transmitral Flow Velocity; a′, Peak Late Diastolic Mitral Annular Velocity Measured by Tissue Doppler; E, Peak Early Diastolic Transmitral Flow Velocity; e′, Peak Early Diastolic Mitral Annular Velocity Measured by Tissue Doppler; e/a, Ratio of Early to Late Diastolic Transmitral Flow Velocities; E/e′, Ratio of Early Transmitral Flow Velocity to Early Diastolic Mitral Annular Velocity; RV A, Peak Late Diastolic Tricuspid Inflow Velocity; RV a′, Peak Late Diastolic Tricuspid Annular Velocity Measured by Tissue Doppler; RV E, Peak Early Diastolic Tricuspid Inflow Velocity; RV e′, Peak Early Diastolic Tricuspid Annular Velocity Measured by Tissue Doppler; RV E/RV e′, Ratio of Early Tricuspid Inflow to Early Diastolic Tricuspid Annular Velocity.

Table 4. Univariate and multivariate logistic regression analysis

	Univariate analysis		Multivariate analysis	
	Exp (B) (95% CI)	P	Exp (B) (95% CI)	P
LVESD	1.07 (1.00–1.15)	0.050	–	–
LAAP	1.12 (1.05–1.19)	0.001*	1.16 (1.04–1.29)	0.006*
LAV	0.88 (0.81–0.95)	0.001*	–	–
e′	0.99 (0.96–1.03)	0.792	–	–
a'	1.14 (1.02–1.27)	0.022	–	–
RV E	0.99 (0.98–1)	0.138	–	–
RV e′	0.99 (0.94–1.04)	0.708	–	–
RAV	0.93 (0.9–0.95)	0.0001*	–	–
IVRT	1.03 (1.02–1.05)	0.0001*	1.04 (1.01–1.06)	0.002*

*Statistically significant (P < 0.05). a′, Peak Late Diastolic Mitral Annular Velocity Measured by Tissue Doppler; e, Peak Early Diastolic Transmitral Flow Velocity; e/a, Ratio of Early to Late Diastolic Transmitral Flow Velocities; é, Peak Early Diastolic Mitral Annular Velocity Measured by Tissue Doppler; IVRT, Isovolumetric Relaxation Time; LAAP, Left Atrial Anteroposterior Diameter; LAV, Left Atrial Volume; LVESD, Left Ventricular End-Systolic Diameter; RAV, Right Atrial Volume; RV e, Peak Early Diastolic Tricuspid Inflow Velocity; RV é, Peak Early Diastolic Tricuspid Annular Velocity Measured by Tissue Doppler.

respectively, highlighting atrial remodeling. These findings reflect structural and functional left heart changes in ED patients, even in the absence of overt cardiovascular disease.

Discussion

In this study, we found significant impairments in LV DD and elevated RV filling pressures in patients with ED. Echocardiographic evaluations of individuals without known CVD, who presented to the urology outpatient clinic with complaints of ED, revealed that LA dilatation, increased LA volume, prolonged IVRT, and a reduced E/A ratio were significantly more prevalent in the ED group compared to the control group. These echocardiographic changes indicate potential subclinical DD in patients with ED. Furthermore, a subgroup analysis within the ED cohort showed that greater severity of ED was associated with a significant decrease in RV é velocity and an increase in the RV E/é ratio. The observed increase in RA volume further supports the relationship between higher ED severity and subclinical RV diastolic dysfunction.

Erectile dysfunction is increasingly recognized as a manifestation of systemic vascular disease, particularly atherosclerosis.[12,13] Compelling evidence indicates that ED frequently precedes overt cardiovascular events, reflecting underlying endothelial dysfunction and arterial insufficiency.[14] The unique characteristics of the penile arteries, due to their smaller caliber, allow atherosclerotic changes to manifest earlier than in larger vessels such as the coronary arteries, positioning ED as a potentially significant early marker of subclinical CVD. Atherosclerosis is fundamentally a systemic condition that affects multiple vascular territories and is characterized by similar pathological alterations

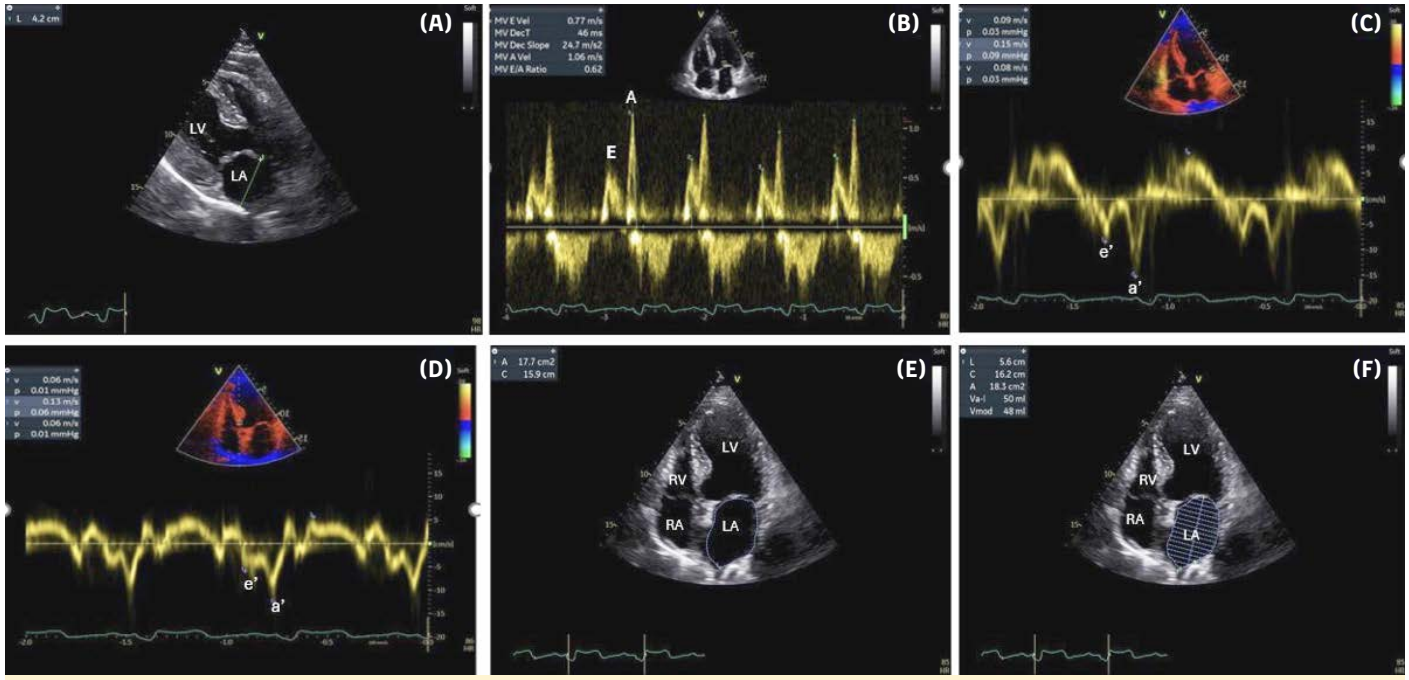

Figure 1. Echocardiographic assessment of left atrial size and left ventricular diastolic function in a patient with erectile dysfunction. *(A) Parasternal long-axis view showing marked left atrial (LA) enlargement posterior to the left ventricle (LV). (B) Pulsed-wave Doppler recording of mitral inflow velocities demonstrating reduced early (E) to late (A) diastolic filling ratio (E/A = 0.62), indicating impaired diastolic relaxation. (C) Tissue Doppler imaging (TDI) from the lateral mitral annulus showing reduced early diastolic annular velocity (e′) and relatively preserved late diastolic velocity (a′), consistent with abnormal LV relaxation. (D) TDI from the septal mitral annulus showing similarly decreased e′ and elevated a′, reinforcing evidence of diastolic dysfunction. (E) Apical four-chamber view with manual planimetry outlining left atrial area (LA), alongside right atrium (RA), right ventricle (RV), and left ventricle (LV). (F) Biplane method of disks for left atrial volume quantification, highlighting enlarged LA dimensions.

LA, Left atrium; LV, Left ventricle; RA, Right atrium; RV, Right ventricle; E, Peak early diastolic mitral inflow velocity; A, Peak late diastolic mitral inflow velocity; e′, Peak early diastolic mitral annular velocity (TDI); a′, Peak late diastolic mitral annular velocity (TDI); TDI, Tissue Doppler imaging.

in the arterial wall.[15] As a result, individuals with arterial ED often face an elevated risk of CVD, even in the absence of overt cardiac symptoms. It is important to note that the clinical onset of symptoms across different vascular beds may not occur simultaneously, primarily due to variations in arterial diameter. Larger arteries tend to be more resilient to comparable degrees of vascular wall thickening than their smaller counterparts.

Moreover, increased arterial stiffness—a common consequence of atherosclerosis—leads to elevated systolic blood pressure and widened pulse pressure.[16] These hemodynamic changes raise myocardial oxygen demand, contribute to LV hypertrophy, and increase myocardial wall stress, ultimately resulting in myocardial ischemia. Collectively, these processes severely impair LV diastolic function, which plays a central role in the development of heart failure with preserved ejection fraction (HFpEF). Impaired myocardial relaxation and increased ventricular stiffness elevate filling pressures, leading to clinical manifestations such as dyspnea, reduced exercise capacity, higher risk of hospitalization, and decreased overall survival. This highlights the importance of early identification of DD, which is vital for effective risk stratification and clinical management.[17,18]

In this study, we systematically assessed diastolic function using key echocardiographic parameters, specifically the E/A ratio and IVRT. Our findings reveal significant impairments in these measures among patients with ED. The E/A ratio, which reflects the dynamic interplay between E and A ventricular filling, serves as a crucial indicator of diastolic function that evolves with disease progression.[19] In the early stages, delayed relaxation presents as a decreased E/A ratio. As DD progresses, pseudo-normalization or even an elevated ratio may occur, resulting from reduced ventricular compliance and altered filling mechanics.

In our patient cohort, we observed a statistically significant reduction in the E/A ratio among those with ED, indicating early-stage DD—even in the absence of overt CVD. Furthermore, IVRT—though influenced by factors such as heart rate and blood pressure—provides valuable insights into myocardial relaxation.[20] It becomes especially informative when interpreted alongside other diastolic indices. In our findings, patients with ED exhibited a notably prolonged IVRT, further reinforcing the presence of subclinical DD.

Moreover, it is essential to recognize that myocardial relaxation and compliance can be significantly influenced by age and metabolic comorbidities, including obesity, insulin resistance, and hypertension—all of which frequently coexist in individuals with ED.[21-23] Importantly, IVRT emerged as an independent variable in our logistic regression analysis of patients with ED, reinforcing its importance in understanding the complex relationship between erectile dysfunction and DD.

Left atrial enlargement also emerged as a robust and independent predictor of ED in this study, underscoring its significance in cardiovascular health. LA enlargement is a clear indicator of atrial remodeling—a phenomenon closely associated with CVD and structural changes in the LV, as supported by previous research.[24] Numerous studies have demonstrated the strong interplay between elevated blood pressure, LV hypertrophy, and atrial size. Conditions such as hypertension and LV hypertrophy can accelerate the onset of diastolic dysfunction, leading to increased filling pressures and subsequent atrial remodeling due to persistent pressure overload. Importantly, LA volume has been proposed as a key marker of both the severity and chronicity of DD, offering a potentially simpler alternative to more complex Doppler echocardiographic assessments of diastolic function and filling pressures. The size of the LA provides valuable insights into the long-term effects of elevated filling pressures. Notably, Nishimura et al.[25] established a direct correlation between elevated LA pressure and the presence of DD, while Matsuda et al.[26] demonstrated that maximal LA volume increases in parallel with the severity of DD, as measured through invasive hemodynamic techniques. Moreover, the progression of DD is linked to increased filling pressures, which not only lead to LA enlargement but also to notable increases in both LA and RA volumes. In our cohort, the statistically significant increases in both LA and RA volumes among patients with ED strongly support the presence of subclinical DD within this population.[27] Despite observing significant differences in individual diastolic parameters such as e′ velocity and IVRT, our study did not demonstrate a statistically significant difference in the E/e′ ratio between the ED and control groups. One plausible explanation is that E/e′, although widely used as a surrogate marker for estimating left ventricular filling pressures, may have limited sensitivity in detecting early stages of DD.[28] This finding is consistent with the results of Hyun et al.,[27] who also reported no statistically significant difference in E/e′ values between ED and control groups in a cardiovascular disease-free population. Similarly, von Bibra et al.[22] showed that in non-diabetic individuals, E/e′ did not increase significantly despite impaired myocardial relaxation, possibly due to early compensatory mechanisms such as volume adaptation that mask elevations in filling pressure. These findings highlight the potential limitations of using E/e′ in isolation to detect early diastolic dysfunction in asymptomatic populations. Instead, parameters such as IVRT, LA volume, and e′ velocity—each of which demonstrated significant differences in our ED group—may serve as more sensitive indicators of subclinical myocardial involvement.[16,27]

Our study underscores the clinical relevance of diastolic function in patients with ED, complementing the more widely recognized LV involvement. Subgroup analysis revealed a significant decline in RV e′ velocity and a rise in the RV E/e′ ratio with increasing ED severity, indicating impaired RV relaxation and elevated filling pressures. These findings were consistent across all ED severity groups and emphasize the utility of tissue Doppler imaging (TDI) in evaluating subclinical RV dysfunction. Prior studies have similarly noted that systemic endothelial dysfunction and vascular pathology can extend to the right heart, supporting a biventricular pathophysiological continuum.[29,30] Our findings suggest a progressive deterioration in RV diastolic function with increasing ED severity, supporting the integration of RV assessment into cardiovascular evaluation in this population.

Our findings support and expand upon prior research linking ED to early DD. Consistent with the studies by Hyun et al.[27] and von Bibra et al.,[22] we found no significant difference in E/e′ ratios between ED and control groups without overt cardiovascular disease, underscoring the limited sensitivity of this index in detecting early-stage DD. In contrast, prolonged IVRT, reduced e′ velocity, and increased LA volume were strongly associated with ED. These results align with the observations of Matsuda et al.[26] and Nishimura et al.,[25] who identified LA enlargement as a marker of chronically elevated filling pressures. The independent predictive value of IVRT and LA size in our multivariate analysis further reinforces their clinical relevance. Furthermore, we observed a significant decline in RV e′ and a rise in RV E/e′ with increasing ED severity, indicating RV diastolic impairment. These findings are consistent with those of Mukhaini et al.[29] and Arısoy et al.,[30] who demonstrated the utility of RV tissue Doppler indices in identifying subclinical RV dysfunction. Collectively, our results highlight the presence of biventricular DD in ED and support the use of echocardiography for early cardiovascular risk assessment in this population.

Given the demonstrated association between ED and subclinical biventricular DD, our findings support the consideration of echocardiographic evaluation in men presenting with ED, particularly when traditional cardiovascular risk factors such as hypertension, diabetes mellitus, obesity, or smoking are present—even in the absence of overt cardiac symptoms. Routine assessment using transthoracic echocardiography, including tissue Doppler parameters and LA volume measurements, may enable early identification of diastolic abnormalities. This proactive approach could facilitate timely cardiovascular risk stratification, guide preventive strategies, and potentially alter the clinical course for individuals at heightened risk of future cardiac events.

It is important to note that smoking, a well-established contributor to endothelial dysfunction and atherosclerosis, was significantly more prevalent in the ED group compared to controls (64.3% vs. 2%, $P < 0.001$). Cigarette smoking impairs endothelial nitric oxide production, increases oxidative stress, and promotes systemic inflammation, all of which contribute to vascular stiffness and microvascular dysfunction.[1,15] These pathophysiological mechanisms underlie both ED and early DD. Moreover, smoking has been independently associated with LV hypertrophy, increased myocardial wall stress, and left atrial remodeling—key contributors to DD.[16] Therefore, while our findings demonstrate a clear association between ED and subclinical biventricular DD, smoking may act as a common upstream pathological factor. This reinforces the importance of controlling for smoking status in future studies evaluating cardiac function in men with ED.

Limitations

This study has several limitations. First, it was conducted at a single center with a relatively small sample size, which may limit the generalizability of the findings. Although patients with known cardiovascular disease were excluded, the presence of undiagnosed or subclinical disease cannot be ruled out. The cross-sectional design also precludes causal inferences regarding the relationship between ED and DD. Advanced imaging techniques, such as LA strain or RV strain analysis, were not employed, which may have reduced the sensitivity for detecting early myocardial dysfunction. Additionally, RV diastolic assessment

was based solely on tissue Doppler imaging, which may not fully capture the complex geometry and function of the RV. While individuals with known hormonal disorders were excluded, serum testosterone and other endocrine parameters were not routinely measured, potentially overlooking hormonal contributions. Lastly, variables such as physical activity, psychological status, and lifestyle factors were not systematically recorded and may have influenced both erectile and cardiac function.

Conclusion

This study reveals a connection between ED and echocardiographic markers of LV DD in individuals without established CVD. Notably, the severity of ED is significantly associated with RV DD in this population. These findings underscore the critical importance of evaluating ED as a potential early indicator of subclinical cardiac dysfunction, suggesting that it may serve as a vital precursor to future cardiovascular disease.

Ethics Committee Approval: Ethics committee approval was obtained from University of Health Sciences Istanbul Training and Research Hospital Clinical Research Ethics Committee (Approval Number: 2504, Date: 04.09.2020).

Informed Consent: All participants received detailed information prior to enrollment, and a written informed consent form was obtained from each individual.

Conflict of Interest: The authors declare no conflict of interest.

Funding: This research received no external funding.

Use of AI for Writing Assistance: The authors confirm that no artificial intelligence (AI) tools, including image generation software, large language models (LLMs) or chatbots, were used in the development, writing, or revision of this manuscript. All content is solely the result of the authors' own work.

Author Contributions: Concept – V.Ç., S.A., T.Ç.; Design – C.E., A.Ö.; Supervision – T.Ç., U.B.; Resource – S.Y., Ş.K.; Materials – A.E., M.B.; Data Collection and/or Processing – S.Y., Ş.K., A.E., M.B.; Analysis and/or Interpretation – A.Ö.; Literature Review – V.Ç., S.A.; Writing – V.Ç., S.A., C.E., T.Ç.; Critical Review – T.Ç., U.B.

Peer-review: Externally peer-reviewed.

References

1. Bonetti PO, Lerman LO, Lerman A. Endothelial dysfunction: A marker of atherosclerotic risk. *Arterioscler Thromb Vasc Biol*. 2003;23(2):168–175. [CrossRef]
2. Gazzaruso C, Solerte SB, Pujia A, et al. Erectile dysfunction as a predictor of cardiovascular events and death in diabetic patients with angiographically proven asymptomatic coronary artery disease: A potential protective role for statins and 5-phosphodiesterase inhibitors. *J Am Coll Cardiol*. 2008;51(21):2040–2044. [CrossRef]
3. Kałka D, Domagała Z, Rusiecki L, et al. Heart rate recovery, cardiac rehabilitation and erectile dysfunction in males with ischaemic heart disease. *Anatol J Cardiol*. 2016;16(4):256–263. [CrossRef]
4. Jovin DG, Sumpio BE, Greif DM. Manifestations of human atherosclerosis across vascular beds. *JVS Vasc Insights*. 2024;2:100089. [CrossRef]
5. Montorsi P, Ravagnani PM, Galli S, et al. The artery size hypothesis: A macrovascular link between erectile dysfunction and coronary artery disease. *Am J Cardiol*. 2005;96(12B):19M–23M. [CrossRef]
6. Paulus WJ, Tschöpe C. A novel paradigm for heart failure with preserved ejection fraction: Comorbidities drive myocardial dysfunction and remodeling through coronary microvascular endothelial inflammation. *J Am Coll Cardiol*. 2013;62(4):263–271. [CrossRef]
7. Taqueti VR, Solomon SD, Shah AM, et al. Coronary microvascular dysfunction and future risk of heart failure with preserved ejection fraction. *Eur Heart J*. 2018;39(10):840–849. [CrossRef]
8. Nehra A, Jackson G, Miner M, et al. The Princeton III Consensus recommendations for the management of erectile dysfunction and cardiovascular disease. *Mayo Clin Proc*. 2012;87(8):766–778. [CrossRef]
9. Rosen RC, Cappelleri JC, Smith MD, Lipsky J, Peña BM. Development and evaluation of an abridged, 5-item version of the International Index of Erectile Function (IIEF-5) as a diagnostic tool for erectile dysfunction. *Int J Impot Res*. 1999;11(6):319–326. [CrossRef]
10. Lang RM, Badano LP, Mor-Avi V, et al. Recommendations for cardiac chamber quantification by echocardiography in adults: An update from the American Society of Echocardiography and the European Association of Cardiovascular Imaging. *J Am Soc Echocardiogr*. 2015;28(1):1–39.e14. [CrossRef]
11. Paulus WJ, Tschöpe C, Sanderson JE, et al. How to diagnose diastolic heart failure: A consensus statement on the diagnosis of heart failure with normal left ventricular ejection fraction by the Heart Failure and Echocardiography Associations of the European Society of Cardiology. *Eur Heart J*. 2007;28(20):2539–2550. [CrossRef]
12. Inman BA, Sauver JL, Jacobson DJ, et al. A population-based, longitudinal study of erectile dysfunction and future coronary artery disease. *Mayo Clin Proc*. 2009;84(2):108–113. [CrossRef]
13. Ulucan Ş, Kaya Z, Keser A, Katlandur H, Karanfil M, Ateş İ. Deterioration of heart rate recovery index in patients with erectile dysfunction. *Anatol J Cardiol*. 2016;16(4):264–269. [CrossRef]
14. Thompson IM, Tangen CM, Goodman PJ, Probstfield JL, Moinpour CM, Coltman CA. Erectile dysfunction and subsequent cardiovascular disease. *JAMA*. 2005;294(23):2996–3002. [CrossRef]
15. Tsujimura A, Hiramatsu I, Aoki Y, et al. Atherosclerosis is associated with erectile function and lower urinary tract symptoms, especially nocturia, in middle-aged men. *Prostate Int*. 2017;5(2):65–69. [CrossRef]
16. Durukan E, Jensen CFS, Skaarup KG, et al. Erectile dysfunction is associated with left ventricular diastolic dysfunction: A systematic review and meta-analysis. *Eur Urol Focus*. 2023;9(6):903–912. [CrossRef]
17. Obokata M, Reddy YNV, Borlaug BA. Diastolic dysfunction and heart failure with preserved ejection fraction: Understanding mechanisms by using noninvasive methods. *JACC Cardiovasc Imaging*. 2020;13(1 Pt 2):245–257. [CrossRef]
18. Mert GÖ, Özlek B, Özlek E, et al. Comparing the diagnostic performance of HFA-PEFF and H2FPEF scoring systems in heart failure with preserved ejection fraction patients: Insights from the APOLLON Registry. *Anatol J Cardiol*. 2023;27(9):539–548. [CrossRef]
19. Nagueh SF, Smiseth OA, Appleton CP, et al. Recommendations for the evaluation of left ventricular diastolic function by echocardiography: An update from the American Society of Echocardiography and the European Association of Cardiovascular Imaging. *J Am Soc Echocardiogr*. 2016;29(4):277–314. [CrossRef]
20. Lo Q, Thomas L. Echocardiographic evaluation of diastolic heart failure. Australas J Ultrasound Med. 2010;13(1):14–26. [CrossRef]
21. Savji N, Meijers WC, Bartz TM, et al. The association of obesity and cardiometabolic traits with incident HFpEF and HFrEF. *JACC Heart Fail*. 2018;6(8):701–709. [CrossRef]
22. Von Bibra H, Paulus WJ, St John Sutton M, Leclerque C, Schuster T, Schumm-Draeger PM. Quantification of diastolic dysfunction via the age dependence of diastolic function - impact of insulin resistance with and without type 2 diabetes. *Int J Cardiol*. 2015;182:368–374. [CrossRef]
23. Özlek B, Özlek E, Kahraman S, et al. Gender disparities in heart failure with mid-range and preserved ejection fraction: Results from APOLLON study. *Anatol J Cardiol*. 2019;21(5):242–252. [CrossRef]
24. Pritchett AM, Mahoney DW, Jacobsen SJ, Rodeheffer RJ, Karon BL, Redfield MM. Diastolic dysfunction and left atrial volume: A population-based study. *J Am Coll Cardiol*. 2005;45(1):87–92. [CrossRef]

25. Nishimura RA, Appleton CP, Redfield MM, Ilstrup DM, Holmes DR Jr, Tajik AJ. Noninvasive doppler echocardiographic evaluation of left ventricular filling pressures in patients with cardiomyopathies: A simultaneous Doppler echocardiographic and cardiac catheterization study. *J Am Coll Cardiol*. 1996;28(5):1226–1233. [CrossRef]
26. Matsuda M, Matsuda Y. Mechanism of left atrial enlargement related to ventricular diastolic impairment in hypertension. *Clin Cardiol*. 1996;19(12):954–959. [CrossRef]
27. Hyun CW, Hwang JY, Yun SW, et al. The association between the severity of erectile dysfunction and left ventricular diastolic dysfunction in patients with and without cardiovascular disease. *Investig Clin Urol*. 2024;65(2):165–172. [CrossRef]
28. Robinson S, Ring L, Oxborough D, et al. The assessment of left ventricular diastolic function: Guidance and recommendations from the British Society of Echocardiography. *Echo Res Pract*. 2024;11(1):16. [CrossRef]
29. Mukhaini M, Prashanth P, Abdulrehman S, Zadjali M. Assessment of right ventricular diastolic function by tissue Doppler imaging in patients with acute right ventricular myocardial infarction. *Echocardiography*. 2010;27(5):539–543. [CrossRef]
30. Arısoy A, Topçu S, Demirelli S, et al. Echocardiographic assessment of right ventricular functions in healthy subjects who migrated from the sea level to a moderate altitude. *Anatol J Cardiol*. 2016;16(10):779–783. [CrossRef]

ARCHIVES OF THE TURKISH SOCIETY OF CARDIOLOGY

Official journal of the TURKISH SOCIETY OF CARDIOLOGY

Prognostic Value of Inflammatory Indices in Patients with Infective Endocarditis: Peak C-Reactive Protein/Albumin Ratio as a Better Biomarker

İnfektif Endokarditli Hastalarda İnflamatuar İndekslerin Prognostik Değeri: Pik C-Reaktif Protein/Albümin Oranı Daha İyi Bir Biyobelirteç

ABSTRACT

Objective: Infective endocarditis (IE) is a severe and potentially fatal infection associated with significant morbidity and mortality. Early identification of patients at high risk of adverse outcomes is essential for improving clinical management and prognosis. This study aimed to evaluate the prognostic value of various inflammatory indices, with a particular focus on the peak C-reactive protein/albumin ratio (CAR), in predicting in-hospital mortality among IE patients.

Method: This retrospective, single-center study included IE patients admitted between June 2020 and June 2023. The primary outcome was in-hospital mortality. For all patients, inflammatory indices, including peak serum CAR levels, were calculated, and their association with mortality was assessed.

Results: Of 165 patients, 62 (37.6%) experienced in-hospital mortality. Non-survivors had significantly higher peak CAR levels (8.1 vs. 5.0, P < 0.001) and elevated levels of other inflammatory indices compared to survivors. Peak CAR demonstrated the highest discriminatory ability for predicting in-hospital mortality, with an area under the curve (AUC) of 0.764, outperforming other indices. Multivariate analysis confirmed that peak CAR was an independent predictor of mortality (adjusted hazard ratio = 1.16, 95% confidence interval: 1.10–1.23, P < 0.001). Net reclassification improvement and integrated discrimination improvement analyses further supported the superior reclassification and discrimination capabilities of peak CAR.

Conclusion: Peak CAR is a significant prognostic marker for in-hospital mortality in IE patients compared to traditional inflammatory indices. Incorporating peak CAR into clinical practice may improve risk stratification and guide treatment decisions.

Keywords: C-reactive protein to albumin ratio, in-hospital mortality, infective endocarditis, inflammatory indices

ÖZET

Amaç: İnfektif endokardit (İE), yüksek morbidite ve mortaliteye ile seyreden, yaşamı tehdit eden bir enfeksiyondur. Advers sonuçlar açısından yüksek risk taşıyan hastaların erken tanımlanması, tedavi yönetimini optimize etmek ve prognozu iyileştirmek açısından kritik öneme sahiptir. Bu çalışmada, infektif endokarditli hastalarda, çeşitli inflamatuar indekslerin prognostik değerininin araştırılması ve özellikle hastane içi mortaliteyi öngörmede pik C-reaktif protein/albümin oranının (CAR) belirleyici rolünü değerlendirilmesi amaçlandı.

Yöntem: Bu retrospektif, tek merkezli çalışmaya Haziran 2020 ile Haziran 2023 tarihleri arasında kesin İE tanısı alan hastalar dahil edildi. Birincil sonlanım noktası hastane içi mortaliteydi. Tüm hastalarda inflamatuar indeksler, özellikle pik CAR düzeyleri kaydedildi ve mortalite ile ilişkileri analiz edildi.

Bulgular: Toplam 165 hastanın 62'sinde (%37,6) hastane içi mortalite tespit edildi. Mortalite grubunda, sağ kalanlara kıyasla anlamlı derecede pik CAR düzeyleri saptandı (8,1 vs. 5,0, P < 0,001). Pik CAR, hastane içi mortaliteyi öngörmede diğer inflamatuar indekslerle kıyaslandığında, yüksek ayırt edici güce sahipti (AUC: 0,764). Çok değişkenli Cox regresyon analizinde pik CAR, bağımsız bir mortalite belirleyicisi olarak saptandı (düzeltilmiş hazard oranı: 1,16; %95 GA: 1,10–1,23; P < 0,001). Net yeniden sınıflandırma iyileştirmesi (NRI) ve entegre diskriminasyon iyileştirmesi (IDI) analizleri de pik CAR'ın üstün öngörü performansını destekledi.

Sonuç: Pik CAR düzeyi, infektif endokarditli hastalarda hastane içi mortalitenin güçlü ve bağımsız bir belirleyicisidir. Klinik uygulamalara entegrasyonu, risk sınıflandırmasını güçlendirebilir ve tedavi kararlarını yönlendirebilir.

Anahtar Kelimeler: C-reaktif protein/albümin oranı, hastane içi mortalite, infektif endokardit, inflamatuar indeksler

ORIGINAL ARTICLE
KLİNİK ÇALIŞMA

Duygu İnan[1]
Alev Kılıçgedik[1]
Ayşe İrem Demirtola Mammadli[2]
Arslan Erdoğan[1]
Duygu Genç Albayrak[1]
Funda Özlem Pamuk[1]
Sevil Tuğrul Yavuz[1]
Fatmatuz Zehra Eroğlu[1]
Cemal Ozanalp[1]
Ahmet İlker Tekkeşin[1]
Ömer Genç[1]

[1]Department of Cardiology, Başakşehir Çam and Sakura City Hospital, Istanbul, Türkiye
[2]Department of Cardiology, Ankara Bilkent City Hospital, Ankara, Türkiye

Corresponding author:
Duygu İnan
✉ dr.duyguinan@gmail.com

Received: July 07, 2025
Accepted: July 25, 2025

Cite this article as: İnan D, Kılıçgedik A, Demirtola Mammadli Aİ, et al. Prognostic Value of Inflammatory Indices in Patients with Infective Endocarditis: Peak C-Reactive Protein/Albumin Ratio as a Better Biomarker. *Turk Kardiyol Dern Ars.* 2025;53(7):501–509.

DOI: 10.5543/tkda.2025.85356

Copyright@Author(s)
Available online at archivestsc.com.
Content of this journal is licensed under a Creative Commons Attribution – NonCommercial-NoDerivatives 4.0 International License.

Infective endocarditis (IE) is a serious, potentially life-threatening infection characterized by involvement of the endocardial surface of the heart. It is associated with relatively high short- and long-term mortality and morbidity rates.[1] Global data from the past 30 years reported 1,090,530 cases and 66,320 deaths in 2019, with an estimated annual increase in IE incidence of 1.2% and a mortality rate of 0.7%.[2] Despite advances in diagnostic techniques and treatment strategies, the challenges managing IE and its associated high costs continue to impose a heavy burden on both the society and the economy.[1] Early identification of patients at high risk of adverse outcomes is crucial for improving clinical management and prognosis.

The clinical course and complication rates of infective endocarditis are influenced by multiple factors, including the timing of diagnosis, baseline clinical status, the causative microorganism, and both the approach to and adequacy of treatment. Several variables have been consistently associated with increased mortality in IE patients, such as heart failure at presentation or New York Heart Association (NYHA) class III/IV symptoms, prosthetic valve involvement, larger vegetation size, Staphylococcus aureus infection, older age, renal dysfunction, and elevated inflammatory or cardiac biomarkers.[1–12]

The clinical features, laboratory findings, and associated complications of IE offer insights into the underlying biological processes and disease severity.[3] Systemic inflammation plays a key role in the pathophysiology of IE.[4] In the development of IE, there is an imbalance between pro-inflammatory and anti-inflammatory responses.[4,5,9] In recent studies, the use of combinations of multiple biochemical markers to diagnose various diseases and to compare the diagnostic and prognostic values has become increasingly popular.[6] In patients with IE, the diagnostic and prognostic value of different inflammatory markers has also been investigated.[1,4,5] White blood cell (WBC) count, procalcitonin, brain-type natriuretic peptide (BNP) levels, D-dimer, C-reactive protein (CRP), serum albumin level, and various indices derived from these parameters are known to have prognostic value in IE.[6-10] Among these, CRP and albumin levels have been used separately to assess the inflammatory and nutritional status of patients.[10–12] The prognostic significance of follow-up CRP levels in IE patients has been particularly emphasized.[13] The CRP/albumin ratio (CAR), which combines these two parameters, has emerged as a novel inflammatory index that may provide better prognostic value than CRP or albumin alone.[14]

Recent studies have suggested that CAR is a significant prognostic marker in various infectious and cardiovascular diseases, including IE.[14–17] However, data on the predictive value of peak CAR, which incorporates the maximum CRP and minimum albumin ratio, are limited. Moreover, while the prognostic values of different inflammatory indices in IE patients have been established individually, no study has clearly evaluated their comparative predictive performance.

In this study, we aimed to evaluate the predictive value of inflammatory indices for in-hospital mortality in IE patients, with a particular focus on peak CAR. We hypothesized that peak CAR would serve as a superior biomarker compared to traditional inflammatory markers, thereby providing clinicians with a valuable tool for risk stratification and management of this challenging patient population.

ABBREVIATIONS

AUC	Area under the curve
BNP	Brain-type natriuretic peptide
BUN	Blood urea nitrogen
CAR	CRP/albumin ratio
CI	Confidence interval
CRP	C-reactive protein
CT	Computed tomography
IDI	Integrated discrimination improvement
IE	Infective endocarditis
IQR	Interquartile range
NLR	Neutrophil-to-lymphocyte ratio
NRI	Net reclassification improvement
NYHA	New York Heart Association
PIV	Pan-immune-inflammation value
ROC	Receiver operating characteristic
SII	Systemic immune-inflammation index
SIRI	Systemic inflammatory response index
WBC	White blood cell count

Materials and Methods

Study Population and Design

This retrospective cohort study was conducted at a tertiary care hospital and involved patients diagnosed with definite IE between June 2020 and 2023. Our center is a tertiary referral facility with a dedicated IE team, receiving IE patients from surrounding cities. The study was approved by the Başakşehir Çam and Sakura Hospital Clinical Research Ethics Committee (Approval Number: 87, Date: 14.02.2024) and was conducted in accordance with the 'Good Clinical Practices' guidelines of the Declaration of Helsinki. Informed consent was waived due to the retrospective nature of the study. The inclusion criteria were adult patients (≥ 18 years) with a definite diagnosis of IE according to the modified Duke criteria.[18] For patients who experienced more than one episode of IE, only the first episode was included in the study. Patients with autoimmune inflammatory diseases, leukemia or other blood system disorders, active corticosteroid or immunosuppressive therapy, chronic liver disease, or insufficient medical records were excluded.

Data Collection

Clinical and demographic data, including age, sex, comorbidities (e.g., diabetes mellitus, hypertension, and coronary artery disease), smoking status, intravenous drug use, body mass index, and NYHA classification, were collected from medical records. Laboratory parameters, including WBC count, peak CRP, procalcitonin, albumin, creatinine, blood urea nitrogen (BUN), troponin, and peak N-terminal pro-B-type natriuretic peptide (NT-proBNP), were recorded. From these data, the peak value of CRP and the lowest value of albumin within the first 48–72 hours, as well as the average values of other parameters at admission, were analyzed. Blood culture samples were obtained from all patients within 24 hours of hospital admission and before the initiation of antibiotic therapy, in accordance with the latest guidelines. Cultures were repeated in cases where clinically indicated.

All patients underwent detailed transthoracic echocardiography using the EPIQ CVx (X5-1 transducer, Philips, USA) within the first 24 hours of admission. Additionally, transesophageal echocardiography was performed for all patients at least once during hospitalization (X8-2t transducer, Philips, USA). Vegetation size was evaluated in multiple imaging planes, and the maximum dimension was recorded. Moreover, new-onset severe valve regurgitation, prosthetic valve dysfunction, abscess, pseudoaneurysm, and perforation were assessed as complications. Computed tomography (CT) or positron emission tomography-CT was used in cases where the diagnosis was uncertain or when it was necessary to evaluate for complications. The main indications for surgery were determined by the IE team in accordance with current guidelines.[18] All patients received appropriate medical treatment, including antibiotic therapy tailored to the clinical presentation and any developing complications.

Inflammatory Indices

Peak CAR was calculated using the maximum CRP value and the minimum albumin value recorded within the first 72 hours. The neutrophil-to-lymphocyte ratio (NLR) was calculated by dividing the neutrophil count by the lymphocyte count.[19] The systemic immune-inflammation index (SII) was calculated by multiplying the platelet count by the neutrophil count and dividing by the lymphocyte count.[19] The systemic inflammatory response index (SIRI) was calculated by multiplying the neutrophil count by the monocyte count and then dividing by the lymphocyte count.[19] The pan-immune-inflammation value (PIV) was calculated by multiplying the neutrophil count by the platelet count, multiplying that result by the monocyte count, and then dividing by the lymphocyte count.[20]

Outcomes

The primary outcome was in-hospital mortality. The predictive power of the inflammatory indices was compared between survivors and non-survivors.

Statistical Analysis

Statistical analyses were conducted using R statistical software (version 4.3.2, Vienna, Austria). The normality of variables was assessed using the Kolmogorov-Smirnov test, supported by visual inspection of histograms and probability plots. Continuous variables were presented as mean ± standard deviation for normally distributed data and as median (interquartile range [IQR25-75]) for non-normally distributed data. Categorical variables were expressed as numbers and percentages. Group-wise comparisons of categorical variables were performed using Fisher's exact test or the χ^2 test, while continuous variables were compared using the independent Student's t-test or the Mann-Whitney U test.

The least absolute shrinkage and selection operator (LASSO) penalized selection method was used to identify and refine significant variables for adjustment in the multivariable Cox proportional hazards regression analyses, by applying an optimal lambda value to prevent overfitting (Appendix 1). The following variables were selected for inclusion in the subsequent analyses for adjustment: age, body mass index, aspartate transaminase level, troponin level, white blood cell count, thyroxine (T4) level, urea level, NYHA class, peak N-terminal pro-B-type natriuretic peptide level, vegetation size, treatment type, and infective endocarditis type (Appendix 1).

The optimal cut-off value for peak CAR in predicting all-cause mortality was identified using X-tile software (Version 3.6.1, Yale University School of Medicine), based on the lowest p-value and highest chi-square value (Appendix 2). Correlations between inflammatory indices were analyzed using Kendall's tau-b coefficient.

Kaplan-Meier plots, the log-rank test, and multivariable Cox proportional hazards models were used for the time-to-event analysis of all-cause mortality. The proportional hazards assumption was tested using Schoenfeld residuals and visual inspections of log-log plots. Hazard ratios (HR) and 95% confidence intervals (CI) were calculated for all regression analyses. The importance of individual variables within the multivariable Cox model, including peak CAR, was assessed using a permutation-based variable importance method, ranking variables based on the root mean squared error metric.

The accuracy of mortality prediction was evaluated using the receiver operating characteristic (ROC) curve, area under the curve (AUC), continuous net reclassification improvement (NRI), and integrated discrimination improvement (IDI) analyses. A decision curve analysis was also conducted to determine whether the biomarkers provided a net benefit compared to all-treatment and no-treatment strategies. All statistical analyses were two-sided, with a significance level (alpha) of 0.05.

Results

A total of 186 patients with a definite diagnosis of IE were enrolled in the study. After excluding 21 patients who met the exclusion criteria, 165 patients were included in the final analysis. Patients were divided into two groups based on in-hospital mortality: survivors and non-survivors. The mean age of the study population was 58.0 ± 15.0 years, and 66 patients (40%) were female. Of the total study population, 62 patients (37.6%) died during hospitalization. Non-survivors were signi§ficantly older than survivors (62.0 ± 14.1 years vs. 55.0 ± 15.7 years, P = 0.005). Comorbidities were comparable between the two groups. NYHA class III or IV clinical presentations were significantly more common in non-survivors than in survivors (P < 0.001). Embolic complications occurred at similar frequencies in both groups; however, acute heart failure at presentation was significantly more prevalent among non-survivors (P = 0.057 and P < 0.001, respectively). Notably, the majority of these patients had vegetation sizes ≥ 10 mm (83.9% vs. 68.0%, P = 0.038). More than half of the patients had native valve endocarditis, with prosthetic valve endocarditis being the second most common type. The rate of surgical treatment was significantly higher among survivors (52.4% vs. 43.5%, P = 0.032). Compared to survivors, non-survivors had similar peak CRP levels (103.8 vs. 77.9 mg/dL, P = 0.056) but statistically significantly lower albumin levels (31.3 ± 8.0 vs. 34.6 ± 5.7 mg/dL, P = 0.002). The peak CAR was significantly higher in non-survivors (8.1 vs. 5.0, P < 0.001). In addition, non-survivors had higher levels of systemic inflammatory indices compared to survivors, including PIV (1991.8 vs. 900.6, P < 0.001), SII (2026.2 vs. 1068.9, P = 0.005), SIRI (11.1 vs. 3.7, P < 0.001), and NLR (9.3 vs. 5.0, P = 0.001) (Central illustration). Table 1 presents additional characteristics of the study population.

Table 1. Baseline characteristics, clinical features, and laboratory findings of the study population

Variables	Survivors (n = 103)	Non-survivors (n = 62)	P*
Age, years	55.0 ± 15.7	62.0 ± 14.1	0.005
Female sex, n (%)	39 (37.9)	27 (43.5)	0.577
DM, n (%)	39 (37.9)	30 (48.4)	0.139
HT, n (%)	61 (59.2)	40 (64.5)	0.609
CAD, n (%)	39 (37.9)	31 (50.0)	0.172
CKD, n (%)	42 (36)	25 (40.3)	> 0.950
COPD, n (%)	11 (10.7)	3 (4.8)	0.310
CVA, n (%)	25 (24.3)	20 (32.2)	0.350
Smoking, n (%)	27 (26.2)	16 (25.8)	> 0.950
IV drug user, n (%)	2 (1.9)	3 (4.8)	0.560
BMI, kg/m^2	26.1 ± 4.8	24.7 ± 5.8	0.099
NYHA class, n (%)			<0.001
I	65 (63.1)	3 (4.8)	
II	23 (22.3)	15 (24.2)	
III	10 (9.7)	26 (41.9)	
IV	5 (4.9)	18 (29.0)	
LVEF, %	53.9 ± 11.4	54.0 ± 10.1	0.914
Embolic events, n (%)	17 (16.5)	18 (29.0)	0.057
Acute HF, n (%)	15 (14.6)	44 (71.0)	< 0.001
Vegetation size, n (%)			0.038
< 10 mm	33 (32)	10 (16.1)	
≥ 10 mm	70 (68)	52 (83.9)	
Infective endocarditis type, n (%)			0.081
Native valve IE	46 (44.7)	40 (64.5)	
Prosthetic valve IE	25 (24.3)	12 (19.4)	
Device-lead IE	15 (14.6)	3 (4.8)	
Transvenous catheter IE	15 (14.6)	5 (8.1)	
Other	2 (1.9)	2 (3.2)	
Treatment type, n(%)			0.032
Surgery	54 (52.4)	27 (43.5)	
Medical treatment only	42 (40.8)	35 (56.5)	
Lead extravasation	7 (6.8)	0 (0)	
WBC, 10^3 µ/L	9.4 (7.1-12.9)	13.8 (9.6-16.6)	< 0.001
Hemoglobin, g/dL	10.1 ± 2.4	10.0 ± 2.3	0.670
Platelet count, 10^3 µ/L	222.7 ± 102.1	215.3 ± 109.7	0.665
Lymphocyte count, 10^3 µ/L	1.2 (0.8-1.9)	1.1 (0.7-1.7)	0.167
Monocyte count, 10^3 µ/L	0.8 (0.5-1.1)	0.9 (0.7-1.6)	0.005
Neutrophil count, 10^3 µ/L	7.1 (4.9-11.5)	11.4 (6.9-14.3)	< 0.001
Peak CRP, mg/dL	77.9 (37.8-148.1)	103.8 (52.7-180.5)	0.056
Procalcitonin, µg/L	0.5 (0.1-2.9)	0.8 (0.2-6.9)	0.111
Albumin, mg/dL	34.6 ± 5.7	31.3 ± 8.0	0.002
AST, IU/L	22 (16-38.5)	29.5 (17.2-67.8)	0.099
Creatinine, mg/dL	1.1 (0.8-3.2)	1.4 (0.9-4.4)	0.167
BUN, mg/dL	43.2 (27.5-62.5)	72.0 (45.1-96.2)	< 0.001
Troponin, ng/L	36.9 (15.6-109.5)	103.5 (49.8-314.0)	< 0.001
Peak NT-proBNP, pg/mL	945.0 (323.5-4352.5)	9277 (5417-15664.5)	< 0.001
TSH, µIU/mL	1.4 (0.9-2.2)	1.7 (0.8-2.6)	0.439
Thyroxine, µg/dL	1.3 (1.1-1.6)	1.3 (1.1-1.6)	0.539
Glucose, mg/dL	131.2 ± 55.5	168.5 ± 85.6	0.001
Sodium, mEq/L	135.0 ± 4.4	134.1± 6.7	0353
Potassium, mEq/L	4.4 ± 0.7	4.4 ± 0.7	0.790
Peak CAR	5.0 (2.5-7.4)	8.1 (6.5-10.9)	< 0.001
PIV	900.6 (320.6-2112.1)	1991.8 (694.2-4094.2)	< 0.001
SII	1068.9 (597.6-2337.6)	2026.2 (968.6-3289.2)	0.005
SIRI	3.7 (1.7-11.4)	11.1 (4.4-28.3)	< 0.001
NLR	5.0 (3.2-12.0)	9.3 (4.8-19.0)	0.001

Values are presented as numbers (n) and percentages (%), mean ± standard deviation, or median (interquartile range, 25th-75th percentiles). *A p-value of <0.05 was considered statistically significant. Abbreviations: AST, Aspartate Aminotransferase; BMI, Body Mass Index; BUN, Blood Urea Nitrogen; CAD, Coronary Artery Disease; CAR, C-Reactive Protein-to-Albumin Ratio; CKD, Chronic Kidney Disease; COPD, Chronic Obstructive Pulmonary Disease; CRP, C-Reactive Protein; CVA, Cerebrovascular Accident; DM, Diabetes Mellitus; HT, Hypertension; IE, Infective Endocarditis; IV, Intravenous; LVEF, Left Ventricular Ejection Fraction; NLR, Neutrophil-to-Lymphocyte Ratio; NT-proBNP, N-Terminal Pro-B-Type Natriuretic Peptide; NYHA, New York Heart Association; PIV, Pan-Immune Inflammation Value; SII, Systemic Immune-Inflammation Index; SIRI, Systemic Inflammatory Response Index; TSH, Thyroid Stimulating Hormone.

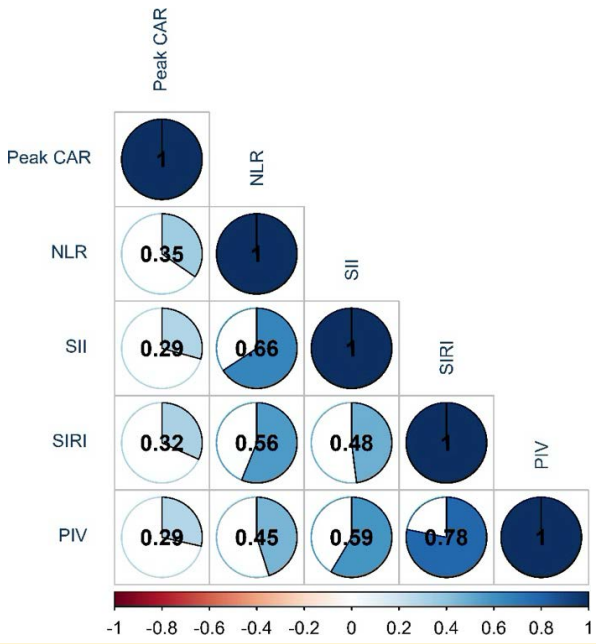

Figure 1. Visualization of the correlation matrix of inflammatory indices. The color legend illustrates the strength of correlation: the intensity of the color reflects the correlation coefficient, with darker shades indicating higher correlation coefficients. Corresponding correlation coefficients are represented using pie charts.

CAR, C-Reactive Protein-to-Albumin Ratio; NLR, Neutrophil-to-Lymphocyte Ratio; PIV, Pan-Immune Inflammation Value; SII, Systemic Immune-Inflammation Index; SIRI, Systemic Inflammatory Response Index.

Multivariate Cox proportional hazards regression analysis, adjusted following univariable analysis of variables selected using the LASSO method, demonstrated that in patients with infective endocarditis, PIV (adjusted HR [aHR] = 1.04, 95% CI: 1.00-1.08, P = 0.039), SII (aHR = 1.13, 95% CI: 1.04-1.23, P = 0.005), NLR (aHR = 1.59, 95% CI: 1.18-2.15, P < 0.001), and peak CAR (aHR = 1.16, 95% CI: 1.10-1.23, P < 0.001) were independently associated with in-hospital mortality (Table 2). Furthermore, multivariable Cox regression analysis including peak CAR revealed that the NYHA class made the largest contribution to the model, followed by peak NT-proBNP and peak CAR (Appendix 1). When examining correlations among hematologic inflammatory biomarkers, peak CAR showed a significant but weak positive correlation with the other indices ($r \leq 0.35$ and $P < 0.05$) (Figure 1).

Results of the ROC analysis indicated that peak CAR had stronger discriminatory power for predicting in-hospital mortality compared to NLR (NRI = 70.1%, IDI = 15.5%), PIV (NRI = 68.8%, IDI = 17.3%), SII (NRI = 71.4%, IDI = 17.8%), and SIRI (NRI = 54.6%, IDI = 14.8%) (Figure 2, Table 3). Kaplan-Meier curve analysis, based on peak CAR dichotomized by X-tile analysis (< 12.7 = low vs. ≥ 12.7 = high), demonstrated that individuals with high peak CAR had increased in-hospital mortality (34.0% vs. 73.3%, plog-rank < 0.001) (Figure 3). Additionally, decision curve analysis showed that models incorporating peak CAR, along with LASSO-derived parameters, provided a net clinical benefit across nearly all thresholds when compared to both the treat-none/treat-all strategies and models without CAR (Figure 4).

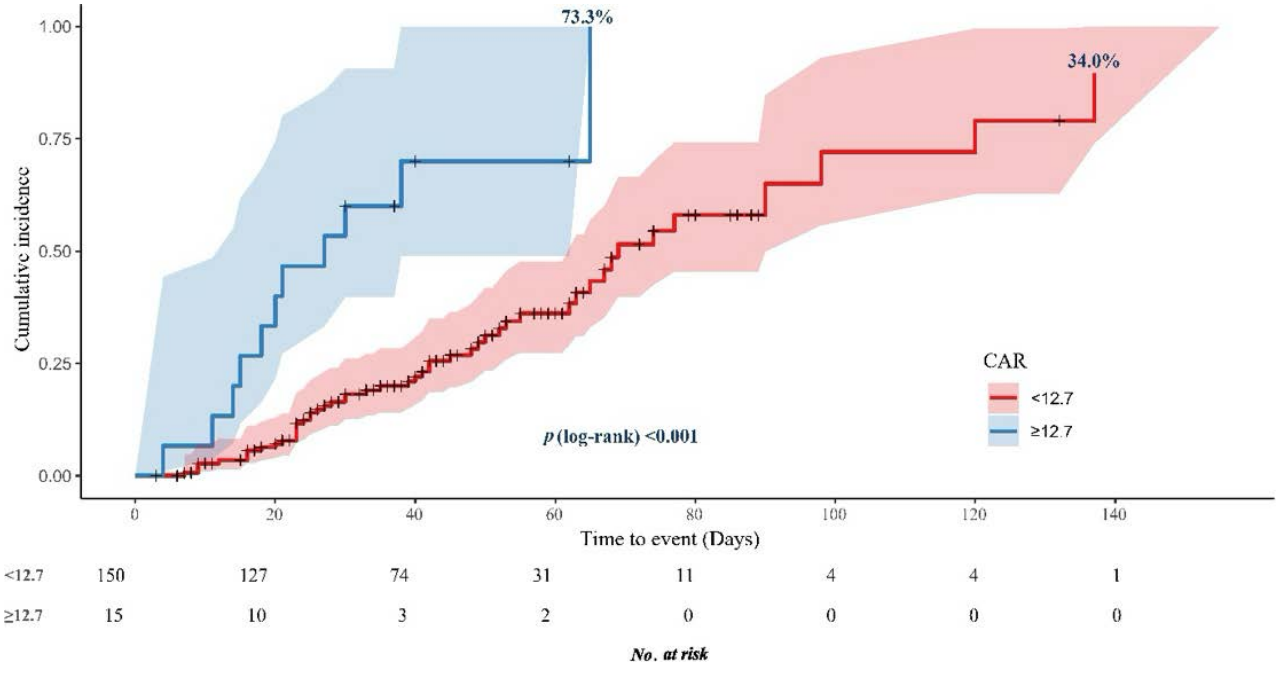

Figure 2. Receiver operating characteristic curve analysis of selected inflammatory biomarkers as predictors of in-hospital mortality among patients with infective endocarditis.

CAR, C-Reactive Protein-to-Albumin Ratio; NLR, Neutrophil-to-Lymphocyte Ratio; PIV, Pan-Immune Inflammation Value; SII, Systemic Immune-Inflammation Index; SIRI, Systemic Inflammatory Response Index.

Table 2. Multivariable proportional hazards regression models for in-hospital mortality

Indices	aHR (95% CI)	P*
PIV, per 1000 units	1.04 (1.00–1.08)	0.039
SII, per 1000 units	1.13 (1.04–1.23)	0.005
SIRI, per 100 units	0.58 (0.22–1.57)	0.300
NLR, per 10 units	1.59 (1.18–2.15)	< 0.001
Peak CAR	1.16 (1.10–1.23)	< 0.001

All models were adjusted for the following covariates; age, body mass index, aspartate transaminase, troponin, white blood cell count, thyroxine (T4) level, urea, NYHA class, peak N-terminal pro-B-type natriuretic peptide level, vegetation size, treatment type, and infective endocarditis type. *A p-value of <0.05 was considered statistically significant. Abbreviations: aHR, Adjusted Hazard Ratio; CAR, C-Reactive Protein-to-Albumin Ratio; CI, Confidence Interval; NLR, Neutrophil-to-Lymphocyte Ratio; PIV, Pan-Immune Inflammation Value; SII, Systemic Immune-Inflammation Index; SIRI, Systemic Inflammatory Response Index.

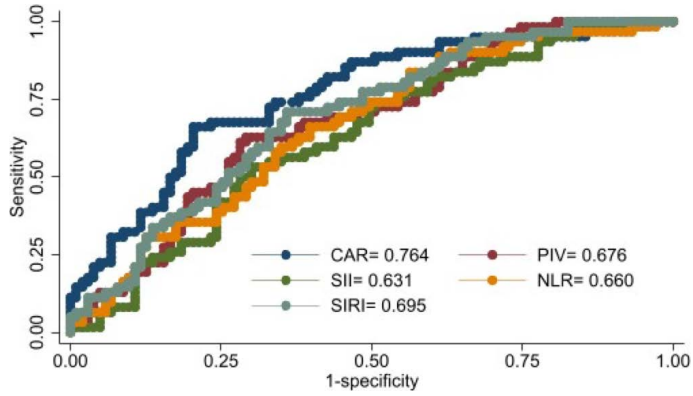

Figure 3. Kaplan-Meier curves illustrating in-hospital mortality stratified by peak C-reactive protein-to-albumin ratio (CAR) levels.

CAR, C-Reactive Protein-to-Albumin Ratio.

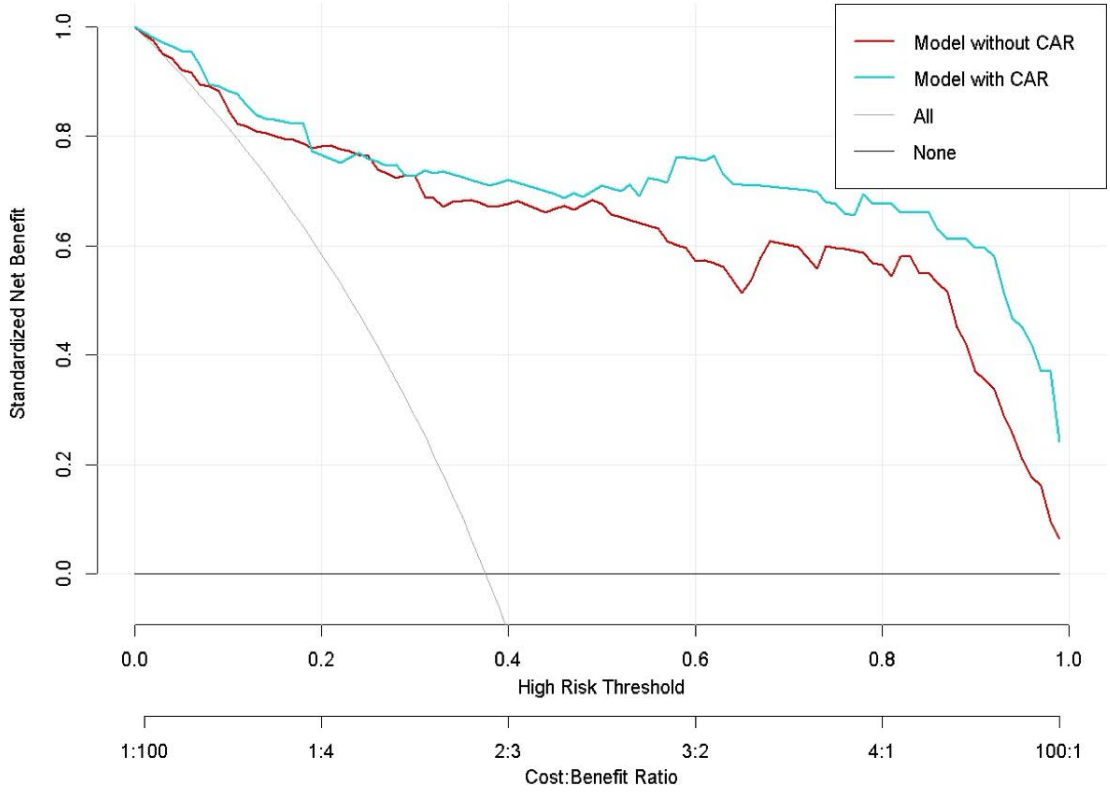

Figure 4. Decision curve analysis illustrating the standardized net benefit of inflammatory indices for predicting in-hospital mortality. The y-axis represents net benefit, while the x-axis indicates the threshold probability of mortality associated with C-reactive protein-to-albumin ratio (CAR).

CAR; C-Reactive Protein-to-Albumin Ratio.

Discussion

In this study, we investigated the predictive value of inflammatory indices for in-hospital mortality in IE patients, with a particular focus on peak CAR, alongside other established risk factors. Our findings highlight the significance of peak CAR as a superior prognostic biomarker in this patient population compared to traditional inflammatory indices.

Despite advances in medical and surgical treatments, high in-hospital mortality rates continue to be reported in patients with IE.[2,3,18] Murdoch et al.[21] reported an in-hospital mortality rate of approximately 18% in a large, international cohort of IE patients, while a multicenter cohort from Türkiye found an in-hospital mortality rate of approximately 33%.[22] In our study, the in-hospital mortality rate was 37.6%, which is relatively higher than those reported in other studies. Several factors may

Table 3. Comparative analyses of the discriminatory and reclassification abilities of certain inflammatory indices in predicting in-hospital all-cause mortality

	Discrimination and reclassification								
	Goodness of fit			Net reclassification improvement			Integrated Discrimination Index		
	C-Index	95% CI	P	NRI	Index (95% CI)	P	IDI	Index (95% CI)	P
CAR	0.764	0.691-0.826	**< 0.001**	ref	ref	-	ref	ref	-
NLR	0.660	0.583-0.732	**0.001**	-0.701	-(0.997-0.405)	**< 0.001**	-0.155	-(0.219-0.091)	**< 0.001**
SII	0.631	0.553-0.705	**0.005**	-0.714	-(1.008-0.420)	**< 0.001**	-0.178	-(0.242-0.114)	**< 0.001**
SIRI	0.695	0.619-0.764	**< 0.001**	-0.546	-(0.850-0.242)	**< 0.001**	-0.148	-(0.215-0.081)	**< 0.001**
PIV	0.676	0.599-0.747	**< 0.001**	-0.688	-(0.985-0.392)	**< 0.001**	-0.173	-(0.237-0.108)	**< 0.001**

*A P-value of <0.05 was considered statistically significant. CAR, C-Reactive Protein-to-Albumin Ratio; CI, Confidence Interval; IDI, Integrated Discrimination Improvement; NLR, Neutrophil-to-Lymphocyte Ratio; NRI, Net Reclassification Improvement; PIV, Pan-Immune Inflammation Value; SII, Systemic Immune-Inflammation Index; SIRI, Systemic Inflammatory Response Index.

explain the elevated mortality rate observed in our study. First, our study population included a higher proportion of patients with critical clinical conditions such as chronic renal failure, stroke, advanced age, and NYHA class III or IV heart failure. Second, as a tertiary referral center, our institution receives patients with more complex and severe clinical presentations, which may contribute to the increased mortality. Third, we observed higher rates of prosthetic valve endocarditis in our cohort, while the rates of surgical intervention, known to be associated with improved outcomes, were relatively low. The challenges of redo surgeries and the high surgical risk associated with comorbidities led both physicians and patients to prefer medical treatment, which was reflected in the mortality rates. In addition to these factors, differences in healthcare systems, diagnostic criteria, and treatment protocols across studies may also contribute to the observed variability in mortality rates.

Owing to the high mortality rate, basic risk classification among IE patients remains a key topic of discussion. Identifying high-risk patients using established predictors aims to improve early referral, surgical management, and treatment-related decision-making. At this point, systemic inflammation, which plays a central role in the pathophysiology of IE, is considered fundamental.[5,7] Numerous studies have focused on the prognostic value of inflammatory markers, and impactful findings continue to emerge for clinical application.[7,10,21] It has been demonstrated that CRP, a well-known marker of inflammation, also holds prognostic value in patients with IE.[7,10,12] The influence of initial CRP levels and/or repeated measurements on outcomes such as mortality and peripheral embolism has been shown in various studies.[12,13] Similarly, serum albumin, another serum parameter, is known to reflect a patient's nutritional and inflammatory status.[23] A low albumin level is a significant determinant of mortality in many cardiovascular diseases, including IE, due to increased inflammation, oxidative stress, and the formation of a pro-thrombotic environment.[11,24-26] Furthermore, combining these two markers into CAR has been shown to enhance prognostic assessment in cardiovascular diseases and more comprehensively reflect the patient's overall condition.[14-17] In a study involving approximately 6,414 sepsis patients, Zhou et al.[27] reported that those with high CAR levels had significantly higher in-hospital mortality compared to those with low CAR. Similarly, Baykız et al.[17] demonstrated that high CAR levels were associated with a composite outcome of mortality and the need for intensive care unit treatment in approximately 196 patients with IE. In the present study, high CAR levels were also associated with in-hospital mortality. Unlike the aforementioned studies, we used peak CAR levels rather than admission CAR, as repeated CRP measurements are known to offer greater sensitivity.[13] Moreover, to increase the sensitivity and accuracy of our analysis, we applied the LASSO regression model to identify predictors of mortality and used X-tile analysis to determine the optimal CAR cutoff value (< 12.7) for clinical risk stratification.

White blood cell subsets and platelets, which are important components of inflammation, are other critical parameters examined to identify risk groups in IE patients.[28] Indices derived from these cell groups, such as SII, NLR, and the platelet-lymphocyte ratio, have been shown to predict outcomes in IE patients in various studies.[17,28,29] In our study, the superiority of peak CAR over other inflammatory indices such as NLR, SII, SIRI, and PIV was notable. As demonstrated in the correlation matrix, peak CAR showed a strong correlation with mortality but only limited correlation with the other indices derived from WBC subsets. While these indices also reflect the systemic inflammatory response, peak CAR exhibited the highest discriminatory ability for predicting in-hospital mortality, as evidenced by ROC curve analysis, as well as NRI and IDI analyses. This suggests that peak CAR captures critical aspects of the inflammatory response not fully accounted for by other indices.

A high CAR level provides prognostic value that complements and enhances the predictive power of traditional markers in infective endocarditis.[7,17] Traditional risk factors such as age, renal insufficiency, cardiac biomarkers, microorganism type, and the presence of heart failure are well-established predictors of adverse outcomes.[3,10] These markers typically reflect individual aspects of the disease process, such as patient demographics, organ dysfunction, or microbial virulence.[3,7] For example, while cardiac biomarkers such as troponins and BNP primarily reflect myocardial stress or injury, CAR provides insight into the systemic burden of inflammation and its impact on the patient's metabolic reserves.[8] Similarly, although renal insufficiency or specific microorganisms like *Staphylococcus aureus* indicate severe disease, these factors do not directly quantify the ongoing inflammatory process.[3] By combining CRP and albumin, CAR offers a dynamic, real-time indicator of the systemic response to infection and the host's capacity to

recover.[15,17] In this study, we observed that patients with higher CAR values had significantly higher in-hospital mortality, even after adjusting for classical prognostic factors. This suggests that CAR captures additional dimensions of patient status that are not fully addressed by traditional markers. Furthermore, the simplicity and accessibility of CAR make it a practical addition to routine clinical assessments.[14,17] Unlike some classical markers that require specialized testing or may have limited availability in resource-constrained settings, CRP and albumin are widely available and cost-effective. This positions CAR as a viable tool for risk stratification, particularly in settings where advanced diagnostic methods are not readily available.

Our study has several limitations. First, the retrospective design may introduce bias and limit the ability to establish a causal relationship between peak CAR and in-hospital mortality. Further prospective studies are needed to validate these findings. Second, this study was conducted at a tertiary care center, and the patient population may not reflect the broader spectrum of IE cases seen in different healthcare settings or geographic regions. This could affect the generalizability of the results. Third, despite rigorous data collection, there may have been missing or incomplete data that could impact the accuracy of inflammatory indices and the overall findings. Fourth, it is important to acknowledge the need for meticulous and cautious interpretation of the results given the limited sample size. To ensure the generalizability of the results, comprehensive studies involving larger and more diverse patient cohorts are required. Lastly, laboratory measurements for CRP and albumin may vary due to differences in assay methods and the timing of sample collection, which could influence the calculation of peak CAR. Additionally, we lacked data on patients' dietary habits, which may have affected albumin levels.

Conclusion

Peak CAR is a valuable prognostic marker for in-hospital mortality in IE patients, outperforming traditional inflammatory markers and other composite indices. Incorporating peak CAR into clinical practice could enhance risk stratification and guide therapeutic decision-making, potentially improving outcomes in this challenging patient population. Future research should aim to validate these findings in larger, multicenter cohorts and explore the potential benefits of targeted interventions based on CAR levels.

Ethics Committee Approval: Ethics committee approval was obtained from Başakşehir Çam and Sakura Hospital Clinical Research Ethics Committee (Approval Number: 87, Date: 14.02.2024).

Informed Consent: Informed consent was waived due to the retrospective nature of the study.

Conflict of Interest: The authors have no conflicts of interest to declare.

Funding: The authors declared that this study received no financial support.

Use of AI for Writing Assistance: Artificial intelligence-assisted technologies were not used in the production of this study.

Author Contributions: Concept – D.İ.; Design – D.İ., A.K., Ö.G.; Supervision – A.İ.D.M., A.E., A.İ.T.; Resource – D.İ., D.G.A., F.Ö.P.; Materials – D.İ., A.İ.D.M., S.T.Y.; Data Collection and/or Processing – D.İ., D.G.A., F.Ö.P., F.Z.E., C.O.; Analysis and/or Interpretation – D.İ., A.K., A.İ.D.M.; Literature Review – D.İ.; Writing – D.İ.; Critical Review – A.E., A.İ.T., Ö.G.

Acknowledgments: The authors thank all doctors, nurses and other health providers involved in caring for our IE patients.

Peer-review: Externally peer-reviewed.

References

1. Hubers SA, DeSimone DC, Gersh BJ, Anavekar NS. Infective endocarditis: A contemporary review. *Mayo Clin Proc*. 2020;95(5):982-997. [CrossRef]
2. Chen H, Zhan Y, Zhang K, et al. The global, regional, and national burden and trends of infective endocarditis from 1990 to 2019: Results from the global burden of disease study 2019. *Front Med (Lausanne)*. 2022;9:774224. [CrossRef]
3. Marques A, Cruz I, Caldeira D, et al. Risk factors for in-hospital mortality in infective endocarditis. *Arq Bras Cardiol*. 2020;114(1):1-8.
4. Cahill TJ, Prendergast BD. Infective endocarditis. *Lancet*. 2016;387(10021):882-893. [CrossRef]
5. Vincent LL, Otto CM. Infective endocarditis: Update on epidemiology, outcomes, and management. *Curr Cardiol Rep*. 2018;20(10):86. [CrossRef]
6. Khan S, Rasool ST. Current use of cardiac biomarkers in various heart conditions. *Endocr Metab Immune Disord Drug Targets*. 2021;21(6):980-993. [CrossRef]
7. Cornelissen CG, Frechen DA, Schreiner K, Marx N, Krüger S. Inflammatory parameters and prediction of prognosis in infective endocarditis. *BMC Infect Dis*. 2013;13:272. [CrossRef]
8. Siciliano RF, Gualandro DM, Mueller C, et al. Incremental value of B-type natriuretic peptide for early risk prediction of infective endocarditis. *Int J Infect Dis*. 2014;29:120-124. [CrossRef]
9. Turak O, Canpolat U, Ozcan F, et al. D-dimer level predicts in-hospital mortality in patients with infective endocarditis: A prospective single-centre study. *Thromb Res*. 2014;134(3):587-592. [CrossRef]
10. Kocazeybek B, Küçükoğlu S, Oner YA. Procalcitonin and C-reactive protein in infective endocarditis: Correlation with etiology and prognosis. *Chemotherapy*. 2003;49(1-2):76-84. [CrossRef]
11. Huang S, Zhou Z, Luo L, et al. Preoperative serum albumin: A promising indicator of early mortality after surgery for infective endocarditis. *Ann Transl Med*. 2021;9(18):1445. [CrossRef]
12. Mohanan S, Nair RG, Vellani H, CG S, George B, MN K. Baseline C-reactive protein levels and prognosis in patients with infective endocarditis: A prospective cohort study. *Indian Heart J*. 2018;70(Suppl):S43-S49. [CrossRef]
13. Verhagen DW, Hermanides J, Korevaar JC, et al. Prognostic value of serial C-reactive protein measurements in left-sided native valve endocarditis. *Arch Intern Med*. 2008;168(3):302-307. [CrossRef]
14. Tanık VO, Akdeniz E, Çınar T, et al. Higher C-reactive protein to albumin ratio portends long-term mortality in patients with chronic heart failure and reduced ejection fraction. *Medicina (Kaunas)*. 2024;60(3):441. [CrossRef]
15. Lindsey MH, Xiong GX, Lightsey HM 4th, et al. C-reactive protein-to-albumin ratio in spinal epidural abscess: Association with post-treatment complications. *J Am Acad Orthop Surg*. 2022;30(17):851-857. [CrossRef]
16. Özcan S, Dönmez E, Yavuz Tuğrul S, et al. The prognostic value of C-reactive protein/albumin ratio in acute pulmonary embolism. *Rev Invest Clin*. 2022;74(2):97-103. [CrossRef]
17. Baykiz D, Govdeli EA, Demirtakan ZG, Elitok A, Umman B, Bugra Z. Prognostic value of the C-reactive protein-to-albumin ratio in patients with infective endocarditis. *Eur Rev Med Pharmacol Sci*. 2022;26(23):8728-8737.
18. Delgado V, Ajmone Marsan N, de Waha S, et al. 2023 ESC Guidelines for the management of endocarditis. *Eur Heart J*. 2023;44(39):3948-4042. [CrossRef]
19. Hua X, Duan F, Zhai W, et al. A novel inflammatory-nutritional prognostic scoring system for patients with early-stage breast cancer. *J Inflamm Res*. 2022;15:381-394. [CrossRef]

20. Fucà G, Guarini V, Antoniotti C, et al. The pan-immune-inflammation value is a new prognostic biomarker in metastatic colorectal cancer: Results from a pooled-analysis of the Valentino and TRIBE first-line trials. *Br J Cancer*. 2020;123(3):403-409. [CrossRef]
21. Murdoch DR, Corey GR, Hoen B, et al. Clinical presentation, etiology, and outcome of infective endocarditis in the 21st century: The International Collaboration on Endocarditis-Prospective Cohort Study. *Arch Intern Med*. 2009;169(5):463-473. [CrossRef]
22. Elbey MA, Akdağ S, Kalkan ME, et al. A multicenter study on experience of 13 tertiary hospitals in Turkey in patients with infective endocarditis. *Anadolu Kardiyol Derg*. 2013;13(6):523-527. [CrossRef]
23. Don BR, Kaysen G. Serum albumin: Relationship to inflammation and nutrition. *Semin Dial*. 2004;17(6):432-437. [CrossRef]
24. Ronit A, Kirkegaard-Klitbo DM, Dohlmann TL, et al. Plasma albumin and incident cardiovascular disease: Results from the CGPS and an updated meta-analysis. *Arterioscler Thromb Vasc Biol*. 2020;40(2):473-482. [CrossRef]
25. Erdogan A, Genc O, Ozkan E, et al. Impact of Naples prognostic score at admission on in-hospital and follow-up outcomes among patients with ST-segment elevation myocardial infarction. *Angiology*. 2023;74(10):970-980. [CrossRef]
26. Pay L, Yumurtaş AÇ, Tezen O, et al. Prognostic value of serum albumin in heart failure patients with cardiac resynchronization therapy. *Biomark Med*. 2024;18(8):363-371. [CrossRef]
27. Zhou X, Fu S, Wu Y, et al. C-reactive protein-to-albumin ratio as a biomarker in patients with sepsis: A novel LASSO-COX based prognostic nomogram. *Sci Rep*. 2023;13(1):15309. [CrossRef]
28. Zencir C, Akpek M, Senol S, et al. Association between hematologic parameters and in-hospital mortality in patients with infective endocarditis. *Kaohsiung J Med Sci*. 2015;31(12):632-638. [CrossRef]
29. Agus HZ, Kahraman S, Arslan C, et al. Systemic immune-inflammation index predicts mortality in infective endocarditis. *J Saudi Heart Assoc*. 2020;32(1):58-64. [CrossRef]

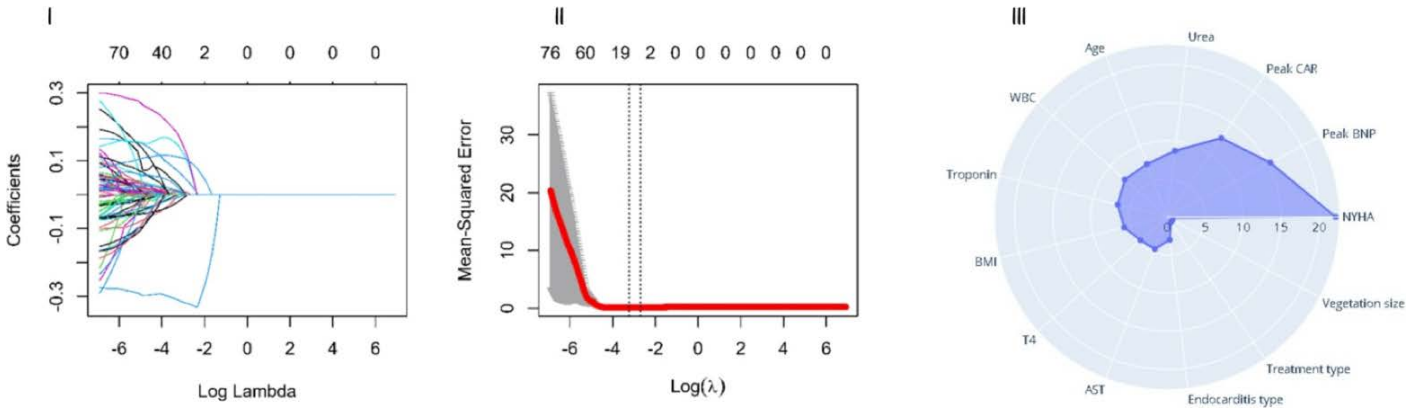

Appendix 1. The least absolute shrinkage and selection operator (LASSO) penalized feature selection to be adjusted for subsequent multivariable Cox regression analyses. I) Coefficient profile plots illustrate how the magnitude of coefficients for covariates decreases as the λ penalty increases. Factors and their corresponding regression coefficients are selected for the model based on the optimal λ value identified by the LASSO model. II) The plot displays the distribution of minimum mean squared errors along with their respective penalization lambda values in the LASSO-penalized model. III) Variable importance plot of the parameters selected with LASSO regression in the model.

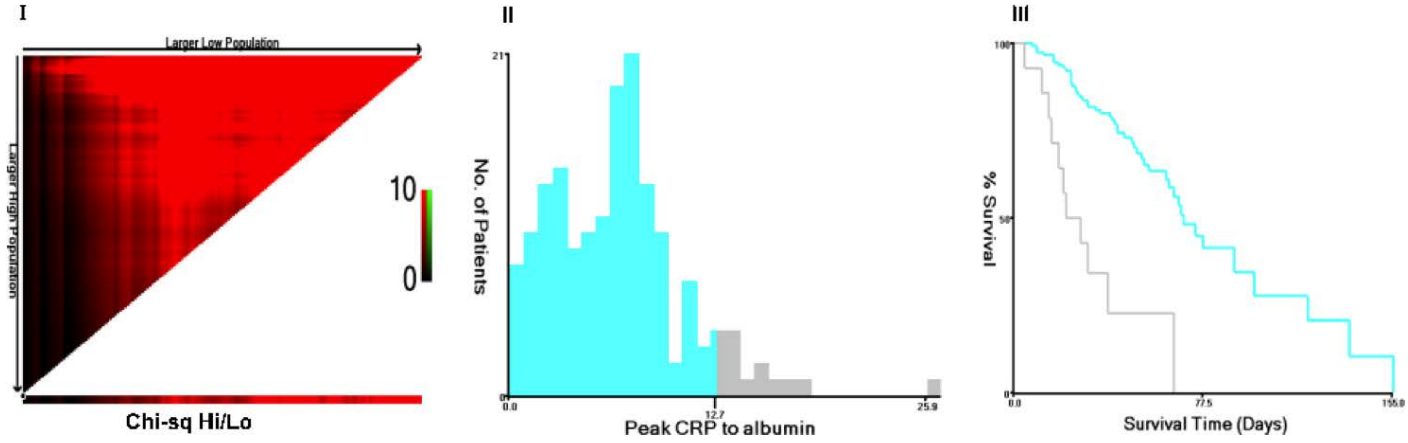

Appendix 2. X-tile analysis used to determine the optimal cut-off value for peak C-reactive protein-to-albumin ratio (CAR).

CAR, C-Reactive Protein-to-Albumin Ratio.

ARCHIVES OF THE TURKISH SOCIETY OF CARDIOLOGY

Official journal of the TURKISH SOCIETY OF CARDIOLOGY

Frontal QRS-T Angle as a Prognostic Marker of Long-Term Mortality in Hemodialysis Patients

Frontal QRS-T Açısının Hemodiyaliz Hastalarında Uzun Dönem Mortaliteyi Öngörmedeki Prognostik Değeri

ABSTRACT

Objective: The electrocardiogram is a crucial, cost-effective, and noninvasive tool for assessing the risk of cardiac morbidity and mortality. The frontal QRS-T angle is a marker of ventricular repolarization. This study investigated whether the frontal QRS-T angle could predict mortality in hemodialysis patients over a seven-year follow-up period.

Method: The study included 110 patients undergoing regular hemodialysis. Frontal QRS-T angles greater than 90 degrees were classified as wide. Patients were categorized based on the width of the QRS-T angle and the presence or absence of mortality. Electrocardiogram (ECG) parameters measured included the QRS, T axis, TP/QT ratio, fragmented QRS, TPe/QTc ratio, and the frontal QRS-T angle, defined as the absolute difference between the frontal QRS and T axes.

Results: A total of 37 patients (34%) had a wide frontal QRS-T angle. The mean age was significantly higher in both the wide frontal QRS-T angle group and the deceased group. Ejection fraction was lower and the frontal QRS-T angle was wider in the mortality group (94 [31-113] vs. 33 [16-80], P < 0.001). In univariate and multivariate logistic regression analyses, having a wide QRS-T angle was associated with increased mortality (odds ratio [OR]: 8.08, confidence interval [CI]: 2.75-23.74, P < 0.001). Additionally, the presence of fragmented QRS also increased mortality risk (OR: 11.25, CI: 2.98-42.49, P < 0.001).

Conclusion: Our findings demonstrate the independent prognostic value of the frontal QRS-T angle in patients undergoing hemodialysis, irrespective of ejection fraction status. This suggests that it may serve as a valuable tool in routine cardiovascular risk assessments, contributing to improved management strategies for this high-risk population.

Keywords: Frontal QRS-T angle, hemodialysis, long-term mortality

ÖZET

Amaç: Elektrokardiyogram (EKG), kardiyak morbidite ve mortalite riskinin değerlendirilmesinde maliyet etkin, hızlı ve noninvaziv bir yöntemdir. Frontal QRS-T açısı, ventriküler repolarizasyonun önemli belirteçlerinden biridir. Bu çalışmada, hemodiyaliz hastalarında frontal QRS-T açısının 7 yıllık takip sürecinde mortaliteyi öngörüp öngöremeyeceği araştırılmıştır.

Yöntem: Çalışmaya 110 hemodiyaliz hastası dahil edilmiştir. Geniş frontal QRS-T açısı, >90° olarak tanımlanmıştır. Hastalar QRS-T açısının genişliğine ve ölüm durumuna göre iki farklı grupta değerlendirilmiştir. Ölçülebilir EKG parametreleri arasında QRS aksı, T dalga aksı, TP/QT oranı, fragmented QRS, TPe/QTc oranı ve frontal QRS-T açısı yer almıştır. Frontal QRS-T açısı, frontal düzlemdeki QRS ve T vektörleri arasındaki mutlak açı farkı olarak tanımlanmıştır.

Bulgular: Hastaların 37'sinde (%34) geniş frontal QRS-T açısı saptanmıştır. Geniş QRS-T açısına sahip ve hayatını kaybeden grupta ortalama yaş daha yüksekti. Ayrıca, mortalite grubunda ejeksiyon fraksiyonu daha düşük saptanmıştır. Frontal QRS-T açısı, mortalite grubunda anlamlı olarak daha geniş bulunmuştur (94 [31-113] vs. 33 [16-80], P < 0,001). Tek - çok değişkenli lojistik regresyon analizlerinde, geniş açılı grupta yer almak mortalite riskini artırmıştır (OR: 8,08; GA: 2,75–23,74; P < 0,001). Benzer şekilde, fragmented QRS varlığı da mortalite ile ilişkili saptanmıştır (OR: 11,25; GA: 2,98–42,49; P < 0,001).

Sonuç: Bulgularımız, frontal QRS-T açısının ejeksiyon fraksiyonundan bağımsız olarak hemodiyaliz hastalarında mortaliteyi öngörmede bağımsız bir prognostik gösterge olduğunu ortaya koymaktadır. Bu açıdan, frontal QRS-T açısının kardiyovasküler risk değerlendirme sürecine entegre edilmesi, bu kırılgan hasta grubunda daha etkili risk yönetimi stratejileri geliştirilmesine fayda sağlayabilir.

Anahtar Kelimeler: Frontal QRS-T açısı, hemodiyaliz, uzun dönem mortalite

ORIGINAL ARTICLE
KLİNİK ÇALIŞMA

Çağlar Kaya[1]
Mustafa Ebik[1]
Cihan Öztürk[1]
Merve Akbulut Çakır[1]
Emirhan Çakır[1]
İlhan Kılıç[2]

[1]Department of Cardiology, Trakya University, Edirne, Türkiye
[2]Department of Nephrology, Çanakkale Onsekiz Mart University, Çanakkale, Türkiye

Corresponding author:
Çağlar Kaya
✉ caglarkaya2626@gmail.com

Received: April 25, 2025
Accepted: June 29, 2025

Cite this article as: Kaya Ç, Ebik M, Öztürk C, Akbulut Çakır M, Çakır E, Kılıç İ. Frontal QRS-T Angle as a Prognostic Marker of Long-Term Mortality in Hemodialysis Patients. *Turk Kardiyol Dern Ars.* 2025;53(7):510–517.

DOI: 10.5543/tkda.2025.98252

Copyright@Author(s)
Available online at archivestsc.com.
Content of this journal is licensed under a Creative Commons Attribution – NonCommercial-NoDerivatives 4.0 International License.

Cardiovascular disease remains the leading cause of mortality among patients with end-stage renal disease undergoing hemodialysis. The electrocardiogram (ECG) is an effective tool for assessing the risk of cardiac morbidity and overall mortality due to its affordability, noninvasive nature, and ability to deliver rapid results. The frontal QRS-T angle (fQRSTa), derived from the QRS axis and the T wave axis on a 12-lead ECG, serves as an important marker of ventricular repolarization.[1,2] Numerous studies have employed both frontal and spatial methods to calculate the fQRSTa. In these studies, the diagnostic and prognostic benefits of each method are often directly compared. Each study has reported different values and established its own threshold values and reference ranges.[3,4] Some studies have established a correlation between a wide fQRSTa and adverse cardiac events in hemodialysis patients.[5] As a result, developing predictive parameters to assess cardiac conditions in patients undergoing hemodialysis has become essential. ECG remains a fundamental, noninvasive tool for the early detection of electrical and structural cardiac abnormalities. This study aimed to evaluate the long-term prognostic value of the frontal QRS-T angle in chronic hemodialysis patients, with particular emphasis on its association with all-cause mortality over a seven-year follow-up period.

ABBREVIATIONS

BMI	Body mass index
CAD	Coronary artery disease
CI	Confidence interval
CRP	C-reactive protein
DM	Diabetes mellitus
ECG	Electrocardiogram
EF	Ejection fraction
fQRSTa	Frontal QRS-T angle
HF	Heart failure
HT	Hypertension
IVSWT	Interventricular septal wall thickness
LV	Left ventricle
LVEDD	Left ventricular end-diastolic diameter
LVEF	Left ventricular ejection fraction
LVESD	Left ventricular end-systolic diameter
MI	Myocardial infarction
PWT	Posterior wall thickness
QTc	Corrected QT interval
RA	Right atrium
ROC	Receiver operating characteristic
SCD	Sudden cardiac death
SPSS	Statistical Package for the Social Sciences
TP-e	Tpeak to Tend Interval
TP/QT	Tpeak to Tend interval/QT interval ratio
TP/QTc	Tpeak to Tend interval/Corrected QT interval ratio

Materials and Methods

A total of 110 hemodialysis patients were enrolled in this retrospective study, which was conducted through a review of archived patient records. Only hemodialysis patients were included; those receiving peritoneal dialysis were excluded. ECG data were collected during the initial cardiology outpatient visits between January 2017 and January 2024. Due to the retrospective nature of the study, the mean follow-up duration was calculated only for deceased patients, averaging 3.62 ± 1.7 years. All patients underwent standard intermittent hemodialysis. Dialysis frequency was either two or three sessions per week, depending on clinical indication. The hemodialysis technique and equipment were consistent across the study population. Patients with atrial fibrillation, pacemakers, right or left bundle branch block, or left anterior hemiblock were excluded from the study. A standard 12-lead ECG was recorded on the day of hemodialysis, using a paper speed of 25 mm/s and an amplitude calibration of 10 mm/mV. QRS duration, QRS axis, and T wave axis were determined automatically. The frontal QRS-T angle was calculated as the absolute difference between the QRS axis and the T wave axis in the frontal plane, in line with previous definitions.[6,7] ECGs were recorded on non-dialysis days (at least one day apart from any hemodialysis session). Specifically, the QRS axis, T wave axis, TP/QT ratio, fragmented QRS, TPe/QTc ratio, and fQRSTa were documented. The frontal QRS-T angle was automatically calculated by the digital ECG system, based on the difference between the frontal plane QRS and T-wave axes, as previously described by Oehler et al.[1] in 2014.[1,6] The fQRSTa is defined as the absolute difference between the frontal plane QRS axis and the T wave axis. In other words, it represents the angle between the frontal QRS and T vectors (Figure 1). Angles exceeding 180° were adjusted using the formula (360 - angle). A wide QRS-T angle, considered abnormal in prior studies, is defined as greater than 90°.[6] The QT interval was measured from the onset of the QRS to the end of the T wave and corrected using Bazett's formula (QTc). The Tp-e interval was defined as the distance from the T-wave peak to its end in the precordial leads. Fragmented QRS was identified by the presence of R' waves or notching in at least two contiguous

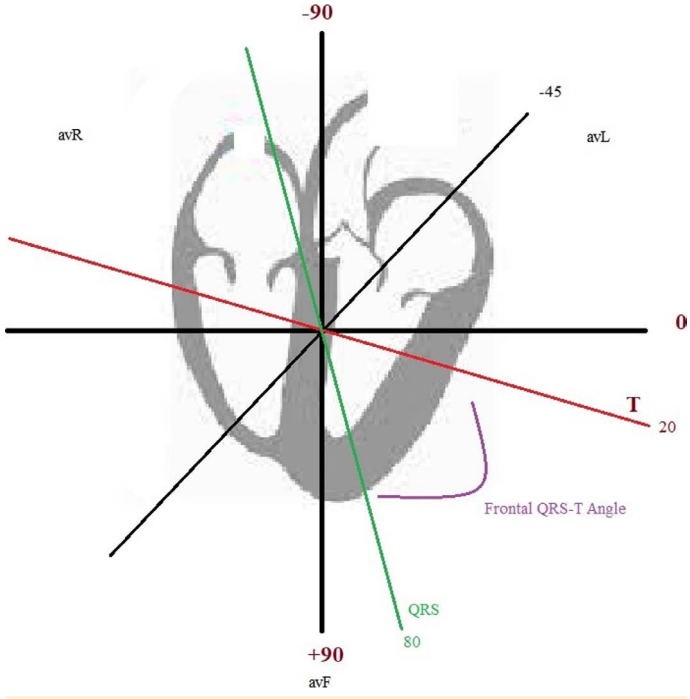

Figure 1. Assessment of the frontal QRS-T angle in a planar plane.

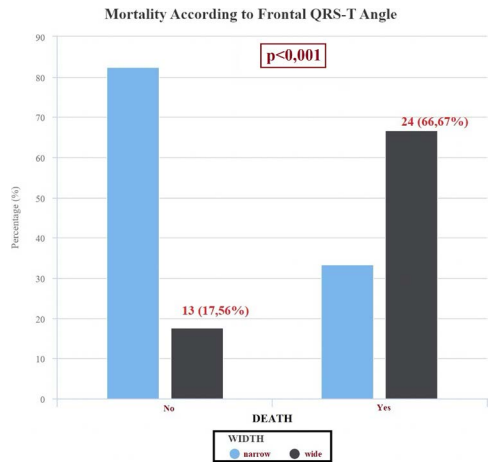

Figure 2. Mortality distribution according to the frontal QRS-T angle.

leads. Patients were grouped based on both the width of the frontal QRS-T angle (wide vs. normal) and mortality status at follow-up (mortality present vs. absent) for comparative analysis. Echocardiographic and laboratory parameters evaluated in the study included left ventricular ejection fraction (LVEF), interventricular septal wall thickness (IVSWT), posterior wall thickness (PWT), left ventricular end-diastolic diameter (LVEDD), and left ventricular end-systolic diameter (LVESD), as well as serum creatinine, potassium (K), hemoglobin (Hb), and calcium (Ca) levels. LVEF was measured using the modified Simpson's method during standard transthoracic echocardiography. Patients with significant left ventricular hypertrophy (wall thickness > 15 mm) were excluded from the study. These parameters were compared between patients with wide and normal frontal QRS-T angles, as well as between those with and without all-cause mortality. Laboratory tests, ECG, and echocardiography were performed on the same day. Ethical approval was obtained from the Institutional Ethics Committee. Additionally, written informed consent was secured from all participants prior to enrollment. The study was approved by the Trakya University Faculty of Medicine Non-Interventional Scientific Research Ethics Committee (Approval Number: 14/10, Date: 02.09.2024). A clinical trial number is not applicable.

Statistical Analysis

All statistical analyses were conducted using SPSS software (version 25.0; SPSS Inc., Chicago, IL). The distribution of continuous variables was assessed using the Shapiro-Wilk test. As most variables were not normally distributed, results were expressed as median (interquartile range, Q1–Q3), and comparisons between groups were performed using the Mann-Whitney U test. Categorical variables were compared using the chi-square or Fisher's exact test, as appropriate. Receiver operating characteristic (ROC) curve analysis was performed to explore the predictive power of the variables, and the area under the curve (AUC) was calculated to assess their overall effectiveness in outcome discrimination. Multivariate logistic regression analysis was conducted to identify independent predictors of the outcome. All statistical tests were two-sided, and a p-value of less than 0.05 was considered statistically significant.

Results

A total of 110 participants were recruited, with a median age of 57 years. Two group comparisons were conducted: one based on the width of the fQRSTa and the other based on mortality status after a seven-year follow-up. During this period, 36 patients (32.73%) were identified as deceased and classified in the mortality group. Among these patients, 24 (67%) exhibited a wide frontal QRS-T angle (fQRSTa), as shown in Figure 2. Patients with an fQRSTa greater than 90 degrees were categorized in the wide group (33.6%), while those with angles below this threshold were classified in the control (normal) group (66.4%). The parameters for both groups are presented in Table 1. The wide group showed a higher prevalence of females and older patients (Table 1). Additionally, body mass index was significantly higher in the wide QRS group (P = 0.005). Older patients were more frequently represented in the mortality group. Notably, both the mortality group and the wide fQRSTa group had a significantly higher incidence of diabetes mellitus (DM). A comparison of electrocardiographic measurements between the groups is shown in Table 2. In the wide group, the median fQRSTa was 96 (range: 94–120). In the mortality group, the fQRSTa was significantly higher (P < 0.001). Fragmented QRS was also more prevalent in the mortality group.

Table 1. Baseline demographic characteristics of the study population by frontal QRS-T angle and mortality status

Variables	Wide frontal QRS-T angle (n = 37)	Normal frontal QRS-T angle (n = 73)	P	Mortality present (n = 36)	Mortality absent (n = 74)	P
Age	63 (57-70)	57 (45-62)	< 0.001	62 (57-71)	57 (45-64)	0.001
Gender - Female	23 (62.16%)	36 (49.31%)	0.202	21 (58.33%)	38 (51.35%)	0.491
HT	32 (86.48%)	54 (73.97%)	0.133	31 (86.11%)	55 (74.32%)	0.160
DM	24 (64.86%)	20 (27.39%)	< 0.001	21 (58.33%)	23 (31.08%)	0.006
Non-smoker	12 (32.43%)	26 (35.61%)	0.533	32 (88.88%)	66 (89.18%)	0.962
CAD	7 (18.91%)	5 (6.84%)	0.055	7 (19.44%)	6 (8.10%)	0.060
Dyslipidemia	9 (24.32%)	6 (8.21%)	0.451	7 (19.44%)	8 (10.81%)	0.216
BMI	29.3 (25-32)	25.4 (22-29)	0.005	29 (26-34)	25 (22-28)	< 0.001

BMI, Body mass index; CAD, Coronary artery disease; DM, Diabetes mellitus; HT, Hypertension.

Table 2. Electrocardiographic parameters of the study population

Variables	Wide fQRSTa (n = 37)	Normal fQRSTa (n = 73)	P	Mortality present (n = 36)	Mortality absent (n = 74)	P
QRS (ms)	92 (84–105)	90 (84–99)	0.403	94 (90–134)	88 (82–98)	0.001
QTc (ms)	439 (416–461)	432 (408–452)	0.268	435 (406–459)	432 (410–452)	0.760
QRS°	-25 (-44–4.5)	34 (1–59)	< 0.001	-2 (-22–49)	19 (-11–50)	0.110
T°	73 (39–98)	58 (41–66)	0.002	68 (51–78)	58 (38–71)	0.054
Tpe	90 (80–110)	70 (65–80)	< 0.001	80 (60–80)	80 (60–80)	0.628
TP/QT	0.22 (0.19–0.30)	0.20 (0.17–0.23)	< 0.001	0.20 (0.18–0.22)	0.20 (0.17–0.24)	0.730
TP/QTc	0.21(0.17–0.25)	0.17 (0.15–0.19)	< 0.001	0.18 (0.16–0.21)	0.18 (0.15–0.21)	0.426
Fragmented QRS	11 (29.72%)	10 (13.69%)	0.043	16 (44.44%)	5 (6.75%)	< 0.001
Frontal QRS–T angle	96 (94–120)	24 (8–50)	< 0.001	94 (31–113)	33 (16–80)	< 0.001

Table 3. Echocardiographic and laboratory parameters of the study population

Variables	Wide fQRSTa (n = 37)	Normal fQRSTa (n = 73)	P	Mortality present (n = 36)	Mortality absent (n = 74)	P
LVEF, %	51 (48–56)	55 (52–60)	0.002	52 (50–57)	55 (50–60)	0.033
IVSWT, mm	12 (10.5–14)	12 (10–15)	0.713	12 (11–14)	12 (10–15)	0.697
PWT, mm	11 (10–12)	11 (10–13)	0.311	11.5 (10.5–13.5)	11 (10–13)	0.675
LVEDD, mm	45 (42.5–48)	46 (42–48.5)	0.696	46.5 (43–48)	46 (41–48)	0.541
LVESD, mm	30 (28–32)	30 (28–32)	0.534	30 (28–33)	29 (27–31)	0.707
Creatinine, mg/dL	4.8 (3.08–6.83)	4.31 (3.3–5.8)	0.599	4.3 (3.3–5.8)	4.56 (3.1–6.6)	0.819
K, mg/dL	4.4 (3.95–4.95)	4.4 (3.9–4.9)	0.685	4.5 (4.05–4.97)	4.4 (3.9–4.9)	0.447
Hb, mg/dL	11.6 (10–12.3)	11.2 (10.4–11.9)	0.325	11.05 (9.8–11.9)	11.55 (10.75–12.35)	0.063
Ca, mg/dL	9.2 (9–10)	9.6 (88.7–9.9)	0.947	9.2 (8.6–9.9)	9.7 (9–10.1)	0.061

Ca, Calcium; Creatinine, Serum Creatinine; CRP, C-Reactive protein; fQRSTa, Frontal QRS-T angle; Hb, Hemoglobin; IVSWT, Interventricular septal wall thickness; K, Potassium; LVEDD, Left ventricular end-diastolic diameter; LVEF, Left ventricular ejection fraction; LVESD, Left ventricular end-systolic diameter; N, Number of patients; PWT, Posterior wall thickness.

Table 3 compares selected echocardiographic and laboratory parameters in the study population, stratified by frontal QRS-T angle width and all-cause mortality status. Patients with a wide frontal QRS-T angle had significantly lower LVEF compared to those with a normal angle (51% (48–56) vs. 55% (52–60), P = 0.002). No statistically significant differences were observed between the groups in IVSWT, PWT, LVEDD, or LVESD (P > 0.05 for all). Similarly, laboratory markers, including serum creatinine, K, Hb, and Ca levels, were comparable between the two groups. In the subgroup analysis based on mortality status, ejection fraction (EF) was again significantly lower in patients in the mortality group compared to those survivors (52% (50–57) vs. 55% (50–60), P = 0.033). No significant differences were observed in structural echocardiographic parameters or serum creatinine and potassium levels between the mortality groups. However, a non-significant trend toward lower hemoglobin and calcium levels was noted among deceased patients compared to survivors (Hb: P = 0.063; Ca: P = 0.061).

A significant correlation was found between the presence of DM and belonging to the wide fQRSTa group (r = 0.3613, P < 0.001). Additionally, a negative correlation was observed between LVEF and the frontal QRS angle (r = -0.2119, P = 0.021). These correlation assessments are presented in Figure 3. The negative relationship between LVEF and fQRSTa is further illustrated in Figure 4. The diagnostic performance of FQRSTa in predicting mortality was evaluated. ROC and sensitivity-specificity curves are shown in Figure 5. The cut-off value determined to predict mortality for fQRSTa was > 92, with sensitivity and specificity estimated at 66.6% and 82.4%, respectively (AUC: 0.71, confidence interval: 0.61–0.79, P < 0.001). Regression analyses were conducted to identify independent predictors of mortality. In the univariate model, age, DM, fQRSTa, wide group classification, and presence of fragmented QRS were all found to be significant (Table 4). In the multivariate analyses, being in the wide fQRSTa group and the presence of fragmented QRS were identified as independent risk factors (Table 4).

Discussion

The main findings of our research are as follows:

1) We established that the fQRSTa, derived from ECG measurements, serves as a significant predictor of mortality in patients undergoing hemodialysis.
2) Our analysis revealed that an fQRSTa exceeding 92 is notably associated with increased mortality.
3) In diabetic patients, we observed both an increased fQRSTa and a significant correlation with other clinical parameters.
4) Furthermore, we found that an increase in fQRSTa in hemodialysis patients is associated with a decrease in LVEF.

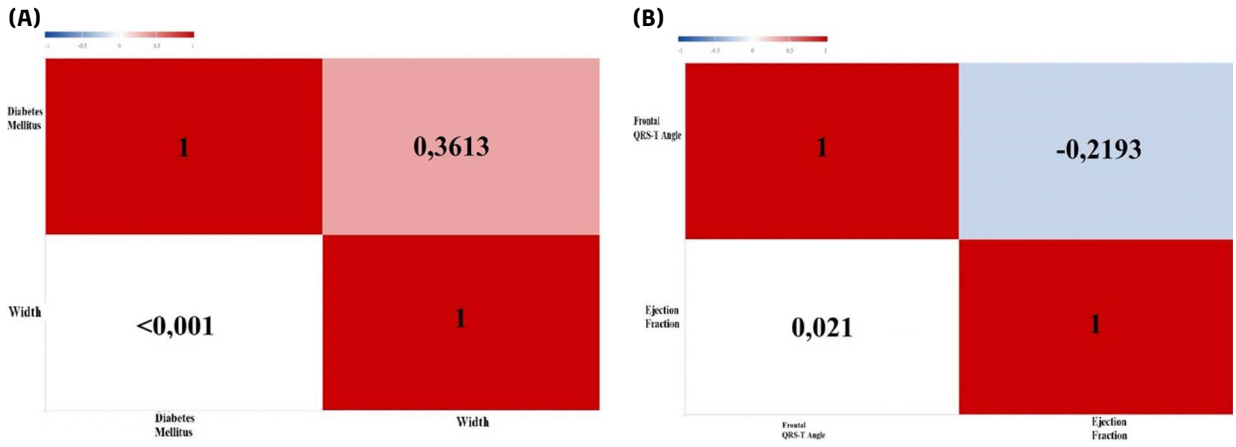

Figure 3. Correlogram showing the relationships between diabetes mellitus, wide frontal QRS-T angle group, and left ventricular ejection fraction (LVEF).

Table 4. Univariate, multivariate, and stepwise binary logistic regression analysis of mortality

Log reg	Univariate model			Multivariate model			Stepwise model		
Variables	**OR**	**95% CI**	**P**	**OR**	**95% CI**	**P**	**OR**	**95% CI**	**P**
Age	1.07	1.03-1.11	< 0.001	1.04	0.98-1.10	0.129	0.03	1	0.138
DM	1.08	1.02-1.16	0.049	0.83	0.25-2.70	0.758	–	–	–
Width	9.38	3.75-23.45	< 0.001	8.60	1.05-70.02	0.044	8.08	2.75-23.74	< 0.001
Frontal QRS-T	1.02	1.00-1.03	< 0.001	1.00	0.97-1.02	0.969	–	–	–
Fragmented QRS	11.04	3.59-33.86	< 0.001	12.17	2.90-51.09	< 0.001	11.25	2.98-42.49	< 0.001
LVEF	0.96	0.91-1.02	0.24	1.01	0.93-1.09	0.755	–	–	–

OR, Odd ratios; CI, Confidence interval; DM, Diabetes mellitus; LVEF, Left ventricular ejection fraction.

In hemodialysis patients, the development of myocardial fibrosis may lead to uremic cardiomyopathy. This condition impairs both depolarization and repolarization processes, resulting in a widened fQRSTa. Additionally, autonomic dysfunction associated with end-stage renal disease, along with dialysis-related fluctuations in electrolytes (particularly potassium and calcium) may contribute to repolarization instability.[1,2,8] These electrical disturbances can increase the risk of arrhythmias and sudden cardiac death (SCD). Based on our findings, the fQRSTa appears to be a simple, noninvasive, and practical risk marker that could be incorporated into routine clinical assessments of dialysis patients.

A recent cohort study conducted in Japan demonstrated that QT prolongation, elevated heart rate, and left ventricular hypertrophy on ECG were strongly associated with an increased risk of SCD in patients undergoing hemodialysis.[9] This important finding highlights the complex cardiac risks faced by this vulnerable population and underscores the need for vigilant monitoring and timely intervention. Building on these insights, our study further reveals that an increased fQRSTa correlates with a heightened risk of overall mortality. This suggests that the fQRSTa may serve as a valuable prognostic marker of cardiac health in hemodialysis patients, requiring further investigation into its role in risk stratification. Collectively, these findings reinforce the importance of comprehensive cardiovascular assessments in individuals receiving hemodialysis, with the goal of improving prediction and management of adverse clinical outcomes.

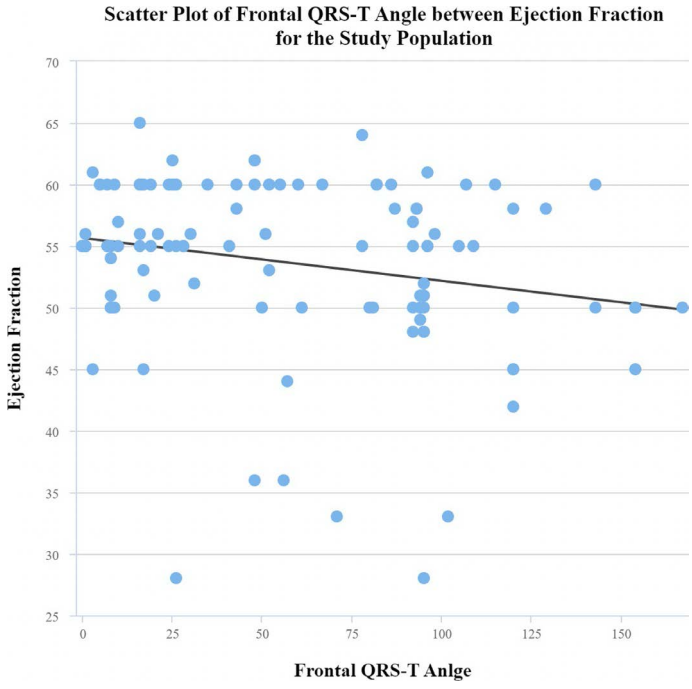

Figure 4. Scatter plot illustrating the correlation between left ventricular ejection fraction (LVEF) and frontal QRS-T angle.

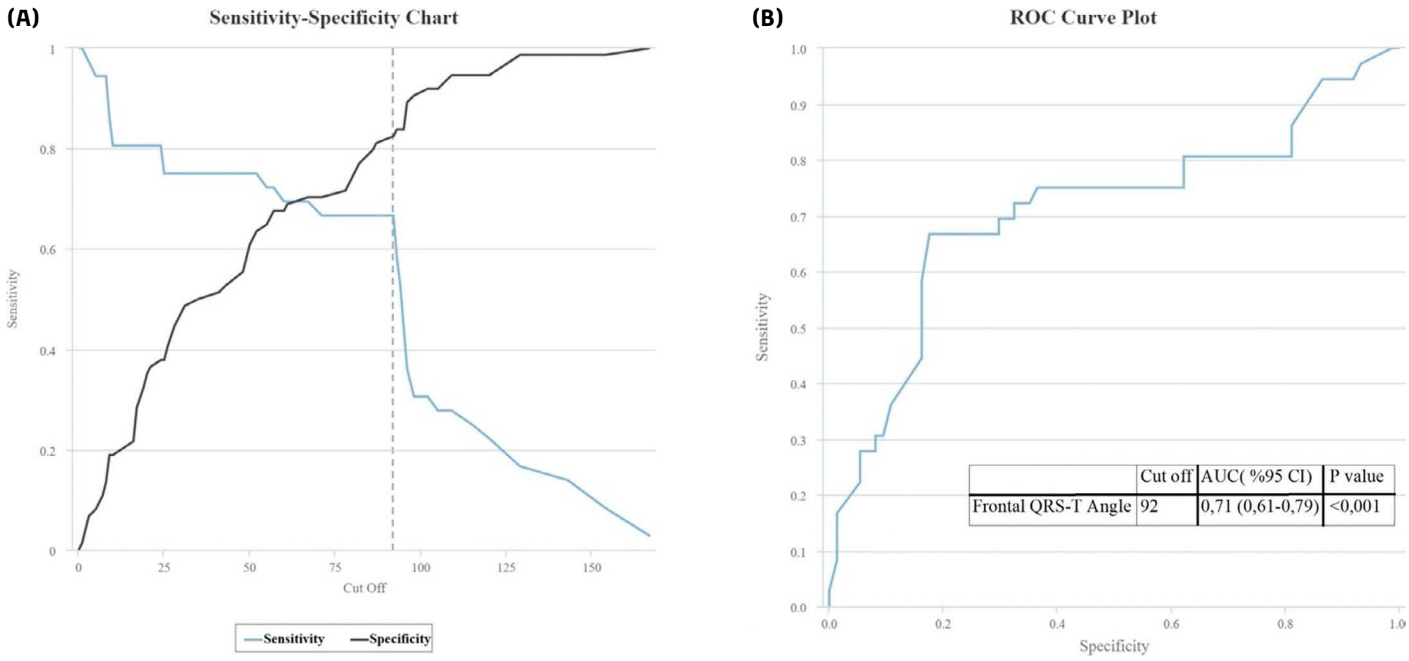

Figure 5. Receiver operating characteristic (ROC) curve and sensitivity-specificity chart of the mortality group.

In a separate investigation focusing on fragmented QRS in dialysis patients, researchers found that patients with fragmented QRS had a higher incidence of ventricular premature contractions and non-sustained ventricular tachycardia on ECG Holter monitoring. This highlights the potential arrhythmic implications of fragmented QRS in this population.[10,11] In our study, we similarly found that the presence of fragmented QRS in hemodialysis patients not only correlates with increased mortality risk but also serves as an independent predictor of adverse clinical outcomes. This finding highlights the importance of monitoring fragmented QRS as a critical parameter in the cardiac assessment of hemodialysis patients, suggesting that it may warrant closer clinical scrutiny and management to mitigate associated risks.

Recent evidence from a study involving diabetic patients indicates that the QRS-T angle is specifically associated with the risk of SCD, rather than with other forms of mortality. This finding suggests a potential pathway for improving SCD risk stratification in patients with type 2 diabetes.[12] A wide fQRSTa has been recognized as a strong, independent, and long-term prognostic indicator for myocardial infarction and all-cause of mortality in diabetic populations, as demonstrated in another study.[6] In our study, we identified a higher prevalence of DM in the wide fQRSTa group, as well as an increased proportion of diabetic patients in the mortality group. These findings support the consideration of DM as a significant contributing factor.

Similarly, in a study conducted by Usalp and Bağırtan on patients with ischemic stroke, a significant association was observed between the fQRSTa and mortality.[13] These findings suggest that the fQRSTa may have prognostic value across various clinical populations, including both stroke and hemodialysis patients, highlighting the potential utility of ECG parameters in broader risk stratification. Our study adds to this evidence by demonstrating that the fQRSTa is also an independent predictor of mortality in the hemodialysis population.

The literature includes studies that have used the fQRSTa as a diagnostic and prognostic marker in patients with myocarditis, valvular diseases, cardiomyopathies, heart failure (HF), and even non-cardiac conditions, demonstrating its utility in assessing cardiac function and predicting adverse clinical outcomes.[7,14–17] In a different investigation focusing on patients with heart failure with preserved ejection fraction (HFpEF), the prognostic relevance of various electrocardiographic parameters, particularly the fQRSTa, was highlighted.[18,19] That study showed that the fQRSTa is a significant indicator of adverse outcomes in this population. Our findings extend this concept by demonstrating that the fQRSTa also holds independent prognostic value for mortality in hemodialysis patients, regardless of LVEF status. Given these insights, the fQRSTa emerges as a valuable metric in the initial cardiovascular assessment of hemodialysis patients, paralleling its established role in the evaluation of individuals with HFpEF. This suggests that incorporating the fQRSTa into routine clinical practice may enhance risk stratification and management strategies for this vulnerable population.

Additionally, patients with a wide fQRSTa showed no evidence of excess left ventricular hypertrophy (LVH), as IVSWT and PWT were similar between groups. Likewise, Cr, K, Hb, and Ca levels were comparable, indicating no significant underlying electrolyte or laboratory imbalances. The only significant difference was a lower LVEF observed in both the wide fQRSTa and mortality groups. In contrast, IVSWT, PWT, chamber size, Cr, and K levels showed no differences by mortality status. Hb and Ca levels were lower in the mortality patients but did not reach statistical significance. These findings suggest that a widened frontal QRS-T angle indicates a higher mortality risk independent of LVH or major metabolic disturbances. In other words, the prognostic value of a wide QRS-T angle in hemodialysis patients is not merely a surrogate for structural heart disease or electrolyte imbalance. This independence from LVH and metabolic factors underscores

the QRS-T angle as a valuable tool for risk stratification in dialysis patients. It complements traditional measures such as LVEF and emphasizes the significance of electrical remodeling in cardiovascular risk.[20]

The future of artificial intelligence (AI) and electrocardiography represents a critical area of focus in cardiovascular research. Recent literature has shown a surge in studies exploring the application of AI in cardiological conditions, including coronary artery disease and arrhythmias.[21] Additionally, research has highlighted the role of AI in predicting hospital admissions due to HF among peritoneal dialysis patients.[22] This study underscores the potential value of integrating electrocardiography and artificial intelligence into the early evaluation of hemodialysis patients to optimize mortality risk prediction and ultimately improve patient outcomes.

Study Limitations

Given the limited sample size in our study, the findings should be interpreted as preliminary. This exploratory analysis lays the groundwork for future investigations in larger patient cohorts, which may enhance the strength and external validity of the results. Another limitation is the absence of serial ECG recordings. Since the frontal QRS-T angle may vary over time, repeated measurements could better capture its prognostic dynamics. Additionally, follow-up duration could not be precisely calculated for all patients due to the retrospective design. Further research involving larger populations will be essential to confirm these findings and refine the clinical implications derived from this initial analysis.

Conclusion

In conclusion, our study highlights the fQRSTa as a significant predictor of mortality in hemodialysis patients, particularly when the angle exceeds 92 degrees. We also found that the fQRSTa is markedly elevated in diabetic patients and correlates with various clinical parameters. Notably, an increased fQRSTa is associated with reduced LVEF, reinforcing its potential as a valuable biomarker for assessing cardiovascular health in this high-risk population. These findings support the integration of fQRSTa into routine clinical evaluations to enhance patient management and improve outcomes.

Ethics Committee Approval: Ethics committee approval was obtained from Trakya University Faculty of Medicine Non-Interventional Scientific Research Ethics Committee (Approval Number: 14/10, Date: 02.09.2024).

Informed Consent: Written informed consent was not required.

Conflict of Interest: The authors have no conflicts of interest to declare.

Funding: The authors declared that this study received no financial support.

Use of AI for Writing Assistance: No artificial intelligence tools were used in the production of this manuscript.

Author Contributions: Concept – Ç.K., C.Ö.; Design – Ç.K., C.Ö.; Supervision – Ç.K., İ.K.; Resource – Ç.K., M.E., E.Ç.; Materials – Ç.K., M.E., C.Ö.; Data Collection and/or Processing – Ç.K., M.E., M.A.Ç., E.Ç.; Analysis and/or Interpretation – Ç.K., C.Ö.; Literature Review – Ç.K., C.Ö.; Writing – Ç.K., M.E., C.Ö., M.A.Ç., E.Ç., İ.K.; Critical Review – Ç.K., İ.K.

Peer-review: Externally peer-reviewed.

References

1. Oehler A, Feldman T, Henrikson CA, Tereshchenko LG. QRS-T angle: a review. Ann Noninvasive Electrocardiol. 2014;19(6):534-542. [CrossRef]
2. Kurisu S, Nitta K, Watanabe N, et al. Associations of frontal QRS-T angle with left ventricular volume and function derived from ECG-gated SPECT in patients with advanced chronic kidney disease. Ann Nucl Med. 2021;35(6):662-668. [CrossRef]
3. Borleffs CJ, Scherptong RW, Man SC, et al. Predicting ventricular arrhythmias in patients with ischemic heart disease: clinical application of the ECG-derived QRS-T angle. Circ Arrhythm Electrophysiol. 2009;2(5):548-554. [CrossRef]
4. Brown RA, Schlegel TT. Diagnostic utility of the spatial versus individual planar QRS-T angles in cardiac disease detection. J Electrocardiol. 2011;44(4):404-409. [CrossRef]
5. Poulikakos D, Hnatkova K, Banerjee D, Malik M. Association of QRS-T angle and heart rate variability with major cardiac events and mortality in hemodialysis patients. Ann Noninvasive Electrocardiol. 2018;23(6):e12570. [CrossRef]
6. May O, Graversen CB, Johansen MØ, Arildsen H. A large frontal QRS-T angle is a strong predictor of the long-term risk of myocardial infarction and all-cause mortality in the diabetic population. J Diabetes Complications. 2017;31(3):551-555. [CrossRef]
7. Gotsman I, Keren A, Hellman Y, Banker J, Lotan C, Zwas DR. Usefulness of electrocardiographic frontal QRS-T angle to predict increased morbidity and mortality in patients with chronic heart failure. Am J Cardiol. 2013;111(10):1452-1459. [CrossRef]
8. Eranti A. The role of electrocardiographic abnormalities, obesity, and diabetes in risk stratification for sudden cardiac death in the general population. Dissertation. University of Ouluens; 2016.
9. Hiyamuta H, Yamada S, Nakano T, et al. Impact of Electrocardiographic Parameters on Sudden Death in Patients Receiving Maintenance Hemodialysis: Ten-Year Outcomes of the Q-Cohort Study. J Atheroscler Thromb. 2024;31(3):214-231. [CrossRef]
10. Kardaş F, Taylan G, Kaya Ç, Kurultak İ. Presence of Fragmented QRS may be Associated with Ventricular Arrhythmias in Hemodialysis Patients. Eskisehir Med J. 2022;3(2):92-100. [CrossRef]
11. Taylan G, Öztürk C, Yalta K. Fragmented QRS Pattern in Patients with COVID-19: Further Insights into Its Temporal and Mechanistic Features. Anatol J Cardiol. 2022;26(3):239-240. [CrossRef]
12. Garcia R, Schröder LC, Tavernier M, et al.; SURDIAGENE and the Mini-Finland study groups. QRS-T angle: is it a specific parameter associated with sudden cardiac death in type 2 diabetes? Results from the SURDIAGENE and the Mini-Finland prospective cohorts. Diabetologia. 2024;67(4):641-649. [CrossRef]
13. Usalp S, Bağırtan B. A Novel Electrocardiographic Marker for Predicting Total Mortality in Ischemic Stroke: Frontal QRS-T Angle. Turk Kardiyol Dern Ars. 2025;53(1):29-34. [CrossRef]
14. Chua KC, Teodorescu C, Reinier K, et al. Wide QRS-T Angle on the 12-Lead ECG as a Predictor of Sudden Death Beyond the LV Ejection Fraction. J Cardiovasc Electrophysiol. 2016;27(7):833-839. [CrossRef]
15. Turen S, Yilmaz E. Predictive value of the frontal QRS-T angle for a permanent pacemaker requirement in patients undergoing transcatheter aortic valve implantation. Eur Rev Med Pharmacol Sci. 2023;27(13):6238-6246.
16. Ucar FM, Ozturk C, Yılmaztepe MA. Evaluation of Tp-e interval, Tp-e/QT ratio and Tp-e/QTc ratio in patients with acute myocarditis. BMC Cardiovasc Disord. 2019;19(1):232. [CrossRef]
17. Abus S, Koparal M, Kaya H, Kapıcı OB, Tasolar MH, Tibilli H. Evaluation of frontal QRS-T angle values in electrocardiography in patients with chronic rhinosinusitis. BMC Cardiovasc Disord. 2023;23(1):160. [CrossRef]
18. He T, Liu C, Liang W. Abnormal electrocardiogram and poor prognosis in heart failure with preserved ejection fraction. Postgrad Med J. 2023;99(1177):1154-1159. [CrossRef]

19. Selvaraj S, Ilkhanoff L, Burke MA, et al. Association of the frontal QRS-T angle with adverse cardiac remodeling, impaired left and right ventricular function, and worse outcomes in heart failure with preserved ejection fraction. J Am Soc Echocardiogr. 2014;27(1):74-82.e2. [CrossRef]
20. Maanja M, Schlegel TT, Kozor R, et al. Improved evaluation of left ventricular hypertrophy using the spatial QRS-T angle by electrocardiography. Sci Rep. 2022;12(1):15106. [CrossRef]
21. Hayıroğlu Mİ, Altay S. The Role of Artificial Intelligence in Coronary Artery Disease and Atrial Fibrillation. Balkan Med J. 2023;40(3):151-152. [CrossRef]
22. Xu L, Cao F, Wang L, et al. Machine learning model and nomogram to predict the risk of heart failure hospitalization in peritoneal dialysis patients. Ren Fail. 2024;46(1):2324071. [CrossRef]

ARCHIVES OF THE TURKISH SOCIETY OF CARDIOLOGY

Official journal of the TURKISH SOCIETY OF CARDIOLOGY

The Outcomes of Concomitant Carotid Endarterectomy and Off-Pump Coronary Artery Bypass Grafting

Eş Zamanlı Karotis Endarterektomi ve Pompasız Koroner Arter Bypass Greftlemesinin Sonuçları

ABSTRACT

Objective: Limited data exist on the concurrent application of carotid endarterectomy (CEA) and off-pump coronary artery bypass grafting (OPCABG).

Method: This retrospective study collected data from 42 patients who underwent simultaneous carotid endarterectomy and off-pump coronary artery bypass grafting between November 2015 and June 2023 at two affiliated institutions. CEA was performed first via eversion endarterectomy, followed by OPCABG using mostly arterial grafts on a beating heart, primarily with a "no-touch" aortic technique. Patient data were obtained from digital hospital records, and follow-up was completed through electronic systems or phone contact.

Results: Among 1,154 OPCABG patients, 42 (3.6%) underwent simultaneous CEA, with a median age of 72 (range: 59-84); 35 patients (83.3%) were male and seven (16.7%) female. All patients were asymptomatic for carotid disease and diagnosed preoperatively via routine Doppler ultrasound. Complete arterial revascularization without aortic manipulation was achieved in 83.3% of cases, with a mean of 3.66 ± 1.22 distal anastomoses. Early mortality occurred in one critically ill patient (2.4%). One patient (2.4%) experienced a postoperative transient ischemic attack and recovered without neurologic sequelae. Seventeen patients (40.4%) were extubated in the operating room. During follow-up, no patients experienced cerebrovascular events; two patients died due to non-cardiac disease. As all events occurred within the first year, the Kaplan–Meier one-, three-, and five-year stroke-free survival rates were identical at 92.6 ± 4.1%.

Conclusion: Concomitant CEA and OPCABG surgery is considered the optimal strategy for patients with extensive carotid and coronary artery stenosis at experienced centers. It is an achievable treatment that minimizes the risk of postoperative cerebrovascular events and cognitive deficits.

Keywords: Carotid endarterectomy, combined surgical procedures, coronary artery bypass, enhanced recovery after surgery (ERAS), off-pump, stroke/prevention & control

ÖZET

Amaç: Karotis endarterektomi (KEA) ve pompasız koroner arter baypas greftlemesinin (OPCABG) birlikte uygulanmasına ilişkin veriler sınırlıdır.

Yöntem: Bu retrospektif çalışmada, Kasım 2015–Haziran 2023 tarihleri arasında iki bağlı merkezde eş zamanlı karotis endarterektomisi (KEA) ve pompasız koroner arter baypas greftleme (OPCABG) uygulanan 42 hastanın verileri incelendi. KEA, önce eversion endarterektomi yöntemiyle yapıldı; ardından çalışan kalpte, çoğunlukla "no-touch" aort tekniğiyle ve çoğunlukla arteriyel greftler kullanılarak OPCABG uygulandı. Hasta verileri dijital hastane kayıtlarından elde edildi ve takip elektronik sistemler veya telefon görüşmesi yoluyla tamamlandı.

Bulgular: Toplam 1.154 OPCABG hastasının 42'sine (%3,6) eş zamanlı KEA uygulandı; medyan yaş 72 (59–84 arası) idi; hastaların 35'i (%83,3) erkek, 7'si (%16,7) kadındı. Tüm hastalar karotis hastalığı açısından asemptomatikti ve preoperatif dönemde rutin Doppler ultrason ile tanı konmuştu. %83,3 olguda aort manipülasyonu olmaksızın tam arteriyel revaskülarizasyon sağlandı; ortalama distal anastomoz sayısı 3,66 ± 1,22 idi. Erken mortalite bir kritik hastada (%2,4) görüldü. Bir hasta (%2,4) postoperatif geçici iskemik atak geçirdi ve nörolojik sekelsiz iyileşti. On yedi (%40,4) hasta ameliyathanede ekstübe edildi. Takip süresince hiçbir hastada serebrovasküler olay görülmedi, iki hasta kardiyak dışı nedenlerle kaybedildi. Tüm olaylar ilk yıl içinde gerçekleştiği için Kaplan–Meier 1., 3. ve 5. yıllık inmesiz sağkalım oranları %92,6 ± 4,1 olarak eşitti.

Sonuç: Eş zamanlı KEA ve OPCABG cerrahisi, yaygın karotis ve koroner arter darlığı olan hastalarda deneyimli merkezlerde optimal strateji olarak bilinmektedir ve postoperatif serebrovasküler olaylar ile bilişsel defisit riskini en aza indirirken uygulanabilir bir tedavi seçeneğidir.

Anahtar Kelimeler: Karotis endarterektomi, kombine cerrahi girişimler, pompasız koroner arter baypas, ameliyat sonrası iyileşmenin hızlandırılması (ERAS), inme/önleme ve kontrol

ORIGINAL ARTICLE
KLİNİK ÇALIŞMA

Mehmet Şanser Ateş[1]
Eray Aksoy[2]
Zümrüt Tuba Demirözü[1]
Sami Gürkahraman[2]

[1]*Department of Cardiovascular Surgery, Koç University Faculty of Medicine, İstanbul, Türkiye*
[2]*Department of Cardiovascular Surgery, Vehbi Koç Foundation American Hospital, İstanbul, Türkiye*

Corresponding author:
Mehmet Şanser Ateş
✉ msanserates@yahoo.com

Received: September 17, 2025
Accepted: September 30, 2025

Cite this article as: Ateş MŞ, Aksoy E, Demirözü ZT, Gürkahraman S. The Outcomes of Concomitant Carotid Endarterectomy and Off-Pump Coronary Artery Bypass Grafting. *Turk Kardiyol Dern Ars.* 2025;53(7):518–523.

DOI: 10.5543/tkda.2025.99650

Copyright@Author(s)
Available online at archivestsc.com. Content of this journal is licensed under a Creative Commons Attribution – NonCommercial-NoDerivatives 4.0 International License.

Coronary artery disease remains an important cause of mortality, particularly in the elderly, with in-hospital mortality rates reported as high as 8.6% in patients aged 75 years and older.[1] Since carotid artery disease frequently coexists with coronary artery disease in this population, the overall risk of stroke and mortality is further increased. Carotid endarterectomy (CEA) remains the gold standard for stroke prevention in patients with carotid artery disease.[2] When both coronary artery bypass grafting (CABG) and coronary artery endarterectomy are necessary, concomitant surgery has been shown to reduce the risk of catastrophic events that may occur when two procedures are performed sequentially.[3,4] However, given the lack of established body of evidence on concomitant surgery, concerns have emerged regarding the simultaneous performance of these procedures.[5,6] There are limited data on concomitant CEA and off-pump coronary artery bypass (OPCABG), and the role of aortic manipulation in stroke risk is uncertain, as most CABG-CEA reports are based on conventional on-pump experiences. The potential benefits of concurrent OPCABG–CEA include eliminating the risk of a potential stroke or acute coronary syndrome between staged operations and avoiding the additional stress of a second surgery and anesthesia.[7,8] The present study aims to evaluate the outcomes of simultaneous OPCABG-CEA for the treatment of critical carotid artery stenosis and coronary artery disease.

ABBREVIATIONS

AF	Atrial fibrillation
BIMA	Bilateral internal mammary arteries
CABG	Coronary artery bypass grafting
CEA	Carotid endarterectomy
COVID-19	Coronavirus Disease 2019
CT	Computed tomography
CVA	Cerebrovascular accident
ERAS	Enhanced recovery after surgery
EuroSCORE	European System for Cardiac Operative Risk Evaluation
IABP	Intra-aortic balloon pump
IQR	Interquartile range
LIMA	Left internal mammary artery
LITA	Left internal thoracic artery
LVEF	Left ventricular ejection fraction
MI	Myocardial infarction
MRI	Magnetic resonance imaging
NYHA	New York Heart Association
ONCABG	On-pump coronary artery bypass grafting
OPCABG	Off-pump coronary artery bypass grafting
RIMA	Right internal mammary artery
RITA	Right internal thoracic artery
STS	Society of Thoracic Surgeons

Materials and Methods

The retrospective study protocol was approved by the Ethics Committee of Koç University (Approval Number: 2023.350.IRB1.124, Date: 02.10.2023). This study included all patients who underwent off-pump CABG and CEA between November 1, 2014 and June 30, 2023, at two affiliated hospitals. Of 1,154 patients who underwent off-pump CABG during this period, 42 also underwent CEA performed concurrently with OPCABG. According to our institutional practice, concomitant CEA–OPCABG was routinely performed when critical carotid artery stenosis was diagnosed in patients scheduled for CABG. The staged procedure for CEA and off-pump CABG was not performed. Patients with a history of preoperative ischemic stroke or severe cerebrovascular accident were censored. Electronic medical records were analyzed. We reviewed the health records of 1,154 off-pump CABG patients and collected data on demographic characteristics and preexisting comorbid conditions, such as hypertension, hyperlipidemia, smoking history, and type 2 diabetes; perioperative status; left ventricular ejection fraction (LVEF); recent myocardial infarction (MI); prior carotid stent, coronary artery stent, or CABG; preoperative inotropic support or intra-aortic balloon pump (IABP); New York Heart Association (NYHA) classification; and European System for Cardiac Operative Risk Evaluation (EuroSCORE).[9] We collected the following data for operative characteristics: territory of anastomoses, number of anastomoses, composite grafts, types of grafts, no-touch aorta technique, and concomitant carotid artery endarterectomy procedures. We collected the following data for postoperative outcomes: re-exploration for bleeding, postoperative atrial fibrillation ([AF], defined as AF occurring after surgery that required treatment during hospitalization), postoperative renal failure (defined as a new requirement for hemodialysis at discharge), prolonged artificial ventilation (defined as > 24 hours of postoperative mechanical support), deep sternal wound infection, postoperative stroke (defined as any confirmed neurologic deficit of abrupt onset caused by a disturbance of cerebral blood supply that did not resolve within 24 hours), transient ischemic attack (TIA, defined as abrupt loss of neurologic function with complete return of function within 24 hours), length of cardiovascular intensive care unit (ICU) stay, length of hospital stay, postoperative total drainage from the chest and mediastinal tubes, required blood products (e.g., erythrocyte suspension and fresh frozen plasma), in-hospital mortality (during the hospital stay) and 30-day mortality, and long-term follow-up (more than 24 months postoperatively). All patients underwent preoperative carotid-subclavian duplex ultrasound screening. Patients suspected of having postoperative neurological events were evaluated by a neurologist and underwent brain imaging with computed tomography (CT), magnetic resonance imaging (MRI), or both, with the diagnosis clinically confirmed. No patients had missing data at follow-up. Follow-up data were obtained via electronic medical records or phone communication.

Statistical Analysis

All statistical analyses were conducted using SPSS Statistics for Windows, version 19.0 (IBM Corp., Armonk, NY, USA). Continuous data were expressed as mean (standard deviation, SD) or median (interquartile range, IQR), and categorical variables were expressed as count (percentage) in complete-case analyses. Survival was estimated by the Kaplan-Meier method, with the date of surgery as the starting point and the date of death or last follow-up as the endpoint. Operative mortality included deaths occurring within 30 days of surgery or during hospitalization. The cut-off value for statistical significance was set as 0.05.

Surgical Procedure and In-Hospital Progress

All surgeries were performed with the patient supine, the neck extended, and rotated 45 degrees to the opposite side. After placement of sterile drapes, the common, internal, and external carotid arteries were dissected free and encircled with vessel loops via a longitudinal incision along the anterior border of the sternocleidomastoid muscle. Intravenous heparin was administered. The common carotid artery was clamped proximally, and the external carotid artery was clamped distally. The internal carotid artery was not clamped but gently elevated with a vessel loop for control. In this way, the entire occlusive plaque could be removed, debris embolization prevented, and backflow of blood from the contralateral side evaluated. The common carotid artery was then transected just proximal to the bifurcation. Using eversion endarterectomy, plaque in the internal and external carotid arteries was first removed from the carotid artery lumen, followed by plaque in the common carotid artery. The common carotid artery was anastomosed end-to-end with 6.0 polypropylene after ensuring adequate backflow. None of the patients received a patch closure, and no drain was placed. After controlling bleeding, the OPCABG procedure was initiated.

Midline sternotomy was used for all primary OPCABG procedures, while left anterolateral thoracotomy was performed in one patient who underwent redo off-pump CABG. Patients underwent full revascularization with bilateral internal mammary arteries (BIMA), the right internal mammary artery (RIMA), or the left internal mammary artery (LIMA), as needed. The radial artery was used to complete revascularization. In addition to arterial grafts, we used saphenous vein grafts for patients who might undergo kidney transplantation to spare the radial artery. Composite T grafts and Y grafts were used for total arterial revascularization. The technique involved inserting 1.0 silk epicardial stay sutures into the four corners of the target coronary artery without the use of a stabilizer or epicardial suction device, as previously described.[10] Heparin was administered (150 IU/kg) to achieve an activated clotting time greater than 300 seconds. Protamine was administered after the anastomoses were completed. All patients received low molecular-weight heparin until hospital discharge. To prevent platelet aggregation, patients received acetylsalicylic acid 100 mg and clopidogrel 75 mg daily and were discharged on the fourth or fifth postoperative day.

Seventeen (40.4%) patients were awakened and extubated on the operating table post-surgery. They were closely monitored in the intensive care unit during the early postoperative period before being transferred to the ward after 24 hours.

Patient Follow-up

The patients were followed up at one week, one month, and three months at scheduled outpatient visits after hospital discharge. At follow-up, all patients underwent physical examination, blood serum analysis, chest radiography, and echocardiography.

Results

The OPCABG-CEA group included 42 patients (3.63%) out of 1,154 OPCABG patients, with a median age of 72 years (IQR: 59–84 years). Thirty-five patients (83.3%) were male. None of the patients had carotid artery disease symptoms on admission and were diagnosed with severe carotid artery disease during routine carotid Doppler ultrasound examination before OPCABG. Baseline characteristics of the patients are presented in Table 1. The mean number of target coronary anastomoses was 3.66 ± 1.22. Complete revascularization without aortic manipulation was performed in 35 patients (83.3%), and 17 patients (40.4%) were extubated in the operating room and transferred to the intensive care unit spontaneously breathing. Operative and early postoperative outcomes are detailed in Tables 2 and 3.

Table 1. Baseline characteristics (n=42)

Characteristic	No. (%)
Age, years	
Mean (SD)	71.59 (7.05)
Median (range)	72 (59-84)
Gender	
Female	7 (16.7)
Male	35 (83.3)
Body mass index (kg/m^2)	
Mean (SD)	26.47 (4.31)
Median (range)	26.31 (16.05–7.18)
Concomitant disease	
Diabetes	16 (38.1)
Hypertension	32 (76.2)
Dyslipidemia	24 (57.1)
Pulmonary disease	11 (26.2)
Previous stroke	7 (16.7)
Tobacco use	13 (31.0)
Impaired renal function	3 (7.1)
Previous myocardial infarction	12 (28.6)
Previous coronary stent	10 (23.8)
Previous CABG	3 (7.1)
Previous carotid stenting	1 (2.4)
Peripheral artery disease	13 (31.0)
Preoperative IABP	2 (4.8)
Preoperative inotropes	1 (2.4)
Atrial fibrillation	3 (7.1)
Emergent/urgent	13 (31.0)
Ejection fraction	
< 30%	0 (0)
30–50%	16 (38.1)
> 50%	26 (61.9)
NYHA classification	
> Class II	30 (71.4)
Euroscore	
0-3	17 (40.5)
4-6	16 (38.1)
≥ 7	9 (21.4)

SD, standard deviation; CABG, Coronary artery bypass grafting; IABP, Intra-aortic balloon pump; NYHA, New York Heart Association.

Table 2. Operative data (n=42)

Variables	No. (%)
Territory	
Left anterior descending artery	39 (92.9)
Left circumflex artery	37 (88.1)
Right coronary artery	32 (76.2)
Number of distal anastomoses	
1	3 (7.1)
2	2 (4.8)
3	13 (31.0)
4	14 (33.3)
> 4	10 (23.8)
Composite graft	
T	33 (78.6)
Y	2 (4.8)
No-touch aorta	35 (83.3)
Grafts	
Radial artery	28 (66.7)
LITA	39 (92.9)
RITA	12 (28.6)
Saphenous vein	4 (9.5)

LITA, Left internal thoracic artery; RITA, Right internal thoracic artery.

Early mortality occurred in one patient, an 83-year-old woman who was critically ill and underwent surgery following cardiopulmonary arrest and resuscitation. She died on the first postoperative day due to multiple organ failure and sepsis. Postoperative morbidities are presented in Table 3. One patient (2.4%) experienced a postoperative transient ischemic attack and recovered without neurologic sequelae. The mean follow-up time was 35.98 ± 28.46 months (range: 1.23-97.03 months). During follow-up, three patients underwent carotid artery stenting of the contralateral side (two elective and one following a transient ischemic attack), and one patient underwent elective CEA of the contralateral side. Two patients died during follow-up: an 80-year-old man with severe left ventricular dysfunction was re-hospitalized in the intensive care unit for severe Coronavirus Disease 2019 (COVID-19) lung involvement and died 51 days after surgery. Another patient, a 65-year-old man on long-term dialysis, died 4.5 months after surgery from severe pneumonia and sepsis. Throughout the follow-up period, no patients experienced cerebrovascular events. As all events occurred within the first year, the Kaplan–Meier one-, three-, and five-year stroke-free survival rates were equal at 92.6 ± 4.1% (Figure 1).

Discussion

In the present study, concurrent OPCABG-CEA produced favorable outcomes in terms of rapid recovery and low morbidity. Complete arterial coronary revascularization was performed in 35 of 42 patients using the no-touch aorta technique. Concomitant CEA with OPCABG facilitated extubation in the operating room for 40% of patients, thereby reducing both intensive care duration and overall hospital stay.

Table 3. Postoperative data

Morbidity*	No. (%)
Re-exploration for bleeding or tamponade	0
Postoperative AF	12 (28.6)
Deep sternal wound infection	1 (2.4)
Inotropic support	3 (7.1)
Renal failure/dialysis	3 (7.1)
Postoperative IABP	0
Transient ischemic attack	1 (2.4)
Postoperative MI	0
In-hospital mortality	1 (2.4)
Outcome parameters**	**Mean (SD) Median (range)**
Artificial ventilation, hours	6.624 (6.73)
	6 (0-25)
Length of ICU stay, hours	32.78 (29.47)
	24.00 (15-190)
Length of hospital stay, days	9.65 (7.25)
	7 (4-44)
Postoperative drainage, mL	672.92 (271.84)
	600.00 (300-1450)
Blood products, unit	
Erythrocyte suspension	0.43 (0.63)
	0 (0-2)
Fresh frozen plasma	0.53 (0.986)
	0 (0-3)

*All patients (n=42); **Among survivors (n=41); AF, Atrial fibrillation; MI, Myocardial infarction; IABP, Intra-aortic balloon pump; ICU, Intensive care unit.

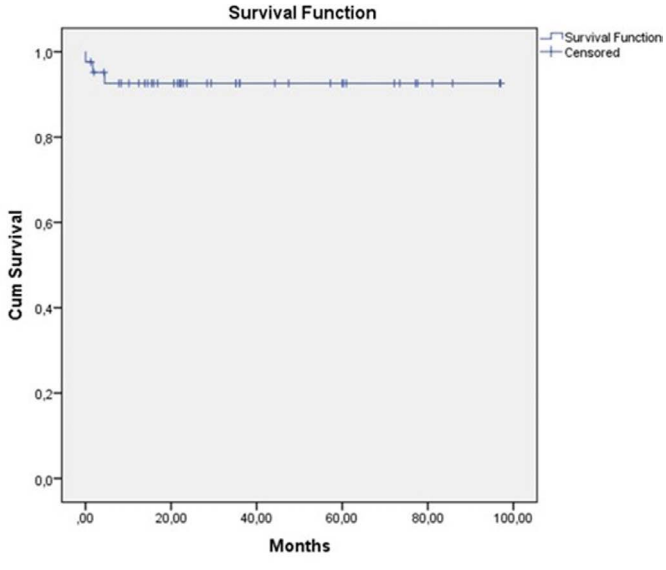

Months	0	12	24	36	48	60	72
Number at risk	42	33	20	16	12	11	8
Cum proportion of overall and CVA-free survival	92.6%	92.6%	92.6%	92.6%	92.6%	92.6%	92.6%

Figure 1. Kaplan-Meier survival curve.

Technical benefits of performing carotid endarterectomy first, followed by CABG without cardiopulmonary bypass, include avoiding the inflammatory and embolic risks associated with cardiopulmonary bypass, reducing the risk of aortic manipulation (no-touch or limited-touch), avoiding the potential side effects of non-pulsatile artificial cerebral perfusion, preventing neck hematoma by using less heparin, reducing the length of the operation, and enabling fast-track extubation to assess neurological status shortly after surgery.

Critical coronary artery disease has been reported in up to one-third of patients before carotid endarterectomy,[11] and the incidence of > 70% carotid stenosis among candidates for CABG ranges from 5.8% to 13.4%. However, routine screening for one condition in the presence of the other has been debated.[12] All patients in our series were asymptomatic for carotid disease, and critical carotid stenosis was diagnosed at a rate of 3.63% during routine carotid duplex scanning.

Contradictory opinions exist regarding staged versus combined surgery for coronary artery disease and critical carotid artery stenosis. Furthermore, if two procedures are to be conducted in stages, there is no definite agreement on which procedure should be performed first, or, more crucially, how much time should be allowed between the two surgeries.[4,13] Due to limited data in the literature, the latest practice guidelines leave this option to institutional practice or patient-specific requirements.[2]

In the series by Kurtoğlu et al.,[8] concurrent CEA–OPCABG in 84 patients yielded an early mortality rate of 3.5%, a stroke rate of 4.8%, and a myocardial infarction rate of 2.3%. In our cohort of 42 patients, early mortality occurred in one patient (2.4%), a transient ischemic attack was observed in one patient (2.4%), and no perioperative myocardial infarction was recorded. Both series employed similar surgical techniques, including complete arterial revascularization when feasible and aortic no-touch techniques. Together, the two studies demonstrate that concurrent CEA–OPCABG can be performed with controllable morbidity and mortality rates.

Haywood et al.[7] reported in a recent study that the combined CEA-CABG group did not differ from the staged cohort in terms of 30-day stroke, mortality, or composite events; however, the myocardial infarction rate was lower. In contrast, Wang et al.[3] reported that outcomes of combined CABG–CEA were primarily determined by the severity of coronary artery disease. Furthermore, in the presence of stable angina, the risk of stroke or death was comparable between the two approaches. The risk of composite events (stroke, death, MI) was higher in patients who underwent combined CEA-CABG, whereas the risk of myocardial infarction was higher in patients with unstable angina who underwent isolated CEA. These findings demonstrate that urgent patients requiring combined CEA-CABG are a subgroup with a unique risk profile and that proficiency in the routine technique should be maintained to reduce the operative risk of CABG. Penton et al.[4] demonstrated, in the largest study to date, that simultaneous CEA-ONCABG yielded a stroke prevalence comparable to CABG five years after CEA.

Off-pump coronary artery bypass grafting not only eliminates the risk of adverse effects associated with cardiopulmonary bypass but also provides stroke prevention, particularly when the aorta is not manipulated and arterial grafts are used.[14] Ramponi et al.[15] recently reported a prospective series of 39 patients undergoing synchronous CEA and anaortic OPCABG, with a 30-day stroke rate of 2.6% and no perioperative myocardial infarction. Their conclusion that synchronous CEA-anaortic OPCABG is both safe and effective is consistent with our outcomes, supporting the role of anaortic OPCABG techniques in minimizing neurologic complications. However, because most previous combined CABG-CEA studies used the ONCABG procedure for coronary revascularization, data on both technical details and specific outcomes for OPCABG-CEA are limited.[16] According to a recent study, 32.5% of 222 patients undergoing combined CABG-CEA received the off-pump technique. The overall postoperative stroke and mortality rates ranged from 1.4% to 9% and 2.2% to 8%, respectively, showing a decline compared with previous decades. Although this study found no difference in neurological outcomes between on-pump coronary artery bypass grafting (ONCABG) and OPCABG patients, technical details about OPCABG, such as the number of revascularized target vessels and use of the aortic no-touch technique, were insufficient to make a strong definitive conclusion.[17]

Limitations

The main limitation of this study is the retrospective nature of the data. It is also difficult to design a study to compare outcomes with on-pump CABG patients. Our group has practiced off-pump CABG with a facile stabilization technique since the late 1990s. No-touch aorta versus single side-biting techniques were not compared, as 83.3% of the patients underwent no-touch aorta procedures. Male versus female patients were not compared, as women comprised only 20% of the study population. The study population consisted of CABG candidates with asymptomatic carotid artery disease diagnosed during preoperative duplex screening. The data available for analysis were primarily obtained from electronic medical records. Additionally, our cardiac surgery outcomes were affected by the COVID-19 pandemic.

Conclusion

Our study showed that concomitant off-pump CABG and CEA, mainly using a no-touch aorta technique and complete arterial revascularization, was safe and effective for patients with coronary artery disease and severe carotid artery disease. Neurological events were a leading cause of mortality after CABG. Neither off-pump nor aortic no-touch techniques can eliminate neurological complications. Therefore, we suggest that concomitant off-pump CABG and CEA with no-touch aorta be considered the preferred revascularization technique at hospitals with skilled cardiovascular surgery and anesthesiology teams. We also suggest that larger randomized studies be conducted to further validate these outcomes while minimizing the risk of postoperative cerebrovascular events and cognitive deficits.

Ethics Committee Approval: Ethics committee approval was obtained from Ethics Committee of Koç University (Approval Number: 2023.350. IRB1.124, Date: 02.10.2023).

Informed Consent: The Institutional Review Board approved this study protocol and waived informed consent, which was obtained for all patients who agreed to the use of their data for research, as all evaluations were made from existing institutional data.

Conflict of Interest: The authors declare no conflicts of interest with respect to the authorship and/or publication of this article.

Funding: The authors received no financial support for the research and/or authorship of this article.

Use of AI for Writing Assistance: No artificial intelligence (AI)–assisted technologies (such as large language models, chatbots, or image generators) were used in the preparation of this manuscript.

Author Contributions: Concept – M.Ş.A., E.A.; Design – M.Ş.A., Z.T.D.; Supervision – M.Ş.A., Z.T.D.; Resource – M.Ş.A., S.G.; Materials – M.Ş.A., S.G.; Data Collection and/or Processing – M.Ş.A., E.A.; Analysis and/or Interpretation – M.Ş.A., E.A., Z.T.D.; Literature Review – M.Ş.A., E.A.; Writing – M.Ş.A., Z.T.D.; Critical Review – M.Ş.A., Z.T.D.

Acknowledgments: The authors would like to express their gratitude to Haldun Y. Karagöz, MD, for sharing his personal experience, mentorship, data, and critical sense greatly contributed to the expertise on the use of arterial grafts for myocardial revascularization in its pioneering era and to staff members Gülhan A. Ünlü, RN, and Hazal Duruk, RN, for project oversight and close follow-up of the patients.

Peer-review: Externally peer-reviewed.

References

1. Taylan G, Kaya Ç, Özbek M, et al. Short-Term Prognosis of Elderly Patients Admitted to the Coronary Care Unit: A Subgroup Analysis of the MORCOR-TURK (Mortality and Morbidity in Coronary Care Units in Türkiye) Trial. Turk Kardiyol Dern Ars. 2024;52(6):411-419. [CrossRef]
2. Mazzolai L, Teixido-Tura G, Lanzi S, et al.; ESC Scientific Document Group. 2024 ESC Guidelines for the management of peripheral arterial and aortic diseases. Eur Heart J. 2024;45(36):3538-3700. [CrossRef]
3. Wang LJ, Mohebali J, Goodney PP, et al. The effect of clinical coronary disease severity on outcomes of carotid endarterectomy with and without combined coronary bypass. J Vasc Surg. 2020;71(2):546-552. [CrossRef]
4. Penton A, Lin J, Kolde G, DeJong M, Blecha M. Investigation of Combined Carotid Endarterectomy and Coronary Artery Bypass Graft Surgery Outcomes and Adverse Event Risk Factors in the Vascular Quality Initiative. Vasc Endovascular Surg. 2023;57(8):884-900. [CrossRef]
5. Klarin D, Patel VI, Zhang S, et al. Concomitant carotid endarterectomy and cardiac surgery does not decrease postoperative stroke rates. J Vasc Surg. 2020;72(2):589-596.e3. [CrossRef]
6. Piotrowski JJ. Carotid endarterectomy should be performed first rather than combined with coronary bypass. J Vasc Surg. 2020;72(6):2214. [CrossRef]
7. Haywood NS, Ratcliffe SJ, Zheng X, et al. Operative and long-term outcomes of combined and staged carotid endarterectomy and coronary bypass. J Vasc Surg. 2023;77(5):1424-1433.e1. [CrossRef]
8. Kurtoğlu M, Ateş MŞ, Duvan İ, Onuk BE, Karagöz YH. Concomitant carotid endarterectomy and off-pump coronary artery bypass grafting in coexistent carotid and coronary artery diseases. Turk J Med Sci. 2012;42(Suppl 1):1247-1251. [CrossRef]
9. Parolari A, Pesce LL, Trezzi M, et al. Performance of EuroSCORE in CABG and off-pump coronary artery bypass grafting: single institution experience and meta-analysis. Eur Heart J. 2009;30(3):297-304. [CrossRef]
10. Kurtoglu M, Ates S, Demirozü T, Duvan I, Karagoz HY, Aybek T. Facile stabilization and exposure techniques in off-pump coronary bypass surgery. Ann Thorac Surg. 2008;85(5):e30-e31. [CrossRef]
11. Illuminati G, Schneider F, Greco C, et al. Long-term results of a randomized controlled trial analyzing the role of systematic pre-operative coronary angiography before elective carotid endarterectomy in patients with asymptomatic coronary artery disease. Eur J Vasc Endovasc Surg. 2015;49(4):366-374. [CrossRef]
12. Masabni K, Raza S, Blackstone EH, Gornik HL, Sabik JF 3rd. Does preoperative carotid stenosis screening reduce perioperative stroke in patients undergoing coronary artery bypass grafting? J Thorac Cardiovasc Surg. 2015;149(5):1253-1260. [CrossRef]
13. Tzoumas A, Giannopoulos S, Charisis N, et al. Synchronous versus staged carotid artery stenting and coronary artery bypass graft for patients with concomitant severe coronary and carotid artery stenosis: A systematic review and meta-analysis. Vascular. 2020;28(6):808-815. [CrossRef]
14. Ramponi F, Seco M, Brereton RJL, et al. Toward stroke-free coronary surgery: The role of the anaortic off-pump bypass technique. J Card Surg. 2021;36(4):1499-1510. [CrossRef]
15. Ramponi F, Seco M, Bannon PG, et al. Synchronous Carotid Endarterectomy and Anaortic Off-Pump Coronary Artery Bypass Surgery. Heart Lung Circ. 2023;32(5):645-651. [CrossRef]
16. Minisandram A, Shah AY, Yao M, et al. Lessons learned during a 30-year experience with simultaneous carotid endarterectomy and coronary artery bypass grafting. J Vasc Surg. 2021;73(2):542-547. [CrossRef]
17. Modugno P, Picone V, Centritto EM, et al. Combined Treatment with Carotid Endoarterectomy and Coronary Artery Bypass Grafting: A Single-Institutional Experience in 222 Patients. Vasc Endovascular Surg. 2022;56(6):566-570. [CrossRef]

ARCHIVES OF THE TURKISH SOCIETY OF CARDIOLOGY

Official journal of the TURKISH SOCIETY OF CARDIOLOGY

How to Perform Open Window Mapping and Ablation in Patients with Wolff-Parkinson-White Syndrome: A Comprehensive Technical Guide Using CARTO™ and EnSite Electroanatomic Mapping Systems

Wolff-Parkinson-White Sendromlu Hastalarda Open Window Haritalama ve Ablasyon Nasıl Yapılır: CARTO™ ve EnSite Elektroanatomik Haritalama Sistemleri Kullanılarak Kapsamlı Teknik Kılavuz

Wolff-Parkinson-White (WPW) syndrome arises from the persistence of one or more accessory pathways (APs) that bypass the atrioventricular (AV) node, leading to pre-excitation. These pathways may conduct in an antegrade, retrograde, or bidirectional manner and may exhibit either decremental or non-decremental properties. Clinically, patients may present with orthodromic atrioventricular reciprocating tachycardia (AVRT), antidromic AVRT, or pre-excited atrial fibrillation, each with distinct risk profiles. Ablation success hinges on precise anatomical and electrophysiological localization of the AP's atrial and/or ventricular insertion.[1] Conventional local activation time (LAT)-based sequential point-by-point activation mapping or differential pacing strategies can be limited by conduction directionality, far-field overlap, signal distortion, and poor catheter-tissue contact. Open Window Mapping (OWM) overcomes these limitations by integrating anatomical and temporal data into a high-resolution, automated annotation schema that surpasses conventional mapping approaches. The subsequent sections elaborate on how OWM addresses these challenges.

Peri-Procedural Strategy

Surface Electrocardiography

Algorithmic localization of APs in patients with WPW syndrome is a critical step in guiding ablation strategy. Validated electrocardiographic algorithms should be employed to predict the anatomical location of the AP based on surface electrocardiogram (ECG) findings. This involves systematic analysis of delta wave polarity across all 12 leads, along with evaluation of the QRS axis and morphology. Notably, variability in QRS patterns may suggest the presence of multiple APs. Furthermore, intermittent pre-excitation observed on ECG or ambulatory monitoring implies variable antegrade conduction, which can affect both risk assessment and procedural planning. Holter or event monitoring complements the diagnostic work-up by quantifying arrhythmia burden, assessing fluctuations in pre-excitation, and detecting episodes of orthodromic or antidromic AVRT or pre-excited atrial fibrillation—both of which are important in risk stratification and therapeutic decision-making.

Cardiac Imaging

Cardiac magnetic resonance imaging (MRI) or computed tomography (CT) is recommended for patients with structural cardiac anomalies or previous failed ablation attempts, as these modalities offer detailed anatomical visualization that is essential for pre-procedural planning and risk assessment (Video 1). In addition, intracardiac echocardiography (ICE) serves as a valuable tool during electrophysiological procedures by providing real-time imaging guidance. ICE facilitates safe and precise transseptal puncture and supports accurate navigation around the annulus, thereby enhancing procedural efficacy and reducing complications in complex structural settings.

HOW TO?
NASIL YAPALIM?

Serkan Çay[1]
Meryem Kara[1]
Serhat Koca[2]
Özcan Özeke[1]
Elif Hande Özcan Çetin[1]
Ahmet Korkmaz[1]
Fırat Özcan[1]
Serkan Topaloğlu[1]

[1]*Division of Arrhythmia and Electrophysiology, Department of Cardiology, University of Health Sciences, Yüksek İhtisas Cardiovascular Building, Ankara City Hospital, Ankara, Türkiye*
[2]*Division of Arrhythmia and Electrophysiology, Department of Pediatric Cardiology, University of Health Sciences, Yüksek İhtisas Cardiovascular Building, Ankara City Hospital, Ankara, Türkiye*

Corresponding author:
Serkan Çay
✉ cayserkan@yahoo.com

Received: June 07, 2025
Accepted: September 05, 2025

Cite this article as: Çay S, Kara M, Koca S, et al. How to Perform Open Window Mapping and Ablation in Patients with Wolff-Parkinson-White Syndrome: A Comprehensive Technical Guide Using CARTO™ and EnSite Electroanatomic Mapping Systems. *Turk Kardiyol Dern Ars.* 2025;53(7):524-535.

DOI: 10.5543/tkda.2025.14636

Copyright@Author(s)
Available online at archivestsc.com.
Content of this journal is licensed under a Creative Commons Attribution – NonCommercial-NoDerivatives 4.0 International License.

Although imaging is primarily recommended in the presence of structural cardiac anomalies or previous failed ablation attempts, it can also provide significant procedural advantages in anatomically normal hearts. First, pre-procedural imaging—particularly cardiac MRI or CT—provides high-fidelity three-dimensional (3-D) anatomical reconstructions that can be integrated into the electroanatomic mapping (EAM) system. This integration improves the anatomical accuracy of chamber geometry, facilitates orientation in anatomically complex regions (e.g., annular structures), and reduces reliance on fluoroscopy. Second, ICE, used intra-procedurally, provides real-time visualization of catheter position and tissue contact, which is particularly advantageous when performing high-density mapping along the atrioventricular annulus. Even in structurally normal hearts, such imaging optimizes the spatial correlation between anatomical landmarks and electrophysiological data, thereby reducing mapping errors related to catheter instability, far-field signal interpretation, or anatomic misregistration.

The imaging data might be co-registered with the EAM system before initiation of OWM. This step allows for more precise delineation of atrial and ventricular boundaries and facilitates targeted mapping along the true annular plane. As a result, the anatomical model used during OWM is highly congruent with the patient's native anatomy, improving localization of AP breakthrough sites and, ultimately, increasing mapping accuracy and procedural efficiency.

Diagnostic/Mapping Catheters

Diagnostic catheter placement includes a quadripolar catheter in the high right atrium, a quadripolar catheter at the His bundle region, a decapolar catheter in the coronary sinus (CS), and a quadripolar catheter at the right ventricular apex. For high-density EAM, the CARTO™ system utilizes either the PentaRay™, OctaRay™, or Optrell™ multipolar mapping catheter, while the EnSite system employs the Advisor™ HD Grid catheter. Ablation is performed using a 3.5 mm open-irrigated, contact force–sensing catheter such as the ThermoCool SmartTouch™, TactiCath™, or TactiFlex™ ablation catheter, with irrigation flow rates typically ranging from 17 to 30 mL/min.

Electrophysiological Study

A comprehensive electrophysiological study to evaluate AP conduction and arrhythmia inducibility typically includes incremental and programmed stimulation from both the atrium and ventricle, using decremental cycle lengths and extrastimulus protocols. Burst pacing may be employed to induce orthodromic or antidromic AVRT. Para-Hisian pacing is performed to differentiate a septal AP from AV nodal conduction. Isoproterenol is infused starting at 1 µg/min and titrated up to 5 µg/min as needed to enhance AP conduction, facilitate arrhythmia induction, or achieve a > 20% increase in sinus rate. Differential pacing maneuvers are also utilized to assess ventriculoatrial (VA) conduction and to exclude the presence of bystander pathways.

Conventional mapping remains a widely used electrophysiological technique for localizing APs, either through identification of the earliest retrograde atrial or anterograde ventricular activation, or by direct recording of discrete AP potentials. This method involves the acquisition of bipolar electrograms (EGMs), which are recorded either from a single electrode pair or simultaneously from multiple electrode pairs using multielectrode catheters. Conventional mapping may be performed with or without the integration of 3-D EAM systems.

When employed without 3-D guidance, the technique relies on the manual correlation of EGM signals with anatomical landmarks and fluoroscopic imaging, which may limit spatial precision. In contrast, the use of 3-D EAM systems enhances this approach by enabling real-time spatial localization of catheter positions within the cardiac chamber. These systems, equipped with automated annotation algorithms, facilitate more accurate mapping by allowing operators to annotate and visualize EGM data within a reconstructed anatomical model.

The introduction of 3-D navigation-compatible, sensor-enabled mapping catheters, particularly multipolar catheters with closely spaced electrodes, permits high-density point acquisition and improves the spatial resolution of EGM recordings. This improved resolution, in association with AP conduction, can lead to more accurate identification of the earliest atrial or ventricular activation sites relative to a reference point.[2]

Electrophysiological Principles of OWM

Open Window Mapping is an advanced EAM strategy designed to overcome the spatial and temporal limitations of traditional LAT mapping. By annotating LATs to a stable reference—typically the surface QRS complex or a pacing spike—OWM establishes a user-defined temporal interval, called the window of interest (WOI) or roving acquisition interval (RAI), to isolate physiologically relevant electrogram activity. Within this constrained window, the system automatically identifies the earliest near-field local activation by prioritizing steep unipolar negative dV/dt signals or sharp bipolar deflections, thereby reducing or eliminating the need for manual annotation. Thus, it is not necessary to distinguish between atrial, ventricular, or accessory pathway EGMs. Moreover, all signals within the WOI/RAI are included during annotation. This decoupling from global chamber activation enables accurate detection of breakthrough sites across the AV annulus, particularly at AP insertions. High-density point collection (> 1,000 evenly distributed annotations) under respiratory gating ensures spatial resolution below 2 mm, and breakthrough identification is validated by cross-referencing bipolar and unipolar electrograms. OWM therefore provides a temporally and spatially precise representation of AP conduction, independent of wavefront direction. If available, the use of automatic algorithms indicating a line of block may help identify block sites and AP conduction breakthroughs at the AV annulus. OWM can be performed during tachycardia, under atrial or ventricular pacing, or during fully pre-excited sinus rhythm.

CARTO™ System-Based OWM Protocol

The use of high-resolution EAM systems—particularly the CARTO™ 3 platform integrated with advanced modules such as CONFIDENSE™—has significantly improved the identification and characterization of AP insertion sites in patients with WPW syndrome. Key features include:

1. Continuous mapping filters such as cycle length range and stability, pattern matching, position and LAT stability, and density;
2. System filters including tissue proximity indication (TPI) and respiration gating;

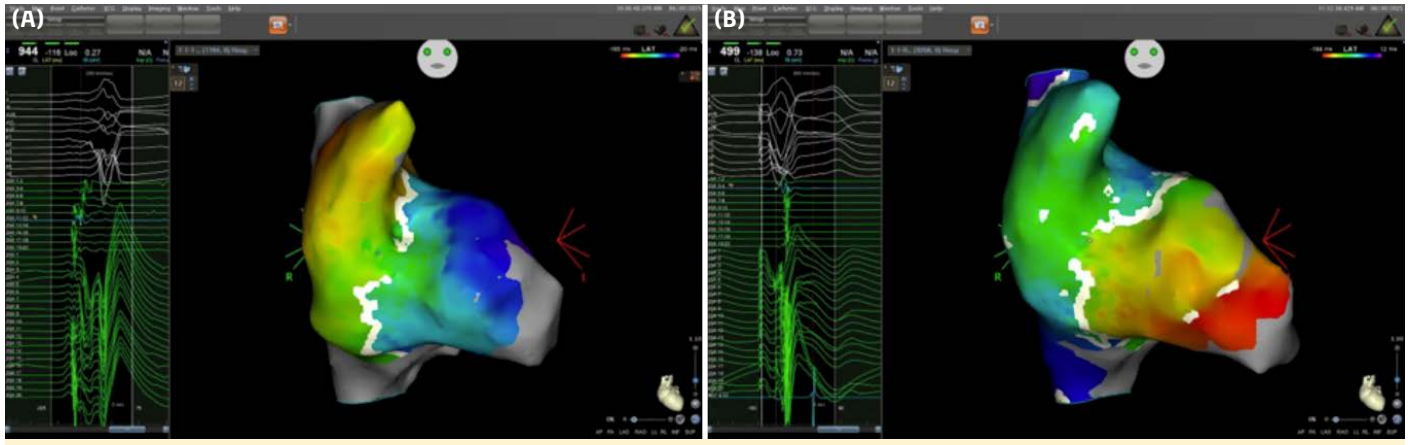

Figure 1. Color-coded LAT mapping derived from the Carto EAM system showing localization of a right-sided free-wall AP using both the OWM and EEML algorithms during sinus rhythm with full pre-excitation (A) and during ventricular pacing (B). The left panels display an extended WOI along with bipolar and unipolar EGMs recorded from the multielectrode mapping catheter, with automatic annotation of the selected point on the map.

AP, Accessory pathway; EAM, Electroanatomic mapping; EEML, Extended early-meets-late; EGM, Electrogram; LAT, Local activation time; OWM, Open Window Mapping; WOI, Window of interest.

3. Map consistency; and especially
4. The wavefront annotation algorithm, which uses both bipolar and unipolar EGMs to generate activation maps and indicate the localization and propagation direction of APs.

The automated wavefront annotation algorithm analyzes the rate of voltage change (dV/dt) in the unipolar EGM. The point exhibiting the steepest dV/dt slope on the unipolar EGM is expected to correspond to a feature on the associated bipolar EGM. Subsequently, the LAT is marked on the unipolar EGM. This dual-signal approach enhances spatial and temporal resolution, allowing the system to distinguish true local electrograms from far-field artifacts with greater confidence.

Previously mentioned additional optimization features, including continuous mapping filters, TPI, respiratory gating, and the map consistency algorithm, are utilized to ensure high-fidelity data capture and to eliminate erroneous or noisy points that are incongruent with their spatial neighbors. Furthermore, these features improve beat discrimination accuracy and reduce reliance on manual LAT reannotation.

The extended early-meets-late (EEML) algorithm, particularly when set at low thresholds (e.g., 15–85%), is employed alongside high-density (HD) Coloring to quantify temporal gradients between adjacent points and to visualize conduction discontinuities, including functional blocks and bridging areas where the AP transmits impulses between chambers.[3,4]

The OWM strategy involves delineating a custom-defined WOI based on the timing of the surface electrocardiogram or a stable intracardiac reference signal (such as CS signals), typically determined using the Advanced Reference Annotation (ARA) algorithm. This window is carefully selected to encompass the earliest and latest atrial and ventricular activations, capturing the full sequence of electrical propagation—from the sinoatrial nodal region to the ventricular basal region—including, in particular, across the AV annulus during sinus rhythm; from the atrial or ventricular pacing site to the region of latest activation in the opposite chamber during continuous pacing; or, during orthodromic or antidromic AVRT, from the ventricle to the atria or vice versa, thereby enabling full chamber acquisition. For instance, in the referenced protocol, a 300 ms WOI is established around the QRS end marker (0 ms), ranging from -225 ms to +75 ms. This allows comprehensive mapping of both the atrial and ventricular chambers, including the atrial and ventricular insertion zones of the AP, during sinus rhythm. Similarly, a 270 ms WOI, centered around the QRS end marker (0 ms) and ranging from -190 ms to +80 ms, enables comprehensive mapping of both the atrial and ventricular chambers, including the atrial and ventricular insertion zones of the AP, during ventricular pacing (Figure 1, Video 2).

Mapping point acquisition is executed using a multielectrode, high-density mapping catheter (the 20-pole PentaRay™ catheter with 2 mm interelectrode spacing), which provides finely resolved spatial data across the cardiac chambers. The CONFIDENSE™ module facilitates automated and continuous point collection while enforcing strict acquisition criteria: narrow cycle length range/stability (≤ ±20 ms, 5%), high pattern-matching threshold (≥ 95%), low position stability (≤ 4 mm), low LAT stability (≤ 5 ms), maximum density, and map consistency with automatic calculation, with TPI and respiratory gating enabled. Filtering parameters are tailored to preserve signal fidelity (bipolar: 30–500 Hz; unipolar: 0.5–100 Hz; notch filters disabled).

With the aid of all these features, anatomical reconstructions of both the atria and the ventricle are created in real time. Activation mapping is superimposed to detect the breakthrough zone across the AV annulus, typically visualized as compact regions of continuous activation (mid-range colors on the color bar), in contrast to other annular regions that show discontinuity in color mapping. These regions are confirmed by the presence of unipolar QS morphology and by early, high-amplitude, fused atrial and ventricular bipolar signals that precede the delta wave onset of the surface QRS complex (Figure 1, Video 2).[5,6]

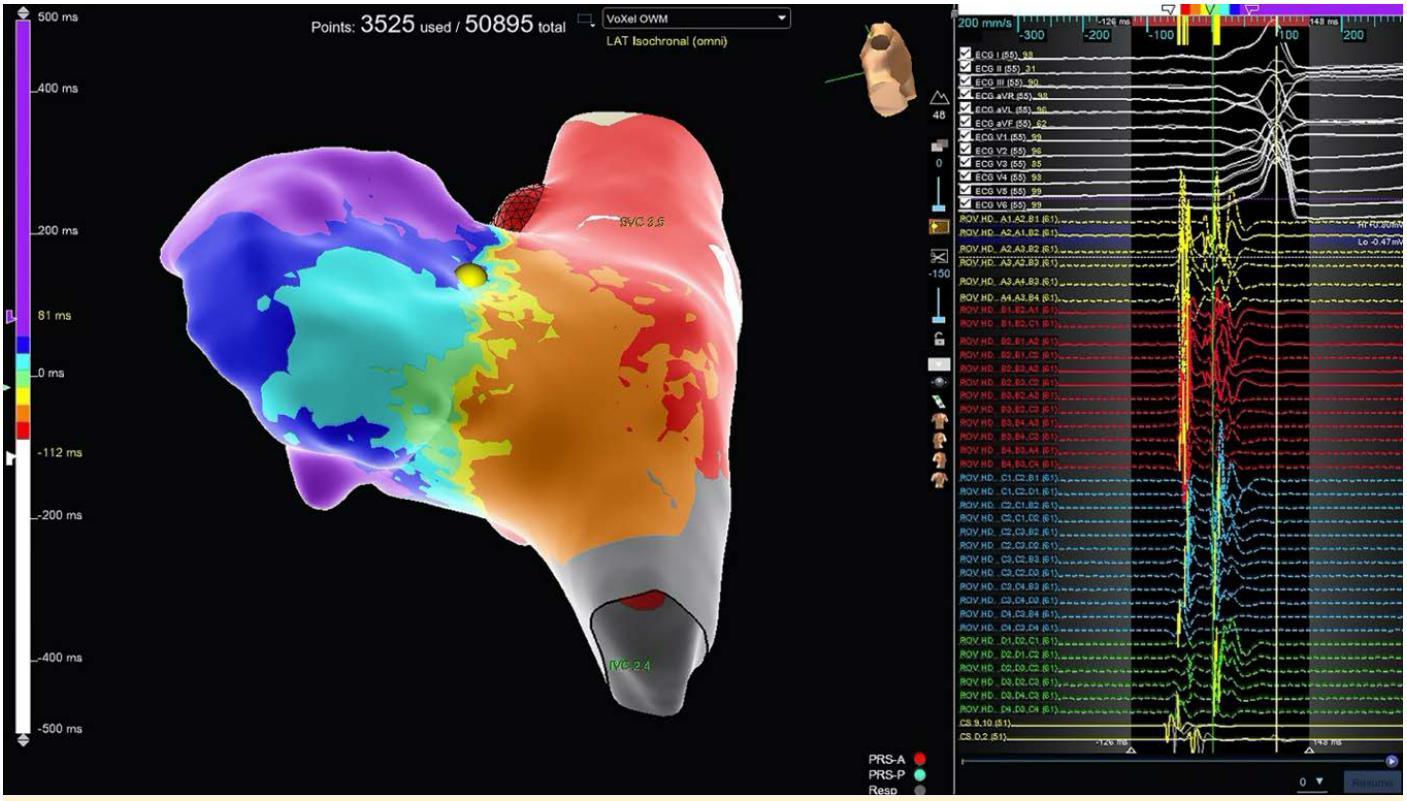

Figure 2. Color-coded LAT mapping derived from the EnSite X EAM system showing localization of a right-sided posteroseptal AP using both the OWM and OT algorithms during sinus rhythm with full pre-excitation. The right panel displays an extended RAI along with bipolar EGMs recorded from the multielectrode mapping catheter, with automatic annotation of the acquired points. The yellow tag indicates the His region.

AP, Accessory pathway; EAM, Electroanatomic mapping; EGM, Electrogram; LAT, Local activation time; OT, Omnipolar technology; OWM, Open Window Mapping; RAI, Roving acquisition interval.

Collectively, this comprehensive and technically rigorous approach to high-density mapping allows for a nuanced, physiologically informed visualization of the AP substrate. It enables electrophysiologists to accurately identify true AP insertion sites, differentiate them from bystander conduction pathways, and plan targeted ablation strategies with maximal precision and efficiency.

EnSite System-Based OWM Protocol

The integration of advanced EAM technologies—namely Omnipolar Technology (OT)—with high-density catheter systems such as the Advisor™ HD Grid has markedly improved the precision and reliability of intracardiac mapping in the evaluation of APs and complex arrhythmogenic substrates. The HD Grid catheter, configured in a 4 × 4 electrode matrix comprising 16 equidistant electrodes, is uniquely designed to capture electrical signals in multiple directions using orthogonal bipolar pairs. This multidirectional configuration allows enhanced spatial sampling of wavefront propagation, particularly in regions with complex conduction patterns or anisotropic tissue properties. Building on this structural advantage, OT further elevates mapping fidelity by combining unipolar and bipolar electrogram data derived from triads of adjacent electrodes, referred to as cliques. This novel omnipolar signal-processing strategy generates local, beat-to-beat quantitative assessments of peak voltage, activation vector orientation, and conduction velocity, all while remaining independent of the catheter's positional alignment relative to the wavefront—thereby overcoming one of the critical limitations of traditional bipolar mapping.

During mapping procedures, OT permits dynamic assessment of the directionality of electrical activation and provides intuitive vector-based visualization of local conduction. In clinical contexts such as AP-related tachycardia, omnipolar activation vectors have been shown to facilitate accurate identification of the electrical insertion site of accessory fibers. Concurrently, the EnSite mapping system enables automated acquisition and annotation of LATs, based on either a surface QRS reference, pacing spike, or intracardiac reference. LAT annotations are algorithmically determined by identifying either the steepest negative slope (maximum dV/dt) or the absolute dV/dt of unipolar signals within a tailored RAI[2]—typically set as a 250–300 ms interval around the reference (Figures 2 and 3). Signal acquisition fidelity is tightly regulated using a combination of automated filters and threshold-based criteria within the AutoMap module. These include a morphology template match score exceeding 80, cycle length tolerance confined to ±20 ms, a speed limit of 10–20 mm/s, distance criterion set to OFF, signal-to-noise ratio between 3 and 5, and enhanced noise rejection set to ON (OFF during pacing). Additionally, map display features are configured with interior projection set to 5 and interpolation to 10.

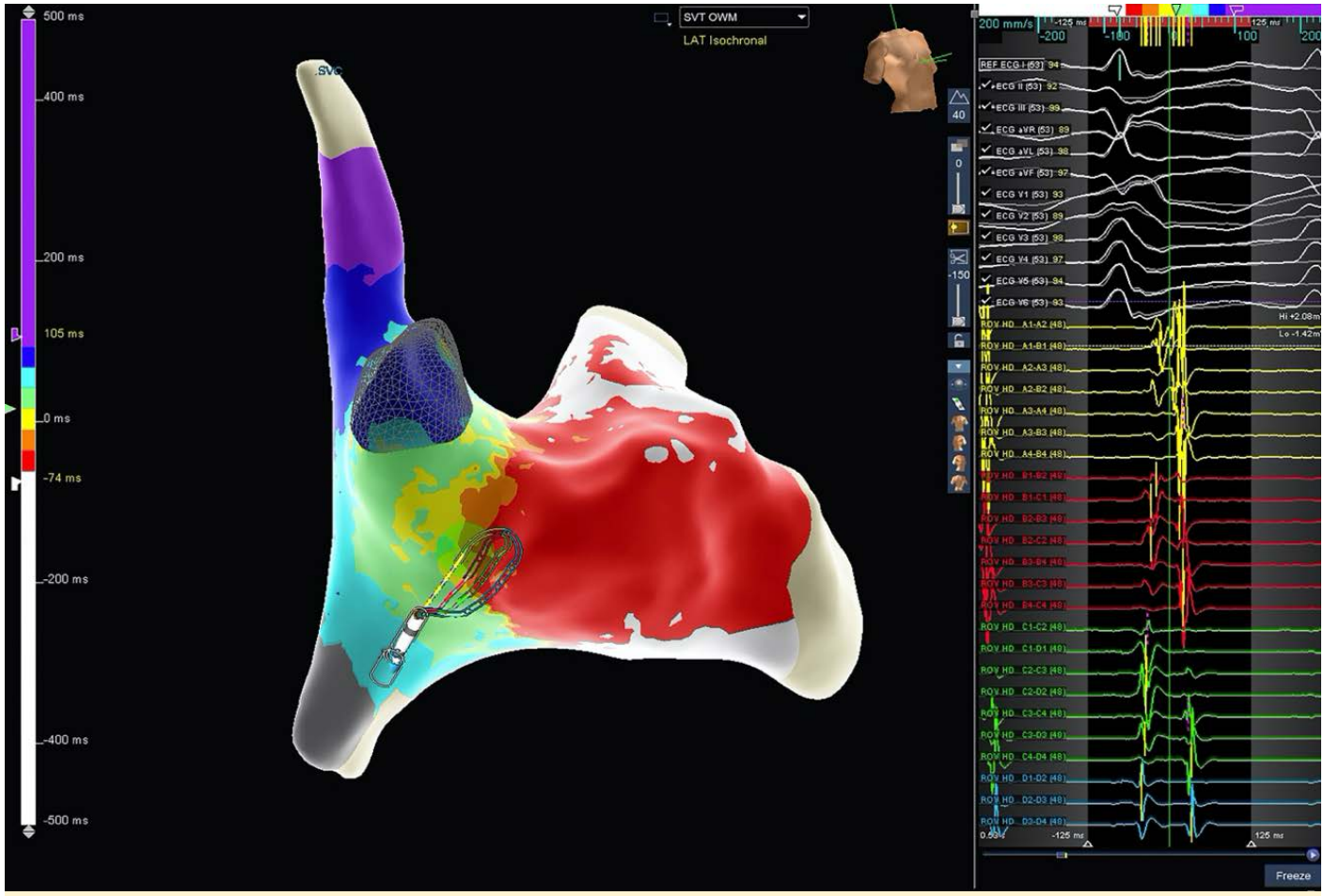

Figure 3. Color-coded LAT mapping derived from the EnSite Precision EAM system showing localization of a right-sided free-wall AP using the OWM algorithm during orthodromic AVRT in a 16-year-old female patient. The right panel displays an extended RAI along with bipolar EGMs recorded from the multielectrode mapping catheter, with automatic annotation of the acquired points using absolute dV/dt. The earliest atrial signal was recorded from the distal bipoles of the yellow spline.

AP, Accessory pathway; AVRT, Atrioventricular reciprocating tachycardia; EAM, Electroanatomic mapping; EGM, Electrogram; LAT, Local activation time; OWM, Open Window Mapping; RAI, Roving acquisition interval.

In both activation and propagation maps, early activation regions are denoted in white, with progressive isochronal contours delineating concentric propagation outward from the AP insertion point. The identification of closely spaced isochrones around the suspected site of insertion, combined with unipolar QS morphology and consistent near-field signals across orthogonal vectors, supports precise and reproducible localization (Figures 2 and 3, Videos 3 and 4).

Collectively, the use of omnipolar electrogram analysis in tandem with automated annotation technologies and a high-density, orthogonal electrode configuration offers an unprecedented level of anatomical and functional resolution. This integrated strategy not only facilitates the detailed characterization of APs and their insertion sites but also provides a robust platform for guiding ablation therapy with greater efficiency and confidence, particularly in challenging arrhythmia substrates where conventional mapping may fail due to limitations in directional sensitivity and signal reproducibility.

General and System-Specific Workflows for OWM

For clarity and ease of application, the complete OWM procedural sequence and key system-specific variations are summarized in Figure 4 and Table 1, which visually complement the detailed protocols described earlier.

While the fundamental workflow of OWM is consistent across platforms, the CARTO™ and EnSite systems incorporate distinct algorithmic, hardware, and visualization features that can influence procedural strategy. Table 2 summarizes the key system-specific advantages relevant to WPW ablation.

OWM integrates anatomical and temporal datasets to generate high-resolution automated maps, mitigating the limitations of conventional techniques related to conduction directionality, signal distortion, and suboptimal catheter–tissue contact.

With respect to poor contact, although multipolar high-density (HD) mapping catheters such as the PentaRay™ or Advisor™ HD Grid do not measure contact force (CF) directly, OWM protocols integrate several indirect yet robust safeguards to preferentially acquire data

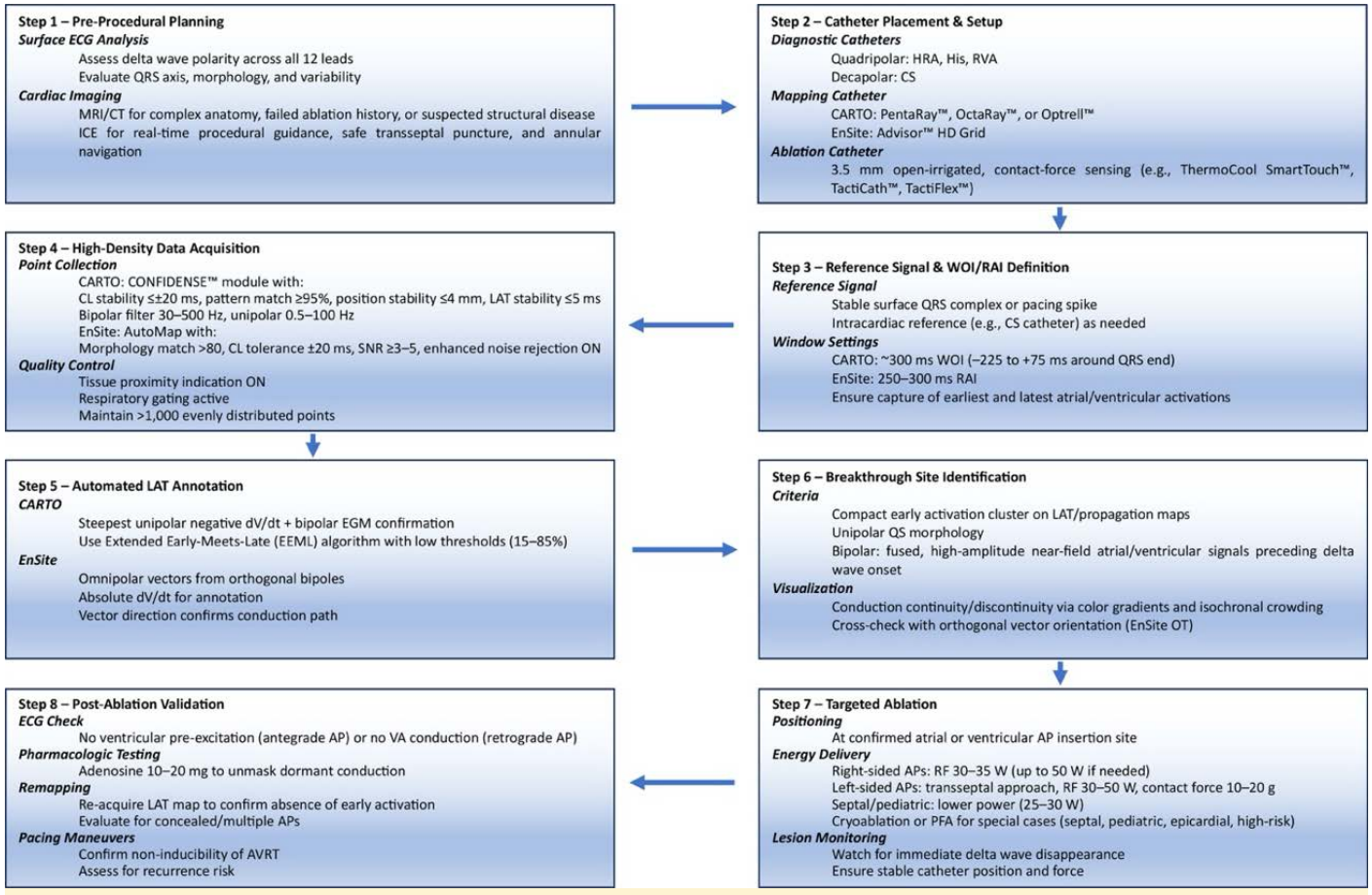

Figure 4. Flow diagram summarizing the stepwise OWM workflow for AP mapping and ablation.

AP, Accessory pathway; AVRT, Atrioventricular reciprocating tachycardia; CL, Cycle length; CS, Coronary sinus; CT, Computed tomography; ECG, Electrocardiogram; EGM, Electrogram; HRA; High right atrium; ICE, Intracardiac echocardiography; LAT, Local activation time; MRI, Magnetic resonance imaging; OT, Omnipolar technology; PFA, Pulse field ablation; RAI, Roving acquisition interval; RVA, Right ventricular apex; SNR, Signal-to-noise ratio; VA, Ventriculoatrial; WOI, Window of interest.

from adequately opposed electrodes. These include the use of tissue proximity indicator modules, which estimate contact quality through impedance- and location-based parameters, and the application of respiratory gating and map consistency algorithms to remove points exhibiting instability—features frequently associated with intermittent or poor contact. In addition, the acquisition process enforces strict positional and timing stability filters, which bias the dataset toward stable, well-positioned catheter contacts. Electrogram morphology criteria further refine data integrity by excluding points with attenuated amplitudes, excessive noise, or inconsistent near-field characteristics, all of which are typical markers of suboptimal tissue contact.

In terms of mitigating signal distortion, OWM employs a combination of anatomical integration and advanced signal-processing strategies. The automated annotation algorithm cross-validates unipolar and bipolar electrograms by identifying the steepest unipolar negative dV/dt and confirming temporal concordance with the sharpest bipolar deflection, thereby reducing the likelihood of far-field contamination. By constraining annotation to a user-defined WOI or RAI, the system isolates physiologically relevant activations and excludes spurious deflections outside the targeted temporal range. Furthermore, with the Advisor™ HD Grid catheter, multidirectional signal capture via OT mitigates the directional sensitivity inherent to conventional bipolar recordings and ensures consistent earliest activation identification regardless of catheter orientation. Automated noise rejection and morphology-matching filters provide an additional safeguard against baseline wander, pacing artifacts, and other sources of distortion, thus preserving signal fidelity.

Collectively, these integrated hardware and software features allow OWM to compensate for the lack of direct CF sensing in HD mapping catheters and substantially attenuate the effects of signal distortion. This combination yields high-resolution, reproducible activation maps with superior spatial and temporal precision compared to conventional LAT-based mapping techniques, even in anatomically and electrically complex substrates.

Ablation Protocols

The cornerstone of successful AP ablation lies in precise target site identification, effective radiofrequency (RF) energy delivery tailored to pathway location, and rigorous endpoint validation to ensure durable lesion formation and long-term arrhythmia-free outcomes.

Table 1. System-specific OWM workflow variations

Step	CARTO™ 3 Workflow	EnSite Precision/X Workflow
Reference Definition	Advanced Reference Annotation (ARA): select a stable reference from surface QRS, pacing spike, or intracardiac signal (e.g., coronary sinus). Used to align the WOI to capture earliest atrial and ventricular activations.	Select a stable reference from surface QRS, pacing spike, or intracardiac signal (e.g., coronary sinus). LAT annotations determined from the steepest unipolar dV/dt or absolute dV/dt within the RAI.
WOI/RAI Setting	Typical: 300 ms WOI around QRS end marker (0 ms); e.g., –225 ms to +75 ms for sinus rhythm; 270 ms (–190 ms to +80 ms) for ventricular pacing.	Typical: 250–300 ms RAI around reference; adjustable to match conduction scenario.
Point Acquisition Module	CONFIDENSE™: automated continuous mapping with strict criteria—cycle length stability ≤ ±20 ms (5%), pattern match ≥ 95%, position stability ≤ 4 mm, LAT stability ≤ 5 ms, high density, map consistency ON, tissue proximity and respiratory gating enabled.	AutoMap: morphology match ≥ 80%, cycle length tolerance ± 20 ms, speed limit 10–20 mm/s, SNR 3–5, noise rejection ON (OFF during pacing), distance criterion OFF, interior projection 5, interpolation 10.
Key Mapping Algorithm	Wavefront annotation: steepest unipolar negative dV/dt aligned with bipolar deflection; dual-signal concordance reduces far-field artifacts. Filtering: bipolar 30–500 Hz, unipolar 0.5–100 Hz, notch filters OFF.	Omnipolar Technology (OT): uses orthogonal bipoles in HD Grid "cliques" to generate vectorbased LAT and conduction velocity independent of catheter orientation.
Conduction Gap Visualization	Extended Early-Meets-Late (EEML) at low thresholds (e.g., 15–85%) plus HD Coloring to reveal conduction discontinuities and AP breakthrough zones.	Isochronal crowding plus omnipolar vector plots to show breakthrough and conduction direction.
Mapping Catheter	PentaRay™ (20-pole, 2 mm spacing)/OctaRay™/Optrell™ for high-density mapping.	Advisor™ HD Grid (16 electrodes, 4 × 4 matrix) for multidirectional mapping.
Unique Strength	High-precision unipolar–bipolar concordance, submillimeter AP localization, robust noise filtering, continuous high-density acquisition.	Orientation-independent activation mapping with quantitative conduction vectors; robust in complex, anisotropic conduction.

LAT, Local activation time; OWM, Open Window Mapping; RAI, Roving acquisition interval; WOI, Window of interest.

Table 2. Comparative advantages of CARTO™ and EnSite Systems for OWM in WPW ablation

Feature/ Capability	CARTO™ 3	EnSite Precision/X
Core OWM Algorithm	Wavefront annotation using steepest unipolar dV/dt aligned to bipolar deflection; Advanced Reference Annotation (ARA) for WOI definition	Roving Acquisition Interval (RAI) with steepest or absolute unipolar dV/dt detection; Omnipolar Technology (OT) for vector-based LAT assignment
High-Density Mapping Catheters	PentaRay™ (20 poles, 2 mm spacing), OctaRay™, Optrell™	Advisor™ HD Grid (16 electrodes in 4 × 4 matrix) enabling orthogonal bipolar pairs
Directional Sensitivity	Enhanced by combining unipolar and bipolar annotation; reduced far-field influence via automated LAT filters	Direction-independent LAT detection via omnipolar vectors, overcoming catheter-wavefront alignment issues
Continuous Mapping Automation	CONFIDENSE™ module with strict acquisition filters (cycle length stability, pattern match ≥ 95%, position stability ≤ 4 mm)	AutoMap with morphology match ≥ 80%, cycle length tolerance ±20 ms, enhanced noise rejection
Noise & Artifact Management	Respiratory gating, tissue proximity indication, map consistency algorithms to reject spatially inconsistent points	Adjustable signal-to-noise ratio thresholds (3–5), speed limit control, interior projection and interpolation settings
Visualization of Conduction Gaps	Extended Early-Meets-Late (EEML) algorithm with HD Coloring for conduction discontinuity mapping	Isochronal crowding with omnipolar vectors; dynamic conduction velocity assessment
Best-Suited Scenarios	Detailed annular mapping in complex AP anatomy where unipolar-bipolar concordance is critical	Mapping in anisotropic tissue or complex conduction patterns where catheter orientation may limit bipolar accuracy
Unique Strength	Highly refined dual-signal annotation (unipolar + bipolar) with advanced map consistency tools	True vector-based omnipolar mapping providing orientation-independent LATs and conduction velocity

AP, Accessory pathway; LAT, Local activation time; OWM, Open Window Mapping; WOI, Window of interest; WPW, Wolff-Parkinson-White (syndrome).

Accurate localization of the AP insertion site is primarily guided by electrophysiological signals. A successful ablation target is characterized by the earliest local bipolar EGMs that precede the onset of the surface delta wave during atrial pacing or antidromic AVRT in antegrade conduction pathways, or by the earliest EGMs that precede the reference atrial electrogram during ventricular pacing or orthodromic AVRT in retrograde conduction. In either conduction direction, early activation timing is critical and indicates proximity to the AP atrial or ventricular insertion site (Figures 5 and 6, Videos 4, 5, and 6).

Unipolar EGMs at the ablation site should demonstrate a QS morphology with a steep negative downstroke, reflecting the site of earliest depolarization with minimal far-field interference.

Figure 5. An irrigated tip force-sensing ablation catheter positioned at the atrial insertion site demonstrates a fused and earliest ventricular bipolar signal relative to the delta wave, with immediate abolition of the AP following ablation. This is evidenced by abrupt prolongation of the ventricular signal and disappearance of the delta wave on the surface electrocardiogram (ECG).

AP, Accessory pathway.

Additionally, local bipolar EGM amplitude should ideally exceed normal voltage thresholds, indicating robust, high-fidelity signals suggestive of close catheter-tissue contact and viable substrate.

Target sites are best selected when they exhibit compact, discrete, and reproducible early signals across sequential beats, with anatomical correlation to the annular insertion—particularly when using EAM systems. The integration of the OWM technique enables high-resolution visualization of LATs and facilitates accurate annotation of earliest activation clusters.

Radiofrequency energy parameters should be titrated according to the anatomical location of the AP, with careful consideration of lesion depth, power delivery, and procedural safety. For right-sided APs, RF power is typically initiated at 30–35 W and may be titrated up to 50 W, with lesion durations ranging from 30 to 60 seconds. In specific cases—such as septal pathways or pediatric patients—power may be limited to 25–30 W due to the proximity of critical conduction tissue.

For left-sided APs, transseptal access is the preferred approach, offering superior catheter stability and a more favorable trajectory compared to the retrograde aortic route. RF power delivery typically ranges from 30–50 W, with contact force maintained between 10 and 20 grams.

When available, advanced lesion metrics—such as Ablation Index (AI), Lesion Size Index (LSI), or average impedance drop—should be used to guide lesion efficacy, serving as reliable surrogates for adequate lesion formation across most anatomical locations. Consistent catheter position and stable contact force throughout the application are essential to ensure transmural and durable lesion formation.

Cryoablation of APs—particularly those located in septal regions and in the pediatric population—is a technically demanding procedure due to the close anatomical proximity to the conduction system. Cryoablation offers a cryomapping phase at sublethal temperatures (typically around –30°C), allowing functional assessment of the target site before creating irreversible lesions at colder temperatures (–70°C to –80°C).

The use of 3-D EAM in conjunction with cryoablation enhances procedural efficacy and safety by enabling precise catheter navigation, real-time lesion annotation, and integration with intracardiac signals and imaging modalities.

Recent feasibility studies have demonstrated the potential utility of pulse field ablation (PFA) for targeting APs in WPW syndrome, particularly in cases refractory to conventional RF ablation or involving epicardial substrates. Focal PFA has been shown to

Figure 6. An irrigated tip force-sensing ablation catheter positioned at the posteroseptal region demonstrates a fused and earliest ventricular bipolar signal relative to the delta wave. The AP is abolished within four seconds of ablation, as evidenced by abrupt prolongation of the ventricular signal and disappearance of the delta wave on the surface electrocardiogram (ECG).

AP, Accessory pathway.

achieve acute conduction block in various AP locations—including left lateral, posteroseptal, and right free wall—through both endocardial and coronary sinus approaches. Preliminary clinical data indicate high acute success rates and a favorable safety profile, with minimal procedural complications and no evidence of collateral damage to the atrioventricular node, coronary vasculature, or surrounding neural structures.[7,8] However, long-term efficacy data remain limited, and further investigation through larger, controlled trials is warranted to establish PFA as a standard therapeutic option for AP-mediated arrhythmias.

Ablation efficacy is assessed using a combination of electrophysiological and pharmacologic criteria. The immediate disappearance of ventricular pre-excitation on the surface ECG during sinus rhythm serves as the primary endpoint for antegrade-conducting pathways. For retrograde-only pathways, the loss of VA conduction during right ventricular pacing indicates successful interruption of AP conduction. Non-inducibility of AVRT using programmed atrial or ventricular stimulation further supports procedural success.

A negative adenosine challenge test—administered as a rapid intravenous bolus of 10–20 mg—should confirm the absence of dormant or latent AP conduction. Adenosine transiently blocks AV nodal conduction and may unmask residual AP activity, making it particularly useful in borderline or equivocal cases.

A robust post-ablation protocol should include pacing maneuvers to assess for residual antegrade or retrograde conduction and to evaluate the presence of multiple or concealed APs. Remapping the previously successful ablation site using OWM or conventional point-by-point techniques is recommended to verify the absence of early local activation or residual AP potentials, thereby confirming durable pathway elimination. In cases of recurrence, remapping can help differentiate between inadequate lesion formation, epicardial or CS connections, and pathway recovery.

In summary, successful AP ablation requires a methodical approach incorporating detailed electrogram analysis, individualized RF energy application, and stringent validation of conduction block using both electrophysiological and pharmacologic endpoints. Advanced mapping technologies and lesion indices further enhance procedural safety and effectiveness, particularly in anatomically complex or high-risk substrates.

Troubleshooting During OWM and Ablation

Contact/Mechanical Artifacts

In our experience, catheter contact artifacts can occur when mapping catheters are positioned close to diagnostic catheters, such as the His bundle catheter. This is an acknowledged technical consideration during high-density EAM, particularly in septal AP cases where catheter trajectories converge. To minimize this risk, we employ several complementary strategies:

1. Maintaining clear fluoroscopic and electroanatomic spatial separation between mapping catheters and the His catheter;
2. Using TPI and respiratory gating features available in EAM systems to ensure that annotated points reflect true endocardial contact rather than incidental catheter-to-catheter interaction;
3. Validating suspected early activation points by cross-referencing bipolar and unipolar electrograms for near-field characteristics, including steep unipolar negative dV/dt and absence of mechanical artifact signatures; and
4. Repeating acquisitions from slightly adjusted mapping catheter positions if signal morphology suggests possible mechanical interference.

Importantly, when the mapping catheter inadvertently contacts the His catheter, we observe a reproducible mechanical deflection artifact that is distinct from true local activation—these points are excluded during map review. Through these procedural safeguards, we have found catheter contact artifacts to be rare and readily identifiable, and they have not compromised our localization accuracy.

Epicardial/Intramural APs

Although OWM offers high spatial and temporal resolution for most endocardial APs, its reliance on steep unipolar downstrokes or sharp bipolar deflections to determine local activation timing may present limitations in the setting of epicardial or intramurally located APs. In such cases, earliest activation may be attenuated, exhibit broad morphology, or demonstrate a delayed steepest dV/dt compared with true endocardial near-field signals, potentially leading to underestimation or mislocalization. To mitigate this, our protocol incorporates high-density point acquisition with bipolar–unipolar correlation, careful morphological assessment for QS patterns with low amplitude or broad deflections, and complementary mapping from the epicardium as well as from the CS or its branches—particularly for posteroseptal or free-wall pathways. ICE, contrast injection, and adjunctive conventional LAT or differential pacing maneuvers are employed when epicardial or intramural origin is suspected. In such scenarios, OWM findings are interpreted in conjunction with multimodal mapping and anatomical imaging to ensure accurate localization and avoid procedural misguidance.

Bystander APs

Open Window Mapping facilitates the distinction between true AP insertion sites and bystander conduction by temporally isolating physiologically relevant electrograms from unrelated activation. This is achieved through the use of a user-defined WOI or RAI referenced to a stable marker, such as the surface QRS complex, pacing spike, or intracardiac reference electrogram. Within this interval, the mapping system automatically identifies the earliest near-field local activation based on EGM characteristics—most notably the steepest unipolar negative dV/dt or sharp bipolar deflection—without requiring manual selection of atrial, ventricular, or pathway-specific signals. By constraining annotation to this physiologically relevant time frame, OWM effectively excludes far-field and sequential wavefront components that commonly obscure or mimic true AP signals in conventional mapping. In the resulting activation maps, true AP insertion sites are visualized as compact, high-density clusters of earliest activation along the AV annulus. EGM analysis at these sites consistently reveals unipolar QS morphology with a steep negative downstroke, indicating immediate local depolarization, and fused, high-amplitude bipolar signals that precede the onset of the delta wave during antegrade conduction or the reference atrial signal during retrograde conduction. In contrast, bystander sites exhibit later activation within the WOI/RAI, lack unipolar QS morphology, and demonstrate electrogram patterns consistent with passive conduction from adjacent tissue rather than direct pathway insertion. Propagation maps further reinforce this distinction by showing conduction continuity across the annulus at true AP sites, whereas bystander regions display discontinuity or delayed wavefront progression. Through this combination of temporally constrained annotation, high-density spatial sampling, and morphology-based signal validation, OWM provides a physiologically faithful representation of AP conduction. This capability enables electrophysiologists to reliably differentiate true AP insertion points from non-conducting annular myocardium or passive conduction sites, thereby informing more targeted and effective ablation strategies.

Para-Hisian APs

Para-Hisian APs are widely recognized as one of the most challenging substrates for catheter ablation due to their close anatomical relationship with the His bundle and the presence of high-frequency His electrograms that can obscure accurate localization. However, the OWM approach remains a valuable tool for guiding ablation even in these complex scenarios. By integrating local activation timing with pace-mapping information and anatomical context, OWM allows accurate differentiation of true pathway potentials from near-field His activity. Importantly, the method helped avoid unnecessary ablation in the immediate vicinity of the His bundle while still enabling successful elimination of the pathway. This observation is in line with previous findings,[5] where OWM proved particularly useful in mapping para-Hisian pathways and provided guidance in circumstances where high-frequency His electrograms might otherwise have caused confusion. These results support the applicability of OWM in difficult perinodal substrates and underscore its potential to improve both the safety and efficacy of ablation in such cases.

AP Potential

Although a discrete AP potential was not visually evident in all of the presented examples, the earliest activation region identified on the 3-D electroanatomic map was systematically correlated with the corresponding bipolar and unipolar electrogram morphology. Specifically, the presence of an early and sharp bipolar deflection, together with a QS-pattern unipolar signal at these sites, was used to confirm local AP activation and to distinguish it from far-field atrial signals. In addition, to account for the well-described oblique course of AP activation, the mapping catheter was intentionally manipulated to record electrograms from different orientations at the same anatomical region, thereby reducing the likelihood of false annotations based solely on color coding. While it is true that the oblique nature of AP activation can occasionally obscure the discrete AP signal, integrating electrogram morphology with the spatial information provided by the activation map effectively mitigates this risk. Through this combined electroanatomic and

electrogram-based approach, we were able to reliably elucidate AP activation despite the absence of a clearly visible discrete AP potential in the raw signals.

Rare APs

In some cases, the earliest activation was recorded at sites projecting into the aortic root or within the CS. This finding does not invalidate the localization strategy, as the determination is based on relative electrogram timing rather than fluoroscopic appearance alone. Epicardial and para-annular pathways may project into these structures despite originating at the AV annulus, a phenomenon that has been described previously.[9,10] Corroborative mapping of adjacent sites, including CS recordings when appropriate, consistently confirmed that these activation sites reflected true AP breakthrough. Accordingly, the method remains valid, provided the localization is interpreted alongside the complete electrophysiological dataset.

Procedure Time

Regarding procedural time, the OWM strategy demonstrates a statistically insignificant reduction in total mapping time, despite acquiring more than 1,000 mapping points compared with the conventional approach. Moreover, OWM is associated with decreased fluoroscopy time and RF time. With respect to overall procedural duration, our experience indicates that the improved targeting capability facilitates more efficient decision-making during ablation, thereby reducing the time required for iterative mapping and catheter repositioning. Although the present study was not specifically powered to assess procedural time as a primary endpoint, only a modest and insignificant reduction in total procedure duration was observed relative to the conventional approach. This is predominantly attributable to fewer mapping iterations and a more rapid final confirmation of ablation efficacy.

Manual Annotation

To avoid subjective bias and ensure reproducibility, all EGMs were annotated fully automatically using the OWM framework. Nonetheless, we recognize that noise and unstable catheter contact may adversely affect automated annotation. To minimize their influence, we implemented two complementary safeguards. First, EGMs with very low amplitude were removed during pre-processing, as they typically correspond to either non-contact or poor-quality recordings. Second, a confidence threshold was applied to the OWM annotations so that only activations with sufficient likelihood were retained. As a result, noisy or pseudo-fragmented signals were effectively excluded prior to subsequent analysis. We therefore emphasize that, although the proposed algorithm does not require manual correction of EGMs, a strict quality control procedure was implicitly incorporated to mitigate the effects of artifacts and noise.

Conclusion

The proposed framework is conceived as a complementary extension of standard 3-D EAM rather than a replacement of current technologies. Conventional mapping systems provide high-resolution anatomical reconstructions and allow for localization of electrograms in 3-D space; however, their ability to resolve spatiotemporal propagation patterns and functionally relevant conduction pathways remains limited. In contrast, the presented approach incorporates activation data directly into the reconstructed geometry and thereby enables the visualization of functional propagation in a reproducible and operator-independent fashion. Importantly, the method relies on information that is already routinely obtained during clinical activation mapping and therefore does not require any additional acquisition step or dedicated hardware. The only modification to current clinical workflows would be a preprocessing step incorporating the reconstruction algorithm, which could be implemented in existing commercial mapping platforms. As such, the proposed approach is feasible in the clinical setting and could enhance current practice by enabling ablation strategies that are based on functional activation patterns rather than solely on local activation time differences.

Open Window Mapping offers a scientifically robust and clinically impactful strategy for the high-precision localization and ablation of APs in WPW syndrome. Unlike traditional activation mapping techniques, which are inherently limited by the confounding effects of global atrial or ventricular wavefront propagation and are subject to spatial averaging artifacts, OWM decouples local electrogram timing from chamber-wide conduction dynamics. This allows isolation of the true site of earliest activation corresponding to the AP insertion point, irrespective of the overall activation sequence. By temporally aligning local electrograms within a user-defined WOI/RAI, OWM creates a more physiologically relevant electroanatomic map that significantly enhances spatial and temporal resolution.

When integrated with high-density mapping catheters and contemporary EAM systems such as CARTO™ and EnSite Precision/X, OWM facilitates rapid and reproducible localization of AP insertion points with submillimeter precision. Both systems support advanced OWM workflows through tailored electrode configurations, real-time signal filtering, and adaptive windowing protocols.

Ethics Committee Approval: Ethics committee approval was not required in accordance with institutional policies.

Informed Consent: All patients provided written informed consent for the publication of this case series and any accompanying images. All identifiable information has been anonymized to protect patient privacy.

Conflict of Interest: The authors declare no conflicts of interest for this article.

Funding: This research did not receive any specific grant from funding agencies in the public, commercial, or not-for-profit sectors.

Use of AI for Writing Assistance: No artificial intelligence (AI)-assisted technologies were used in the production of this work.

Author Contributions: Concept – S.Ç.; Design – S.Ç.; Supervision – S.Ç.; Resource – S.Ç.; Materials – S.Ç.; Data Collection and/or Processing – S.Ç.; Analysis and/or Interpretation – S.Ç.; Literature Review – S.Ç.; Writing – S.Ç.; Critical Review – M.K., S.K., Ö.Ö., E.H.Ö.Ç., A.K., F.Ö., S.T.

Acknowledgments: We gratefully acknowledge the technical support provided by the CARTO technicians Gozde Senol and AhmetMelih Demirhan, as well as the Ensite technician Hilal Kuzay. Their expertise and assistance were instrumental in the successful execution of the procedures described in this study. We also acknowledge the contributions of the first author, who performed all the cases and played a central role in the practical implementation of the study.

Peer-review: Internally peer-reviewed.

Video 1. Three-dimensional (3-D) reconstruction and importation of cardiac chambers and vessels into the CARTO EAM system in a patient with three previous failed ablation attempts, including an epicardial ablation. EAM, Electroanatomic mapping.

Video 2. Propagation maps illustrating the direction of activation from the earliest to the latest site, with breakthrough observed on the right lateral tricuspid annulus. This demonstrates the localization and insertion sites of the AP during sinus rhythm with full pre-excitation (left video) and during ventricular pacing (right video). AP, Accessory pathway.

Video 3. Color-coded LAT maps (upper left panel) and propagation maps—classical (upper right panel), sparkle (lower left panel), and full-color (lower right panel)—illustrating the direction of activation from the earliest to the latest site. Breakthrough is observed at the right posteroseptal tricuspid annulus, demonstrating the localization and insertion sites of the AP during sinus rhythm with full pre-excitation. AP, Accessory pathway; LAT, Local activation time.

Video 4. Color-coded LAT (upper left panel) and propagation maps—classical (upper right panel) and sparkle (lower left panel)—illustrating the direction of activation from the earliest to the latest site. Breakthrough is observed at the right lateral tricuspid annulus, indicating the localization and insertion sites of the AP during orthodromic AVRT. RF application at the site of the earliest atrial activation (lower right panel) eliminates the AP and terminates the tachycardia within a few seconds. AP, Accessory pathway; AVRT, Atrioventricular reciprocating tachycardia; LAT, Local activation time; RF, Radiofrequency.

Video 5. Corresponding to Figure 5, this video illustrates the ablation effect on the AP. The timeline on the right shows fused and earliest ventricular bipolar signals relative to the delta wave, along with a QS morphology on the unipolar EGMs. The AP is abolished just four seconds after the onset of ablation (see white bar and time marker at the bottom). AP, Accessory pathway; EGM, Electrogram.

Video 6. Corresponding to Figure 6, this video illustrates the ablation effect on the AP. The timeline at the bottom shows fused and earliest ventricular bipolar EGMs relative to the delta wave. The AP is abolished just four seconds after the onset of ablation, as indicated by the RF session time in the box and the roving yellow line on the timeline. AP, Accessory pathway; EGM, Electrogram; RF, Radiofrequency.

References

1. Jackman WM, Wang XZ, Friday KJ, et al. Catheter ablation of accessory atrioventricular pathways (Wolff-Parkinson-White syndrome) by radiofrequency current. *N Engl J Med*. 1991;324(23):1605-1611. [CrossRef]
2. Schricker AA, Winkle R, Moskovitz R, et al. Open-window mapping of accessory pathways utilizing high-density mapping. *J Interv Card Electrophysiol*. 2021;61(3):525-533. [CrossRef]
3. Wang NC. Open-window mapping and the extended early-meets-late algorithm for the Wolff-Parkinson-White syndrome. *J Arrhythm*. 2022;38(4):642-645. [CrossRef]
4. Sande JLM, Minguito-Carazo C, Melchor LG, et al. Open window mapping with extended early meets late algorithm vs. conventional mapping for accessory pathway ablation. *J Interv Card Electrophysiol*. 2025;68(3):643-653. [CrossRef]
5. Çay S, Özeke Ö, Özcan F, Kara M, Topaloğlu S. Para-Hisian Accessory Pathway: Mapping Using Open-Window and Ablation From the Aortic Cusp. *Turk Kardiyol Dern Ars. 2023*;51(5):364-366. [CrossRef]
6. Yagishita A, Yamauchi Y, Sagawa Y, et al. Utility of open-window mapping for catheter ablation of an accessory pathway in patients with Wolff-Parkinson-White syndrome. *Pacing Clin Electrophysiol*. 2023;46(8):882-889. [CrossRef]
7. Brešković T, Lisica L, Jurišić Z, et al. Ablation of accessory pathways in different anatomic locations using focal pulsed field ablation. *Heart Rhythm*. 2024;21(8):1211-1217. [CrossRef]
8. Shen C, Jia Z, Yu Y, et al. Efficacy and safety of pulsed field ablation for accessory pathways: a pilot study. *Europace*. 2024;26(7):euae139. [CrossRef]
9. Kubota S, Nakasuga K, Maruyama T, et al. A unipolar coronary sinus mapping study of patients with left-sided atrioventricular accessory pathways. *Int Heart J*. 2005;46(4):657-667. [CrossRef]
10. Akiyama M, Kaneko Y, Taniguchi Y, et al. Coronary sinus recordings of double potentials associated with retrograde conduction through left atrioventricular accessory pathways. *J Cardiovasc Electrophysiol*. 2004;15(12):1371-1376. [CrossRef]

ARCHIVES OF THE TURKISH SOCIETY OF CARDIOLOGY

Official journal of the TURKISH SOCIETY OF CARDIOLOGY

Left Anterior Descending Artery to Right Coronary Artery Bifurcation Stenting with Culotte Technique in Acute Inferior Myocardial Infarction

Akut Alt Duvar Miyokard Enfarktüsünde Sol Ön İnen Koroner Arterden Sağ Koroner Artere Culotte Tekniği ile Bifurkasyon Stentleme İşlemi

ABSTRACT

Coronary artery anomalies are defined as abnormal origin, course, or termination of any of the three main epicardial coronary arteries. These anomalies are typically asymptomatic and are often discovered incidentally. However, certain anomalies may be associated with an increased risk of myocardial infarction, syncope, ventricular arrhythmias, and exercise-induced sudden cardiac death. A single coronary artery anomaly is a very rare form of coronary artery anomaly and typically supplies a large myocardial perfusion area. Here, we describe an extremely rare case of a single coronary artery anomaly in which the right coronary artery (RCA) originates from the mid-segment of the left anterior descending (LAD) coronary artery. The patient presented with acute inferior myocardial infarction and underwent LAD/RCA bifurcation stenting using the Culotte technique.

Keywords: Acute myocardial infarction, coronary artery anomaly, Culotte technique, left anterior descending artery/right coronary artery (LAD/RCA) bifurcation

ÖZET

Koroner arter anomalileri, üç ana epikardiyal koroner arterden herhangi birinin anormal kökeni, seyri ya da sonlanması olarak tanımlanır. Genellikle kardiyak şikâyete neden olmazlar ve tesadüfen saptanırlar. Ancak bazı koroner arter anomalileri, miyokard enfarktüsü, bayılma, ventriküler aritmiler ve egzersize bağlı ani kardiyak ölüm riskinde artış ile ilişkili olabilirler. Koroner arter anomalileri içerisinde tek koroner arter anomalisi çok nadir görülür ve tek koroner arter, geniş miyokardiyal beslenme alanı sağlar. Biz burada, akut alt duvar miyokard enfarktüsü ile başvuran hastada sol ön inen koroner arterden (LAD) çıkan sağ koroner arterin (RCA) olduğu tek koroner arter anomalisinde LAD/RCA bifurkasyon lezyonunun Culotte tekniği ile revaskülarize edildiği sıra dışı vakayı sunduk.

Anahtar Kelimeler: Akut miyokard enfarktüsü, koroner arter anomalisi, Culotte tekniği, sol ön inen koroner arter/çıkan sağ koroner arter bifurkasyonu

CASE REPORT
OLGU SUNUMU

Murat Akçay[1]
Ahmet Çınar[2]
Aydın Can Ulusoy[1]
Fatma Rümeysa Karaçeşme[1]
Metin Çoksevim[1]

[1]*Department of Cardiology, Faculty of Medicine, Ondokuz Mayıs University, Samsun, Türkiye*
[2]*Department of Cardiology, Merzifon Kara Mustafa Paşa State Hospital, Amasya, Türkiye*

Corresponding author:
Murat Akçay
✉ drmuratakcay@hotmail.com

Received: July 20, 2024
Accepted: November 03, 2024

Cite this article as: Akçay M, Çınar A, Ulusoy AC, Karaçeşme FR, Çoksevim M. Left Anterior Descending Artery to Right Coronary Artery Bifurcation Stenting with Culotte Technique in Acute Inferior Myocardial Infarction. *Turk Kardiyol Dern Ars.* 2025;53(7):536–540.

DOI: 10.5543/tkda.2024.77257

Copyright@Author(s)
Available online at archivestsc.com. Content of this journal is licensed under a Creative Commons Attribution – NonCommercial-NoDerivatives 4.0 International License.

Coronary artery anomalies are defined as any abnormality in the origin, course, or termination of the three main epicardial coronary arteries and may coexist with congenital heart disease. These anomalies are generally asymptomatic and are most often discovered incidentally during coronary angiography, computed tomography, or autopsy in individuals without congenital heart disease.[1,2] However, certain anomalies have been associated with an increased risk of myocardial infarction, syncope, ventricular arrhythmias, and exercise-induced sudden cardiac death.[2-4]

Isolated coronary artery anomalies are observed in approximately 0.5% of patients undergoing coronary angiography and in 0.3% of autopsy series.[1-3] The most common coronary anomaly involves the left anterior descending (LAD) and left circumflex (Cx) arteries originating separately from the left main coronary artery (LMCA), accounting for roughly 35% of cases. Other frequent anomalies include the right coronary artery (RCA) originating from the left coronary sinus (22%) and the Cx artery arising from the right coronary artery (20%).[3] A single coronary artery is another rare coronary anomaly, seen much less frequently, approximately 8% of all coronary anomalies.[4,5]

Here, we describe an extremely rare case documented in the literature, in which the RCA originates from the mid-segment of the LAD, as visualized on coronary angiography. The patient presented with an acute inferior myocardial infarction and was treated with LAD/RCA bifurcation stenting using the Culotte technique.

Case Report

A 69-year-old male presented with typical anginal chest pain for approximately 3-4 hours. He had no prior history of cardiac disease or other comorbidities. While in the emergency department, the patient suffered a sudden cardiac arrest, requiring cardiopulmonary resuscitation (CPR) for 10 minutes. Following successful stabilization of blood pressure and heart rhythm, electrocardiography revealed ST-segment elevation in leads D2, D3, and aVF, along with ST depression in the anterior leads (Figure 1A). The patient was intubated and remained hypotensive and tachycardic. After administration of acetylsalicylic acid (ASA) and clopidogrel via nasogastric tube, as well as intravenous heparin, the patient was taken for emergency coronary angiography. On coronary angiography, a 95% stenosis was observed in the mid-segment of the LAD, along with a subtotal thrombosed lesion in the distal Cx (Figure 1B). The RCA was not visualized initially, and the culprit lesion responsible for the myocardial infarction was presumed to be in the Cx artery. The lesion was predilated using a 2.5 × 15 mm balloon, followed by implantation of a 3.5 × 44 mm Supraflex stent (Sirolimus-Eluting Coronary Stent System, Sahajanand Medical Technologies Ltd.) (Figure 1C). Despite administration of intracoronary nitrate (100 mcg), ST-segment elevation persisted on the monitor, and the patient's chest pain response could not be assessed. Subsequently, the RCA originating from the mid-LAD region was identified using a 6-F Amplatz left 2 (AL2) guide catheter. The LAD-RCA bifurcation lesion was classified as Medina (1,0,1) (Figures 2A-B), and percutaneous coronary intervention (PCI) to the RCA was planned using the provisional technique (Video 1). Both the LAD and RCA were wired (Figure 2B). The RCA was predilated using a 2.5 × 15 mm balloon, followed by implantation of a 3.0 × 32 mm Promus PremierTM Select stent (Everolimus-Eluting Coronary Stent System, Boston Scientific, USA) (Figure 2C). Kissing percutaneous transluminal coronary angioplasty (PTCA) was performed at the mid-LAD lesion using 2.75 × 15 mm and 4.0 × 12 mm non-compliant (NC) balloons for the RCA and LAD, respectively (Figure 2D). Following the kissing PTCA, it was decided to stent the LAD using the Culotte technique. After rewiring, a 3.5 × 32 mm Promus PremierTM Select stent (Everolimus-Eluting Coronary Stent System, Boston Scientific, USA) was implanted in the mid-LAD lesion (Figure 2E). A second kissing PTCA was then performed using 3.5 × 15 mm and 4.0 × 12 mm NC balloons for the LAD and RCA, respectively (Figure 2F). Proximal optimization technique (POT) was subsequently performed with a 4.0 × 12 mm NC balloon, achieving an optimal final result (Figures 2G-H, Video 2). The patient was extubated approximately two days later. Ejection fraction (EF) was measured at 40%, with evidence of inferior and posterior hypokinesia. He was discharged one week

ABBREVIATIONS

AL2	Amplatz left 2
ASA	Acetylsalicylic acid
CABG	Coronary artery bypass grafting
Cx	Circumflex
EF	Ejection fraction
LAD	Left anterior descending
LMCA	Left main coronary artery
NC	Non-compliant
PCI	Percutaneous coronary intervention
POT	Proximal optimization technique
PTCA	Percutaneous transluminal coronary angioplasty
RCA	Right coronary artery

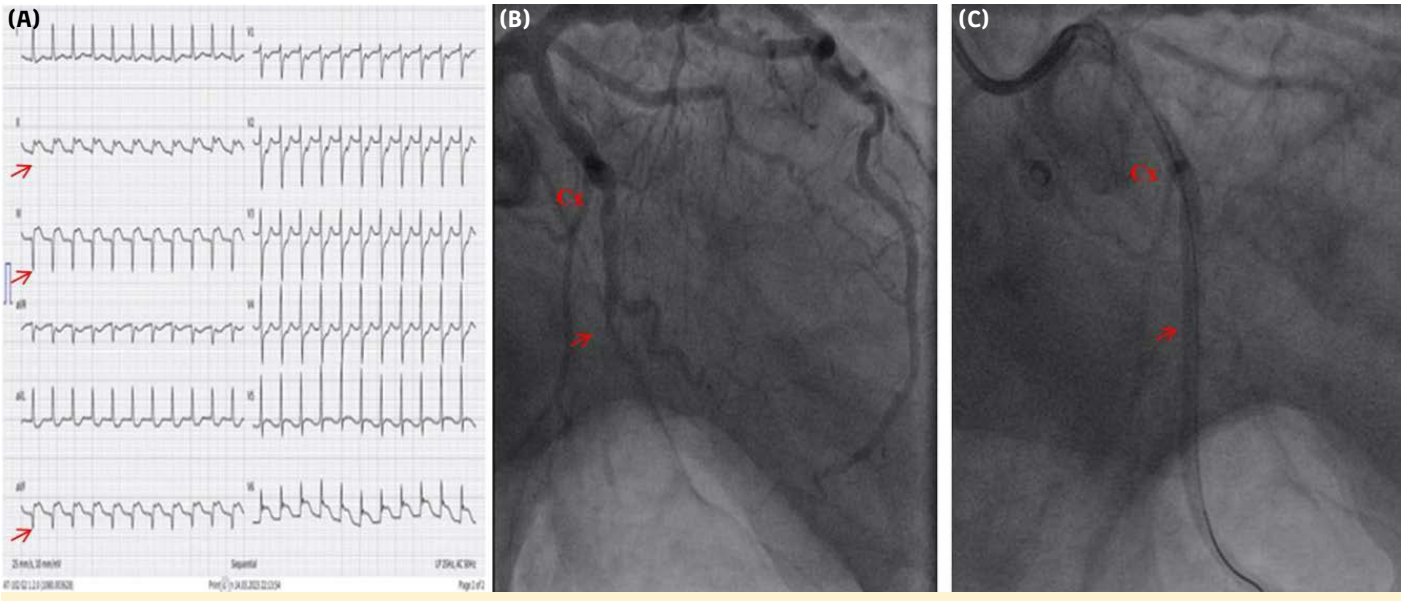

Figure 1. (A) Electrocardiogram showing ST-segment elevation in leads DII, DIII, and aVF, with ST-segment depression in leads V1-V3. (B) Coronary angiography showing a subtotal thrombosed lesion in the left circumflex (Cx) artery. (C) Coronary angiography showing the left circumflex (Cx) artery after stent implantation.

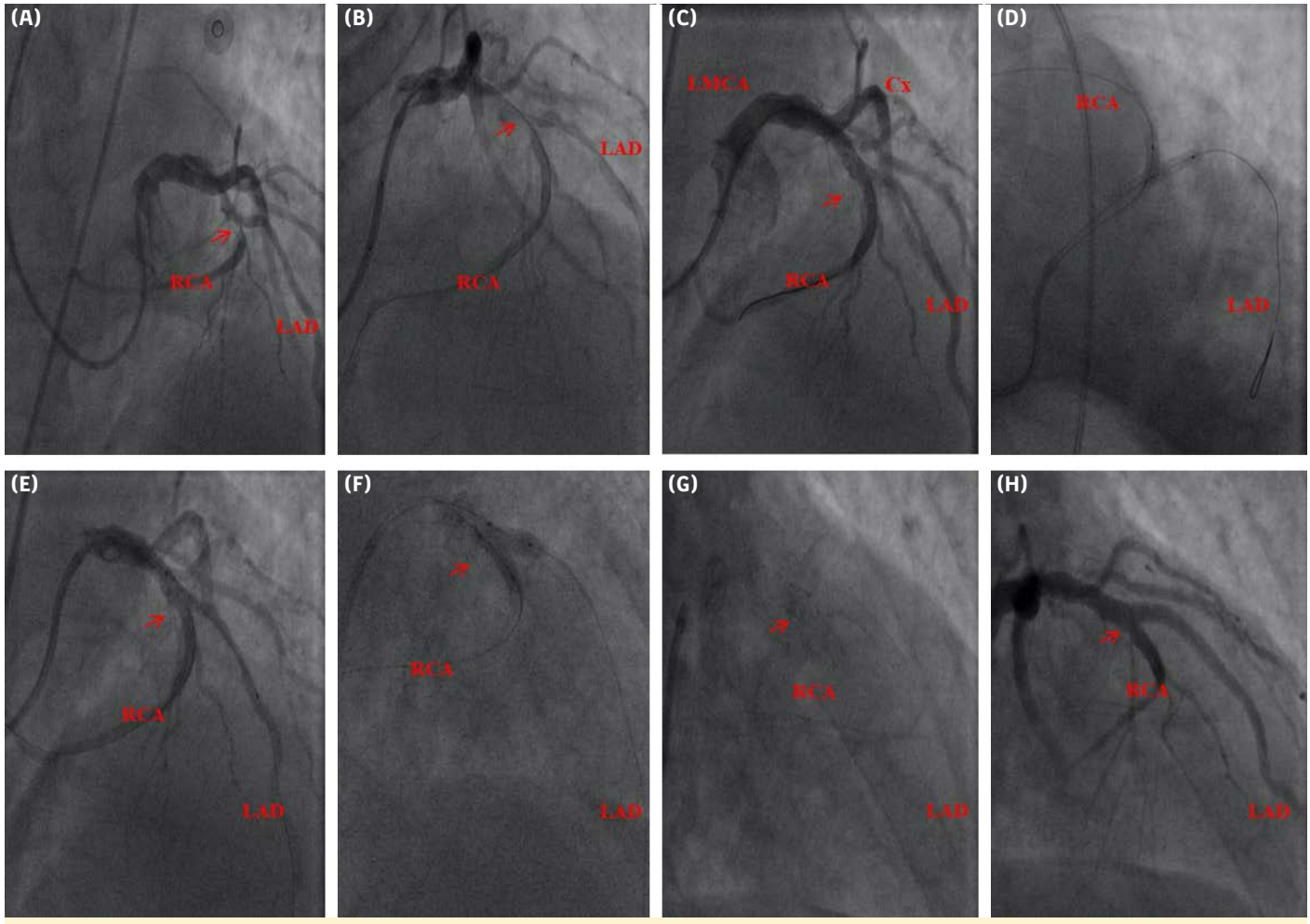

Figure 2. (A) Coronary angiographic imaging using a 6-French Amplatz Left 2 (AL2) guiding catheter, showing 95% stenosis at the ostium of the right coronary artery (RCA), which originates from the mid-left anterior descending (LAD) artery. (B) Coronary angiography showing both the right coronary artery (RCA) and left anterior descending (LAD) artery lesions wired. (C) Coronary angiographic imaging following implantation of a 3 × 32 mm stent into the right coronary artery (RCA). (D) Coronary angiographic imaging of the first kissing balloon procedure involving the left anterior descending (LAD) artery and the right coronary artery (RCA). (E) Coronary angiographic imaging showing implantation of a 3.5 × 32 mm stent into the left anterior descending (LAD) artery using the Culotte technique. (F) Coronary angiographic imaging of the second kissing balloon procedure involving the left anterior descending (LAD) artery and the right coronary artery (RCA). (G) Coronary angiographic non-contrast imaging showing implanted stents in the left anterior descending (LAD) artery and the right coronary artery (RCA) using the Culotte technique. (H) Coronary angiographic contrast imaging showing implanted stents in the left anterior descending (LAD) artery and the right coronary artery (RCA) using the Culotte technique.

later on acetylsalicylic acid, clopidogrel, bisoprolol, perindopril, spironolactone, and atorvastatin. The patient provided written informed consent for publication of this case.

Discussion

Our case represents an exceptionally rare single coronary artery anomaly, in which stenting was performed from LAD to the RCA using the Culotte technique. A single coronary artery anomaly is a rare congenital coronary abnormality, in which a single coronary artery arises from the aorta or provides perfusion to the entire myocardium.[6,7]

Coronary artery anomalies may occur in isolation or in association with other congenital cardiac defects, such as transposition of the great vessels, bicuspid aortic valve, tetralogy of Fallot, or arteriovenous fistulae.[2,7] In the largest angiographic series reported in the literature, comprising 126,595 cases, Yamanaka et al.[2] identified a 1.3% prevalence of isolated coronary artery anomalies. Among these, 225 cases were identified as coronary artery fistulae, and 1,461 cases involved abnormalities in the origin or course of the coronary arteries. Single coronary artery anomaly was found to be extremely rare, with a reported incidence of 0.05%. Although often asymptomatic, single coronary artery anomalies can present with chest pain, dyspnea, palpitations, syncope, myocardial infarction, ventricular fibrillation, and even sudden cardiac death. In one study, the incidence of coronary artery anomalies was reported to be as high as 12–19% among individuals who experienced sudden death at a young age.[8,9] These anomalies may also alter myocardial perfusion and predispose to atherosclerosis by reducing

the vasodilatory response.[10,11] When atherosclerotic stenosis is detected, treatment options include medical management, PCI, or surgical intervention. PCI in such cases presents several challenges, including limited guiding catheter support, the need for specialized equipment, selection of the appropriate PCI strategy, and the necessity for an experienced operator.[12–15]

In the literature, there are very few reported cases of an anomalous RCA originating from the mid-LAD, and no standardized revascularization strategy has been established due to the anatomical complexity of these cases. In some instances, coronary artery bypass grafting (CABG) has been used for revascularization, while in others, PCI has been successfully performed depending on the operator's expertise.[11–15] In the case reported by Calabrò et al.,[13] provisional LAD bifurcation stenting was performed for a 90% stenosis in the mid-LAD adjacent to the origin of the anomalous RCA. In reviewing other rare cases in the literature, Prasad et al.[14] used the reverse crush technique, and Khan et al.[15] employed the Culotte technique for treating mid-LAD/RCA lesions in two non-ST-segment elevation myocardial infarction (non-STEMI) patients. Considering that a single coronary artery supplies most of the myocardial territory, any complication can significantly affect a large portion of the myocardium. Therefore, such anomalies have been described in the literature as similar to unprotected left main coronary artery lesions.[13–15] In these cases, unlike conventional catheterization procedures, several challenges may arise, including the need for adequate catheter support, precise cannulation, appropriate imaging during PCI, selecting a less commonly used catheter, providing the optimal curvature to the guidewire, and difficulty advancing balloons or stents.[14,15] For optimal catheter support, the use of a wide-angle AL2 catheter may be more effective, as demonstrated in our case. Initially, we were unable to visualize the RCA due to insufficient contrast filling using a JL4 catheter. If the coronary arteries are excessively tortuous, a hydrophilic wire may be required to reduce the risk of perforation. Additionally, intravascular imaging may be necessary in areas with overlapping stents.[14,15] In our case, intravascular imaging was not utilized due to the lack of hemodynamic stability. However, in stable patients, intravascular imaging can be considered in bifurcation lesions to help prevent incomplete or suboptimal PCI. Initially, provisional stenting from the LAD to the RCA was planned. However, following the kissing balloon procedure, the LAD lesion was reassessed as significant. The strategy was subsequently changed to the Culotte technique, taking into account the similarity in vessel diameters and the favorable vessel angle.

Conclusion

In conclusion, our case highlights a rare single coronary artery anomaly in which the RCA originated from the mid-LAD, presenting as an acute inferior myocardial infarction, and successfully treated with LAD/RCA bifurcation stenting using the Culotte technique. A single coronary artery anomaly is a very rare congenital coronary condition that supplies a large myocardial perfusion area. Treating such cases presents certain challenges, including determining the optimal revascularization technique, selecting appropriate equipment, and requiring an experienced operator. Our case is unusual in that complex and complete revascularization was successfully performed in the setting of a rare single coronary artery anomaly.

Ethics Committee Approval: This is a single case report, and therefore ethics committee approval was not required in accordance with institutional policies.

Informed Consent: The patient provided written informed consent for publication of this case.

Conflict of Interest: The authors have no conflicts of interest to declare.

Funding: The authors declared that this study received no financial support.

Use of AI for Writing Assistance: The authors confirm that no artificial intelligence (AI)-supported technologies were used in the writing of this case report.

Author Contributions: Concept – M.A., A.Ç., A.C.U., F.R.K., M.Ç.; Design – M.A., A.Ç., A.C.U., F.R.K., M.Ç.; Supervision – M.A., A.Ç., A.C.U., F.R.K., M.Ç.; Resource – M.A.; Materials – M.A., A.Ç., A.C.U., F.R.K., M.Ç.; Data Collection and/or Processing - M.A., A.Ç., A.C.U., F.R.K., M.Ç.; Analysis and/or Interpretation - M.A.; Literature Review – M.A., A.Ç., A.C.U., F.R.K., M.Ç.; Writing – M.A.; Critical Review – M.A.

Peer-review: Both externally and internally peer-reviewed.

Video 1. Angiographic imaging showing significant stenosis at the ostium of the right coronary artery, originating from the mid-left anterior descending (LAD) artery.

Video 2. Angiographic imaging showing the implanted stents in the left anterior descending (LAD) artery and the right coronary artery (RCA) using the Culotte technique.

References

1. Pérez-Pomares JM, de la Pompa JL, Franco D, et al. Congenital coronary artery anomalies: A bridge from embryology to anatomy and pathophysiology--A position statement of the development, anatomy, and pathology ESC Working Group. *Cardiovasc Res*. 2016;109(2):204-216. [CrossRef]
2. Yamanaka O, Hobbs RE. Coronary artery anomalies in 126,595 patients undergoing coronary arteriography. *Cathet Cardiovasc Diagn*. 1990;21(1):28-40. [CrossRef]
3. Lipton MJ, Barry WH, Obrez I, Silverman JF, Wexler L. Isolated single coronary artery: Diagnosis, angiographic classification, and clinical significance. *Radiology*. 1979;130(1):39-47. [CrossRef]
4. Harikrishnan S, Jacob SP, Tharakan J, et al. Congenital coronary anomalies of origin and distribution in adults: A coronary arteriographic study. *Indian Heart J*. 2002;54(3):271-275.
5. Taylor AJ, Rogan KM, Virmani R. Sudden cardiac death associated with isolated congenital coronary artery anomalies. *J Am Coll Cardiol*. 1992;20(3):640-647. [CrossRef]
6. Said SA, de Voogt WG, Bulut S, et al. Coronary artery disease in congenital single coronary artery in adults: A Dutch case series. *World J Cardiol*. 2014;6(4):196-204. [CrossRef]
7. Cho SH, Joo HC, Yoo KJ, Youn YN. Anomalous origin of right coronary artery from left coronary sinus: Surgical management and clinical result. *Thorac Cardiovasc Surg*. 2015;63(5):360-366. [CrossRef]
8. Van Camp SP, Bloor CM, Mueller FO, Cantu RC, Olson HG. Nontraumatic sports death in high school and college athletes. *Med Sci Sports Exerc*. 1995;27(5):641-647. [CrossRef]
9. Virmani R, Kolodgie FD, Burke AP, Farb A, Schwartz SM. Lessons from sudden coronary death: A comprehensive morphological classification scheme for atherosclerotic lesions. *Arterioscler Thromb Vasc Biol*. 2000;20(5):1262-1275. [CrossRef]
10. Morales AR, Romanelli R, Boucek RJ. The mural left anterior descending coronary artery, strenuous exercise and sudden death. *Circulation*. 1980;62(2):230-237. [CrossRef]
11. Click RL, Holmes DR Jr, Vlietstra RE, Kosinski AS, Kronmal RA. Anomalous coronary arteries: Location, degree of atherosclerosis

and effect on survival--A report from the Coronary Artery Surgery Study. *J Am Coll Cardiol*. 1989;13(3):531–537. [CrossRef]
12. Izumiyama O, Yamashita A, Sugimoto S, Baba M, Hasegawa T. Coronary artery bypass grafting in two patients with single coronary artery. Kyobu Geka. *The Japanese Journal of Thoracic Surgery*. 1999;52(2):143–147.
13. Calabrò P, Bianchi R, Palmieri R, Sordelli C, Bigazzi MC, Calabrò R. Evidence of right coronary from mid-left anterior descending coronary: A rare case of coronary anomalous origin. *Eur Heart J*. 2009;30(5):565. [CrossRef]
14. Prasad K, Chhikara S, Kumar MN, Gupta A. Left anterior descending/right coronary artery bifurcation angioplasty in a rare case of single coronary artery: A case report. *Eur Heart J Case Rep*. 2021;5(4):ytab047. [CrossRef]
15. Khan UA, Sharma D, McGlinchey P, Peace A. Percutaneous coronary intervention to left anterior descending artery/right coronary artery bifurcation: This is not a typo! A case report. *Eur Heart J Case Rep*. 2019;3(3):ytz137. [CrossRef]

ARCHIVES OF THE TURKISH SOCIETY OF CARDIOLOGY

Official journal of the TURKISH SOCIETY OF CARDIOLOGY

Paradoxical Cerebral and Coronary Embolism in a Young Patient Due to Right Atrial Appendage Aneurysm: A Case Report

Sağ Atriyal Apendiks Anevrizmasına Bağlı Genç Bir Hastada Paradoksal Serebral ve Koroner Emboli: Bir Olgu Sunumu

ABSTRACT

A 32-year-old male patient was admitted to the hospital with an ischemic stroke. Transesophageal echocardiography revealed an echogenic structure consistent with a thrombus within the aneurysm of the right atrium, along with a patent foramen ovale (PFO) in the interatrial septum. Cardiac magnetic resonance imaging (MRI) confirmed the presence of a right atrial appendage aneurysm (RAAA) with thrombus formation. Coronary angiography demonstrated occlusion of the circumflex artery. Concurrently, the patient was diagnosed with antiphospholipid syndrome. Given the presence of a PFO, paradoxical embolism was postulated as the etiology for both the coronary and cerebral artery occlusions. Antithrombotic and anticoagulant therapy was initiated, and surgical intervention for the RAAA and PFO was recommended. However, the patient declined surgical treatment, and medical management was continued. The patient has been regularly followed for approximately two years without any complications.

Keywords: Acute coronary syndrome, acute ischemic stroke, right atrial appendage aneurysm

ÖZET

Otuz iki yaşında erkek hasta iskemik inme nedeniyle hastaneye kaldırıldı. Transözofageal ekokardiyografi, sağ atriyum anevrizması içinde trombüsle uyumlu ekojenik bir yapının ve interatriyal septum içinde foramen ovale'nin (PFO) varlığını gösterdi. Kardiyak MRI, trombüslü sağ atriyal apendiks anevrizmasının (RAAA) varlığını ortaya koydu. Koroner anjiyografi, sirkumfleks arterin tıkalı olduğunu gösterdi. Eş zamanlı olarak, antifosfolipid sendromu tanımlandı. PFO'nun varlığı göz önüne alındığında, paradoksal emboli, hem koroner hem de serebral arter tıkanıklığının etiyolojisi olarak varsayıldı. Antitrombotik ve antikoagülan tıbbi tedavi başlatıldı ve RAAA ve PFO için cerrahi müdahale önerildi. Ancak, hasta cerrahi tedaviyi reddetti ve bu nedenle tıbbi tedavisine devam edildi. Hasta yaklaşık iki yıldır düzenli muayene edilmekte ve herhangi bir sorun olmadan takip edilmektedir.

Anahtar Kelimeler: Akut koroner sendrom, akut iskemik inme, sağ atrial apendiks anevrizması

CASE REPORT
OLGU SUNUMU

Songül Usalp[1]

Safiye Sanem Dereli Bulut[2]

Filiz Çelebi[1]

Emine Altuntaş[3]

[1]*Department of Cardiology, Sancaktepe Sehit Prof. Dr. Ilhan Varank Training and Research Hospital, Istanbul, Türkiye*
[2]*Department of Radiology, Umraniye Training and Research Hospital, Istanbul, Türkiye*
[3]*Department of Cardiology, Mehmet Akif Ersoy Training and Research Hospital, İstanbul, Türkiye*

Corresponding author:
Songül Usalp
✉ dr.songulusalp@hotmail.com

Received: August 11, 2024
Accepted: December 03, 2024

Cite this article as: Usalp S, Dereli Bulut SS, Çelebi F, Altuntaş E. Paradoxical Cerebral and Coronary Embolism in a Young Patient Due to Right Atrial Appendage Aneurysm: A Case Report. *Turk Kardiyol Dern Ars.* 2025;53(7):541-544.

DOI: 10.5543/tkda.2024.36737

Copyright@Author(s)
Available online at archivestsc.com. Content of this journal is licensed under a Creative Commons Attribution – NonCommercial-NoDerivatives 4.0 International License.

Ischemic stroke (IS) is a relatively rare condition in young adults, with an incidence ranging from 7 to over 100 per 100,000 person-years, depending on the population studied.[1] Among the most common causes of IS in individuals under 50 years of age are atrial myxoma, intracardiac thrombus, dilated cardiomyopathy, nonbacterial thrombotic endocarditis, atrial septal defects, patent foramen ovale (PFO), and hematologic disorders predisposing to thrombosis.[1]

Acute coronary syndromes are also rarely observed in young patients, with underlying causes including genetic abnormalities, hyperlipidemias, coagulation disorders, and coronary artery anomalies. It is exceedingly uncommon for an individual to present with both acute coronary artery syndrome and acute IS concurrently. Such a presentation should prompt consideration of a systemic coagulation disorder or an intracardiac thrombus/embolism.

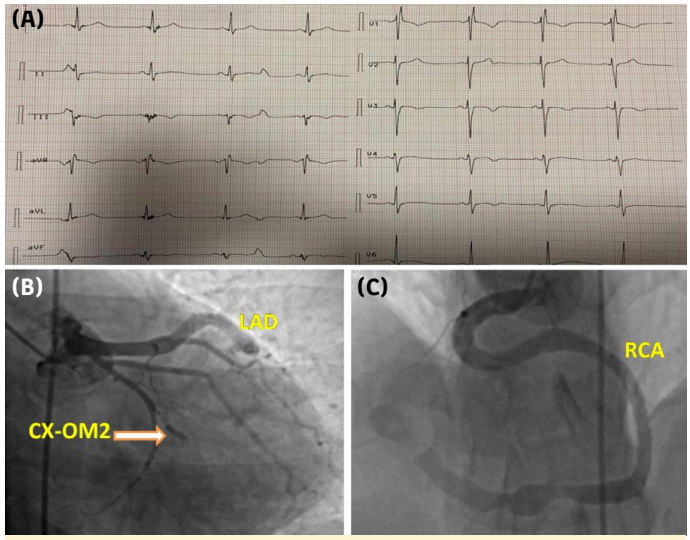

Figure 1. (A) Electrocardiogram obtained at the patient's initial hospital admission. (B) Coronary angiography image showing total occlusion of the left circumflex artery starting from its distal segment. (C) Coronary angiography image showing a severely ectatic right coronary artery.

In this article, we present an intriguing case of a 32-year-old male patient with positive antiphospholipid antibodies, diagnosed with both IS and acute coronary syndrome, along with a rare right atrial appendage aneurysm (RAAA) containing a thrombus.

Case Report

A 32-year-old male patient was admitted to the hospital with complaints of sudden-onset speech difficulty, confused speech, and amnesia, which began approximately 30 minutes prior to presentation. He had no known medical history, was a non-smoker, and had no history of drug or substance use. Upon admission, the patient was conscious, and his vital signs were within normal limits. There was no evidence of speech or motor aphasia/paraphasia. The absence of pathological findings during the initial neurological examination in the emergency department suggested that the occluded cerebral artery might have spontaneously recanalized.

Laboratory investigations revealed the following results: Troponin I: 0.056 µG/L (reference range: 0-0.014), Anti-beta-2 glycoprotein 1 immunoglobulin M (IgM): 36.06, (normal <20 U/mL), Anti-beta-2 glycoprotein 1 IgG: <2 U/mL (within normal range). Other laboratory findings were within normal limits.

Electrocardiography revealed sinus rhythm with an incomplete right bundle branch block and a heart rate of 51 beats per minute. T-wave inversions were observed in leads V3-V6 (Figure 1). A 24-hour Holter rhythm monitor showed no abnormalities.

Cranial diffusion magnetic resonance imaging demonstrated hyperintense signal changes on diffusion-weighted images and hypointensities on apparent diffusion coefficient (ADC) maps in the subcortical area at the level of the ventricle corpus, left cerebral hemisphere, and left posterior frontal lobe. These findings were consistent with acute cerebral infarction. Brain computed tomography (CT) and carotid-vertebral artery CT angiography findings were normal.

ABBREVIATIONS

ADC	Apparent diffusion coefficient
APS	Antiphospholipid syndrome
CT	Computed tomography
EULAR	European League Against Rheumatism
IS	Ischemic stroke
MRI	Magnetic resonance imaging
PFO	Patent foramen ovale
RAAA	Right atrial appendage aneurysm
TEE	Transesophageal echocardiography
TTE	Transthoracic echocardiography

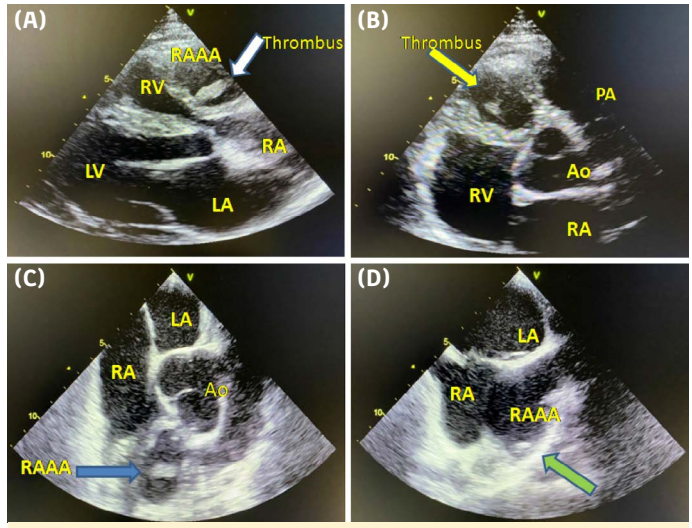

Figure 2. (A) Transthoracic echocardiography, longitudinal axis view: an aneurysmal structure with suspected thrombus is observed in the upper vicinity of the right ventricle (white arrow). (B) Transthoracic echocardiography, short axis view: an aneurysmal structure with suspected thrombus is observed between the right ventricle and right atrium (yellow arrow). (C) Transesophageal echocardiography mid-esophageal view: a mobile echogenic structure is observed within the aneurysmal formation, adjacent to the aorta and right ventricle (blue arrow). (D) Transesophageal echocardiography, bicaval view: a right atrial aneurysm is visualized with a suspicious thrombus (green arrow).

Transthoracic echocardiography (TTE) showed an ejection fraction of 60%, and a cystic structure with a mobile echogenic component was observed exerting pressure on the lateral wall of the right ventricle (Figure 2A-B, Video 1). Transesophageal echocardiography (TEE) revealed an aneurysmal formation adjacent to the right atrium, with an echogenic structure consistent with a thrombus and a PFO tunnel (Figure 2C-D, Videos 2–4). However, the right atrial appendage aneurysm could not be clearly visualized on TEE. Cardiac MRI was subsequently performed both to better evaluate the right atrial appendage and to rule out extracardiac masses. Treatment with acetylsalicylic acid (100 mg), and subcutaneous enoxaparin was initiated. A fourfold increase in troponin levels compared to baseline was noted. Coronary angiography demonstrated occlusion of the obtuse marginal branch of the circumflex artery and an ectatic

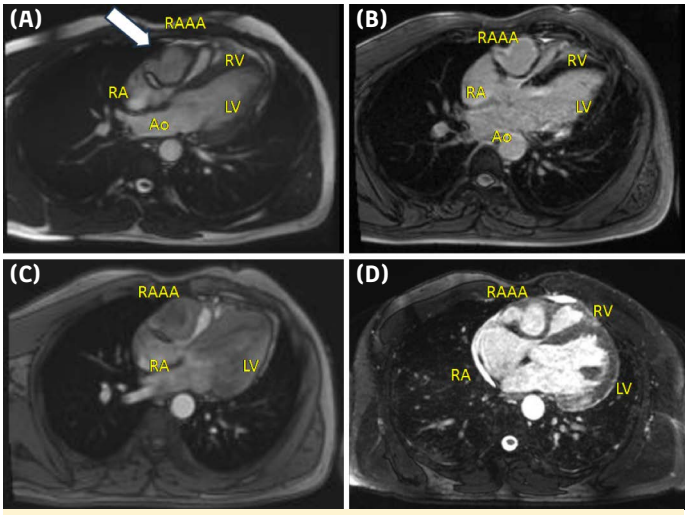

Figure 3. (A–D) Cardiac magnetic resonance imaging of the right atrial appendage aneurysm from various sequences (white arrow). The thrombus within the aneurysm is clearly visible.

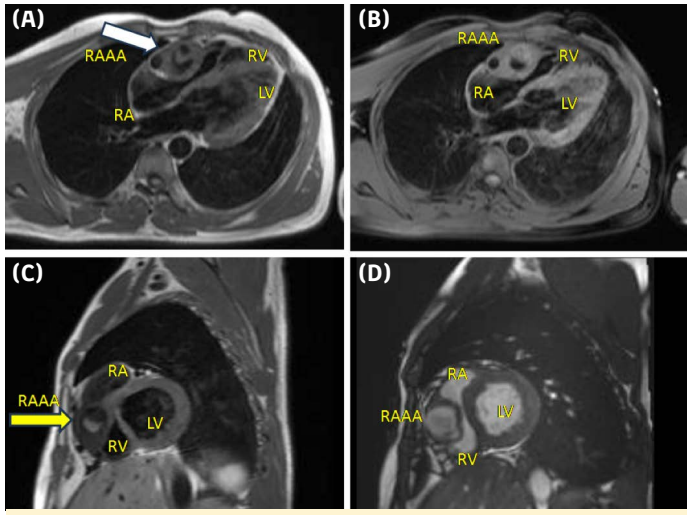

Figure 4. (A–D) Cardiac magnetic resonance images obtained from different segments show a thrombus embedded in the tissue of the right atrial appendage (white and yellow arrows).

right coronary artery (Figure 1B-C). As the obtuse marginal branch was non-dominant, had a small vessel diameter, and supplied a relatively limited territory, a decision was made to manage the patient with medical therapy.

Cardiac MRI confirmed the presence of a thrombus within a large RAAA (Figures 3, 4).

Discussion

To the best of our knowledge, this is the first and only reported case in the literature of a young male patient presenting with a RAAA containing thrombus, acute coronary syndrome, antiphospholipid syndrome (APS), and acute IS concurrently.

It is hypothesized that the thrombus formed in the RAAA embolized to the left atrium, and subsequently to the coronary and cerebral vessels, through the PFO. Additionally, the presence of anti-beta-2 glycoprotein 1 IgM antibodies likely contributed to an increased tendency toward arterial thrombosis.

The occurrence of IS and acute coronary syndrome in young patients is exceedingly rare.[2] TTE is typically the first imaging modality used to investigate cardiac etiologies. However, RAAA, usually located on the free wall of the right atrium, can be easily misidentified or overlooked on TTE. TEE is the preferred modality for evaluating RAAA, typically visualized in the mid-esophageal bicaval view by rotating the probe between 90° and 130°. Nevertheless, even with TEE, RAAA can be missed in up to 16% of cases.[3] Indeed, in our case, the RAAA could not be clearly visualized on TEE. Therefore, cardiac MRI was performed to better evaluate the RAAA. Studies conducted using TEE have found that RAAAs are approximately 12 times less common than left atrial aneurysms.[4] Compared to the left, RAAA often exhibit low-flow velocity spontaneous contrast echoes, and this slow flow predisposes to thrombus formation. Surgical resection is recommended for patients with thromboembolic events or large aneurysms, while regular follow-up is advised for asymptomatic patients.[5]

Beta-2 glycoprotein 1 plays a role in the etiopathogenesis of various conditions characterized by both arterial and venous thrombosis.[5] The presence of anti-beta-2 glycoprotein antibodies is one of the diagnostic criteria for APS.[5] These antibodies can induce platelet activation *in vivo*, thereby increasing the risk of thrombosis.[6] One study suggested that more than 20% of strokes occurring in individuals under the age of 45 are associated with APS.[6] Warfarin therapy is generally recommended for patients diagnosed with APS.[6]

B2 glycoprotein 1 is a molecule composed of amino acids synthesized by hepatocytes, endothelial cells, and trophoblast cells. By binding electrostatically to negatively charged phospholipids on the plasma membrane, it becomes a target for antiphospholipid antibodies.[5] *In vitro*, phospholipid antibodies that cause prolongation of coagulation tests involving phospholipids are referred to as "lupus anticoagulants."[5] Although these antibodies are called "anticoagulants" because they prolong coagulometric test results *in vitro*, they induce platelet activation *in vivo* and therefore increase the risk of thrombosis. For the diagnosis of APS, at least one of the beta-2 glycoprotein 1 antibodies or lupus anticoagulant antibodies must be positive in laboratory analyses, accompanied by clinical features such as thrombosis, recurrent fetal loss, or signs of low platelet count.[5,6] In our patient, anti-beta 2 glycoprotein IgM was positive, and he presented with arterial thrombosis.

The European League Against Rheumatism (EULAR) recommends targeting an international normalized ratio (INR) of 3 to 4 is APS patients with ischemic stroke.[6] In contrast, the American College of Chest Physicians recommends an INR target range of 2 to 3. Additionally, the initiation of antiplatelet therapy in combination with warfarin is advised for patients with antiphospholipid syndrome who experience arterial thrombosis for the first time.[7]

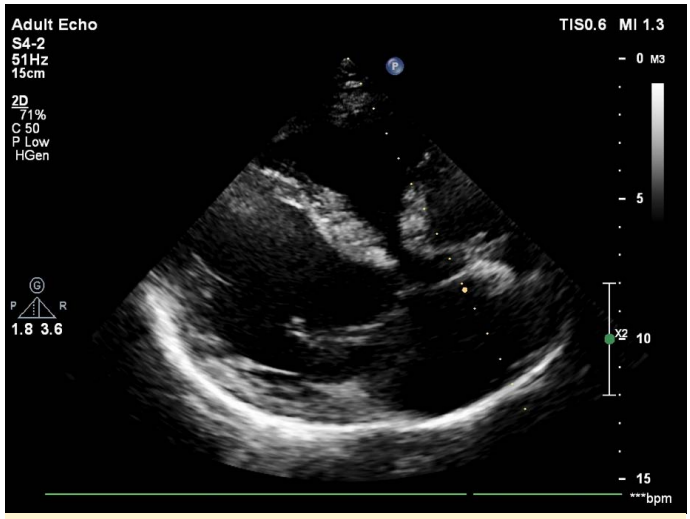

Figure 5. Transthoracic echocardiography performed four months after initiation of treatment shows no evidence of thrombus formation within the right atrial appendage aneurysm.

In our case, systemic embolism occurred due to a thrombus originating from the RAAA and passing through the PFO. There is a high incidence of coexisting prothrombotic conditions in young adults who experience stroke secondary to PFO. Recent studies have shown that newly developed devices, in combination with antiplatelet therapy, are superior to anticoagulant or antiplatelet therapy alone in preventing IS in patients with PFO.[6]

According to current knowledge, only a small number of RAAA cases have been reported in adults.[8,9] Most case reports in the literature involve pediatric patients. However, since most adult patients with RAAA are asymptomatic, they are typically managed conservatively. One case in the literature reported a patient presenting with simultaneous ischemic stroke, acute coronary syndrome, and pulmonary embolism, but without the presence of RAAA.[10] To date, there are no documented cases in the literature of RAAA causing both cerebrovascular accident and acute coronary syndrome, with associated thrombus formation and concurrent APS, as observed in our patient.

Our patient is currently being managed with a combination of acetylsalicylic acid and warfarin, as he declined invasive treatment. On the most recent transthoracic echocardiography performed four months after initiating treatment, no thrombus was detected within the RAAA (Figure 5). The patient has been attending regular follow-ups for approximately two years to monitor INR levels and has remained stable without any complications.

Conclusion

Ischemic stroke in young patients requires a thorough and comprehensive diagnostic evaluation. When conventional diagnostic methods are inconclusive, advanced diagnostic techniques should be employed.

Ethics Committee Approval: This is a single case report, and therefore ethics committee approval was not required in accordance with institutional policies.

Informed Consent: Written consent was obtained from the patient for the publication of this case report and associated personal information.

Conflict of Interest: The authors have no conflicts of interest to declare.

Funding: The authors declared that this study received no financial support.

Use of AI for Writing Assistance: Artificial intelligence assisted technologies were not used in the writing of this article.

Author Contributions: Concept – S.U.; Design – S.S.D.B.; Supervision – S.U.; Resource – F.Ç.; Materials – E.A.; Data Collection and/or Processing – F.Ç.; Analysis and/or Interpretation – S.S.D.B.; Literature Review – S.U.; Writing – S.U.; Critical Review – E.A.

Peer-review: Externally peer-reviewed.

Video 1. Transthoracic echocardiography showing a mobile thrombus within the right atrial appendage aneurysm.

Video 2–5. Transesophageal echocardiography recordings of the patient.

References

1. Ekker MS, Boot EM, Singhal AB, et al. Epidemiology, aetiology, and management of ischaemic stroke in young adults. *Lancet Neurol*. 2018;17(9):790-801. [CrossRef]
2. Li F, Yang L, Yang R, et al. Ischemic stroke in young adults of Northern China: Charac-teristics and risk factors for recurrence. *Eur Neurol*. 2017;77(3-4):115-122. [CrossRef]
3. Ozer O, Sari I, Davutoglu V. Right atrial appendage: Forgotten part of the heart in atrial fibrillation. *Clin Appl Thromb Hemost*. 2010;16(2):218-220. [CrossRef]
4. García-Fernández MÁ, Cresti A. Right Atrial appendage thrombus: "Can be found if you look for it". *JACC Case Rep*. 2023;5:101702. [CrossRef]
5. Bustamante JG, Goyal A, Rout P, Singhal M. Antiphospholipid syndrome. In: *StatPearls*. Treasure Island (FL): StatPearls Publishing; 2024.
6. Bertsias G, Ioannidis JP, Boletis J, et al. EULAR recommendations for the management of systemic lupus erythematosus. Report of a Task Force of the EULAR Standing Committee for International Clinical Studies Including Therapeutics. *Ann Rheum Dis*. 2008;67(2):195-205. [CrossRef]
7. Sayar Z, Moll R, Isenberg D, Cohen H. Thrombotic antiphospholipid syndrome: A prac-tical guide to diagnosis and management. *Thromb Res*. 2021;198:213-221. [CrossRef]
8. Le Ven F, Orhan E, Jobic Y. Aneurysm of right atrial appendage in a young patient. *Arch Cardiovasc Dis*. 2010;103(10):559-560. [CrossRef]
9. Sivakumaran L, Sayegh K, Mehanna E, Sanchez FW, Fields J, Cury R. Use of cardio-vascular magnetic resonance in the evaluation of a giant right atrial appendage aneurysm: A case report and review of the literature. *BMC Res Notes*. 2017;10(1):681. [CrossRef]
10. Shirani A, Daraei M, Shirani A. Antiphospholipid syndrome with major arterial throm-bosis, presenting as pulmonary thromboembolism, cerebrovascular accident, and coro-nary artery disease: A case report and literature review. *Clin Case Rep*. 2024;12(8):e9254. [CrossRef]

ARCHIVES OF THE TURKISH SOCIETY OF CARDIOLOGY

Official journal of the TURKISH SOCIETY OF CARDIOLOGY

Optical Coherence Tomography-Guided Nano-Culotte Stenting for Woven Coronary Artery Bifurcation Lesion

Woven Koroner Bifürkasyon Lezyonuna Optik Koherens Tomografi Kılavuzlu Nano-Culotte Stentleme

A 31-year-old male patient presented with non-ST-segment elevation myocardial infarction. Coronary angiography revealed a bifurcation lesion involving a bifid left anterior descending (LAD) artery with a woven coronary artery anomaly (Video 1) and a high obtuse marginal (OM) lesion. Both the LAD and septal LAD branches were successfully wired using a Fielder XT guidewire in combination with a Corsair microcatheter. Optical coherence tomography (OCT) imaging confirmed the presence of a woven coronary anomaly with thrombus formation in both branches and demonstrated that the guidewires had traversed separate microchannels (Figure 1 A, B, Video 2). Based on the OCT findings, percutaneous coronary intervention (PCI) was planned for the LAD. After confirming that the Fielder XT wires were in the distal true lumen of both branches, they were exchanged for 0.014-inch floppy guidewires.

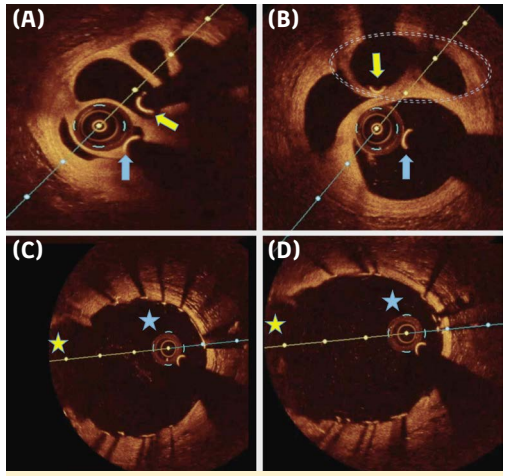

Figure 1. Optical coherence tomography (OCT) imaging. (A) Proximal LAD. (B) The branching point level (in the circle: septal LAD ostium). (C) Post-procedural imaging of the carina level. (D) Post-procedural imaging of the polygon of confluence (blue arrowhead/star: LAD wire, yellow arrowhead/star: septal LAD wire).

LAD, Left anterior descending artery.

Given the high risk of side branch occlusion with provisional stenting, a planned two-stent strategy using the Szabo technique was selected (Figure 2). After wiring and predilatation of both woven coronary bifurcation vessels (Figure 3A, Video 3), a 3.0 × 18 mm sirolimus-eluting stent was manually prepared outside the catheter (Figure 3B). The proximal strut was partially opened, the LAD wire was passed through the strut, and the strut was then re-crimped. The stent was advanced over the septal LAD wire until it was restrained by the LAD guidewire and subsequently implanted, minimizing the risk of LAD occlusion (Video 4).

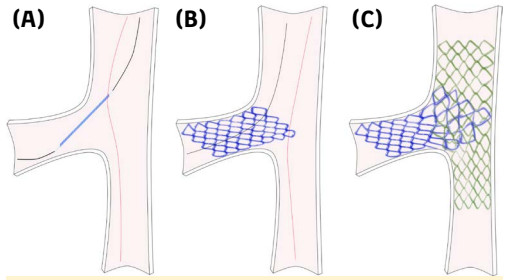

Figure 2. Stenting procedure with Szabo technique. (A) Stent positioning with the Szabo technique. (B) Side branch stent implantation. (C) Final stent configuration.

CASE IMAGE
OLGU GÖRÜNTÜSÜ

Serkan Kahraman
Ahmet Yaşar Çizgici
Kadir Sadıkoğlu
Ali Kemal Kalkan
Mehmet Ertürk

Department of Cardiology, University of Health Sciences, Mehmet Akif Ersoy Thoracic and Cardiovascular Surgery Center, Training and Research Hospital, İstanbul, Türkiye

Corresponding author:
Serkan Kahraman
✉ serkankahraman_86@outlook.com

Received: August 14, 2025
Accepted: September 04, 2025

Cite this article as: Kahraman S, Çizgici AY, Sadıkoğlu K, Kalkan AK, Ertürk M. Optical Coherence Tomography-Guided Nano-Culotte Stenting for Woven Coronary Artery Bifurcation Lesion. *Turk Kardiyol Dern Ars.* 2025;53(7):545-546.

DOI: 10.5543/tkda.2025.83841

Copyright@Author(s)
Available online at archivestsc.com.
Content of this journal is licensed under a Creative Commons Attribution – NonCommercial-NoDerivatives 4.0 International License.

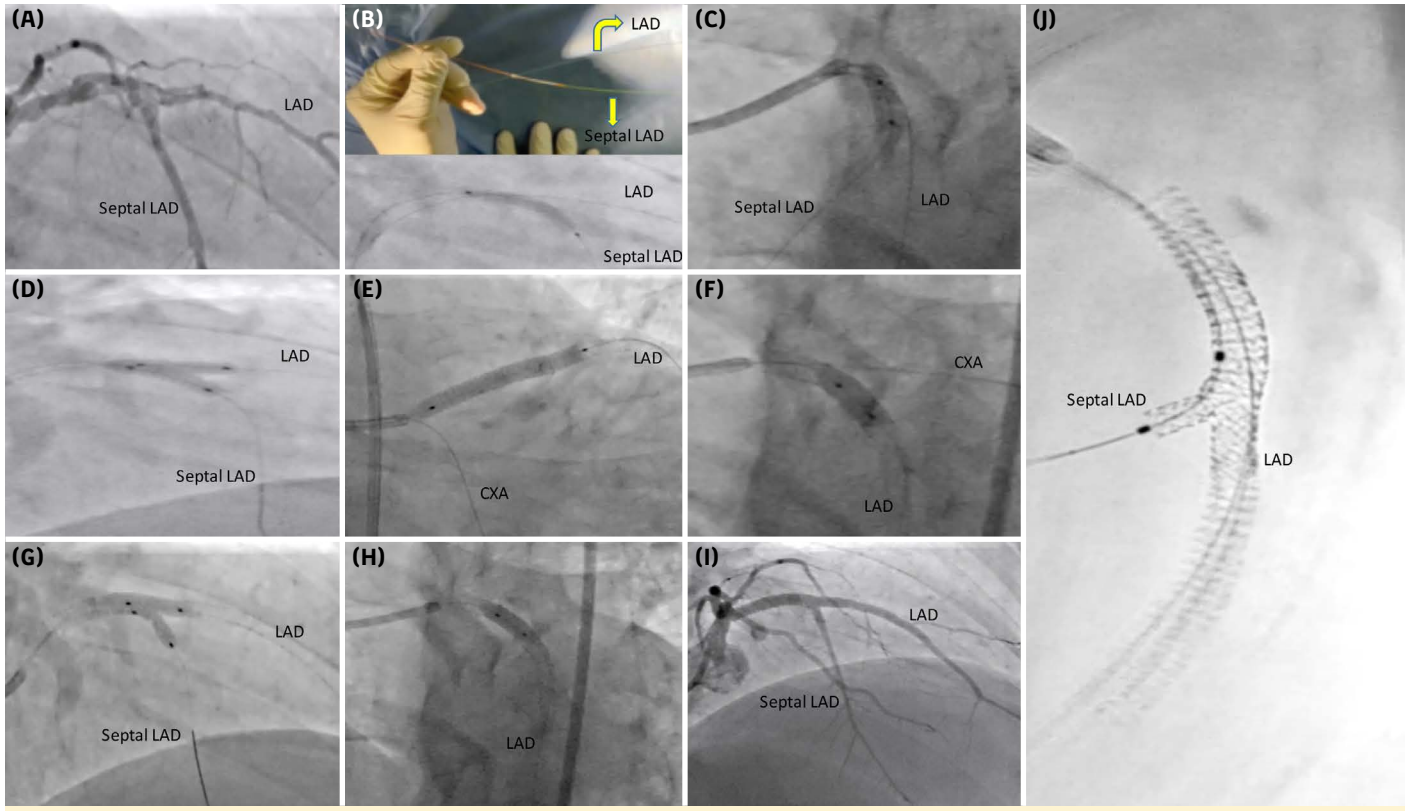

Figure 3. Percutaneous intervention of a woven coronary bifurcation lesion. (A) Woven coronary bifurcation lesion. (B) Septal LAD stent preparation and implantation with the Szabo technique. (C) The POT technique. (D) First KBD. (E) LAD stent implantation. (F) Second POT technique. (G) Second KBD. (H) Final POT. (I) Final angiographic imaging. (J) Stent enhancement imaging.

KBD, Kissing balloon dilatation; LAD, Left anterior descending artery; POT, Proximal optimization technique.

Proximal optimization technique (POT) was performed using a 4.5 × 8 mm non-compliant balloon (NCB) (Figure 3C), followed by kissing balloon dilatation (KBD) with 3.0 × 12 mm (septal LAD) and 3.5 × 12 mm (LAD) NCBs (Figure 3D). A 3.5 × 31 mm sirolimus-eluting stent was deployed in the LAD (Figure 3E). A second POT and final KBD were completed using the same balloon dimensions (Figure 3F, G). The procedure concluded with a final POT using a 4.5 × 8 mm NCB (Figure 3H, Video 5). Post-procedural OCT imaging confirmed optimal stent apposition and expansion (Figure 1 C, D, Video 6). Additionally, the OM lesion was treated with a 2.75 × 21 mm sirolimus-eluting stent (Video 7). The right coronary artery was also patent in the patient (Video 8).

Although a woven coronary artery is a rare congenital anomaly, performing a PCI on it alongside a bifurcation lesion is an extremely difficult procedure. This report demonstrates that OCT-guided bifurcation PCI using the Szabo technique is feasible and effective. To the best of our knowledge, this represents the first documented case of its kind.

Ethics Committee Approval: This is a single case report, and therefore ethics committee approval was not required in accordance with institutional policies.

Informed Consent: The authors confirm that informed consent was obtained from the patient for the use and publication of their case details and images in this manuscript.

Conflict of Interest: The authors report no financial or personal conflicts of interest related to this manuscript.

Funding: No funding was received for this study.

Use of AI for Writing Assistance: AI-assisted technologies were not used.

Author Contributions: Concept – S.K.; Design – S.K.; Supervision – A.K.K., M.E.; Resource – A.Y.Ç., K.S.; Materials – A.Y.Ç., K.S.; Data Collection and/or Processing - S.K.; Analysis and/or Interpretation - S.K., A.K.K., M.E.; Literature Review – S.K.; Writing – S.K.; Critical Review – S.K., M.E.

Peer-review: Internally peer-reviewed.

Video 1. Angiographic imaging of a woven coronary bifurcation lesion.

Video 2. Pre-procedural optical coherence tomography imaging of the left anterior descending artery.

Video 3. Wiring of both the left anterior descending artery (LAD) and septal LAD branches.

Video 4. Septal left anterior descending artery (LAD) stent preparation and implantation with the Szabo technique.

Video 5. Percutaneous coronary intervention of the woven coronary bifurcation lesion.

Video 6. Post-procedural optical coherence tomography imaging of the left anterior descending artery.

Video 7. Percutaneous coronary intervention of the obtuse marginal branch.

Video 8. Angiographic imaging of the right coronary artery.

ARCHIVES OF THE TURKISH SOCIETY OF CARDIOLOGY

Official journal of the TURKISH SOCIETY OF CARDIOLOGY

Can Artificial Intelligence Replace Human Peer Review in Cardiovascular Journals?

Kardiyovasküler Bilimsel Yayınlarda Hakemlik Sürecini Yapay Zeka Üstlenebilir mi?

LETTER TO THE EDITOR
EDİTÖRE MEKTUP

To the Editor,

In recent years, one of the most pressing challenges facing scientific journals—particularly in high-output fields such as cardiology—has been the difficulty in recruiting competent and willing peer reviewers. The growing volume of submissions, a limited pool of qualified reviewers, the absence of financial compensation, and increasing academic workloads have all contributed to significant delays in the peer-review process. Many editors report prolonged publication timelines due to the unavailability of suitable reviewers. At the same time, some authors are now drafting their manuscripts with the help of artificial intelligence (AI)-powered tools. It is also known that some reviewers are using AI during the evaluation process. These developments raise a critical question: Can artificial intelligence replace human reviewers in academic publishing?

AI applications have demonstrated remarkable progress in recent years. Natural language processing models can improve academic writing, generate summaries, check grammar and style, verify references, and even support statistical analysis.[1] However, peer review is not solely a matter of technical competence. It requires identifying novel hypotheses, evaluating methodological rigor, conducting comparative assessments against existing literature, and interpreting clinical or practical implications—skills that are inherently human. AI is predicted to fall short in such intuitive and context-dependent evaluations.[2] Furthermore, because AI models tend to favor "averages," they may undervalue innovative or unconventional approaches, perceiving them as risky or irrelevant.

International ethical guidelines concerning the use of AI tools in academic writing, editorial evaluation, and peer review processes must also be considered. In this context, the International Committee of Medical Journal Editors (ICMJE) stated in a 2023 report that such tools cannot be listed as "authors," and that scientific and ethical responsibility for the resulting content lies entirely with the human author(s).[3] Similarly, the Committee on Publication Ethics (COPE) emphasized in its guidelines on the use of AI in editorial processes that AI should serve only as a supporting tool, not as a decision-maker.[4] According to COPE, all final decisions in editorial evaluations, particularly regarding the acceptance or rejection of articles, must be made exclusively by human editors. The report also presented examples of how AI can pose ethical risks. Recent studies have demonstrated both the potential and limitations of AI-supported peer review applications. Gao et al.[5] observed that while scientific abstracts generated by ChatGPT exhibit high linguistic fluency, they lag behind those written by human authors in terms of content accuracy and contextual depth.

Recently, in a national cardiology journal where we served as academic referees, we observed that some articles were written with the help of a ChatGPT-like language model, and that the text structures were overly general and lacked references. In such cases, high similarity scores (40%) and repeated content were frequently encountered. If these texts, despite passing systematic similarity checks, go unnoticed by human reviewers, there is a risk that erroneous or weak content may enter the scientific literature.

Sefa Tatar

Department of Cardiology, Necmettin Erbakan University, Meram Faculty of Medicine, Konya, Türkiye

Corresponding author:
Sefa Tatar
✉ ssefa_tatar@hotmail.com

Received: May 02, 2025
Accepted: June 10, 2025

Cite this article as: Tatar S. Can Artificial Intelligence Replace Human Peer Review in Cardiovascular Journals? *Turk Kardiyol Dern Ars.* 2025;53(7):547–548.

DOI: 10.5543/tkda.2025.67002

Copyright@Author(s)
Available online at archivestsc.com.
Content of this journal is licensed under a Creative Commons Attribution – NonCommercial-NoDerivatives 4.0 International License.

Recent evidence underscores the growing ethical scrutiny surrounding the use of generative AI tools in the peer-review process. A 2024 cross-sectional analysis by Li et al.,[6] published in JAMA Network Open, systematically examined the policies of the top 100 medical journals regarding AI use in peer review. The study found that 78% of these journals had explicit policies on the matter, and among them, 59% strictly prohibited the use of AI in peer review, mainly due to concerns about confidentiality, lack of contextual judgment, and accountability.[1] This institutional consensus aligns with our own observations as peer reviewers. In a national cardiology journal, we identified submissions likely written using ChatGPT-like tools, characterized by repetitive content, a lack of references, and high similarity scores. These examples illustrate the risks associated with unchecked AI involvement in academic publishing and underscore the importance of maintaining human oversight in peer evaluation.[6]

In conclusion, a fully AI-based peer review system does not appear feasible at this stage. However, a hybrid model that combines human judgment with AI support could enhance both the speed and quality of the scientific review process. The thoughtful integration of AI into editorial workflows is likely to become an essential component of the future of academic publishing. We believe this short piece may contribute to ongoing discussions about the integration of AI in cardiovascular publishing.

Conflict of Interest: The author have no conflicts of interest to declare.

Funding: The author declared that this study received no financial support.

Use of AI for Writing Assistance: AI-assisted technologies were not used in this article.

Peer-review: Internally peer-reviewed.

References

1. Fecher B, Hebing M, Laufer M, Pohle J, Sofsky F. Friend or foe? Exploring the implications of large language models on the science system. *AI & Society*. 2025;40(2):447-459. [CrossRef]
2. Thelwall M. Can ChatGPT evaluate research quality? *JDIS*. 2024;9(2):1-21. [CrossRef]
3. International Conference of Medical Journal Editors. Recommendations for the Conduct, Reporting, Editing, and Publication of Scholarly Work in Medical Journals (updated January 2025). Accessed Feb 5, 202. http://www.icmje.org/icmje-recommendations.pdf
4. Committee on Publication Ethics. Ethical guidelines for peer reviewers. Accessed May 10, 2019.https://publicationethics.org/resources/guidelines-new/cope-ethical-guidelines-peer-reviewers.
5. Gao CA, Howard FM, Markov NS, et al. Comparing scientific abstracts generated by ChatGPT to real abstracts with detectors and blinded human reviewers. *NPJ Digit Med*. 2023;6(1):75. [CrossRef]
6. Li ZQ, Xu HL, Cao HJ, Liu ZL, Fei YT, Liu JP. Use of Artificial Intelligence in Peer Review Among Top 100 Medical Journals. *JAMA Netw Open*. 2024;7(12):e2448609. [CrossRef]

ARCHIVES OF THE TURKISH SOCIETY OF CARDIOLOGY

Official journal of the TURKISH SOCIETY OF CARDIOLOGY

Would the Hemoglobin, Albumin, Lymphocyte, and Platelet Score Help Predict Atrial Fibrillation Recurrence After Cryoballoon Ablation?

Hemoglobin, Albümin, Lenfosit ve Trombosit Skoru Kriyoballon Ablasyon Sonrası Atriyal Fibrilasyon Tekrarını Tahmin Etmeye Yardımcı Olur mu?

LETTER TO THE EDITOR
EDİTÖRE MEKTUP

To the Editor,

I read with great interest the recently published article by Kalenderoğlu et al.,[1] titled "*Assessment of the Efficacy of the Hemoglobin, Albumin, Lymphocyte, and Platelet (HALP) Score in Predicting Recurrence of Atrial Fibrillation Following Cryo-Balloon Ablation*".[1] The authors have presented a timely and clinically relevant study that investigates the predictive value of the hemoglobin, albumin, lymphocyte, and platelet (HALP) score for atrial fibrillation (AF) recurrence after cryoballoon ablation (CBA), addressing a key challenge in arrhythmia management. The identification of a low HALP score as an independent predictor of AF recurrence adds to the growing body of evidence linking systemic inflammation and nutritional status with adverse cardiac outcomes. Given the simplicity, availability, and cost-effectiveness of the HALP score, incorporating it into pre-procedural risk stratification protocols could significantly enhance patient selection and post-ablation monitoring strategies. The reported association between a lower HALP score, particularly in the first tertile, and a 2.1-fold increased risk of AF recurrence after CBA underscores the potential clinical utility of this score.

The HALP score is a recently introduced "immune-nutritional marker" that combines several routinely measured blood parameters reflecting immune function, such as platelet and lymphocyte counts, and nutritional status, as indicated by albumin and hemoglobin (a marker of anemia).[2] Initially, the score was defined as a negative prognostic marker rather than a diagnostic or therapeutic tool in oncology patients.[3,4] Later, the HALP score was also studied for its ability to predict cardiovascular and all-cause mortality in specific patient groups, including those with diabetes,[5] atherosclerotic cardiovascular disease,[6] atrial fibrillation,[7] and even in the general population.[8] An analysis of data from the National Health and Nutrition Examination Survey (NHANES) between 2017 and 2020, involving 8,245 participants, revealed an association between the HALP score and various demographic, socioeconomic, and health-related factors in the adult population in the United States.[9] The study showed that male participants had higher HALP scores than female participants, and that age was inversely correlated with the HALP score. In line with this, Kalenderoğlu et al.[1] also reported that older patients had lower HALP scores. *Therefore, the authors may consider further discussing their study findings regarding the association between age and HALP score, as well as the role of age in AF recurrence.*

Furthermore, the proportion of non-paroxysmal AF patients (particularly those with long-standing persistent AF) was higher in the lower HALP score group,[1] and this subtype is a well-known predictor of AF recurrence after CBA.[10,11] The impact of "*diagnosis-to-catheter ablation time*" on AF recurrence, especially in non-paroxysmal AF, is well established.[12] *However, the study by Kalenderoğlu et al.[1] did not provide data on diagnosis-to-catheter ablation time or its association with the HALP score*.

Nevertheless, as the authors rightly noted, the retrospective and single-center design of the study, along with the use of single-timepoint laboratory values (rather than

Uğur Canpolat

Department of Cardiology, Hacettepe University Faculty of Medicine, Ankara, Türkiye

Corresponding author:
Uğur Canpolat
✉ dru_canpolat@yahoo.com

Received: June 24, 2025
Accepted: June 26, 2025

Cite this article as: Canpolat U. Would the Hemoglobin, Albumin, Lymphocyte, and Platelet Score Help Predict Atrial Fibrillation Recurrence After Cryoballoon Ablation? *Turk Kardiyol Dern Ars.* 2025;53(7):549-550.

DOI: 10.5543/tkda.2025.50051

Copyright@Author(s)
Available online at archivestsc.com. Content of this journal is licensed under a Creative Commons Attribution – NonCommercial-NoDerivatives 4.0 International License.

temporal trends), calls for cautious interpretation. Prospective, multicenter studies and external validation cohorts would be valuable for confirming these findings and establishing standardized HALP score thresholds for clinical use. In conclusion, this study represents a significant step toward integrating immune-nutritional biomarkers into the management of AF.

Conflict of Interest: The author have no conflicts of interest to declare.

Funding: The author declares that this study received no financial support.

Use of AI for Writing Assistance: This paper did not use AI-assisted technologies.

Peer-review: Internally peer-reviewed.

References

1. Kalenderoğlu K, Hayıroğlu M, Çınar T. Assessment of the Efficacy of the Hemoglobin, Albumin, Lymphocyte, and Platelet Score in Predicting Recurrence of Atrial Fibrillation Following Cryo-Balloon Ablation. *Turk Kardiyol Dern Ars*. 2025;53(4):263-269. [CrossRef]
2. Farag CM, Antar R, Akosman S, Ng M, Whalen MJ. What is hemoglobin, albumin, lymphocyte, platelet (HALP) score? A comprehensive literature review of HALP's prognostic ability in different cancer types. *Oncotarget*. 2023;14:153-172. [CrossRef]
3. Chen XL, Xue L, Wang W, et al. Prognostic significance of the combination of preoperative hemoglobin, albumin, lymphocyte and platelet in patients with gastric carcinoma: a retrospective cohort study. *Oncotarget*. 2015;6(38):41370-41382. [CrossRef]
4. Xu H, Zheng X, Ai J, Yang L. Hemoglobin, albumin, lymphocyte, and platelet (HALP) score and cancer prognosis: A systematic review and meta-analysis of 13,110 patients. *Int Immunopharmacol*. 2023;114:109496. [CrossRef]
5. Zhao P, Zhang Z, Li M, Hao J, Wang Y. Association between Hemoglobin-albumin-lymphocyte-platelet score and all-cause or cardiovascular mortality in patients with diabetes or prediabetes: mediated effects of renal function. *BMC Cardiovasc Disord*. 2025;25(1):331. [CrossRef]
6. Zou Y, Cong J, Fu J, Yang X. Association between hemoglobin, albumin, lymphocyte, and platelet scores and all-cause and cardiovascular mortality among adults with atherosclerotic cardiovascular disease in the United States: An analysis of NHANES. *Medicine (Baltimore)*. 2025;104(19):e42386. [CrossRef]
7. Eyiol A. The relationship of pan-immune-inflammation value (PIV) and HALP score with prognosis in patients with atrial fibrillation. *Medicine (Baltimore)*. 2024;103(36):e39643. [CrossRef]
8. Pan H, Lin S. Association of hemoglobin, albumin, lymphocyte, and platelet score with risk of cerebrovascular, cardiovascular, and all-cause mortality in the general population: results from the NHANES 1999-2018. *Front Endocrinol (Lausanne)*. 2023;14:1173399. [CrossRef]
9. Antar R, Farag C, Xu V, Drouaud A, Gordon O, Whalen MJ. Evaluating the baseline hemoglobin, albumin, lymphocyte, and platelet (HALP) score in the United States adult population and comorbidities: an analysis of the NHANES. *Front Nutr*. 2023;10:1206958. [CrossRef]
10. Oto A, Aytemir K, Canpolat U, et al. Pulmonary vein isolation with the cryoballoon technique in atrial fibrillation treatment: Single centre experience. *Turk Kardiyol Dern Ars*. 2013;41(4):299-309. Turkish. [CrossRef]
11. Canpolat U, Kocyigit D, Yalcin MU, et al. Long-term outcomes of pulmonary vein isolation using second-generation cryoballoon during atrial fibrillation ablation. *Pacing Clin Electrophysiol*. 2019;42(7):910-921. [CrossRef]
12. Amin AM, Elbenawi H, Khan U, et al. Impact of Diagnosis to Ablation Time on Recurrence of Atrial Fibrillation and Clinical Outcomes After Catheter Ablation: A Systematic Review and Meta-Analysis With Reconstructed Time-to-Event Data. *Circ Arrhythm Electrophysiol*. 2025;18(2):e013261. [CrossRef]

ARCHIVES OF THE TURKISH SOCIETY OF CARDIOLOGY

Official journal of the TURKISH SOCIETY OF CARDIOLOGY

Reply to the Letter to the Editor: ''Would the Hemoglobin, Albumin, Lymphocyte, and Platelet Score Help Predict Atrial Fibrillation Recurrence After Cryoballoon Ablation?''

Editöre Mektup Yanıtı: ''Hemoglobin, Albümin, Lenfosit ve Trombosit Skoru Kriyoballon Ablasyon Sonrası Atriyal Fibrilasyon Tekrarını Tahmin Etmeye Yardımcı Olur mu?''

LETTER TO THE EDITOR REPLY
EDİTÖRE MEKTUP YANITI

To the Editor,

We would like to express our appreciation to the author[1] for their keen interest in our article titled "*Assessment of the Efficacy of the Hemoglobin, Albumin, Lymphocyte, and Platelet (HALP) Score in Predicting Recurrence of Atrial Fibrillation Following Cryo-Balloon Ablation*."[2] Your thoughtful comments and observations have provided valuable insights.

As highlighted, the HALP score, which was originally introduced as a vital prognostic tool in oncology, is now gaining significant traction in the field of cardiovascular research. We firmly believe that the HALP score stands out as an easily accessible and cost-effective immunonutritional biomarker capable of effectively stratifying the risk of atrial fibrillation (AF) recurrence after cryoballoon ablation (CBA). Our findings clearly demonstrated that lower HALP scores are associated with older age, corroborating previous studies from the National Health and Nutrition Examination Survey (NHANES), which revealed a clear inverse relationship between age and HALP levels.[3]

However, it is important to acknowledge the limitation posed by the lack of data regarding the duration from AF diagnosis to CBA, commonly referred to as "diagnosis-to-ablation time." This gap in information is a notable drawback, as the retrospective nature of our data collection made consistent documentation of this variable challenging. Addressing this limitation in future prospective studies may further clarify the role of the HALP score in relation to diagnosis-to-ablation time, which remains an area for further research.

References

1. Canpolat U. Would the Hemoglobin, Albumin, Lymphocyte, and Platelet Score Help Predict Atrial Fibrillation Recurrence After Cryoballoon Ablation? *Turk Kardiyol Dern Ars*. 2025;53(7):549-550.
2. Kalenderoğlu K, Hayıroğlu M, Çınar T. Assessment of the Efficacy of the Hemoglobin, Albumin, Lymphocyte, and Platelet Score in Predicting Recurrence of Atrial Fibrillation Following Cryo-Balloon Ablation. *Turk Kardiyol Dern Ars*. 2025;53(4):263-269. [CrossRef]
3. Antar R, Farag C, Xu V, Drouaud A, Gordon O, Whalen MJ. Evaluating the baseline hemoglobin, albumin, lymphocyte, and platelet (HALP) score in the United States adult population and comorbidities: an analysis of the NHANES. *Front Nutr*. 2023;10:1206958. [CrossRef]

Koray Kalenderoğlu[1]
Mert İlker Hayıroğlu[1]
Tufan Çınar[2]

[1]*Department of Cardiology, Health Sciences University, Dr Siyami Ersek Cardiovascular and Thoracic Surgery Center, İstanbul, Türkiye*
[2]*Department of Medicine, University of Maryland Midtown Campus, Baltimore, Maryland, USA*

Corresponding author:
Koray Kalenderoğlu
✉koray_kalenderoglu@hotmail.com

Cite this article as: Kalenderoğlu K, Hayıroğlu Mİ, Çınar T. Reply to the Letter to the Editor: ''Would the Hemoglobin, Albumin, Lymphocyte, and Platelet Score Help Predict Atrial Fibrillation Recurrence After Cryoballoon Ablation?'' *Turk Kardiyol Dern Ars.* 2025;53(7):551.

DOI: 10.5543/tkda.2025.55305

Copyright@Author(s)
Available online at archivestsc.com.
Content of this journal is licensed under a Creative Commons Attribution – NonCommercial-NoDerivatives 4.0 International License.

ARCHIVES OF THE TURKISH SOCIETY OF CARDIOLOGY

Official journal of the TURKISH SOCIETY OF CARDIOLOGY

Factors Affecting QT Interval in Patients with Type 2 Diabetes Mellitus and the Effect of Sodium-Glucose Cotransporter 2 Inhibitors

Tip 2 Diabetes Mellituslu Hastalarda QT Aralığını Etkileyen Faktörler ve Sodyum-Glukoz Kotransporter 2 İnhibitörlerinin Etkisi

LETTER TO THE EDITOR
EDİTÖRE MEKTUP

To the Editor,

We read with great interest the article titled "*Sodium-Glucose Cotransporter 2 Inhibitors Significantly Lower the Cardiac Electrophysiological Balance Index in Type 2 Diabetes Patients*" by Özdemir et al.,[1] published in Volume 53 of the Archives of the Turkish Society of Cardiology (March 2025). We would like to highlight several important points regarding this well-written study.

Although Balcıoğlu et al.[2] demonstrated that treatment with sodium-glucose cotransporter 2 (SGLT-2) inhibitors for at least six months resulted in lower values of the sympathetic activity index and the ratio of low-frequency to high-frequency power in patients with type 2 diabetes mellitus (DM), these findings support the hypothesis that SGLT-2 inhibitors may modulate cardiovascular autonomic function by reducing sympathetic nervous system (SNS) activity. Therefore, we believe the authors should specify the duration of SGLT-2 inhibitor use in their patient cohort.

Hadgu et al.[3] investigated the relationship between thyroid dysfunction and diabetes mellitus. According to their meta-analysis, thyroid dysfunction was more common in patients with type 2 diabetes mellitus. Based on their findings, the authors recommended regular thyroid function testing in patients with type 2 DM. In a separate study, Altun et al.[4] showed that QT dispersion was prolonged in patients with hypothyroidism. We believe that thyroid function may influence QT interval in patients with type 2 DM and should therefore be considered in statistical analysis.

Mobasheri-Shiri et al.[5] were the first to describe the relationship between insulin resistance (IR) and QT interval, reporting a positive correlation between the two. Furthermore, Gerich[6] noted that IR is not a prerequisite for type 2 DM and emphasized that each patient with type 2 DM has a unique level of IR. Recent studies have demonstrated that the triglyceride-glucose index is an indirect measure of IR. Lee et al.[7] found an association between QTc prolongation and the triglyceride-glucose index. Although triglyceride and glucose values are presented in the study tables, the authors did not comment on IR levels in their patients. By calculating the triglyceride-glucose index, the authors could indirectly assess IR and explore its relationship with the cardiac electrophysiological balance index. This may provide a pathophysiological explanation for how SGLT-2 inhibitors influence these parameters.

In conclusion, we think that factors such as thyroid function and insulin resistance should be taken into account in studies evaluating QT interval because of their potential impact on QT interval.

Conflict of Interest: The authors have no conflicts of interest to declare.

Funding: The authors declared that this study received no financial support.

Use of AI for Writing Assistance: AI-assisted technologies were not used in this article.

Ali Çoner

Can Ramazan Öncel

Cemal Köseoğlu

Department of Cardiology, Alanya Alaaddin Keykubat University, Faculty of Medicine, Antalya, Türkiye

Corresponding author:
Cemal Köseoğlu
✉ drcemalkoseoglu@hotmail.com

Received: June 11, 2025
Accepted: June 26, 2025

Cite this article as: Çoner A, Öncel CR, Köseoğlu C. Factors Affecting QT Interval in Patients with Type 2 Diabetes Mellitus and the Effect of Sodium-Glucose Cotransporter 2 Inhibitors. *Turk Kardiyol Dern Ars.* 2025;53(7):552-553.

DOI: 10.5543/tkda.2025.70970

Copyright@Author(s)
Available online at archivestsc.com.
Content of this journal is licensed under a Creative Commons Attribution – NonCommercial-NoDerivatives 4.0 International License.

Author Contributions: Concept – A.Ç.; Design – C.K.; Supervision – C.R.Ö.; Resource – A.Ç.; Materials – C.K.; Data Collection and/or Processing – C.R.Ö.; Analysis and/or Interpretation – A.Ç.; Literature Review – C.K.; Writing – C.R.Ö.; Critical Review – A.Ç

Peer-review: Internally peer-reviewed.

References

1. Özdemir E, Ziyrek M, Dönmez E, et al. Sodium-Glucose Cotransporter 2 Inhibitors Significantly Lower the Cardiac Electrophysiological Balance Index in Type 2 Diabetes Patients. *Turk Kardiyol Dern Ars*. 2025;53(2):113-119. [CrossRef]
2. Balcıoğlu AS, Çelik E, Aksu E, Aykan AÇ. Impact of Sodium-Glucose Cotransporter-2 Inhibitors on Sympathetic Nervous System Activity Detected by Sympathetic Activity Index and LF/HF Ratio in Patients with Type 2 Diabetes Mellitus. *Turk Kardiyol Dern Ars*. 2022;50(6):415-421. [CrossRef]
3. Hadgu R, Worede A, Ambachew S. Prevalence of thyroid dysfunction and associated factors among adult type 2 diabetes mellitus patients, 2000-2022: a systematic review and meta-analysis. *Syst Rev*. 2024;13(1):119. [CrossRef]
4. Altun A, Altun G, Ozbay G. QT dispersion in hypothyroidism. *Int J Cardiol*. 1999;72(1):93-95. [CrossRef]
5. Mobasheri-Shiri M, Bazmi S, Soleimani-Meigoli MS, Karimimoghadam Z, Tabrizi R, Farjam M. The association between insulin resistance and QT interval: A systematic review and Meta-Analysis. *BMC Cardiovasc Disord*. 2025;25(1):139. [CrossRef]
6. Gerich JE. Insulin resistance is not necessarily an essential component of type 2 diabetes. *J Clin Endocrinol Metab*. 2000;85(6):2113-2115. [CrossRef]
7. Lee TL, Hsuan CF, Wu CC, et al. Association between Triglyceride Glucose Index and Corrected QT Prolongation in Chinese Male Steelworkers. *Int J Environ Res Public Health*. 2021;18(8):4020. [CrossRef]